Investigating host and pathogen factors that modulate the phagocytosis of *Cryptococcus neoformans* by macrophages.

by

Chinaemerem Uju Onyishi

UNIVERSITY OF BIRMINGHAM

A thesis submitted to the University of Birmingham for the degree of

DOCTOR OF PHILOSOPHY

Institute of Microbiology and Infection

School of Biosciences

College of Life and Environmental Sciences

University of Birmingham

September 2023

Abstract

Infection with the opportunist fungal pathogen, *Cryptococcus neoformans,* is thought to begin with the inhalation of spores or desiccated yeast into the lungs, where phagocytes of the innate immune system serve as the first line of defence against infection. However, for a long time, very little was understood about the mechanism by which *C. neoformans* is detected and phagocytosed by macrophages. Therefore, my PhD research sought to investigate the role of pattern recognition receptors (PRR) such as TLR4 and scavenger receptors in the non-opsonic phagocytosis of *C. neoformans*. I also investigated broader aspects of phagocyte-*Cryptococcus* interactions, including how pathogen factors such as extracellular vesicle (EV) production impact the host and how resistance to amoebal phagocytosis may relate to the mammalian immune response.

I found that TLR4 was not directly involved in the uptake of *C. neoformans*. Instead TLR4 deficiency led to increased non-opsonic uptake via increased expression of the scavenger receptor, MSR1. *MSR1* knock out and immunofluorescence imaging identified MSR1 as a key receptor for the non-opsonic phagocytosis of *C. neoformans*. Therefore, I identify TLR4/MSR1 crosstalk in modulating *C. neoformans* uptake.

In parallel, I found that the scavenger receptor MARCO is only involved in uptake in certain contexts but has a hitherto unrecognised role as a broadly relevant modulator of non-lytic expulsion. Finally, in collaborative projects with other groups, I discovered that loss of EV production led to decreased phagocytosis of cryptococci and that

resistance to amoebal uptake was not a predictor of cryptococcus virulence to macrophages as measured by phagocytosis rate and intracellular proliferation. Taken together, my work highlights the importance of *C. neoformans* interactions with macrophages as a possible predictor of disease outcome, suggesting that strategies to manipulate non-opsonic uptake of cryptococci may serve as useful therapeutic targets in the future.

Declaration

The work presented in this thesis is my own original work and has resulted in two publications. The first is a review article titled *'Human immune polymorphisms associated with the risk of cryptococcal disease'*, with my supervisor, Professor Robin C. May as a co-author. I am the first author on this publication and wrote the manuscript. The parts of this publication that may share similarities with Chapter 1 of the thesis were written with no significant contribution from Robin C. May.

Chapter 3 of this thesis is adapted from a published research article titled '*Toll-like receptor 4 and macrophage scavenger receptor 1 crosstalk regulates phagocytosis of a fungal pathogen'* with Dr Guillaume Desanti, Dr Alex Wilkinson, Dr Samuel Lara-Reyna, Dr Eva-Maria Frickel, Dr Gyorgy Fejer, Dr Olivier Christophe, Professor Clare Bryant, Dr Subhankar Mukhopadhyay, Professor Siamon Gordon and Professor Robin May as co-authors. I am the first author on this paper and was responsible for conducting all experiments and writing the manuscript. The contribution of the co-authors to the text were not substantial.

Chapter 6 of the thesis discusses work I carried out in collaboration with Dr Thomas Sauters and Professor Paul Magwene. As at 19/10/2023, the work has been accepted for publication in PLOS Pathogens. Chapter 6 only includes original work that I specifically contributed to this collaborative project. In all cases where information was derived from others, I confirm that I have stated these explicitly in the thesis.

To my family, whose love brought me into this moment.

Acknowledgments

Firstly, I would like to thank my supervisor Prof Robin May for taking a chance on an aspirational BSc who had no idea what she was getting herself into. Thank you for believing in my potential to become a successful scientist. I will forever be grateful for your endless support and guidance over the past four years. Many thanks to my co-supervisors, Dr Eva-Maria Frickel and Dr Elizabeth Ballou, for your expertise and advice during my research. Thank you to Dr Hung-Ji Tsai, for your wealth of knowledge and scientific and career advice. I would also like to extend my gratitude to the Darwin Trust of Edinburgh for providing the PhD studentship and financial support that made this entire experience possible.

I would like to thank Prof Clare Bryant for the provision of iBMDMs that laid the foundation for my project. A massive thank you to Prof Siamon Gordon and Dr Subhankar Mukhopadhyay who not only provided me with the MPI cell lines that were critical to the completion of my project but took personal interest in the success of my research. Thank you to my other collaborators Dr Juliana Rizzo and Dr Guilhem Janbon at the Pasteur Institute in Paris, and Dr Thomas Sauters and Dr Paul Magwene at Duke University in North Carolina who invited me into their exciting research and shared their knowledge with me. Thank you to Dr Guillaume Desanti, Dr Samuel Lara-Reyna, Dr Lamin Saidykhan, Dr Joao Correia and Dr Maria Makarova who all made time to teach me new techniques at various points during my PhD research. Thank you to all the past and present members of the HAPI lab who I've had the pleasure of working alongside

over the past four years. I greatly appreciate your words of encouragement, scientific and life advice, and being a reliable source of necessary distraction.

Lastly, I would like to thank my friends who endured my monologues about my experimental successes and failures. Thank you for your words of encouragement at the most critical moments, keeping me grounded and making sure I celebrate even the smallest wins. A massive thank you to my siblings, Chinedu, Uche, Chisom, Somto, Chisimdi and Chijindu, whose steadfast support came in the form of never-ending laughter. Thank you to my father, Dr Samuel Maduka Onyishi, and my mother, Dr Ifeyinwa Emilia Onyishi for your endless self-sacrifice and prayers. Thank you for being a consistent source of encouragement, strength, and for your unwavering belief in me. Thank you for all I cannot put into words. They say you don't get to pick your family, but I certainly feel like I picked mine. And finally, I thank God with whom all things are possible.

Table of Contents

List of Figures

List of Tables

List of Abbreviation

Abbreviation	Explanation
ADCC	Antibody-Dependent Cellular Cytotoxicity
AF594	AlexaFluor594
AIDS	Acquired Immune Deficiency Syndrome
ANOVA	ANalysis Of VAriance
AP1	Activator Protein 1
ARE	Antioxidant Response Elements
ARP2/3	Actin Related Protein 2/3
ART	Anti-Retroviral Therapy
ATF	Activating Transcription Factor
BAL	BronchoAlveolar Lavage
BB515	Brilliant Violet 515
BBB	Blood Brain Barrier
BCL10	B-Cell Lymphoma 10
BLI	BioLuminescence Imaging
BMDC	Bone-Marrow derived myeloid Dendritic Cells
BMDM	Mice Bone Marrow Derived Macrophages
BSA	Bovine Serum Albumin
BZP	Zinc Finger E-Box Binding Homeobox 1
CARD9	CAspase Recruitment Domain-containing protein 9
CCL	Chemokine (C-C motif) Ligand 7
CCR2	C-C Chemokine Receptor type 2
CD	Cluster of Differentiation
CFU	Colony Forming Unit
CFW	CalcoFluor White
CHO	Chinese Hamster Ovary
CHS	Chitin Synthase
CI	Confidence Interval
CLR	C-type Lectin Receptor
CM	Cryptococcal Meningitis
CNS	Central Nervous System
CO2	Carbon Dioxide
CR	Complement Receptor
CryoEM	Cryogenic Electron Microscopy
CSF1	Colony Stimulating Factor 1
μCT	micro-Computed Tomography
CXCL	C-X-C motif Chemokine Ligand

DAPI	4’,6-Diamidino-2-phenylindole
DC-SIGN	Dendritic Cell-Specific ICAM- 3-Grabbing Non-integrin
DKO	Double Knockout
DMEM	Dulbecco’s Modified Eagle medium,
DMSO	DiMethyl SulfOxide
DNA	DeoxyriboNucleic Acid
DPBS	Dulbecco's Phosphate-Buffered Saline
EDTA	EthyleneDiamineTetraacetic Acid
EGFP	Enhanced Green Fluorescent Protein
ELISA	Enzyme-Linked Immunosorbent Assay
ERG11	Sterol 14-demethylase
ERK	Extracellular signal-Regulated Kinase
ESCRT	Endosomal Complex Required for Transport
EV	Extracellular Vesicles
FACS	Fluorescence-Activated Cell Sorting
FBS	Fetal Bovine Serum
FCGR	FC Gamma Receptor
FMO	Fluorescent Minus One
FSC	Forward SCatter
GAT	GATA-type zinc fingers
GalXM	Galactoxylomannan
GCS	Glucosylceramide
GFP	Green Fluorescent Protein
GMCSF	Granulocyte-Macrophage Colony Stimulating Factor
GTPase	GTP-binding protein
GWAS	Genome Wide Association Study
GXM	Glucuronoxylomannan
HAP	CCAAT-binding Heme Activator Protein
HEK293	Human Embryonic Kidney 293
HIV	Human Immunodeficiency Virus
HMDM	Human Monocyte Derived Macrophages
HSO	Human Serum Opsonised
iBMDM	immortalised Bone Marrow Derived Macrophage
IFN	Interferon
IFNAR	Interferon-α/β Receptor
IKK	Inhibitor of nuclear factor Kappa-B Kinase subunit
IL	InterLeukin
IPR	Intracellular Proliferation Rate
IRAK	IL-1R-associated kinase

IRF	Interferon regulatory factor 3
ISG	IFN-stimulated genes
ITAM	Immunoreceptor Tyrosine-Based Activation Motif
ITIM	Immunoreceptor Tyrosine-Based Inhibitory Motifs
JAK	JAnus Kinase
JNK	c-Jun N-terminal Kinase
KO	KnockOut
LBP	LPS Binding Protein
LDL	low-density lipoproteins
LPS	Lipopolysaccharide
LRR	Leucine Rich Repeat
LT50	Time to 50% Lethality
MALT1	Mucosa-Associated Lymphoid Tissue lymphoma-translocation gene 1
MAPK	Mitogen Activated Protein Kinase
MARCO	MAcrophage Receptor with COllagenous structure
MBL	Mannose Binding Lectin
M-CSF	Macrophage Colony Stimulating Factor
MD2	Myeloid Differentiation factor 2
MDA5	Melanoma Differentiation-Associated protein-5
MEK	Mitogen-activated Extracellular signal-regulated Kinase
MHC	Major Histocompatibility Complex
MIP	Macrophage Inflammatory Protein
MOI	Multiplicity Of Infection
MPI	Max Plank Institute cells
MR	Mannose Receptor
MRC1	Mannose Receptor C-Type 1
MRI	Magnetic Resonance Imaging
MSR1	Macrophage Scavenger Receptor 1
MYD88	MYeloid Differentiation primary response 88
NFE2L2	Nuclear Factor Erythroid-derived 2-Like 2
NHNT	Non-HIV, Non-Transplant
NHSBT	National Health Service Blood Transfusion service
NK	Natural Killer
NKp30	NK cell cytotoxicity triggering receptor
NLR	NOD-Like Receptor
NO_2	Nitrogen Dioxide
iNOS	inducible Nitric Oxide Synthase
OPT1	OligoPeptide Transporter 1
OR	Odds Ratio

ox-LDL	oxidized Low-Density Lipoprotein
PAMP	Pathogen Associated Molecular Pattern
PAP	Pulmonary Alveolar Proteinosis
PBMC	Peripheral Blood Mononuclear Cell
PBS	Phosphate Buffered Saline
PCR	Polymerase Chain Reaction
PE	Phycoerythrin
PI3K	PhosphoInositide 3-Kinase
pICLC	poly-IC
PKC	Protein Kinase C
PLB1	Phospholipase B1
PMϕ	Peritoneal Macrophages
PMA	Phorbol 12-Myristate 13-Acetate
PRR	Pattern Recognition Receptor
QTL	Quantitative Trait Loci
RBC	Red Blood Cell
RNA	RiboNucleic Acid
RNS	Reactive Nitrogen Species
ROS	Reactive Oxygen Species
RPMI	Roswell Park Memorial Institute
SCARF	Scavenger Receptor Class F
SD	Sabouraud Dextrose
SEM	Standard Error of the Mean
SFDMEM	Serum Free Dulbecco's Modified Eagle Medium
SLE	Systemic Lupus Erythematosus
SNARE	Soluble N-ethylmaleimide-sensitive-factor attachment protein receptor
t-SNARE	plasma membrane SNARE
v-SNARE	vesicles SNARE
SNC2	Synaptobrevin homolog 2
SNP	Single Nucleotide Polymorphism
SOCS3	Suppressor Of Cytokine Signalling 3
SP	Surfactant Protein
SR	Scavenger Receptor
SREC	Scavenger Receptor expressed by Endothelial Cells
SSC	Side SCatter
STAT	Signal Transducer and Activator of Transcription
SYK	Spleen Tyrosine Kinase
TAK1	Transforming growth factor-β-Activated Kinase 1
TANK	TRAF family member Associated NFκB activator

TBK1	TANK-Binding Kinase 1
TGF-β	Transforming Growth Factor-β
TIR	Toll/Interleukin 1 Receptor
TIRAP	TIR domain–containing Adaptor molecule
TLR	Toll-Like Receptor
TNF-α	tumour necrosis factor-α
TRAF	Tumor necrosis factor Receptor-Associated Factor
TRAM	TRIF related adaptor molecule
TRIF	TIR-domain-containing adapter-inducing interferon-β
UK	United Kingdom
USA	United States of America
UTR	UnTranslated Region
UV	UltraViolet
V-ATPase	Vacuolar-type Adenine TriPhosphatase
VPS	Vacuolar Protein Sorting
WASP	Wiskott–Aldrich Syndrome Protein
WT	WildType
YPD	Yeast extract-Peptone-Dextrose

Chapter 1 Introduction

Parts of the work in Chapter 1 have already been published: ***Onyishi, C.U****. and May, R.C. (2022) Human immune polymorphisms associated with the risk of cryptococcal disease. Immunology, 165 (2): 143–157. doi:10.1111/imm.13425.*

1.1 *Cryptococcus neoformans* and Cryptococcosis

Cryptococcus neoformans is an encapsulated yeast with a diameter of 5-7µm that causes a potentially fatal disease called cryptococcosis mainly in immunocompromised individuals (May et al., 2016; Maziarz and Perfect, 2016). Although *C. neoformans* is commonly found in soil and avian excreta all over the world (Srikanta et al., 2014), human cryptococcosis became a major health concern following the AIDS pandemic in the 1980s and is now considered an AIDS-defining illness and the leading cause of fungal meningitis in sub-Saharan Africa (May et al., 2016). Infection with *C. neoformans* is thought to begin with the inhalation of spores or desiccated yeast cells from the environment into the lungs (Figure 1-1) (May et al., 2016). Within the lungs, *C. neoformans* is phagocytosed by alveolar, interstitial and infiltrating monocyte-derived macrophages that attempt to clear the infection. However, the fungi have evolved mechanisms to survive and replicate within macrophages, possibly due to evolutionary selection through amoebae (Campuzano and Wormley, 2018; May et al., 2016). In immunocompetent individuals, *C. neoformans* can be cleared by the immune system or establish asymptomatic latent infection within macrophages. Most adults are believed to carry latent *C. neoformans* infection since one study identified antibodies against *C. neoformans* in 56% of 2.1 to 5-year-olds and in 70% of children over 5 years old living in

the Bronx, New York (Goldman et al., 2001). In immunocompromised individuals, it can successfully colonise the lungs leading to pulmonary disease that is characterised by acute pneumonia, chronic pneumonia and non-calcified granulomas (Warkentien and Crum-Cianflone, 2010). Following successful primary pulmonary infection or following reactivation of latent infection, *C. neoformans* can spread through the peripheral blood circulation, cross the blood-brain barrier (BBB) and infect the meninges, ultimately leading to fatal cryptococcal meningitis (CM) (May et al., 2016; Srikanta et al., 2014).

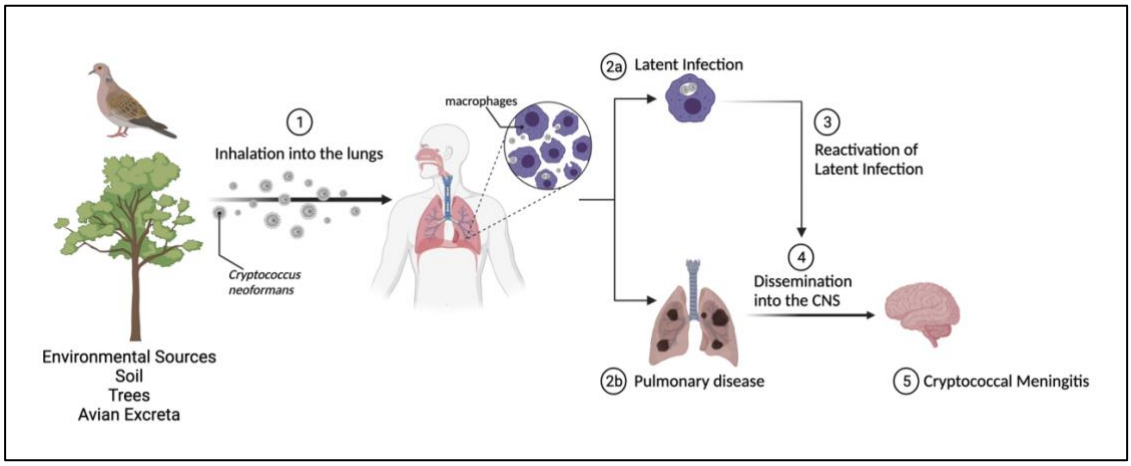

Figure 1-1: *Cryptococcus neoformans* mode of infection. *C. neoformans* is commonly found in soil and avian excreta all over the world. Infection with the fungus begins with the inhalation of fungal cells into the lungs. Within the lungs, *C. neoformans* can establish asymptomatic latent infection or cause pulmonary disease. The fungi can then disseminate to the central nervous system (CNS), cross the blood-brain barrier, and infect the meninges, leading to fatal cryptococcal meningitis (CM). Figure created with BioRender.com.

Several mechanisms have been proposed to explain the ability of *C. neoformans* to cross the BBB and gain entry into the highly sterile environment that is the central nervous system (CNS) (May et al., 2016; Vu et al., 2014). The first proposed mechanism is called paracytosis, which is where cryptococcus cells squeeze their way through loosened tight junction of brain endothelial cells (May et al., 2016). The second mechanism, called

transcytosis, states that cryptococci adhere to the surface of brain endothelial cells via CD44 receptors on the blood side (Jong et al., 2008). They are then internalized, travel across the cytoplasm of the endothelial cell and finally exit into the brain side of the BBB (Vu et al., 2014; Chang et al., 2004). A secreted *C. neoformans* metalloprotease (CnMpr1) has been found to also play a role in fungal attachment to the brain endothelium (Vu et al., 2014). Interestingly, the expression of CnMpr1 in *Saccharomyces cerevisiae*, which naturally lacks the ability to cross the BBB, allowed these cells to cross the brain endothelium (Vu et al., 2014). The final proposed mechanism by which cryptococcus cross the BBB is called the "Trojan Horse" hypothesis. In this model, cryptococcus cells hijack phagocytic cells and use them as a vehicle to enter the CNS. Once infected macrophages cross the BBB, it is thought that fungal cells escape from within macrophage via a mechanism called vomocytosis, a non-lytic expulsion mechanism where fully phagocytosed fungi are expelled from the macrophage with no evidence of host cell damage (Alvarez and Casadevall, 2006; Ma et al., 2006). In support of the "Trojan Horse" hypothesis, it has been found that mice depleted of alveolar macrophages have increased survival and decreased fungal spread to the CNS (Kechichian et al., 2007; Shao et al., 2005; Charlier et al., 2009), thereby implicating phagocytes in the spread of *C. neoformans* to the CNS. However, whether vomocytosis is directly involved in the escape of fungi from macrophages remains unclear since vomocytosis is yet to be observed in brain tissue. There is some evidence to support all three hypotheses, thus, it is highly plausible that *C. neoformans* can utilise all three mechanisms to promote its dissemination in a context-dependent manner.

1.1.1 The Epidemiology of Cryptococcosis

Fungal diseases are greatly underrepresented in public health discourse even though they are estimated to cause over 1.5 million deaths annually (Bongomin et al., 2017). Not only is there a lack of accurate and rapid diagnostic tools, but there is also poor access to antifungal drugs leading to case-fatality rates ranging from 15% to 80% (Bongomin et al., 2017; Rodrigues and Nosanchuk, 2020). In the case of *C. neoformans*, the estimated global burden of CM in HIV patients is 223,100 cases per year with 73% of global cases (162,500) occurring in sub-Saharan Africa (Rajasingham et al., 2017). HIV-associated CM is estimated to cause 181,100 deaths annually of which 135,900 occur in sub-Saharan Africa. Additionally, CM is responsible for 15% of AIDS-related deaths globally, making it the second-leading cause of death in AIDS patients after tuberculosis (Rajasingham et al., 2017). It has been reported that HIV-associated CM has a 17% 2-week mortality rate, 34% at 10 weeks and 41% after 1 year despite treatment with antifungal drugs (Jarvis et al., 2014). This clearly emphasizes the need for better antifungal drugs and the development of host-directed immune therapy, a development that will require a greater understanding of cryptococcus-host interaction.

1.1.2 Risk factors for *C. neoformans* infection

As an opportunistic fungal pathogen, conditions and medical interventions that suppress host immunity, such as HIV/AIDS, solid organ transplantation, diabetes, and chronic glucocorticoid use, increase the risk of cryptococcosis and CM (May et al., 2016; Brizendine et al., 2013).

HIV/AIDS

The significantly low levels of $CD4^+$ T-cells in AIDS patients (CD4 count less than 100 cells/µL) make them particularly vulnerable to opportunistic infections including infection with *C. neoformans* (Rajasingham et al., 2017). In developed countries, such as the United States, with better and faster access to Anti-Retroviral Therapy (ART) and antifungal treatments, hospitalization due to HIV-associated CM decreased by 53.6% between 1997 and 2009 (Pyrgos et al., 2013). Unfortunately, this has not been the case in low- and middle-income countries where access to ART and high-quality antifungal drugs is still limited likely due to the high cost of drugs and poorly funded healthcare systems (Loyse et al., 2013; Driemeyer et al., 2022).

Solid Organ Transplant

Solid organ transplant increases the risk of *C. neoformans* infection due to the prescription of aggressive immunosuppressive agents, such as alemtuzumab and antithymocyte globulin, to these patients in order to prevent organ rejection (Shoham and Marr, 2012; Vilchez et al., 2001). *C. neoformans* is responsible for ~8% of invasive fungal infections among organ transplant recipients, making it the third leading cause of fungal infection in this cohort behind candidiasis and aspergillosis (Pappas et al., 2010; Shoham and Marr, 2012).

Cryptococcosis in Immunocompetent Individuals

Although CM is usually an opportunistic disease in immunocompromised individuals, there are growing reports of CM in immunocompetent individuals (Pappas, 2013; Mada

et al., 2017; Poley et al., 2019; Brizendine et al., 2013; George et al., 2018). This suggests that the risk of cryptococcal disease may also be driven by host genetics and/or environmental factors (Cunha and Carvalho, 2018; Pappas, 2013). The impact of host genetics on risk of cryptococcal disease will be discussed in Chapter 1.4.

A retrospective study of 302 patients with cryptococcosis found that HIV-positive and organ transplant recipients had a lower risk of death compared to non-HIV, non-transplant patients (NHNT) (Brizendine et al., 2013). This is possibly due to delays in diagnosis and treatment in otherwise healthy individuals. It was shown that it took about 68 days to diagnose otherwise healthy people with cryptococcosis, compared to 22 days for HIV patients and 26 days for organ transplant recipients (Brizendine et al., 2013). It is known that cryptococcosis is a possible complication in HIV patients, thus regular screening allows cryptococcus infection to be detected early. Even after diagnosis with cryptococcosis in otherwise healthy individuals, the currently available treatment regimens are based mainly on data from studies on HIV patients. Hence, a better understanding of pathogen interaction with seemingly healthy individuals is needed to develop better treatment options for immunocompetent individuals (Garelnabi et al., 2018).

1.2 Host Innate Immune Response

With a case-fatality rate between 20% to 70% (Rajasingham et al., 2017), there is an urgent need to understand the precise immune signalling pathway(s) triggered by *C. neoformans* infection and identify the key immune modulators that could serve as novel

avenues for host-directed immunotherapies. The next section will review our understanding of the host innate immune response to *C. neoformans* infection.

1.2.1 Phagocytosis as a Defence Mechanism

Following the inhalation of *C. neoformans* into the lungs, professional phagocytes such as macrophages, dendritic cells and neutrophils are at the forefront of host defence (Osterholzer et al., 2009a; Wozniak et al., 2006). Lung-resident macrophages are among the first cells cryptococcus encounter, thus, the interaction between host macrophages and invading fungi is believed to be an important determinant of disease progression and outcome (Shao et al., 2005; Osterholzer et al., 2009a).

Phagocytosis, defined as the uptake of particles greater than 0.5μm, is a significant process in the innate immune response as it leads to the degradation of invading pathogens and the presentation of microbial ligands on MHC molecules thereby activating the adaptive arm of the immune system (Campuzano and Wormley, 2018). Phagocytosis is initiated by the recognition of pathogen-associated molecular patterns (PAMPs) that are unique to microbes by Pattern Recognition Receptors (PRRs) on the surface of phagocytes (Figure 1-2) (Campuzano and Wormley, 2018). Components of *C. neoformans* cell wall, such as β-glucan, mannan and chitin, and components of the capsule, such as glucuronoxylomannan (GXM), serve as PAMPs (May et al., 2016). Most *C. neoformans* PAMPs are on the cell wall, which presents a challenge for host immune cells since they are masked by the capsule polysaccharide (Bloom et al., 2019; Cross and Bancroft, 1995). However, there is evidence to suggest that the infectious *C. neoformans*

particle from the soil is nonencapsulated and encapsulation occurs while in lung tissue (Farhi et al., 1970). This suggests that there may be a period during the early stages of infection where the cell wall components of *C. neoformans* are exposed allowing for detection by host PRRs.

With regards to host PRRs, it is notable that not all PRRs are considered bona fide phagocytic receptors, meaning that they are not directly responsible for the internalisation of microorganisms (Freeman and Grinstein, 2014). Instead, some are involved in priming and modulating phagocytosis and do not directly initiate particle engulfment (Freeman and Grinstein, 2014; Uribe-Querol and Rosales, 2020). One such receptor is the Toll-like Receptor (TLR) family which is able to recognise microbial ligands and initiate a signalling cascade that activates other receptors at the surface of the cell, such as phagocytic integrins, which are then responsible for pathogen engulfment (Freeman and Grinstein, 2014; Uribe-Querol and Rosales, 2020). Other PRRs include members of the C-type Lectin Receptor (CLR) family, NOD-like Receptor (NLR) family and Scavenger Receptor (SR) family. These are all examples of non-opsonic receptors; however, there also exists opsonic receptors such as Fcγ receptors (FcγR) and complement receptor 3 (CR3), which recognize the Fc portion of IgG antibody-coated targets and complement fragment iC3b coated targets, respectively (Lim et al., 2018; Saylor et al., 2010).

Following the recognition of a microbial ligand by PRRs, a receptor-specific signalling cascade is triggered that results in the remodelling of the actin cytoskeleton such that

the plasma membrane surrounds the pathogen and a phagosome is formed (Johnston and May, 2013; Pauwels et al., 2017). The phagosome then goes through three basic maturation steps where it interacts with early endosome, late endosome and lysosome, ultimately becoming a phagolysosome (Pauwels et al., 2017). These interactions result in the production of reactive oxygen species (ROS) and reactive nitrogen species (RNS), the acidification of the phagosome and finally the acquisition of a mixture of antimicrobial peptides and degradative enzymes from the lysosome thereby creating an environment that promotes microbial killing (Johnston and May, 2013). The phagocytosis of microbes by macrophages and subsequent phagosome maturation is usually protective to the host and leads to the degradation of the microbe. However, *C. neoformans* can survive and replicate within macrophages (Davis et al., 2015). Instead, neutrophils, dendritic cells and natural killer (NK) cells have a greater killing capacity than macrophages (Diamond et al., 1972; Miller and Kohl, 1983; Hole et al., 2012; Hidore et al., 1991). This is likely because macrophages require further stimulation by cytokines produced by adaptive immune cells to become fully fungicidal while neutrophils, NK cells and dendritic cells naturally have this ability (Kawakami et al., 1995; Voelz et al., 2009). For example, NK cell-mediated cytotoxicity is initiated by the detection of *C. neoformans* by the NK cell receptor NKp30 leading to NK cell-fungal conjugate formation (Li et al., 2013). NKp30 binding to cryptococci then activates PI3K and ERK1/2 signalling (Wiseman et al., 2007), ultimately leading to the release of perforin, a pore-forming protein that disrupts the cell membrane, ultimately killing the fungal cell (Ma et al., 2004).

Our understanding of macrophage response to *C. neoformans* infection is further complicated by the findings that macrophages can promote fungal growth and dissemination. Shao *et al.* (2005) showed that mice depleted of alveolar macrophages had decreased lung fungal burden at 3 days and 14 days post-infection compared to non-depleted cells. However, when rats were depleted of alveolar macrophages there was an increase in lung fungal burden (Shao et al., 2005). In a similar study by Kechichian et al. (2007), a T-cell and NK-cell immunodeficient mice model was depleted of alveolar macrophages and infected with a *C. neoformans* mutant lacking glucosylceramide (Δgcs1), which makes the fungi avirulent and unable to disseminate to the CNS. They found that with the depletion of alveolar macrophages, immunodeficient mice showed increased survival and decreased fungal spread to the CNS (Kechichian et al., 2007). Thus, macrophages may be hijacked to promote cryptococcal disease. The next section will expand on the macrophage response to *C. neoformans* infection.

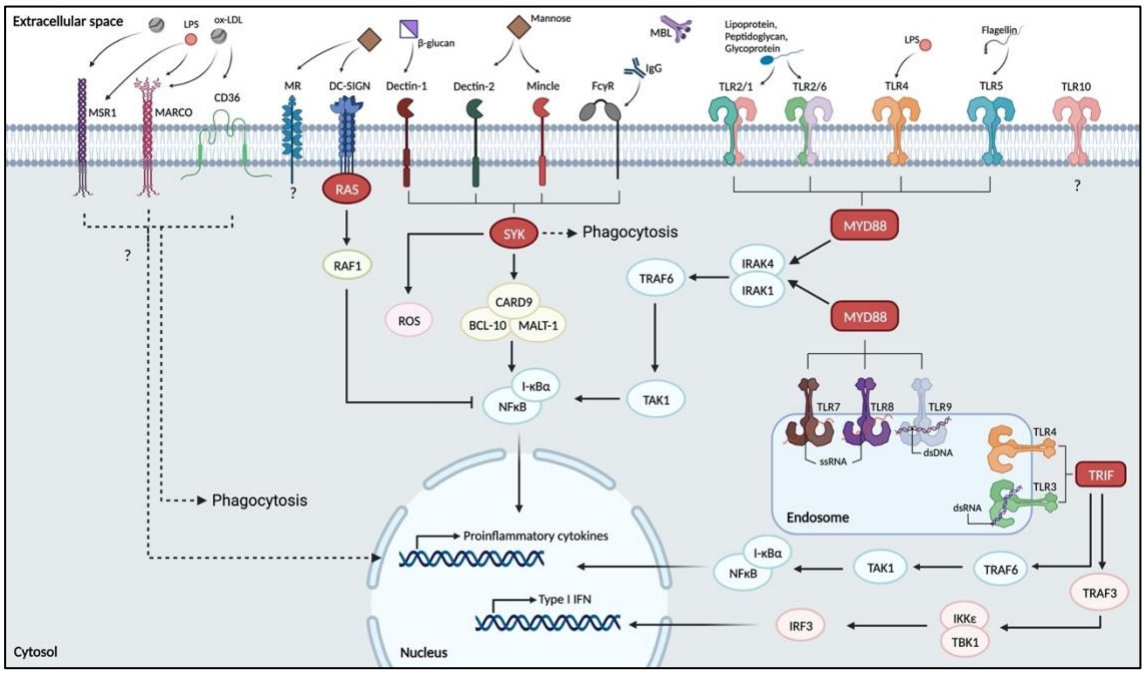

Figure 1-2: Pattern recognition receptors (PRRs) and their signalling pathways. The recognition of foreign particles is initiated by PRR binding to Pathogen Associated Molecular Patterns (PAMPs) unique to microbes. Toll-like receptors (TLRs) recognise a wide range of microbial ligands such as lipopolysaccharide (LPS), glycoproteins and nucleic acids. Ligand binding to a TLR activates a signalling cascade that leads to the transcription and secretion of proinflammatory cytokines or type I interferons. The C-type lectin receptor (CLR) family is composed of receptors such as Dectin-1, Dectin-2, Mannose Receptor (MR), dendritic cell-specific ICAM- 3-grabbing non-integrin (DC-SIGN), macrophage inducible C-type lectin (Mincle) and MBL, which recognise carbohydrate molecules on fungal cells. Ligand binding leads to the phosphorylation of CLRs by spleen tyrosine kinase (SYK) which then drives a signalling cascade involving the caspase recruitment containing protein 9 (CARD9)–B-cell lymphoma 10 (BCL10)–mucosa-associated lymphoid tissue lymphoma-translocation gene 1 (MALT1) complex. Members of the scavenger receptor family such as Macrophage Scavenger Receptor 1 (MSR1), MAcrophage Receptor with COllagenous domain (MARCO) and CD36 recognise a diverse range of ligands including oxidised low-density lipoprotein (ox-LDL) and LPS. Foreign agents are also recognised by molecules such as IgG and Mannose Binding Lectin (MBL) that bind and opsonise the pathogen promoting efficient host cell recognition and clearance through Fcγ Receptors and complement receptors, respectively. Figure created with BioRender.com.

1.2.2 Macrophage Response to *C. neoformans* infection

The ability of macrophages to successfully eliminate phagocytosed *C. neoformans* is influenced by the macrophage polarization state (Voelz et al., 2009; Zhang et al., 2009). The cytokines and inflammatory regulators present in the host microenvironment after infection polarise macrophages to display two main phenotypes: classically activated macrophages (M1) and alternatively activated macrophages (M2), which is further

subdivided into M2a, M2b and M2c (Campuzano and Wormley, 2018; Wager and Wormley, 2014). The M1 phenotype is induced by the signal transducer and activator of transcription 1 (STAT1)-dependent recognition of Interferon- γ (IFN-γ) and tumour necrosis factor- α (TNF- α) secreted by CD4+ T helper 1 (Th1) cells (Wager and Wormley, 2014; Leopold Wager et al., 2015). This Th1 and subsequent M1 responses are known to promote fungal clearance by increasing the production of ROS and RNS and the expression of cytokines such as Interleukin 12 (IL12), IL6 and TNFα (Martinez and Gordon, 2014). The markers of M1 phenotype include inducible nitric oxide synthase (iNOS), C-X-C Motif Chemokine Ligand 9 (CXCL9), CXCL10, CXCL11, IL-12 and suppressor of cytokine signalling 3 (SOCS3) (Wager and Wormley, 2014). The iNOS enzyme acts on L-arginine to produce nitric oxide (NO), a RNS involved in creating an antimicrobial environment in the phagosome (Wager and Wormley, 2014).

On the other hand, M2a macrophages are activated by the secretion of the anti-inflammatory cytokines IL-4 and IL-13 by Th2 cells leading to a phenotype that is associated with increased intracellular fungal survival and proliferation and exacerbates disease (Campuzano and Wormley, 2018; Wager and Wormley, 2014; Voelz et al., 2009). The most common markers of the M2a response are arginase-1 (Arg-1), found in inflammatory zone 1 (Fizz1), and CD206 (or Mannose receptor, MR) (Wager and Wormley, 2014). Arg1 competes with iNOS for interaction with L-arginine. Arg1 acts on L-arginine to produce L-ornithine and urea which are more relevant to tissue repair and not infection control (Rath et al., 2014). Many groups have reported a Th2/M2 bias following murine infection with *C. neoformans*, presenting Th2/M2 polarisation as a *C.*

neoformans-mediated immune evasion strategy (Jain et al., 2009; Zhang et al., 2009; Abe et al., 2000; Müller et al., 2007).

Before the establishment of the cytokine profile that results in a Th1/M1 bias or Th2/M2 bias, there is the initial recognition of a microbial ligand by host PRRs. Not only do PAMP-PRR interactions lead to phagocytosis, but they also activate signalling cascades that result in the activation of transcription factors and the expression and secretion of pro- and anti-inflammatory cytokines. In the next section, I will highlight the major macrophage PRRs that have been studied in the context of *C. neoformans* infection.

1.2.3 *C. neoformans* and Toll-like Receptors

TLRs are a family of transmembrane PRRs expressed by various immune cells including macrophages (Vidya et al., 2018). There are 10 functional TLRs in humans (TLR1-10) (Figure 1-3). TLR1, 2, 4, 5, 6 and 10 are embedded in the plasma membrane where they recognize components of microbial cell surface, meanwhile, TLR3, 7, 8 and 9 are found on the endosomal membrane and mainly recognize nucleic acid (Skevaki et al., 2015). TLRs have a Toll/Interleukin 1 Receptor (TIR) domain in their cytoplasmic end which interacts with intracellular signalling proteins. Meanwhile, the extracellular domain of TLRs contain leucine-rich repeats (LRR) and is responsible for ligand binding (Gay et al., 2014).

The recognition of PAMPs by TLRs activate a signal transduction pathway mediated by the adaptor proteins Myeloid differentiation primary response 88 (MyD88) or TIR-

domain-containing adapter-inducing interferon-β (TRIF) (Garelnabi and May, 2018; Kawasaki and Kawai, 2014). The MyD88-dependent pathway is used by all TLRs except TLR3 (Leopold Wager et al., 2016). MyD88 is recruited to TLRs by a sorting adaptor called TIR domain-containing adaptor molecule (TIRAP), which is associated with both plasma membrane and endosomal TLRs (Kawasaki and Kawai, 2014). On the other hand, TRIF is only involved in TLR3 and TLR4 signalling. TRIF related adaptor molecule (TRAM) is a sorting adaptor protein that associates with TLR4 and transmits TLR4 signalling to TRIF (Kagan et al., 2008). However, TLR3 has been found to directly interact with TRIF (Kawasaki and Kawai, 2014). Activation of the adaptors leads to the formation of higher-order scaffolds called the 'Myddosome' and the 'Triffosome' composed of members of the IL-1R-associated kinase (IRAK) family and Tumor necrosis factor receptor-associated factors (TRAF) family respectively (Gay et al., 2014). The MyD88-dependent pathway and the TRIF-dependent pathway ultimately lead to the activation of the transcription factor Nuclear Factor κB (NF-κB) and the mitogen-activated protein kinase pathway (MAPK) (Kawasaki and Kawai, 2014). The TRIF pathway also leads to the activation of Interferon regulatory factor 3 (IRF3). These then act to activate the expression and secretion of proinflammatory cytokines (MyD88 and TRIF pathway) and Type I interferons (TRIF pathway) (Figure 1-3) (Campuzano and Wormley, 2018; Vidya et al., 2018; Garelnabi and May, 2018; Kawasaki and Kawai, 2014).

TLR signalling also leads to a conformational change in cell surface adhesion molecules called integrins (Freeman and Grinstein, 2014). Integrins are made up of combinations of one of 18 α- and one of 8 β-subunits to give 24 possible heterodimers. In their

inactivate state, integrins have a bent conformation that is incapable of binding ligands (Freeman and Grinstein, 2014). There are various inside-out signalling pathways that ultimately lead to integrin extension and exposure of the ligand binding site. TLR signalling acts through Rap GTPase to drive integrin extension and acts through Rac GTPase to promote membrane ruffling. Integrin then facilitates outside-in signalling to trigger actin polymerization and phagocytosis. On the other hand, ligand binding to TLR also results in the internalisation of the cell surface receptors through clathrin-mediated endocytosis (Gay et al., 2014). Hence the balance between receptor internalization and trafficking of newly synthesized receptors to the plasma membrane is important for sustained signal transduction (Gay et al., 2014). In the context of *C. neoformans* infection, TLR2, TLR4 and TLR9 have gained significant attention (Wager and Wormley, 2014).

TLR4 is most known for its role in recognising lipopolysaccharide (LPS) of Gram-negative bacteria (Chow et al., 1999), but is thought to also recognise fungal mannans (Tada et al., 2002) and GXM (Shoham et al., 2001). LPS-induced signalling begins with its recognition by extracellular LPS binding protein (LBP) (Park et al., 2009; Wright et al., 1990). This LPS-LBP complex allows for the transfer of LPS to CD14 protein anchored on the cell membrane. CD14 then facilitates the transfer of LPS to MD2 which is already in complex with a TLR4 monomer (Park et al., 2009). LPS binding is followed by the dimerization of two TLR4/MD2 complexes which then induces signalling via the Myd88-dependent pathway (Tsukamoto et al., 2018). TLR4-MD2 dimer on the plasma membrane is then internalised into an endosome and dissociates from MyD88 which then allows for TRIF-dependent signalling (Kagan et al., 2008). The endocytosis of TLR4

dimer is necessary for TRIF-mediated activation of Interferon Regulatory Factor 3 (IRF3), a transcription factor that promotes the expression of type 1 Interferons (Kagan et al., 2008). TNF Receptor Associated Factor 3 (TRAF3) is involved in both MyD88- and TRIF-dependent signalling (Häcker et al., 2006). However, only intracellular TLRs induce TRAF3 mediated type 1 interferon production (Häcker et al., 2006). It was shown that the re-localization of TRAF3 to the plasma membrane led to the production of type I interferons by TLR2 signalling, which does not normally produce it since its signalling is mediated by the MyD88-dependent pathway (Kagan et al., 2008). Thus, the spatial distribution of TLRs is an important regulator of innate immune response.

To investigate the contribution of TLR4 during *C. neoformans* infection, Shoham et al. (2001) showed that Chinese hamster ovary (CHO) cells transfected with both TLR4 and CD14 were able to bind *C. neoformans* GXM and promote nuclear NF-κB translocation, thereby suggesting that TLR4 and CD14 are PRRs for *C. neoformans* GXM (Table 1.1) (Shoham et al., 2001). This finding was supported by a later study that showed that TLR4 and CD14 were involved in the uptake of GXM by human monocyte-derived macrophages (Monari et al., 2005). Adding onto the two studies that demonstrated a role for TLR4 and CD14 in GXM-binding (Monari et al., 2005; Shoham et al., 2001), a study that sought to explore the role of PRRs in GXM clearance *in vivo* found that *Tlr4*$^{-/-}$ and *Cd14*$^{-/-}$ mice injected intravenously with GXM had decreased serum GXM clearance compared to wildtype mice over 8 days (Yauch et al., 2005). However, the difference between wildtype and knockout mice was relatively modest suggesting that there are likely other receptors involved. Having demonstrated the involvement of TLR4 as a *C.*

neoformans PRRs, the next logical question is whether this receptor is involved in host defence against infection. The first study to explore this question was carried out by Yauch et al. (2004). In their study, TLR4 mutant mice were infected intranasally or intravenously with *C. neoformans* and they found no difference in survival between wildtype and TLR4 mutant mice (Yauch et al., 2004). They also observed that compared to wildtype mice, *Cd14*$^{-/-}$ mice had decreased survival following intravenous but not intranasal infection (Yauch et al., 2004). A similar study found no difference in TNFα expression by macrophages isolated from wildtype and TLR4 mutant mice (Biondo et al., 2005). In another *in vivo* study, Nakamura et al. (2006), reported that TLR4 deficiency had no impact on pro-inflammatory cytokine production and lung fungal burden following intratracheal infection. They went on to show that the infection of HEK293 cells transfected with TLR4/MD2/CD14 did not result in NF-κB activation, leading to the conclusion that TLR4 is dispensable during anti-cryptococcal response (Nakamura et al., 2006). Finally, the stimulation of microglial cells with the TLR4 agonist, LPS, resulted in increased phagocytosis and killing of *C. neoformans* (Redlich et al., 2013). Taken together, it is evident that the research on the role of TLR4 is rather limited and inconsistent. There remains a need to decipher the mechanisms by which TLR4 impacts immune response to *C. neoformans*.

TLR2 forms heterodimers with TLR1 (TLR2/1) and TLR6 (TLR2/6) to recognize a wide range of PAMPs including, bacterial lipopeptides, peptidoglycan of gram-positive bacteria, viral envelope glycoprotein, zymosan (a fungal cell wall extract particle composed mainly of β-glucan, but also mannans, chitin, protein and lipids) (Kawai and

Akira, 2010; Underhill et al., 1999) and GXM (Shoham et al., 2001). Similar to TLR4, the role of TLR2 during anticryptococcal immune response remains inconclusive. According to Yauch et al. (2004), *Tlr2*$^{-/-}$ mice had reduced survival after intranasal infection *C. neoformans*, but not after intravenous infection. However, there was no significant difference in lung fungal burden and proinflammatory cytokine expression between *Tlr2*$^{-/-}$ mice and wildtype mice infected intranasally. Similarly, Nakamura et al. (2006) found no significant difference in pro-inflammatory cytokine production and lung fungal clearance between wildtype and *Tlr2*$^{-/-}$ mice. Both studies suggest that TLR2, at least on its own, is dispensable during host response to C*. neoformans* infection. By contrast, Biondo et al. (2005) reported that *Tlr2*$^{-/-}$ mice had a significantly higher lung, brain and spleen fungal burden, lower cytokine expression and decreased survival compared to wildtype mice after intraperitoneal infection. TLR2 has also been shown to bind GXM and activate NF-κB (Shoham et al., 2001; Fonseca et al., 2010); however, it was only marginally involved in GXM clearance *in vivo* (Yauch et al., 2005).

Once a pathogen is internalised and degraded, microbial nucleic acid can be detected by endosomal TLRs. TLR9 is one such receptor and is known for its role in the recognition of unmethylated CpG DNA. In *C. neoformans* infection, TLR9 is thought to act specifically in dendritic cells (Wager and Wormley, 2014). It has been shown that TLR9 is necessary for the activation of bone marrow-derived myeloid dendritic cells (BM-DCs) (Nakamura et al., 2008). *C. neoformans* infection of *Tlr9*$^{-/-}$ mice impaired fungal clearance and resulted in increased production of IL-4 and M2 response markers (Zhang et al., 2010). There was also decreased recruitment of CD4+, CD8+ and CD19+ lymphocytes to the site

of infection suggesting that TLR9 signalling contributes to the adaptive immune response (Zhang et al., 2010). Further investigation into the role of TLR9 in host response to *C. neoformans* revealed that the impaired fungal clearance in *Tlr9*$^{-/-}$ mice was caused by a lack of dendritic cell activation via chemokine (C-C motif) ligand 7 (CCL7) induction, which limited the recruitment of other immune cells needed to clear the infection (Qiu et al., 2012).

TLR3 is another endosomal PRRs; however, very little is known about the role of this receptor during *C. neoformans* infection. This is likely because TLR3 is the receptor for dsRNA; therefore, there is no obvious TLR3 ligand in *C. neoformans* (Gay et al., 2014). Interestingly, TLR3 has been shown to recognise dsRNA in *Aspergillus fumigatus* conidia leading to type I interferon (IFN) response (Beisswenger et al., 2012). The source of dsRNA in *A. fumigatus* conidia and, potentially, in other fungi may come from secondary structures on fungal mRNA, since it has been shown that endogenous mRNA can serve as a ligand for TLR3 (Karikó et al., 2004). Alternatively, dsRNA can come from infection of fungi with dsRNA mycoviruses, which have also been found to induce type 1 IFN response (Kinsella et al., 2022; Takahashi-Nakaguchi et al., 2020; Bhatti et al., 2011; Applen Clancey et al., 2020).

A few studies have explored the significance of the type 1 IFN response during *C. neoformans* infection. Using mice deficient in IFN α/β receptor 1 (IFNAR1), it has been shown that the type 1 IFN response is involved in the control of *C. neoformans* infection (Biondo et al., 2005; Sionov et al., 2015). Biondo et al. (2005) observed that *Ifnar1*$^{-/-}$ mice

had increased expression of Th2 cytokines, such as IL4, IL10 and IL13, decreased expression of Th1 cytokines such as TNFα, IFNγ and iNOS, and increased lung and brain fungal burden compared to wildtype mice. Meanwhile, Sionov et al. (2015) found that the treatment of *C. neoformans* infected mice with pICLC, a dsRNA mimic, within 72 hours after infection, improved mice survival. The improved survival was dependent on the type 1 IFN response since treatment of *Ifnar1*$^{-/-}$ mice with pICLC did not improve survival. Interestingly, they also found that pICLC-mediated protection occurred through the cytosolic dsRNA receptor melanoma differentiation-associated protein-5 (MDA5) and not TLR3 (Sionov et al., 2015). Contrary to these studies, Sato et al. (2015) reported increased survival and increased Th1 response in *Ifnar1*$^{-/-}$ mice. More recently, it has been shown that the stimulation of macrophages with IFNα and IFNβ increases the rate of vomocytosis; however, it remains unclear whether this phenomenon is beneficial or detrimental to the host (Seoane et al., 2020). Seeing as pICLC-mediated protection was time-dependent (Sionov et al., 2015), and that IFNα and IFNβ expression peaked at day 1 and day 3 post-infection (Sato et al., 2015), the type 1 IFN response may be protective during the early stages of infection but hijacked by the fungi during the later stages where it can promote vomocytosis in the CNS (Seoane et al., 2020).

Although there are discrepancies in the significance of individual TLRs during *C. neoformans* infection, studies using MyD88 deficient mice consistently show that this adaptor molecule plays a major role in anti-fungal immune response (Biondo et al., 2005; Yauch et al., 2004), thereby implicating the upstream TLRs in host response. The precise upstream TLR involved remains unclear; though there may be a combination of

receptors involved and not a specific receptor with a large effect. Attempts to uncover the mechanisms by which individual TLRs contribute to anti-cryptococcal immune response have revealed contradictory results. These contradictions may be due to differences in experimental design. For example, some studies utilise an intravenous infection route, while others utilise an intranasal or intratracheal or intraperitoneal mode of infection (Table 1.1). In fact, one study found that TLR2 was dispensable following intravenous infection, but significant during intranasal infection (Yauch et al., 2004). This demonstrates that the chosen route of infection can significantly alter experiential results. Additionally, there is variation in the dose of cryptococcus used during infection, with inoculum ranging from 1×10^4 to 1×10^6. It is possible that the dose of cryptococci used influences the effect of receptor deficiencies, thereby leading to conflicting results. Finally, the genetic background of the mice could also contribute to the discrepancies. It is recognised that BALB/c mice are more proinflammatory and capable of clearing pulmonary *C. neoformans* infection, while C57BL/6 mice are intrinsically more susceptible to *C. neoformans* and produce the Th2 response (Zaragoza et al., 2007; Huffnagle et al., 1998). There are many confounding variables when using mice models of infection; therefore, it may be beneficial to utilise an *in vitro* model of infection instead to gain foundational understanding.

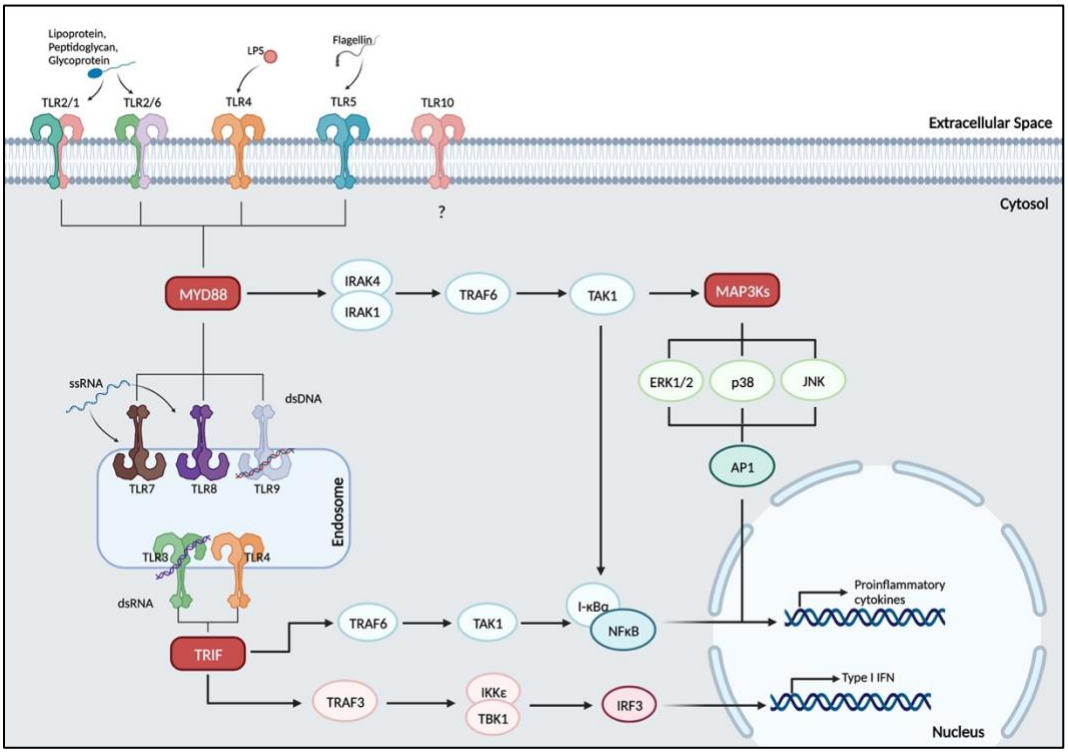

Figure 1-3: Toll-like Receptor (TLR) Signalling Pathway. The recognition of microbial ligands by TLRs activates a signalling cascade that is mediated by the adaptor proteins Myeloid Differentiation primary response 88 (MyD88) or TIR-domain-containing adapter-inducing interferon-β (TRIF). The signalling cascade ultimately leads to the activation of transcription factors nuclear factor kappa B (NF-κB) and interferon regulator factor 3 (IRF3) that drive the expression of proinflammatory cytokines and Type I interferons, respectively. MyD88 and TRIF signalling also lead to the activation of the mitogen-activated protein kinase (MAPK) pathway via transforming growth factor-β-activated kinase 1 (TAK1) activity. Figure created with Biorender.com.

1.2.4 *C. neoformans* and C-type Lectin Receptors

Another class of PRRs involved in the recognition of foreign agents are CLRs. CLRs recognise carbohydrate moieties and are highly expressed at the surface of macrophages (Figure 1-2) (Taylor et al., 2002; Freeman and Grinstein, 2014). Dectin-1 is a bona fide phagocytic receptor that recognises β-1,3-glucans and β-1,6-glucans as well as zymosan (Brown, 2006; Brown and Gordon, 2001). Ligand binding leads to the activation of a signalling pathway that involves spleen tyrosine kinase (SYK) and the caspase recruitment containing protein 9 (CARD9)–B-cell lymphoma 10 (BCL10)–

mucosa-associated lymphoid tissue lymphoma-translocation gene 1 (MALT1) complex (Campuzano and Wormley, 2018). This then leads to the activation of NF-κB and the production of ROS.

Chemically inhibiting SYK and Dectin-1 activity in the J774.A1 macrophage cell line and in primary human macrophages has been shown to reduce the phagocytosis of non-opsonised *C. neoformans*, but not *C. gattii* (Table 1.1) (Lim et al., 2018). However, in an *in vivo* model, it was found that Dectin-1 KO mice and wildtype mice had a similar infection course and cytokine production, implying that Dectin-1 is not necessary for effective anti-cryptococcal immune response (Nakamura et al., 2007). In a study by Walsh *et al.* (2017), Chinese Hamster Ovary (CHO) cells expressing Dectin-1 or an empty vector were challenged with *C. neoformans* and none of the cell lines showed significant binding of *C. neoformans* spores or yeast cells compared to the positive control. Even macrophages derived from *Dectin1*$^{-/-}$ mice did not show a significant difference in association with *C. neoformans* spores or yeast (Walsh et al., 2017). Phagocytosis of spores by alveolar macrophages was also investigated and they observed a modest, but statistically significant decrease in phagocytosis in *Dectin1*$^{-/-}$ mice compared to wildtype mice. However, when these mice were infected with *C. neoformans* spores intranasally there was no significant difference in mice survival rate compared to wildtype. The result of this cell-based assay is very different from the significant reduction in phagocytosis seen when Dectin-1 receptors are blocked using neutralizing antibodies or excess soluble ligands, thus revealing the impact of experimental design on results. Although Dectin-1 is recognised as the major PRR for the detection of the fungi *Candida albicans*

(Gantner et al., 2005; Taylor et al., 2007), most of the data presented above suggest that Dectin-1 is dispensable during host response to *C. neoformans*. This could be due to the masking of *C. neoformans* cell wall β-glucans by the capsule (Bloom et al., 2019).

The role of other CLRs during *C. neoformans* infection has also been explored. Dectin-2 has been shown to recognize α-mannans on fungal cell wall (Saijo et al., 2010), while Dectin-3 is thought to recognize GXM on *C. neoformans* capsule (Huang et al., 2018). PAMP recognition triggers the same SYK-dependent signalling pathway used by Dectin-1. However, unlike Dectin-1, Dectin-2 and Dectin-3 form heterodimeric complexes with FcγR because they lack the immunoreceptor tyrosine-based activation motif (ITAM) in their cytoplasmic tail that is needed for SYK-dependent signalling and it is thought that this interaction requires Mincle (Campuzano and Wormley, 2018; Li and Underhill, 2020). It has been shown that a CHO cell line co-expressing Dectin-2 and FcγR, binds *C. neoformans* spores and activates the signalling cascade; however, the signal was 5 times lower than that seen for other fungi (Walsh et al., 2017). *Dectin2*$^{-/-}$ alveolar macrophage had a modest decrease in phagocytosis, but it was not statistically significant. Additionally, *Dectin-2*$^{-/-}$ mice infected with *C. neoformans* spores intranasally showed no significant difference in mice survival rate compared to wildtype (Walsh et al., 2017). This implies that Dectin-2 is not a major PRR involved in the detection of *C. neoformans* Surprisingly, even the deletion of the downstream adaptor protein, CARD9, did not seem to affect binding and phagocytosis (Walsh et al., 2017), although early studies found that CARD9 KO mice had increased susceptibility to *C. neoformans* infection and reduced IFN-γ expression (Yamamoto et al., 2014). A recent study found that Dectin-2 and CARD9

were required for the phagocytosis of acapsular *C. neoformans* by bone marrow-derived dendritic cells (Kitai et al., 2021). However, when *Dectin-2*$^{-/-}$ and *Card9*$^{-/-}$ cells were infected with capsular *C. neoformans*, there was no difference in phagocytosis between knockout and wildtype cells (Kitai et al., 2021), supporting the hypothesis the capsular polysaccharide masks cell wall components of the fungi limiting the contribution of CLRs during host response to *C. neoformans*. *Dectin-3*$^{-/-}$ mice were not more susceptible to *C. neoformans* infection and did not show any difference in cytokine production compared to wildtype mice, demonstrating that this receptor is not involved in host response to infection (Campuzano et al., 2017).

Another important CLR is Mannose Receptor C-Type 1 (MRC1), encoding the mannose receptor (MR) protein that recognizes oligosaccharides terminating in N-Acetylglucosamine (GlcNAc) (e.g. chitin), fucose, and mannose (van de Veerdonk et al., 2008; Rodman et al., 1978). MR mediates receptor-mediated endocytosis and phagocytosis by macrophages (Porcaro et al., 2003). MR is important for the uptake of fungal pathogens such as *C. albicans* (Porcaro et al., 2003) and *Pneumocystis carinii* (Ezekowitz et al., 1991). Stimulation with *C. albicans*-derived chitin leads to the production of anti-inflammatory IL-10 and pro-inflammatory TNFα and IL-6 by human peripheral blood mononuclear cells (hPBMCs) (Wagener et al., 2014). This chitin-induced IL-10 production was found to be TLR9 dependent (Wagener et al., 2014). The precise role of MR during *C. neoformans* infection remains unclear. One study found that pulmonary infection of *Mrc1*$^{-/-}$ mice with *C. neoformans* resulted in a much faster time to death compared to wildtype mice (Dan et al., 2008). *Mrc1*$^{-/-}$ mice also had a

higher fungal burden 4 weeks post-infection, but the uptake of cryptococcal mannoproteins was similar. Meanwhile, another study reported that macrophages derived from *Mrc1*$^{-/-}$ mice did not show any significant difference in binding and phagocytosis of *C. neoformans* spores and yeast form (Walsh et al., 2017). When J774 macrophages were treated with soluble mannan, which serves as a competitive inhibitor of MR, the phagocytosis of *C. neoformans* was not affected (Lim et al., 2018). There was also no difference in the level of phagocytosis using macrophages derived from *Mrc1*$^{-/-}$ mice; however, human macrophages treated with mannan showed a significant 80% reduction in phagocytosis compared to untreated cells (Lim et al., 2018).

There exist some contradictions in the role of CLRs during *C. neoformans* infection; however, it appears that many studies find no involvement or very minimal involvement of CLR in anti-cryptococcal immune response.

1.2.5 *C. neoformans* and Scavenger Receptors

Scavenger receptors (SRs) are phagocytic receptors found on the plasma membrane of various immune cells including macrophages (Abdul Zani et al., 2015) (Figure 1-2). They were first found to bind modified low-density lipoproteins (LDL), but are now known to recognize a wide range of host and microbial ligands such as apoptotic cells, phospholipids, proteoglycan, LPS, and fungal β-glucans (Abdul Zani et al., 2015; Canton et al., 2013; Murshid et al., 2016). Scavenger receptors have been classified into 10 families, called Class A to J (PrabhuDas et al., 2014). A few SRs have been found to play a role in immune response to *C. neoformans*.

Macrophage receptor with collagenous structure (MARCO) is found extensively on alveolar macrophages (Bin et al., 2003). It has also been shown that compared to wild-type mice, *Marco*$^{-/-}$ mice infected with *C. neoformans* had a significantly higher lung fungal burden at 7 dpi, but not 21 dpi, suggesting that MARCO is important during the afferent (early/innate) phase of infection (Xu et al., 2017b). In wildtype mice, there is a significant increase in MARCO expression following *C. neoformans* infection, implying that it has an important role in controlling the infection (Xu et al., 2017b). MARCO was also found to be required for the phagocytosis of *C. neoformans* by alveolar macrophages and monocyte-derived dendritic cells (Xu et al., 2017b). Interestingly, a later study by the same group investigating the role of MARCO during the efferent/ adaptive phase of *C. neoformans* infection found that *Marco*$^{-/-}$ mice had better fungal clearance in the lungs, decreased CNS dissemination, and decreased Th2 cytokines (Xu et al., 2017a). Thus, it is possible that the initial protective nature of MARCO during the innate immune response is hijacked by *C. neoformans* leading to a non-protective response that promotes fungal persistence and dissemination (Table 1.1).

Macrophage scavenger receptor 1 (MSR1), also known as scavenger receptor A1 (SR-A1), is known to recognize a range of ligands including LPS and heat shock proteins; however, the cryptococcal ligand remains unknown (Heung, 2017; Qiu et al., 2013). Interestingly, during *C. neoformans* infection, it was found that SR-A can be hijacked by the fungi to promote the deleterious Th2 response (Qiu et al., 2013). *Msr1*$^{-/-}$ mice infected with *C. neoformans* had reduced fungal burden 3 weeks post-infection (efferent

phase) compared to wildtype mice. The enhanced fungal clearance in *Msr1*$^{-/-}$ mice correlated with decreased levels of IL-4 and IL-13 and increased presentation of classical macrophage activation (Qiu et al., 2013). Thus, in the case of *C. neoformans* infection, *Msr1*$^{-/-}$ seems to play a detrimental role.

The scavenger receptors CD36 and scavenger receptor expressed by endothelial cells-I (SREC-1) (also known as SCARF1) were shown to recognize and phagocytose *C. neoformans* in a β-glucan-dependent manner using CHO cells transfected with CD36 and SCARF1 (Means et al., 2009). They were also found to activate a protective immune response against *C. neoformans* in *Caenorhabditis elegans* and mice *in vivo* (Means et al., 2009). Moreover, SREC-1 and CD36 cooperated with TLR2, but not TLR4 and TLR9 for optimal activation of immune response following infection (Means et al., 2009).

Most SRs, except SREC1 and SREC2, have very short cytoplasmic tails that lack any discernible signalling domains (Canton et al., 2013). As a result, these receptors cannot induce an inflammatory response on their own even though they have been implicated in a range of inflammatory disorders such as Alzheimer's disease (Mukhopadhyay et al., 2011). Hence it is thought that they act as part of multimolecular signalling complexes or through interactions with other PRRs such as TLRs. Crosstalk between SRs and TLRs will be discussed in Chapter 1.2.8. It is also unclear how SRs mediate phagocytosis; however, it has been demonstrated that SR-mediated phagocytosis is dependent on actin polymerisation, functional microtubule, protein kinase C (PKC), protein tyrosine kinase, c-Jun N-terminal kinases (JNKs), extracellular signal-regulated kinase (ERK) and

phosphoinositide 3-kinase (PI3K) (Sulahian et al., 2008). Whether or not SRs directly interact with these proteins remains unknown.

Table 1.1: Non-opsonic Pattern Recognition Receptors and their role during host response to *C. neoformans* infection.

PRR	Model System	Result	Reference
TLR4	CHO cells	CHO cells transfected with both TLR4 and CD14 were stimulated following challenge with *C. neoformans* GXM, as measured by NF-κB translocation.	(Shoham et al., 2001)
	C3H/HeJ Mice (TLR4 mutant)	Mortality rate was similar between wildtype and TLR4 mutant mice following intravenous or intranasal infection with *C. neoformans*.	(Yauch et al., 2004)
		There was no significant difference in TNFα production and mice survival compared to wildtype mice (intraperitoneal infection).	(Biondo et al., 2005)
	Tlr4$^{-/-}$ Mice	*Tlr4*$^{-/-}$ mice injected intravenously with GXM showed decreased serum GXM clearance compared to wildtype mice.	(Yauch et al., 2005)
		There was no significant difference in pro-inflammatory cytokine production and lung fungal clearance between wildtype and *Tlr4*$^{-/-}$ mice. Moreover, HEK293 cells expressing TLR4, MD2 and CD14 were not active in response to *C. neoformans challenge* (intra-tracheal infection).	(Nakamura et al., 2006)
	Microglial cells from WT and *Myd88*$^{-/-}$ mice	Microglial cells treated with TLR4 agonist (LPS) showed increased phagocytosis and killing of *C. neoformans*. This increase required MyD88 signalling	(Redlich et al., 2013)
TLR2	CHO cells	CHO cells transfected with both TLR2 and CD14 were not stimulated by challenge with *C. neoformans* GXM.	(Shoham et al., 2001)

	Tlr2$^{-/-}$	*Tlr2*$^{-/-}$ mice had a significantly higher fungal burden, lower cytokine expression and decreased survival compared to wildtype mice after intraperitoneal infection.	(Biondo et al., 2005)
		Tlr2$^{-/-}$ mice infected intravenously with GXM did not show significant difference in serum GXM clearance compared to wildtype mice.	(Yauch et al., 2005)
		There was no significant difference in pro-inflammatory cytokine production and lung fungal clearance between wildtype and *Tlr2*$^{-/-}$ mice. Moreover, HEK293 cells expressing TLR2 and Dectin-1 were not active in response to *C. neoformans* challenge (intra-tracheal infection).	(Nakamura et al., 2006)
		Tlr2$^{-/-}$ mice had increased mortality after intranasal infection (10^6 cells) with *C. neoformans*, but not after intravenous (10^4 cells) infection. However, there was no significant difference in lung fungal burden and proinflammatory cytokine levels between *TLR2*$^{-/-}$ mice and wildtype mice infected intranasally.	(Yauch et al., 2004)
	HEK293A cells	HEK293A cells transfected with TLR2/1 and TLR2/6 heterodimers showed dose-dependent activation of an NF-κB reporter construct in response to GXM. Meanwhile cells transfected with an empty vector were unresponsive.	(Fonseca et al., 2010)
	Microglial cells from WT and *Myd88*$^{-/-}$ mice	Microglial cells stimulated with TLR1/2 agonist (Pam3CSK4) showed increased phagocytosis and killing of *C. neoformans*. This agonist-mediated increase required MyD88 signalling.	(Redlich et al., 2013)

TLR9	*Tlr9*$^{-/-}$ Mice	*Tlr9*$^{-/-}$ mice infected intranasally with *C. neoformans* showed reduced survival compared to WT mice. However, there was no difference in fungal burden in the lungs, brain or spleen. There was also no difference in pro inflammatory cytokine concentration.	(Wang et al., 2011)
		TLR9 is necessary for the activation of bone-marrow derived myeloid dendritic cells (BM-DCs) by cryptococcal DNA.	(Nakamura et al., 2008)
		TLR9 deletion impairs pulmonary fungal clearance during the adaptive immune phase.	(Zhang et al., 2010)
		TLR9 inhibition compromised the accumulation and activation of CD11b+ dendritic cells, CD4+ and CD8+ T cells, IFNg and the CCR2 chemokines CCL7 and CCL12. All of which are important for the development of protective immunity.	(Qiu et al., 2012)
	Microglial cells from WT and *Myd88*$^{-/-}$ mice	Microglial cells stimulated with TLR9 agonist (CpG ODN) showed increased phagocytosis and killing of *C.neoformans*. This agonist-mediated increase required MyD88 signalling.	(Redlich et al., 2013)
	WT mice intranasally immunized with the TLR9 agonists, CpG ODN	Mice intranasally immunized with CpG ODN before infection with Cn showed reduced pulmonary inflammation and reduced lung fungal burden. In vitro, marophages pretreated with CpG ODN alone had an elevated IL-12, TNFα and CCL2.	(Edwards et al., 2005)
MyD88	*Myd88*$^{-/-}$ Mice	Compared with wild-type C57BL/6 mice, *Myd88*$^{-/-}$ mice had significantly reduced survival, increased lung fungal burden, and impaired GXM clearance following intranasal and intravenous infection with *C. neoformans*.	(Yauch et al., 2004)

		Myd88$^{-/-}$ mice had decreases survival, increased brain, lung and spleen fungal burden, and decrease proinflammatory cytokine production compared to wildtype mice after intraperitoneal infection.	(Biondo et al., 2005)
Dectin-1	Chemical inhibiton of Dectin-1 in J774A.1 macrophages	Dectin-1 inhibition results in decreased phagocytosis of non-opsonsied *C. neoformans*	(Lim et al., 2018)
	Dectin-1$^{-/-}$ Mice	There was no difference between wildtype and *Dectin1*$^{-/-}$ mice infected intratracheally and intravenously with *C. neoformans*.	(Nakamura et al., 2007)
	CHO cells and *Dectin1*$^{-/-}$ mice	Chinese Hamster Ovary (CHO) cells expressing Dectin-1 were unable to bind *C. neoformans* spores. Similarly, Dectin1$^{-/-}$ mice infected with C*. neoformans* spores showed no difference in survival.	(Walsh et al., 2017)
Dectin-2	CHO cells and *Dectin2*$^{-/-}$ mice	CHO cell line co-expressing Dectin-2 and FcγR binds *C. neoformans* spores and activates downstream signalling. However, *Dectin2*$^{-/-}$ mice infected with *C. neoformans* spores intranasally showed no significant difference in mice survival rate compared to wildtype	(Walsh et al., 2017)
	BMDC from *Dectin2*$^{-/-}$ miice	Dectin-2 is required for the phagocytosis of acapsular, but not capsular, *C. neoformans* by bone marrow derived dendritic cells	(Kitai et al., 2021)
Dectin-3	*Dectin3*$^{-/-}$ Mice	Dectin-3 is dispensible during mice resposne to infection with *C. neoformans*.	(Campuzano et al., 2017)
Mannose Receptor	*Mrc1*$^{-/-}$ Mice	*Mrc1*$^{-/-}$ mice infected with *C. neoformans* had increased mortality and increased lung fungal burden compared to wildtype mice	(Dan et al., 2008)
	Alveolar macrophage from *Mrc1*$^{-/-}$ mice	*Mrc1*$^{-/-}$ macrophages showed no difference in binding and phagocytosis of *C. neoformans* spores cmopared to wildtype macropages.	(Walsh et al., 2017)

	J774A.1 macropahges treated with soluble mannan	MR is dispensible in the phagocytosis of non-opsonised *C. neoformans.*	(Lim et al., 2018)
MARCO	*Marco*$^{-/-}$ mice	MARCO is protective against *C. neoformans* infection during the innate phase of infection. But is hijacked by the fungi during the adaptive phase of the immune response.	(Xu et al., 2017b, 2017a)
MSR1 (aka SR-A1)	*Msr1*$^{-/-}$ mice	*Msr1*$^{-/-}$ mice infected with *C. neoformans* had reduced fungal burden, decreased levels of IL-4 and IL13 and increased presentation of classical macrophage activation compared to wildtype mice.	(Qiu et al., 2013)
CD36	CHO cells and macrophages from *Cd36*$^{-/-}$ mice	CD36 expression was needed for the binding and phagocytosis of *C. neoformnas.*	(Means et al., 2009)
SREC-1 (aka SCARF1)	CHO cells	CHO cells transfected with SREC-1 were able to bind and phagcytose *C. neoformans*	(Means et al., 2009)

PRR: Pattern Recognition Receptor; TLR: Toll-like Receptor; CHO: Chinese Hamster Ovary; HEK293: Human embryonic kidney 293; MyD88: Myeloid differentiation primary response 88; BMDC: Bone marrow derived dendritic cells; MRC1: Mannose Receptor C-Type 1; MR: Mannose Receptor; MSR1: Macrophage Scavenger Receptor 1; SR-A1: Scavenger receptor A1; MARCO: MAcrophage Receptor with COllagenous structure; SREC-1: Scavenger receptor expressed by endothelial cells.

1.2.6 *C. neoformans* and Opsonic Receptors

It is proposed that the initial phagocytosis of *C. neoformans* cells in the lungs is through the various non-opsonic PRRs mentioned above since the environment in lung alveoli is deficient in serum opsonins (Lim et al., 2018; Mitchell and Perfect, 1995). However, in the circulatory system, uptake usually involves opsonisation (coating) with antibodies and complement proteins in the serum (Lim et al., 2018). The most common opsonic receptors involved in phagocytosis are Fcγ receptors (FcγR), which recognize IgG antibody-coated cells, and complement receptor type 3 (CR3), which recognizes

complement protein-coated cells (Figure 1-2) (Lim et al., 2018; Saylor et al., 2010). The capsule of *C. neoformans* masks various cell wall components recognized by non-opsonic receptors thereby resulting in inefficient uptake of *C. neoformans* yeast cells (Lim et al., 2018). Thus, pre-treatment of *C. neoformans* with IgG or complement proteins is a common practice in experimental procedures to promote efficient phagocytosis (Saylor et al., 2010; Hünniger and Kurzai, 2019).

FcγRs are found on the plasma membrane of immune cells such as macrophages, dendritic cells, neutrophils, T-cells and B-cells (Li et al., 2009). FcγRs recognize the Fc region of IgG molecules, which are the most common antibody class in the blood (Hargreaves et al., 2015; Stoop et al., 1969). Ligand recognition results in the phosphorylation of the Immunoreceptor Tyrosine-Based Activation motif (ITAM) found on the cytoplasmic tail of activating Fc receptor or the Immunoreceptor Tyrosine-Based Inhibitory motifs (ITIMs) on inhibitory Fc receptors (Lennartz and Drake, 2018; Getahun and Cambier, 2015). This then recruits SYK to activate downstream processes ultimately leading to phagocytosis, cytotoxicity and cytokine production and release (Hargreaves et al., 2015; Nimmerjahn and Ravetch, 2008). FcγRI, FcγRIIA, FcγRIIC and FcγRIII have an activatory function, while FcγRIIB is the only inhibitory receptor (Hargreaves et al., 2015). Thus, the balance of these receptors on the plasma membrane and the ratio of inhibitory to activatory receptor engagement is integral in triggering phagocytosis and achieving appropriate immune response (Nimmerjahn and Ravetch, 2008; Freeman and Grinstein, 2014).

Aside from inhibitory versus activatory classifications, FcγRs are also classified by their affinity to IgG. FcγRI (CD64) is the sole high-affinity receptor, meaning it effectively captures monomeric IgG molecules (Hargreaves et al., 2015). Meanwhile, FcγRIIA (CD32A), FcγRIIB (CD32B), FcγRIIC (CD32C), FcγRIIIA (CD16A) and FcγRIIIB (CD16B) are low-affinity receptors that require the engagement of multiple FcγR-Fc region immune complexes (Hargreaves et al., 2015). Low-affinity receptors promote cell activation, phagocytosis and antibody-dependent cellular cytotoxicity (Bournazos et al., 2016; Willcocks et al., 2009). While high-affinity receptors have been implicated in MHC Class II antigen presentation (Brandsma et al., 2017; Bournazos et al., 2016). Among these, FcγRIIA is the best studied in macrophages and the most relevant in promoting efficient phagocytosis and pathogen killing (Hoepel et al., 2019; Mosser and Zhang, 2011). There are four IgG subclasses in humans (IgG1 to IgG4) and they exhibit variable binding affinity to the different FcγRs (Nimmerjahn and Ravetch, 2008). IgG2 is the dominant subclass directed against pathogens and its main receptor is FcγRIIA (Vogelpoel et al., 2015).

It has been shown that stimulation of FcγRs alone only results in moderate cytokine production. Instead, FcγRIIA acts in synergy with TLRs to promote the expression of proinflammatory cytokines such as TNFα, IL-1β, and IL-23 (den Dunnen et al., 2012). This crosstalk was initially described in dendritic cells but has also been reported in macrophages and monocytes (Vogelpoel et al., 2015). Vogelpoel et al. (2005) showed that FcγRIIA is responsible for cytokine expression in dendritic cells, macrophages and monocytes. Moreover, FcγRIIA selectively communicates with TLR2, TLR4, TLR5, TLR7/8,

IL-1R and IFNγR, but not Dectin-1 (Vogelpoel et al., 2015; den Dunnen et al., 2012). In a study that sought to determine the molecular basis of FcγR-TLR crosstalk-mediated cytokine production, Hoepel et al. (2019) found that TLR-induced phosphorylation and nuclear translocation of the transcription factor interferon regulatory factor 5 (IRF5) is a key mediator in the crosstalk in both dendritic cells and macrophages. IRF5 also increased the rate of glycolysis thereby providing a carbon source to support increased translation of proinflammatory cytokines.

A study that explored the phosphoproteome profile of murine macrophage in response to TLR2, TLR4 and TLR7 stimulation found increased phosphorylation of proteins involved in FcγR mediated phagocytosis following TLR2 and TLR4 stimulation, but not TLR7 stimulation (Sjoelund et al., 2014). Interestingly, it has been shown that inhibiting the phagocytosis of IgG-opsonised *Staphylococcus aureus* did not prevent proinflammatory cytokine production (den Dunnen et al., 2012). Thereby suggesting that pathogen internalization is not necessary for FcγR-TLR cross talk possibly because FcγR-mediated phagocytosis and cytokine production follow independent signalling pathways. The uncoupling of phagocytosis and cytokine production can also be observed from the finding that *Msr1*$^{-/-}$ macrophages are impaired in the phagocytosis of *Neisseria meningitidis* without significantly impacting TLR4-mediated cytokine production (Peiser et al., 2002). Notably, there is also evidence of signalling overlaps between phagocytosis and cytokine production. For example, the activation of SYK is central to FcγR-mediated phagocytosis; however, SYK phosphorylation also leads to NF-

κB activation and the transcription of proinflammatory cytokines via the CARD9/BCL10/MALT1 complex (Fu and Harrison, 2021).

The activation of the complement pathway during *C. neoformans* infection recruits phagocytic immune cells to the site of infection and promotes the phagocytosis and elimination of *C. neoformans* by these cells (Levitz and Tabuni, 1991; Voelz and May, 2010). There are three pathways to activate the complement system: classical-, alternative- and lectin- pathways (Zipfel and Skerka, 2009). The classical pathway is activated by antibody-antigen interaction, the alternative pathway is continuously active and the lectin pathway is activated by mannose-binding lectin (MBL) interaction with mannose molecules on the surface of pathogens (Zipfel and Skerka, 2009; Voelz and May, 2010). In the alternative pathway, C3 protein spontaneously splits to generate complement component 3a (C3a), an anti-microbial peptide, and C3b, an opsonin (Zipfel and Skerka, 2009). Following activation, all three pathways lead to the formation of C3 convertase, which further amplifies C3 cleavage. Complement Receptor type 3 (CR3) and CR4 on the surface of immune cells can then result in the phagocytosis of C3b-opsonised cells (Zipfel and Skerka, 2009). In addition to its role as an opsonin, C3b also leads to the generation of C5 convertase, an enzyme that cleaves C5 into C5a and C5b. C5b then recruits other complement proteins including C6, C7, C8 and C9 to form a membrane attack complex that destroys pathogens (Voelz and May, 2010). Several studies have found that the alternative complement pathway is the main pathway involved in the immune response to *C. neoformans* infection (Diamond et al., 1974; Kozel et al., 1991; Diamond et al., 1973). However, a recent transcriptomics study revealed that all three

arms of the complement system are significantly upregulated in mice infected intranasally with *C. neoformans* for 14 days, with components of the classical pathway being among the top 10 most upregulated genes (Holcomb et al., 2022). It has also been shown that tumour necrosis factor-α (TNF- α) and granulocyte-macrophage colony-stimulating factor (GM-CSF) promote CR3-mediated phagocytosis of complement-opsonised *C. neoformans* by murine macrophages (Cross et al., 1997; Collins and Bancroft, 1992). The absence of CR3 results in a significant increase in mice mortality (Cross et al., 1997) and mice also had increased mortality when treated with cobra venom to deplete the late complement components, C3 to C9, prior to infection with cryptococci (Diamond et al., 1973).

1.2.7 Is opsonisation important during the initial phagocytosis of *C. neoformans*?

Aside from IgG- and C3b-mediated opsonisation in the circulatory system, analysis of bronchoalveolar lavage (BAL) fluid has revealed the existence of soluble PRRs (sPRRs) in the lungs that may serve as opsonins (Wong et al., 2020; Smole et al., 2020; Litvack and Palaniyar, 2010). Soluble PRRs survey body cavities for the presence of pathogens or allergens (Smole et al., 2020). To determine whether these sPRRs are involved in the early stages of host-pathogen interaction in the lungs, we must first establish whether they are present in the airway mucosa, and then determine their level of activity in this environment.

Well-known sPRRs in the lungs include surfactant protein A (SP-A) and SP-D, which have been shown to opsonise and promote the clearance of invading microbes (Pikaar et al.,

1995; LeVine et al., 2004; Giannoni et al., 2006; Pastva et al., 2007). SP-A and SP-D belong to the collectin family of C-type lectins, indicating that they recognise carbohydrate moieties (Haagsman et al., 1987). They are produced by type II alveolar epithelial cells and released into the alveolar space (Phelps and Floros, 1991; Voorhout et al., 1992). They have been found to opsonise herpes simplex virus-1 (van Iwaarden et al., 1991), *Mycobacterium tuberculosis* (Gaynor et al., 1995), allergens (Malhotra et al., 1993; Wang et al., 1996), and *Aspergillus fumigatus* (Madan et al., 1997), leading to increased phagocytosis by alveolar macrophages and activation of host immune defence. Interestingly, with regards to *C. neoformans*, SP-A is capable of binding to minimally encapsulated and acapsular yeast; however, it does not result in enhanced phagocytosis (Walenkamp et al., 1999; Giles et al., 2007). This implies that SP-A does not act as an opsonin for *C. neoformans*. Notably, a later study found that SP-A is incapable of binding encapsulated or acapsular H99 *C. neoformans* strain (Geunes-Boyer et al., 2009); however, this might be due to the low concentration of SP-A used in this study; 1 μg/ml compared to up to 25 μg/ml and 40 μg/ml used by Walenkamp et al. (1999) and Giles et al. (2007), respectively. Giles et al. (2007) went further to show that *Sftpa1*$^{-/-}$ mice and wildtype mice have similar responses to intranasal infection with *C. neoformans*, suggesting a negligible role of SP-A during infection.

On the other hand, SP-D binds acapsular, and to a much lesser extent, encapsulated *C. neoformans* (Geunes-Boyer et al., 2009; Walenkamp et al., 1999). Opsonisation of acapsular, but not encapsulated *C. neoformans* with SP-D increased its phagocytosis by macrophages (Geunes-Boyer et al., 2009). Similarly, alveolar macrophages from

wildtype mice phagocytosed more encapsulated and acapsular cryptococcus than macrophages from *Sftpd*$^{-/-}$ mice (Geunes-Boyer et al., 2009). Interestingly, this SP-D mediated opsonisation to drive increased phagocytosis is thought to be beneficial to the pathogen and not the host since *Sftpd*$^{-/-}$ mice showed decreased fungal burden, increased survival compared to wildtype mice, and improved killing of cryptococci (Geunes-Boyer et al., 2012, 2009). Therefore, SP-D opsonisation of *C. neoformans* is thought to protect the fungi from damage by host defence mechanisms, such as oxidative stress (Geunes-Boyer et al., 2012), thereby allowing the fungi to survive and replicate within phagocytes and disseminate to the brain. Taken together, SP-D, but not SP-A, is involved in the opsonisation of *C. neoformans* during the early stages of infection in a pathogen-protective manner.

MBL is another sPRR that belongs to the collectin family of C-type lectins. However, unlike SP-A and SP-D, MBL is primarily present in the serum where it activates the lectin pathway of the complement system (Zipfel and Skerka, 2009; Jambo et al., 2007; Davies et al., 2001); though there is evidence of MBL in the BAL fluid during respiratory disease (Vogt et al., 2020; Fidler et al., 2009). On the other hand, MBL deficiency has also been implicated in genetic susceptibility to *C. neoformans* infection (Wagemakers et al., 2019; Ou et al., 2011). Moreover, MBL has been found to opsonise cryptococcus and enhance phagocytosis (Chaka et al., 1997; van Asbeck et al., 2008). It is yet to be determined whether MBLs in the lungs are functional or whether they merely reflect mucosa permeability due to tissue damage. Thus, MBL is clearly involved in host defence against disease, but due to its primary localisation to the serum (Jambo et al., 2007; Wong et al.,

2020), it may not be involved in the initial opsonisation and phagocytosis of *C. neoformans* at the airway mucosa. Though it may be recruited to the lungs at a later stage of infection.

Complement by-products such as C3b (alternative pathway) and C1q (classical pathway) also serve as opsonins that promote phagocytosis (Zipfel and Skerka, 2009; Wong et al., 2020). The importance of the complement system during *C. neoformans* infection was briefly described in section 1.2.6. As mentioned previously, the alternative complement pathway is thought to be the key pathway involved in the immune response to *C. neoformans* infection (Diamond et al., 1974; Kozel et al., 1991; Diamond et al., 1973). Complement proteins are most well known for their activity in serum; however, they have also been detected, but to a lower extent, in BAL fluid from both healthy and diseased lungs (Robertson et al., 1976; Watford et al., 2000; Chen et al., 2008). They were also shown to be expressed by alveolar macrophages (Cole et al., 1983; Ackerman et al., 1978) and alveolar type II epithelial cells *in vitro* (Strunk et al., 1988). Interestingly, when the functionality of complement proteins in the lungs was examined, it was found that the classical complement pathway in BAL fluid had approximately 16% to 39% of serum complement activity; meanwhile, no alternative pathway activity (the pathway thought to be most important during host response to *C. neoformans*) was detected in BAL fluid (Watford et al., 2000). Others showed that BAL fluid from rat poorly opsonised *Klebsiella pneumoniae*, while serum rapidly opsonised bacteria (Coonrod, 1981). Similarly, Wong et al. (2020) showed that BAL fluid was able to deposit C3b opsonin on *Aspergillus fumigatus* conidia; however, the intensity of C3b deposition was less than

that observed with serum-opsonised conidia (Wong et al., 2020). When *C. neoformans* was isolated from mice lungs and stained for C3, it was found that C3 was located at the deeper layers of the capsule, such that it would be difficult for the C3 opsonin to interact with complement receptors on the surface of phagocytes (Zaragoza and Casadevall, 2004). Therefore, the presence of complement proteins in the lungs does not necessarily equate to a significant contribution of complement pathways in immune response in the lung mucosa, especially since these studies report the presence of one or a few components of the complement system, but not the presence of other components needed to complete the signal transduction pathway. For example, Wong et al. (2020) found the presence of C4, a component of the classical complement pathway, in BAL fluid, but not C2, a key activator of this pathway. There is also evidence to suggest that the level of complement proteins is higher in individuals with pulmonary disease compared to healthy individuals (Bolger et al., 2007; Pandya and Wilkes, 2014). Thus, although it is clear that the complement pathway plays a critical role during host response to *C. neoformans* infection (Holcomb et al., 2022; Diamond et al., 1973), its significance during initial cryptococcus-phagocyte interaction remains unclear. It will be important for future research to explore the significance of BAL fluid-specific complement components in host response to *C. neoformans* infection.

The primary antibody in the airway mucous membrane is secretory IgA (sIgA), also known as IgA2 (Peebles et al., 1995). Although sIgA from respiratory secretions was able to opsonise *Pseudomonas aeruginosa*, it did not enhance the phagocytosis of this bacteria by alveolar macrophages (Reynolds et al., 1975). Similarly, opsonisation with

sIgA did not enhance the uptake of *Staphylococcus aureus* by bovine polymorphonuclear neutrophils (Barrio et al., 2003); suggesting that despite its prevalence in the mucosa, sIgA has poor opsonisation activity. Instead, sIgA functions by preventing the attachment of microbes to epithelial cells via steric hinderance, promoting microbe clumping and entrapment within the mucus, and neutralising microbes and toxins (Mantis et al., 2011). It is also unknown whether sIgA mAbs that recognize epitopes on *C. neoformans* exist in the lung mucosa; though, anti-GXM IgA1 has been detected in human serum (Deshaw and Pirofski, 1995; Subramaniam et al., 2005) and was shown to be protective to mice when administered prior to infection (Mukherjee et al., 1992).

IgG, the dominant immunoglobulin in the blood, IgM and IgE have also been detected in lung secretions (Burnett, 1986). IgE is known for its role in mediating allergic responses and has been shown to opsonise *C. neoformans in vitro* (Balzar et al., 2007; Janda et al., 2015). However, the percent phagocytosis was very low compared to IgG-opsonised cryptococcus (Janda et al., 2015). Moreover, it has not been reported whether IgE is involved in host response to *C. neoformans in vivo*. The presence of IgG on the capsule of cryptococcus cells isolated from the lungs of infected mice has been observed following intranasal *C. neoformans* infection (Zaragoza and Casadevall, 2004). Meanwhile, IgM was not detected on yeast cells isolated from the lungs (Zaragoza and Casadevall, 2004); possibly due to the absence of IgM in the lungs during *C. neoformans* infection or the poor reactivity of IgM with the fugal capsule. It was further shown that IgG-coated cells from lungs were not readily phagocytosed compared to uncoated yeast cells, suggesting that during pulmonary infection, IgG coating of cryptococcus did not

promote opsonic phagocytosis (Zaragoza and Casadevall, 2004). Pre-treatment of mice with IgM and IgG mAbs have been shown to be protective, deleterious or insignificant to mice during experimental infection with *C. neoformans* (Mukherjee et al., 1995; Sanford et al., 1990; Zaragoza and Casadevall, 2004; Fleuridor et al., 1998; Dromer et al., 1987; Beenhouwer et al., 2007); however, it remains unclear whether natural antibody-mediated responses significantly contribute to host response to infection.

Given the current knowledge, we cannot neglect the potential involvement of sPRRs in the opsonisation of *C. neoformans* to promote phagocytosis by macrophages at the lung mucosa. However, at present, it appears that non-opsonic interactions between cryptococcus and host innate immune cells would be just as relevant as potential opsonic interaction during the early stages of infection.

1.2.8 Crosstalk between Pattern Recognition Receptors

The existence of crosstalk between PRRs has been hinted at throughout this chapter, with one such relationship being described between FcγRs and TLRs. Crosstalk between PRRs is thought to confer specificity to the innate immune system, robustness against infection and redundancy that protects against immunodeficiency (Tan et al., 2014; Underhill, 2007). The collaboration between PRRs can facilitate a scaled response, but it can also serve as a negative regulator of immune response (Tan et al., 2014). The following section will provide further examples of crosstalk between PRRs.

A single microbe contains several PAMPs that can be recognised by different PRRs. For example, LPS from a Gram-negative bacteria can be recognised by TLR4; however, after phagocytosis, DNA from the same bacteria can be recognised by TLR9. Moreover, we are often exposed to multiple pathogens at a time, thus, no individual PRR is likely the sole contributor to the observed immune response (Underhill, 2007). It has been shown that Dectin-1, the key PRR involved in the detection of *C. albicans*, synergises with TLR2 for optimal production of TNFα following macrophage stimulation with *C. albicans* or zymosan (Ferwerda et al., 2008; Dennehy et al., 2008). It was later shown that this collaboration requires Dectin-1 and TLR2 to be within a 500 nm distance from each other, implicating spatial distribution of receptors in the regulation of immune response (Li et al., 2019).

Although TLRs are not directly responsible for pathogen uptake, it has been shown that stimulating macrophages with TLR4, TLR2 or TLR9 agonists results in upregulation of phagocytic receptors such as FcγR, CR3, MSR1 and MARCO (Zhou et al., 2019; Doyle et al., 2004). Thus, priming cells with TLR agonists can influence the phagocytic capacity of the cell. It has also been shown that MSR1 enhanced LPS-induced and TLR4-mediated NF-κB activation (Yu et al., 2012). Supporting the existence of crosstalk and synergism between TLR4 and MSR1.

Alternatively, complete or partial loss of TLRs could influence the phagocytic capacity of other PRRs. A pivotal study described synergy between TLR4 and MSR1 and TLR2 and MSR1 in the phagocytosis of *Escherichia coli* (gram negative) and *Staphylococcus aureus*

*(*gram positive), respectively (Amiel et al., 2009). They showed that bone marrow-derived dendritic cells (BMDC) isolated from wildtype, *Msr1*$^{-/+}$, or *Tlr4*$^{-/+}$ mice had similar levels of phagocytosis. However, when BMDC was double heterozygote (*Msr1*$^{-/+}$ *Tlr4*$^{-/+}$) there was impaired phagocytosis of *E. coli*. The same was seen in *Msr1*$^{-/+}$ *Tlr2*$^{-/+}$ heterozygotes infected with *S. aureus* (Amiel et al., 2009). Similarly, Mukhopadhyay et al. (2011), showed that MSR1 and MARCO contribute to the clearance of the gram-negative bacteria, *Neisseria meningitidis,* while modulating TLR4-mediated cytokine response to *N. meningitidis*. Additionally, MSR1 has been identified as a receptor for extracellular dsRNA and is thought to act as a carrier to deliver dsRNA to TLR3, thereby enhancing TLR3-mediated immune response (Limmon et al., 2008; DeWitte-Orr et al., 2010; Mukhopadhyay et al., 2011). It is likely that this TLR-SR crosstalk to regulate phagocytosis and cytokine expression is a general phenomenon of host-pathogen interaction, and not unique to bacterial infection.

There also exists collaboration within the same family of receptors with evidence showing that co-stimulation of macrophages with a TLR3 agonist (MyD88-independent) or TLR4 agonist and a TLR2, TLR9, or TLR5 agonist (MyD88-dependent) resulted in synergistic production of TNFα (Bagchi et al., 2007). Meanwhile, a combination of agonists for two MyD88-dependent TLRs did not induce synergy, suggesting that MyD88-TRIF adaptor crosstalk is one possible mechanism for synergism.

This concept of crosstalk may explain why, to date, no PRR has been definitively recognised as the receptor responsible for *C. neoformans* detection by macrophages.

The research thus far has focused on genetic knockdown of individual receptors; however, several receptors may be working together. Alternatively, the genetic knockout of one receptor may be compensated for by differential expression of another receptor leading to unexpected phenotypes.

1.3 *Cryptococcus neoformans* Virulence Factors

Although there are various mechanisms employed by the host immune system to control infection with *C. neoformans*, the ability of the fungus to survive and replicate within macrophages implies the existence of immune evasion strategies, some of which act even before the fungus is phagocytosed.

Although most *C. neoformans* cells do not experience a human host for their entire existence, they have evolved several virulence factors that allow them to establish successful infection in humans (May et al., 2016). Thus, it is interesting to consider the evolutionary pressures that selected for these virulence factors (May et al., 2016; Johnston and May, 2013). One proposed explanation for the acquisition of these virulence factors is called accidental pathogenesis (May et al., 2016; Casadevall, 2008). This is the idea that the virulence factors did not evolve selectively to perturb the human immune system, instead, it originally evolved as a mechanism to deal with environmental threats, but also happens to be advantageous within human hosts (Casadevall, 2008). For example, Cryptococcus has been co-evolving with amoebae for millions of years and the mechanism used by amoebae to phagocytose and digest prey shares similarities with mammalian macrophages, so adaptation to this alternative host

during its evolution might have aided in its ability to survive in mammalian macrophages (May et al., 2016; Coelho et al., 2014). Some of these virulence mechanisms include their capsule polysaccharide, their ability to form titan cells, melanin production and extracellular vesicles.

1.3.1 Capsule Polysaccharide

The cryptococcus polysaccharide capsule is known to possess anti-phagocytic capabilities (Kozel and Gotschlich, 1982). Firstly, the dynamic polysaccharide capsule, which can be as large as 30 μm, protects C*. neoformans* from getting phagocytosed by masking PAMPs found on the cell wall (Johnston and May, 2013; Kozel and Gotschlich, 1982). Acapsular *C. neoformans* mutants are readily phagocytosed by macrophages, supporting the idea that the polysaccharide capsule forms a barrier that hinders the recognition of PAMPs, such as β-glucans and mannan, which are more easily recognised by macrophage PRRs (Johnston and May, 2013; Cross and Bancroft, 1995; Kozel and Gotschlich, 1982).

Secondly, the GXM and GalXM polysaccharides that make up the cryptococcal capsule are shed during infection and have been shown to suppress the activation of NF-κB and decrease plasma levels of the TNFα, IL-1β and IL-6 (Piccioni et al., 2013). Shed GXM is phagocytosed by neutrophils and macrophages and the accumulation of GXM within neutrophils attenuated their anti-cryptococcal response (Monari et al., 2003). Additionally, the enlargement of *C. neoformans* capsule was found to confer protection against ROS and RNS by acting as a scavenger of free radicals (Zaragoza et al., 2008).

Therefore, not only does the capsule limit the ability of phagocytes to ingest *C. neoformans*, but it also enhances fungal survival after phagocytosis.

1.3.2 Titanization

When in the host, *C. neoformans* can take on a 'giant' morphology referred to as 'titan cells' (Love et al., 1985; Zaragoza et al., 2010). These cells have a diameter of over 10 µm excluding the capsule, and a diameter of 40 µm to 100 µm when the capsule is included. They also exhibit a polyploid genome, greatly crosslinked capsule and a thickened cell wall with elevated levels of chitin (Okagaki et al., 2010; Zaragoza et al., 2010). Titanization enables *C. neoformans* cells to evade phagocytosis due to their large size (Crabtree et al., 2012). At the same time, the presence of titan cells decreases the phagocytosis of normal-sized cells (Okagaki and Nielsen, 2012). This reduction in phagocytosis increased cryptococcal viability and dissemination to the CNS (Crabtree et al., 2012). Moreover, titan cell formation pushed the murine immune response towards the non-protective Th2 response (García-Barbazán et al., 2016).

1.3.3 Laccase activity and Melanisation

C. neoformans laccase catalyses the production of melanin through the oxidation of exogenous compounds such as 3,4-dihydroxyphenylalanine (L-dopa) (Liu et al., 1999; Casadevall et al., 2000). This melanin is then associated with the fungal cell wall and protects *C. neoformans* from antifungal activity (Casadevall et al., 2000). Various studies have shown that melanin-deficient *C. neoformans* are much less virulent to mice than wildtype *C. neoformans* (Kwon-Chung et al., 1982; Salas et al., 1996). Melanin protects

C. neoformans from killing by anti-microbial compounds possibly by binding and sequestering these antimicrobial compounds (Doering et al., 1999). Melanin has been shown to protect *C. neoformans* from oxidative damage (Wang and Casadevall, 1994b; Khajo et al., 2011) and contribute to antifungal drug resistance, including resistance to amphotericin B and caspofungin (Wang and Casadevall, 1994a; Ikeda et al., 2003; Duin et al., 2002).

1.3.4 Extracellular Vesicles

Extracellular vesicles (EVs) are 30 to 500 nm double-layered membrane particles released by all types of cells into the extracellular environment (Meldolesi, 2018). Fungal EV-like structures were first described in the 1970s in *Aspergillus nidulans*, *C. albicans* and *C. neoformans* (Gibson and Peberdy, 1972; Takeo et al., 1973; Chigaleĭchik et al., 1977). In 2007, EVs were isolated for the first time in *C. neoformans* and were originally identified for their role in the transport of *C. neoformans* capsular polysaccharide to the extracellular space for capsule assembly and release (Rodrigues et al., 2007). However, EVs are also recognised as 'virulence bags' because they were found to contain a range of virulence-associated molecules such as GXM, laccase, urease, superoxide dismutase, chitin deacetylase, phospholipids, ergosterol and RNA (Rodrigues et al., 2007; de Oliveira et al., 2020; Rizzo et al., 2021). Therefore, fungal EVs carry molecules that not only modulate their physiology but also their response to the host. Since the discovery of cryptococcal EVs in 2007, there has been some progress in our understanding of how EVs impact cryptococcus-host interaction. Murine macrophages can take up *C. neoformans* EVs and the treatment of macrophages with isolated EVs resulted in

increased expression of TNFα, TGF-β and IL-10, enhanced phagocytosis of non-opsonised *C. neoformans*, and enhanced fungal killing (Oliveira et al., 2010a), suggesting that EVs can prime macrophages and improve their antifungal activity. However, EVs can also promote fungal virulence. For example, several groups have reported that EVs from a highly virulent *C. neoformans* strain was able to increase the pathogenicity of a less virulent strain, implying a function for EVs in fungi-to-fungi communication and transfer of virulence (Hai et al., 2020; Bielska et al., 2018). Moreover, cryptococcal EVs were found to promote fungal crossing of the BBB in an *in vitro* model (Huang et al., 2012). *In vivo*, *C. neoformans* EVs were found around cystic lesions in the brain of infected mice and were associated with increased brain fungal burden (Huang et al., 2012).

EVs have also been implicated in antifungal drug response. A recent study showed that *C. neoformans* decrease their production of EVs to acquire resistance to the cell membrane disrupting drug, fluconazole (Rizzo et al., 2023). Compared to wildtype control, EV-deficient mutants showed no difference in ERG11 expression, a well-known antifungal drug resistance gene (Rizzo et al., 2023). Therefore, a decrease in EV production may be an independent mechanism by which *C. neoformans* acquire drug resistance. It is possible that cryptococci suppress EV production when exposed to fluconazole to maintain membrane homeostasis. On the other hand, *Saccharomyces cerevisiae* EVs were found to be enriched with FKS1 involved in β-1,3-glucan synthesis and CHS3 involved in chitin synthesis (Zhao et al., 2019). Pre-incubation of yeast cells with EVs prior to treatment with the cell wall synthesis inhibiting drug caspofungin

rescued yeast cell survival. In fact, caspofungin treatment increased EV production in a dose-dependent manner, suggesting a model where yeast cells increased EV production in response to caspofungin treatment to promote cell wall remodelling to counteract the effects of caspofungin treatment in recipient cells (Zhao et al., 2019). All the above examples support a role for EVs in both yeast-to-yeast communication and yeast-to-host communication.

There remains much to be understood about the mechanism of EV production, EV release across the cell wall and polysaccharide capsule, the effects of cryptococcal EVs on the host response to infection, and the mechanism of EV-mediated yeast-to-yeast communication. Studies have identified genes belonging to the conventional ER/Golgi secretory pathways such as SEC6 and SEC4/SAV1 in the release of EVs (Panepinto et al., 2009; Yoneda and Doering, 2006; Oliveira et al., 2010b). *SEC6* silencing and *SEC4* deletion led to an accumulation of intracellular vesicles, but failure to detect extracellular vesicles, suggesting that this pathway is specifically involved in EV secretion and not production or composition (Panepinto et al., 2009; Yoneda and Doering, 2006). According to studies in *Saccharomyces cerevisiae* and mammalian cells, post-Golgi secretory vesicles are tethered to the plasma membrane via the highly conserved exocyst complex of which SEC6 is one of 8 members, while SEC4 mediates recruitment of components of the exocyst complex to vesicle membrane (Mei and Guo, 2018; Xu et al., 2022). Following tethering, SNAp Receptors (SNARE) on vesicles (v-SNARE) and on the plasma membrane (t-SNARE) interact, driving membrane fusion and release of EVs (Mei and Guo, 2018). The t-SNARE protein SSO1 and the v-SNARE protein SNC2 have

been found on *C. neoformans* EVs (Rizzo et al., 2021), supporting the involvement of the exocyst complex and SNARE proteins in EV secretion in this fungi. EVs must also traverse the thick cell wall of fungi but the mechanism is poorly understood. What has been found is that crossing of the cell wall does not require trans-cell wall channels (Wolf et al., 2014). Instead, the *C. neoformans* and *C. albicans* cell walls are thought to be viscoelastic, allowing particles larger than the porosity of the cell wall to pass through (Walker et al., 2018).

With regards to EV production, studies in mammalian cells have identified a key role for members of the endosomal sorting complex required for transport (ESCRT) machinery in EV biogenesis (Meldolesi, 2018). Similar studies in fungi have found that deletion of ESCRT complex components, VPS2, VPS23 and VPS36, in *S. cerevisiae* led to reduced protein content in EVs (Zhao et al., 2019). Meanwhile, deletion of VPS23 and VPS36 led to increased EV diameter (Zhao et al., 2019). In *C. albicans*, deletion of ESCRT components led to decreased EV production (Zarnowski et al., 2018). *VPS27* knockout in *C. neoformans* led to defective EV maturation and increased EV size (Park et al., 2020). Therefore, there appears to be a shared ESCRT-dependent EV biogenesis pathway across eukaryotes.

1.3.5 Secreted Virulence Effectors

Secreted effector proteins and toxins that directly act on host cells are a common phenomenon in bacterial pathogens (Galán, 2009); however, very few such molecules have been identified in *C. neoformans.*

First identified as a virulence factor in 1997, Phospholipase B1 (PLB1) is an extracellular enzyme released by *C. neoformans* that cleaves host phospholipids (Chen et al., 1997a, 1997b). Mice infected with *plb1Δ C. neoformans* showed reduced mortality compared to those infected with wildtype fungi (Cox et al., 2001; Hamed et al., 2023). Fewer CFUs were recovered from the brain of mice infected with *plb1Δ C. neoformans* (Cox et al., 2001; Santangelo et al., 2004). This is thought to represent the involvement of PLB1 in the dissemination of *C. neoformans* from the lungs to the bloodstream, but not from the bloodstream to the CNS (Santangelo et al., 2004); a role for PLB1 in the transcytosis of cryptococci across the BBB (Maruvada et al., 2012); and/or PLB1-mediated survival of *C. neoformans* in the brain via its role in regulating cytokine production, microglia recruitment and microglial morphological changes (Hamed et al., 2023). In line with the decreased CFU observed in mice infected with *plb1Δ C. neoformans*, in an *in vitro* model of infection, *plb1Δ C. neoformans* had decreased intracellular proliferation and increased killing by macrophages (Evans et al., 2015). Further work is needed to understand the precise consequence of PLB1-mediated phospholipid hydrolysis on cryptococcus pathogenesis.

Another secreted *C. neoformans* virulence factor is urease, an enzyme that catalyses the hydrolysis of urea into carbon dioxide and ammonia (Cox et al., 2000; Almeida et al., 2015). Mice infected with *ure1Δ C. neoformans* showed decreased mortality (Cox et al., 2000). Moreover, urease was shown to be involved in the dissemination of cryptococci to the brain and crossing of the BBB, but it was not necessary for the subsequent

proliferation of cryptococcus within the brain (Olszewski et al., 2004). Several groups have shown that urease promotes *C. neoformans* sequestration/ trapping within small capillaries in the brain (Olszewski et al., 2004; Shi et al., 2010); it is thought that sequestration is followed by ammonia-induced toxicity to endothelial cells of the brain leading to weakening of tight junctions and permeabilization of the BBB allowing cryptococcus tissue invasion (Olszewski et al., 2004; Shi et al., 2010). Moreover, mice infected with *ure1Δ C. neoformans* produced less IL-4, IL-13 and Arginase-1, suggesting that urease promotes the nonprotective type 2 immune response (Osterholzer et al., 2009b).

CPL1 is a newly identified cryptococcus molecule found to promote fungal pathogenesis (Dang et al., 2022). CPL1 is a secreted protein (Liu et al., 2008; Cai et al., 2015), but is also found at the *C. neoformans* cell surface (Cai et al., 2015). Cells deficient in CPL1 have impaired capsule formation (Liu et al., 2008). Recently, CPL1 was found to play a role in virulence by polarizing macrophages towards the nonprotective M2 response characterized by increased Arginase-1 production (Dang et al., 2022). CPL1-mediated induction of Arginase-1 required TLR4 signalling. CPL1 also increased macrophage sensitivity to IL-4, a cytokine that promotes type 2 immune response, such that Arginase-1 expression was higher when macrophages were stimulated with recombinant CPL1 and IL-4 simultaneously compared to individually. Mice infected with *cpl1Δ C. neoformans* survived longer and produced less Arginase-1 than those infected with wildtype *C. neoformans*. Moreover, uptake of *C. neoformans* was enriched in

macrophages expressing Arginase-1, suggesting the fungi exploit these alternatively activated macrophages as a replicative niche (Dang et al., 2022).

1.4 Host Genetic Susceptibility to *Cryptococcus neoformans*

Reports of CM in immunocompetent individuals, a lack of CM in many HIV/AIDS patients with low CD4+ T-cell count and the existence of donor-to-donor variation in macrophage response to *C. neoformans* infection suggests that disease risk may be driven by other factors outside of host immune state (Garelnabi and May, 2018). It is well recognised that there is a strong genetic component to susceptibility to infectious diseases (Sørensen et al., 1988). Moreover, infectious agents are among the strongest selection pressures to act on the human genome (Fumagalli et al., 2011). Therefore, host genetics may impact an individual's susceptibility to cryptococcal disease. Though research in the area is limited, SNPs in various immune signalling proteins have been associated with susceptibility to cryptococcal disease.

Several studies have investigated the relationship between *FCGR* genes and *Cryptococcus* infection in HIV-negative and HIV-positive individuals with CM (Meletiadis et al., 2007; Hu et al., 2012; Rohatgi et al., 2013). Meletiadis et al. (2007) reported that two common allelic variants in Fc receptors, *FCGR2A (CD32a*) 131R/R and *FCGR3A (CD16a)* 158V/V, were associated with an increased risk of cryptococcal disease in HIV-negative individuals (OR = 1.67; 95% CI [1.05-2.63]; p = 0.04 and OR = 2.04; 95% CI [1.06-4.00]; p = 0.04, respectively). Similarly, Rohatgi et al. (2013) genotyped the *FCGR2A* 131H/R and the *FCGR3A* 158F/V polymorphisms in 164 mostly white male volunteers

and found that the *FCGR3A* 158V allele was associated with an increased risk of cryptococcal disease in HIV- positive individuals (OR = 2.1; 95% CI [1.2-3.5]; p = 0.005). They went on to show that heterozygotes had a 2.1-fold increased risk of developing cryptococcal disease while *FCGR3A* 158V/V homozygotes had a 21-fold increase in infection risk. In contrast to the study by Meletiadis et al. (2007), Rohatgi et al. (2013) found no association between *FCGR2A* 131H/R polymorphism and cryptococcal disease. Both of these studies had a predominantly Caucasian cohort; however, another study using 117 HIV-uninfected Han Chinese individuals with CM and 190 healthy controls also found no association between *FCGR2A* 131H/R polymorphism and cryptococcal disease (Hu et al., 2012). Surprisingly, they also found no association between *FCGR3A* 158F/V and CM. Instead Hu et al. (2012) found that the *FCGR2B (CD32b)* 232I/I genotype was enriched in CM patients (OR = 1.65; 95% CI [1.02-2.67]; p = 0.039), while the *FCGR2B* 232I/T genotype was rare in CM patients (OR = 0.54; 95% CI [0.33-0.90]; p = 0.016) (Hu et al., 2012). It is possible that ethnic differences may influence the impact of particular genetic polymorphisms on *C. neoformans* infection. It may also be the case that the sample size used in some studies hindered the detection of certain polymorphisms.

Some progress has been made to determine the mechanism by which these FCGR polymorphisms influence response to infection. The histidine (H) to arginine (R) substitution at position 131 of *FCGR2A* results in reduced affinity of the receptor to IgG2 (Warmerdam et al., 1991). Since *FCGR2A* is the major receptor for IgG2, the reduced affinity associated with the arginine substitution likely results in decreased phagocytosis of IgG2-coated fungal cells, ultimately leading to poor fungal clearance. FcγRIIB is the

only known inhibitory FcγR and its binding to IgG molecules acts to suppress immune cell activation (Hargreaves et al., 2015). It has been shown that FcγRIIB with a threonine residue at position 232 have a 3-to-4-fold decrease in their affinity to IgG, as a result, they are less able to inhibit immune cell activation, leading to unobstructed activatory FcγR signalling and persistent proinflammatory response which can damage healthy tissue (Floto et al., 2005; Hu et al., 2019). This likely explains why it has consistently been shown that the *FCGR2B* 232T/T genotype increases susceptibility to the autoimmune disease Systemic lupus erythematosus (SLE), but has a protective function against malaria infection (Willcocks et al., 2009; Kyogoku et al., 2002). This implies that the threonine substitution increases the risk of autoimmune disease, but is protective against infectious disease, supporting the underrepresentation of the *FCGR2B* 232I/T genotype in CM patients. An investigation into the functional consequence of the *FCGR3A* 158 polymorphism revealed that CHO-K1 cells engineered to express the *FCGR3A* 158V allele bound human serum- or IgG-opsonised *C. neoformans* more effectively than cells expressing the *FCGR3A* 158F allele (Rohatgi et al., 2013). Moreover, natural killer (NK) cells expressing *FCGR3A* 158V allele induced greater antibody-dependent cellular cytotoxicity (ADCC) towards *C. neoformans*-infected monocytes than those expressing 158F allele. It is known that monocytes secrete chemokines that damage the BBB, thus the elevated cytotoxicity caused by cells expressing *FCGR3A* 158V allele may promote *C. neoformans* dissemination into the CNS. Since the *FCGR3A* 158V allele increases *C. neoformans* binding to CHO cells, the increased risk of HIV-associated cryptococcal disease may also be caused by increased phagocytosis of *C. neoformans* by phagocytes (Figure 1-4). One may assume that elevated phagocytosis would promote

fungal clearance; however, it was shown that clinical *C. neoformans* strains that were more easily phagocytosed (termed high uptake *C. neoformans*) led to greater CNS fungal burden and increased expression of nonprotective Th2 cytokines (Hansakon et al., 2018; Sabiiti et al., 2014a). In essence, increased phagocytosis counterintuitively leads to poor disease outcome. This supports the 'Trojan horse' hypothesis that states that *C. neoformans* hijack macrophages to disseminate throughout the host, cross the BBB, and promote pathogenesis (May et al., 2016).

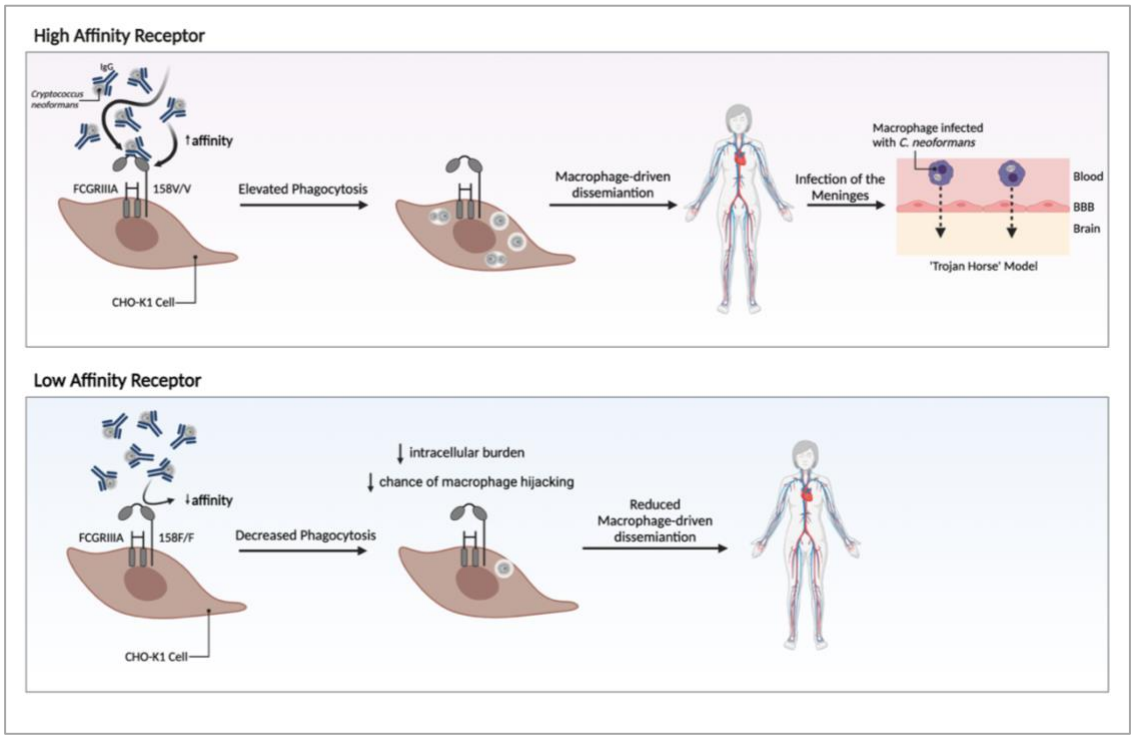

Figure 1-4: Proposed consequence of *FCGR3A (CD16a)* 158F/V polymorphism on host response to infection. Chinese hamster ovary (CHO-K1) cells engineered to express *FCGR3A* 158V allele had a higher affinity to IgG-opsonised *C. neoformans* than those expressing the *FCGR3A* 158F allele. The high-affinity FCGR3A 158V receptor may result in elevated phagocytosis by phagocytes. Intracellular *C. neoformans* can then use macrophages as a vehicle to cross the blood-brain barrier (BBB) in what is called the 'Trojan Horse' model and infect the meningitis leading to fatal cryptococcal meningitis (CM). Meanwhile, those expressing the low-affinity *FCGR3A* 158F receptor have decreased phagocytosis, decreased intracellular burden of *C. neoformans* and, therefore, a decreased risk of macrophage-driven dissemination to the brain leading to decreased risk of CM. Figure created with BioRender.com.

Aside from FCGRs, polymorphisms in MBL2, a soluble PRR that activates the lectin pathway of the complement system, that lead to MBL2 deficiency were associated with non-HIV CM (Ou et al., 2011). In a 2019 case report, a 60-year-old HIV-negative man with chronically relapsing CM had a decreased concentration of MBL in his serum, supporting the finding that MBL deficiency increases CM risk (Wagemakers et al., 2019). Unfortunately, the patient's MBL2 gene was not genotyped, otherwise, it may have revealed whether the observed deficiency in serum MBL had a genetic basis.

TLRs are a highly polymorphic protein family and various studies have implicated TLRs in susceptibility to infections such as malaria (Mockenhaupt et al., 2006), tuberculosis (Ben-Ali et al., 2004), herpes simplex virus (Zhang et al., 2007) and sepsis (Wurfel et al., 2008). In a 2018 study, Jiang et al. carried out the first study to investigate the impact of genetic polymorphisms in TLR genes on *C. neoformans* infection. The study looked at SNPs in the *TLR1, TLR2, TLR4, TLR6* and *TLR9* genes of individuals with non-HIV associated CM of Chinese ancestry. They identified eight TLR SNPs that were associated with CM susceptibility. Among the eight SNPs, six were associated with an increased risk of CM, five were associated with cerebrospinal fluid (CSF) cytokine concentration and two were associated with disease severity. The only SNP that was associated with CM risk, disease severity and CSF cytokine concentration was the rs3804099 SNP on *TLR2* which causes a synonymous mutation. The C/T genotype of the rs3804099 SNP is associated with lower expression of 12 out of the 18 cytokines shown to be associated with severe disease. This genotype was also rare in individuals with severe disease (OR = 0.39; 95% CI [0.15-1.00]; p = 0.046), suggesting that heterozygosity of the rs3804099

SNP decreases risk of severe disease by preventing the over-expression of these cytokines in the CNS. Meanwhile, the T/T genotype of rs3804099 was associated with increased risk of CM (OR = 1.47; 95% CI [1.02-2.11]; p = 0.036). Overall, the study concluded that polymorphisms in TLRs have a causal role in *C. neoformans* pathogenesis (Jiang et al., 2018), thereby supporting the need for further research to clarify the mechanisms by which TLRs are involved in macrophage response to infection.

The genetic studies described so far have mainly included volunteers of Han Chinese or European Ancestry. Despite sub-Saharan Africa having the highest burden of cryptococcal disease, few genetic studies have focused on people of African descent. To combat this lack of representation, Kannambath et al. (2020) performed the first genome-wide association study (GWAS) of genetic susceptibility to cryptococcosis in HIV-positive people of African descent. They found that the top hits were located within 2.5kb upstream of the Colony Stimulating Factor 1 (*CSF1)* gene which codes for Macrophage (M)-CSF, a cytokine that promotes monocyte or macrophage differentiation, activation, and phagocytosis. It has been shown that exogenous M-CSF promotes anti-cryptococcal immune response (Nassar et al., 1994; Kannambath et al., 2020); thus, polymorphisms in and around the *CSF1* gene that result in decreased expression of the gene may increase risk of cryptococcal disease.

Granulocyte-macrophage colony-stimulating factor (GM-CSF) is another cytokine involved in macrophage phagocytosis, chemotaxis, and in the regulation of macrophage shift towards a proinflammatory phenotype (Ushach and Zlotnik, 2016). Autoantibodies

against GM-CSF are known to cause acquired pulmonary alveolar proteinosis (PAP), a condition where surfactant, composed of 90% lipids, 9% surfactant protein and 1% carbohydrate, build up in the alveoli leading to impaired gas exchange in the lungs (Trapnell et al., 2003; Kitamura et al., 1999; Tanaka et al., 1999). In these patients, anti-GM-CSF autoantibodies impair the function of alveolar macrophages leading to an inability of macrophages to clear pulmonary surfactant and maintain surfactant homeostasis (Trapnell et al., 2003). Individuals with PAP are at an increased risk of a range of lung infections, including reports of patients presenting with cryptococcosis (Sunderland et al., 1972; Salvator et al., 2022; Rosen et al., 1958; Bergman and Linell, 1961). However, anti-GM-CSF autoantibodies can also increase the risk of cryptococcosis and CM in immunocompetent hosts independent of PAP diagnosis (Salvator et al., 2022; Rosen et al., 2013; Goupil de Bouillé et al., 2022; Arango-Franco et al., 2023). Anti-GM-CSF autoantibodies increase risk of disease caused by both *C. neoformans* and *C. gattii* (Saijo et al., 2014; Viola et al., 2021). Anti-GM-CSF autoantibodies from CM patients were able to inhibit GM-CSF-dependent STAT-5 activation and MIP-1α chemokine production (Rosen et al., 2013; Arango-Franco et al., 2023), indicating that these autoantibodies have neutralizing activity. Thus, anti-GM-CSF autoantibodies impair macrophage function, enabling cryptococcus survival, proliferation and dissemination. Further work is needed to understand the mechanisms by which GM-CSF signalling directly impacts host response to cryptococcus.

There has also been a case of cryptococcosis in a patient with autoantibodies against IFNγ; however, this patient was also positive for *Mycobacterium abscessus* and varicella-

zoster virus infection (Rujirachun et al., 2020). Anti-IFNγ autoantibodies are typically associated with increased risk of nontuberculous mycobacterial infection (Browne et al., 2012; Kampmann et al., 2005); therefore, the presence of cryptococcosis in this patient may not be directly related to anti-IFNγ autoantibodies.

Continued research into identifying polymorphisms that increase cryptococcosis risk will have clinical applications as well as revealing unexpected genes and pathways involved in immune response to *C. neoformans* infection.

1.5 Genetic factors that contribute to Cryptococcus virulence

In addition to the human genotypic factors that impact disease outcome, it is relevant to note that there also exist cryptococcal genetic factors that contribute to its pathogenicity and virulence (Montoya et al., 2021). *C. neoformans* is divided into three major lineages VNI, VNII and VNB and there is significant diversity within and between lineages (Cuomo et al., 2018). Cryptococcus strains vary in their ability to infect mammalian cells, their ability to disseminate from the lungs to the CNS, and the severity of the disease they cause (Kwon-Chung et al., 2010; Esher et al., 2018; Litvintseva and Mitchell, 2009). For example, the VNB lineage is further divided into VNBI and VNBII with the VNBII lineage being predominantly confined to clinical isolates while VNBI is present in both clinical and environmental isolates (Desjardins et al., 2017; Vanhove et al., 2017). A GWAS study comparing VNBI and VNBII lineages found that VNBI clinical isolates were significantly more melanised and more resistant to ROS than VNBII clinical isolates (Desjardins et al., 2017). Moreover, within the VNBI lineage, environmental

isolates were more melanised and resistant to ROS than clinical isolates, suggesting that melanisation is more relevant during exposure to environmental stressors than host stress. Loss of function mutations in the transcription factor, BZP4, was associated with reduced melanisation capabilities in four clinical strains, two of which were from the VNB1 lineage and two from the VNBII lineage (Desjardins et al., 2017).

In another GWAS study, human survival and other clinical parameters were compared with the whole-genome sequence of 38 *C. neoformans* isolates (Gerstein et al., 2019). They identified 40 Cryptococcus genes that were significantly associated with patient survival, cytokine expression, and clinical parameters. To examine the biological relevance of these genes, 17 deletion strains were created and used to infect mice. Compared to the control strain, three of the deletion strains led to increased mice survival, while three led to decreased mice survival (Gerstein et al., 2019).

It is also thought that the natural genetic variation in *C. neoformans*, evolved from its interaction with its natural environmental predator, the amoeba, and contribute to its virulence to mammalian cells (Steenbergen et al., 2001). This is supported by findings that *C. neoformans* strains deficient in capsule polysaccharide are readily phagocytosed and killed by the amoeba, *Acanthamoeba castellanii* (Steenbergen et al., 2001). Which is consistent with the knowledge that the *C. neoformans* capsule is a major virulence factor during mammalian infection. It was also shown that *C. neoformans* have a similar transcriptional profile after phagocytosis by amoebae and macrophages (Derengowski et al., 2013). However, the extent to which cryptococcus' co-evolution with amoebae

impacts its pathogenesis towards mammalian host and the genetic architecture of virulence remains poorly understood.

1.6 Research Rationale and Aims

Despite advances in medicine, infections with fungal diseases have a case-fatality rate ranging from 20% to 70% and are responsible for over 1.5 million deaths annually (Bongomin et al., 2017; Rodrigues and Nosanchuk, 2020; Rajasingham et al., 2017). The poor outcome observed following *C. neoformans* infection reveals an urgent need to understand the precise immune signalling pathway(s) triggered by the infection and identify the key immune modulators that could serve as novel avenues for immunotherapeutic development.

One of the first interactions following *C. neoformans* inhalation is between *C. neoformans* and macrophages. It is clear that there exists a positive correlation between the level of phagocytosis and *C. neoformans* virulence (Hansakon et al., 2018; Diamond et al., 1972). Moreover, this interaction between macrophages and *C. neoformans* is likely a predictor of disease outcome; however, there is no clear understanding of the mechanism by which macrophages detect and phagocytose *C. neoformans,* neither is there an understanding of the physiological properties of *C. neoformans,* such as EV production, that could modulate phagocytosis. Researchers have used mice deficient in individual PRRs to investigate the involvement of those receptors during host response to infection. However, all the receptors investigated thus far, including TLR4, TLR2, Dectin-1, and Dectin-2, have revealed contradictory results. Mice present a relatively

complex system and the contradictions observed between studies could be attributed to minor differences in experimental design such as the mode of infection (intranasal vs intravenous) and/or the infection load. Hence this project aims to utilise an *in vitro* approach to identify the pattern recognition receptor(s) critical to the detection and phagocytosis of non-opsonised *C. neoformans*, beginning with the hypothesis that TLR4 is one such critical receptor. Using an *in vitro* approach will reduce the number of confounding variables and allow for the investigation of phagocytosis specifically. The contribution of TLR4 during phagocytosis was first studied using chemical inhibitors of TLR4, then macrophages isolated from TLR4-deficient mice were utilised for validation. Moreover, the study focused on infection with non-opsonised *C. neoformans* since the role of opsonins in the lung mucosa remains unclear and opsonising antibodies are thought to be negligible within the healthy lung (Mitchell and Perfect, 1995), therefore, the level of non-opsonic uptake is likely a critical determinant of the subsequent course of an infection. It is also thought that the presence of opsonin-coated microbes reflect activation of the adaptive immune response so the resulting macrophage response may not be as robust as that triggered by the recognition of microbes displaying only PAMPs (Fu and Harrison, 2021). Hence, a focus on non-opsonised infection will reflect host-pathogen interaction at the earliest stages of infection. Secondly, this PhD seeks to investigate the consequence of *C. neoformans* factors on phagocytosis by exploring the role of EV production on phagocytosis. Finally, it will explore the correlation between natural variation in cryptococcus resistance to amoebae and virulence in mammalian macrophages as measured by phagocytic index and intracellular proliferation. This will

provide some insight into the validity of the accidental pathogenesis theory by revealing whether cryptococcus virulence in amoebae correlates with virulence in macrophages.

Chapter 2 Materials & Methods

2.1 Tissue Culture

To investigate the role of TLR4 during anti-cryptococcal immune response, I reasoned that utilising an *in vitro* based approach that focused on early cryptococcus-macrophages interaction, specifically, the process of phagocytosis, would minimise the impact of confounding variables on experimental outcomes. A range of murine macrophage cell lines were used in *in vitro* infection assays.

2.1.1 J774A.1 Macrophages

J774A.1 [ECACC] is a murine macrophage cell line that was derived from a female BALB/c mouse with reticulum cell sarcoma (Ralph et al., 1975). J774A.1 cell line was cultured in T-75 flasks [Fisher Scientific] in Dulbecco's Modified Eagle medium, low glucose (DMEM) [Sigma-Aldrich], containing 10% non-heat inactivated fetal bovine serum (FBS) [Sigma-Aldrich], 2 mM L-glutamine [Sigma-Aldrich], and 1% Penicillin and Streptomycin solution [Sigma-Aldrich] at 37°C and 5% CO_2. Cells were passaged when 70% to 90% confluent by scraping and resuspending in fresh complete DMEM at a ratio of 1:3 to 1:6. Macrophage cultures were used in infection assays between passage 3 and 15. During these infection assays, J774A.1 macrophages were seeded at a concentration of $1x10^5$ cells/mL on a 24-well plate [Greiner Bio-One].

2.1.2 Immortalised Mice Bone Marrow Derived Macrophages (iBMDMs)

Bone marrow derived macrophages (a kind gift from Prof Clare Bryant, University of Cambridge, Cambridge, UK) were originally isolated from C57BL/6 wildtype, *Tlr4*$^{-/-}$, *Myd88*$^{-/-}$ and *Trif*$^{-/-}$ mice as previously described (Harris et al., 2011; Sakai et al., 2017; Latty et al., 2018). The cells were immortalised via transformation with retrovirus expressing Raf and Myc, two well-known oncogenes (Harris et al., 2011). Gene knockouts were validated in house by measuring LPS-induced IL12p40 production using ELISA. Immortalised BMDMs were cultured in DMEM, low glucose [Sigma-Aldrich] supplemented with 10% heat-inactivated FBS [Sigma-Aldrich], 2 mM L-glutamine [Sigma-Aldrich], and 1% Penicillin and Streptomycin solution [Sigma-Aldrich] at 37°C and 5% CO_2. Cells were passaged when 70% to 90% confluent by scraping and resuspending in fresh complete DMEM at a ratio of 1:3 to 1:6. Macrophage cultures were used in assays between passage 3 and 10. During these infection assays, iBMDMs were seeded at a concentration of $3x10^5$ cells/mL on a 24-well plate.

2.1.3 Max Plank Institute (MPI) Cells

MPI cells are a non-transformed, GM-CSF-dependent murine macrophage cell line that is functionally similar to alveolar macrophages (Fejer et al., 2013). In this project, MPI cells from wildtype, *Msr1*$^{-/-}$, *Marco*$^{-/-}$ and *MSR1/MARCO* double knockout (*DKO*) C57BL/6 mice were utilised (kind gift from Prof Siamon Gordon, Oxford University, UK and Dr Subhankar Mukhopadhyay, King's College London, UK). MPI cells were validated as macrophages by measuring the expression of myeloid cell-specific surface markers and their global gene expression profile (Fejer et al., 2013). Knockout MPI cells were

authenticated using immunofluorescence staining and qPCR. Macrophages were cultured in Roswell Park Memorial Institute (RPMI) 1640 Medium [ThermoFisher] supplemented with 10% heat-inactivated FBS [Sigma-Aldrich], 2 mM L-glutamine [Sigma-Aldrich], and 1% Penicillin and Streptomycin solution [Sigma-Aldrich] at 37°C and 5% CO_2. To subculture macrophages, culture media was recovered into a 50 mL Falcon tube, and cells were washed twice with Dulbecco's phosphate buffered saline (DPBS) without calcium chloride and magnesium [Sigma-Aldrich]. They were then incubated with PBS-EDTA for 10 mins at 37°C to detach cells [Lonza]. Detached cells were recovered and centrifuged at 200xg for 5 mins to pellet cells. The pellet was resuspended in 4 mL complete RPMI and reseeded in T75 flasks at a ratio of 1:6. Finally, GM-CSF conditioned media was added to each flask at 1% to 5% vol/vol. GM-CSF conditioned media was prepared by seeding the X-63-GMCSF cell line (Zal et al., 1994) at a density of $2.5x10^5$cells/mL in T75 flasks in complete RPMI. Cells were incubated at 37°C and 5% CO_2 for 7 days. After 7 days, the supernatant was collected, clarified by centrifugation at 200xg for 5 mins and filtered through a 0.45 μm filter. GM-CSF conditioned media was stored in 1 mL aliquots at -80°C. When being used in infection assays, MPI cells were seeded at a density of $2x10^5$ cells/mL on a 24-well plate supplemented with 1% GM-CSF.

2.1.4 Freezing cells for long-term storage

Long-term storage of macrophage cell lines was achieved by freezing in liquid nitrogen. To do this, cells were recovered either by scraping (J774.A1 and iBMDMs) or via incubation with PBS-EDTA (MPI cells). Once detached, cell suspensions were centrifuged

at 200xg for 5mins, the supernatant was discarded and the pellet was resuspended in freezing media composed of 50% FBS, 40% complete media and 10% dimethyl sulfoxide (DMSO) [Sigma-Aldrich]. Cells were aliquoted in 1.5 mL cryogenic vials at a volume of 1mL, placed in a cell freezing containing, and frozen down at -80°C. After 24 hours, the cells were transferred to liquid nitrogen.

Frozen cells were thawed by recovering from liquid nitrogen, incubating in a 37°C water until fully thawed, transferring into 9 mL fresh media, and centrifuging at 200xg for 5 mins. The supernatant was discarded, and the pellet was resuspended in 10 mL fresh media. All 10 mL suspension was then transferred to a T75 flask and made up to 15 mL.

2.1.5 Isolation of human monocytes and macrophage differentiation

Leukocyte cones used for this study were obtained with ethical approval from the University of Birmingham Science, Technology Engineering and Mathematics Ethical Committee (ERN15_0804c).

Leukocyte cones, from healthy donors, were obtained from the National Health Service Blood Transfusion service (NHSBT) and promptly processed within 4 h. Peripheral blood mononuclear cells (PBMCs) were isolated from the cones using a standard density gradient centrifugation method. Following a DPBS wash, the blood was mixed with an equal volume of DPBS (containing 2% FBS) and carefully layered onto Lymphoprep (StemCell). Centrifugation was carried out at 1100×g for 20 minutes without applying brakes. The resulting white buffy layer was collected and further washed with DPBS by

centrifuging at 300×g for 10 min. Red blood cells (RBC) were removed by using a RBC lysis solution (BioLegend) for 10 min at room temperature. $CD14^+$ monocytes were then isolated from the PBMCs using immunomagnetic positive selection (Miltenyi Biotec). Isolated human monocytes were seeded at a density of 0.5×10^6 cells per well in tissue culture-treated 24-well plates and cultured in complete RPMI 1640 medium supplemented with 10% Human Serum and 20 ng/mL human GM-CSF (PeproTech) for macrophage differentiation. Cells were incubated for 6 days, with medium replacement on day 3.

2.1.6 Isolation of murine peritoneal macrophages

Mice culling and isolation of resident peritoneal macrophages was performed by Dr Subhankar Mukhopadhyay at the Sir William Dunn School of Pathology, University of Oxford under their local ethical approval. After mice killing, 8 mL cold 1xDPBS (without calcium and magnesium) was injected into the peritoneal cavity. The abdomen was then massaged gently and fluid containing all peritoneal exudate cells was collected into 15mL Falcon tubes. I placed the collected cell suspension into a polystyrene box with ice packs and transported them on the train from Oxford to Birmingham.

Once in Birmingham, tubes were centrifuged at 200xg for 5 min. Red blood cells were removed by using a RBC lysis solution for 10 min at room temperature. Cells were counted and seeded at a density of $3x10^5$ cells per well in RPMI and incubated overnight at 37°C and 5% CO_2.

2.2 *Cryptococcus neoformans* strains

To study the role of TLR4 during phagocytosis, the *Cryptococcus neoformans* var. *grubii* serotype A strain KN99 mating type α (KN99α) that was biolistically transformed to express green fluorescent protein (GFP) was used (Voelz et al., 2010). KN99α-GFP cells were recovered from MicroBank vials stored at -80°C by streaking onto yeast extract-peptone-dextrose (YPD) agar (50 g/L YPD broth powder [Sigma-Aldrich], 2% Agar [MP Biomedical]), thereby creating stock plates used for about 1 month. The stock plates were incubated at 25°C for 48 h then stored at room temperature until needed.

To study the contribution of *Cryptococcus* EVs in phagocytosis, WTKN99α, *gat5Δ*, *hap2Δ*, *gat5Δ::GAT5* and *hap2Δ::HAP2* were received from collaborators at the Pasteur Institute (Dr Juliana Rizzo and Dr Guilhem Janbon) (Rizzo et al., 2023). These mutants were identified by screening a transcription factor knockout library produced by (Jung et al., 2015) for EV production. The WTKN99α, *gat5Δ*, *hap2Δ*, *gat5Δ::GAT5* and *hap2Δ::HAP* cells in a KN99α background were sent on filter paper and recovered by placing each filter paper on YPD agar plate and incubating at 25°C for 48 h. After 48 h, cells were picked with a 1μl inoculation loop, resuspended in 3mL YPD broth (50 g/L YPD broth powder [Sigma-Aldrich]) and incubated at 25°C overnight under constant rotation (20rpm). The following day 200 μl of cell suspension was added to a Microbank vial and stored at -80°C. When needed for a phagocytosis assay, stock plates were prepared as described above.

To study the parallels between *C. neoformans* virulence in amoebae and macrophages, 11 *Cryptococcus* strains, 9 of which were F1 progeny from crosses of genetically diverse parental strains (Bt22 x Ftc555-1), were received from collaborators at Duke University (Dr Thomas Sauters and Prof Paul Magwene) (Table 2.1). The cells were sent on filter paper and recovered by placing each filter paper on YPD agar plate and incubating at 25°C for 48 h as described above. The parental strains, Bt22 and Ftc555-1, used in the crosses for quantitative trait loci (QTL) mapping were chosen to maximise genetic diversity. The Bt22 strain is a clinical isolate from the VNBI lineage while Ftc555-1 is an environmental strain also from the VNBI lineage. My end of this collaboration focused on measuring the phagocytosis and intracellular proliferation of cryptococcus parents and segregants in J774A.1 macrophages to investigate the association between cryptococcus virulence to mammalian cells and their resistance to amoebal predation.

Table 2.1: List of Cryptococcus parents and segregants received from Dr Thomas Sauters and Prof Paul Magwene (Duke University, Durham, North Carolina, USA).

Collection number	Cross designation	Strain name	Resistance to Amoebae
PMY2649	Parent	Bt22	Medium
PMY2650	Parent	Ftc555-1	High
PMY2776	Segregant		High
PMY2765	Segregant (S5)		High
PMY2768	Segregant (S4)		High
PMY2745	Segregant		Medium
PMY2747	Segregant		Medium
PMY2715	Segregant		Medium
PMY2570	Segregant (S3)		Low

PMY2581	Segregant (S1)		Low
PMY2911	Segregant (S2)		Low

2.3 *Candida albicans* strains

To investigate macrophage response to *Candida albicans*, a CAF2-1 *Candida albicans* expressing dTomato fluorescent protein (Caf2-dTomato) was used (Gratacap et al., 2013). Prior to the phagocytosis assay, a colony was suspended in 10 mL YPD broth and incubated overnight at 30°C and 180 rpm. Prior to their use in infection, the *C. albicans* overnight culture was diluted 1:100 in fresh YPD broth, then incubated at 30°C and 180 rpm for 3 h till cells were in exponential phase. Cells in exponential phase were washed with PBS, counted and macrophages were infected at a multiplicity of infection of 5 *C. albicans* to 1 macrophage for 45 mins.

To explore non-lytic expulsion of *Candida albicans,* a yeast-locked *C. albicans* strain was used (a kind gift from Hung-Ji Tsai, University of Birmingham, Birmingham, United Kingdom). The yeast-locked TetOn-NRG1 *C. albicans* strain constitutively express the Nrg1 transcription factor, thereby preventing yeast to hypha transition (Ost et al., 2021). Macrophages were infected at MOI 2:1. Timelapse imaging began immediately after macrophage infection.

2.4 Phagocytosis Assay

Phagocytosis assays were performed to measure the uptake of cryptococci by macrophages under various conditions (Figure 2-1). Twenty-four hours before the start

of the phagocytosis assay, the desired number of macrophages were seeded onto 24-well plates in 400 µl complete culture media. The cells were then incubated overnight at 37°C and 5% CO_2. At the same time, a colony of the desired cryptococcus strain(s) was picked from the stock plate and resuspended in 3 mL liquid YPD broth. The culture was then incubated at 25°C overnight under constant rotation (20 rpm).

On the day of the assay, macrophages were activated using 150 ng/ml phorbol 12-myristate 13-acetate (PMA) [Sigma-Aldrich] for 1 h at 37°C. PMA is a known activator of protein kinase C (PKC), a kinase that activates a wide range of proteins involved in apoptosis, membrane remodelling and NF-κB activation (Smith et al., 1998). PMA is also used to differentiate the THP1 human monocyte cell line into a macrophage-like cell (Chanput et al., 2014). PMA stimulation was performed in media containing heat-inactivated serum (iBMDMs, MPI cells and peritoneal macrophages) or in serum-free media (J774A.1) to eliminate the contribution of complement proteins during phagocytosis. In some cases, MPI cells were stimulated with 100 ng/mL LPS for 1 h instead of PMA since there is evidence to show that LPS stimulation induces MARCO expression (Kissick et al., 2014; Jing et al., 2013). Primary human monocyte-derived macrophages were not exposed to PMA. Instead, naïve M0 macrophages were serum starved for 2 h prior to the assay to remove the effects of serum opsonins and minimise serum-induced cryptococcus capsule enlargement (Zaragoza et al., 2008).

Where applicable, macrophages were then treated with the desired concentration of soluble inhibitors of PRRs or known ligands of PRRs (Table 2.2) and incubated at 37°C for

1 h. Meanwhile pre-treatment with the general scavenger receptor ligand, oxidized low-density lipoprotein (ox-LDL), or the MARCO ligand polyG occurred for 30 min. Pre-treatment with neutralising antibodies occurred for 30 min. The concentration of each molecule is indicated in Table 2.2 and in the corresponding results.

To prepare *C. neoformans* for infection, overnight *C. neoformans* cultures were washed two times in 1X DPBS and centrifuged at 6500 rpm for 2.5 mins. To infect macrophages with non-opsonised *C. neoformans*, after the final wash, the *C. neoformans* pellet was resuspended in 1 mL PBS, counted using a hemacytometer, and fungi was incubated with macrophages at a multiplicity of infection (MOI) of 10:1. The infection was allowed to take place for 2 h at 37°C and 5% CO_2. Infection occurred in the presence of soluble inhibitors. When treatment with soluble inhibitors was not needed, PMA stimulation of macrophages was directly followed by infection with *C. neoformans*.

In some instances, macrophages were infected with antibody-opsonised *C. neoformans*. To opsonise the fungi, pellet was resuspended in 1 mL PBS, and the number of yeast cells was counted using a haemocytometer. Then $1x10^6$ yeast cells in 100 µl PBS were opsonised for 1 hour using 10 µg/mL anti-capsular 18B7 antibody (a kind gift from Arturo Casadevall, Johns Hopkins University, Baltimore, Maryland, USA).

After 2 h of infection, macrophages were washed 4 times with PBS to remove as much extracellular *C. neoformans* as possible. The cells were then imaged as described in Chapter 2.6.1.

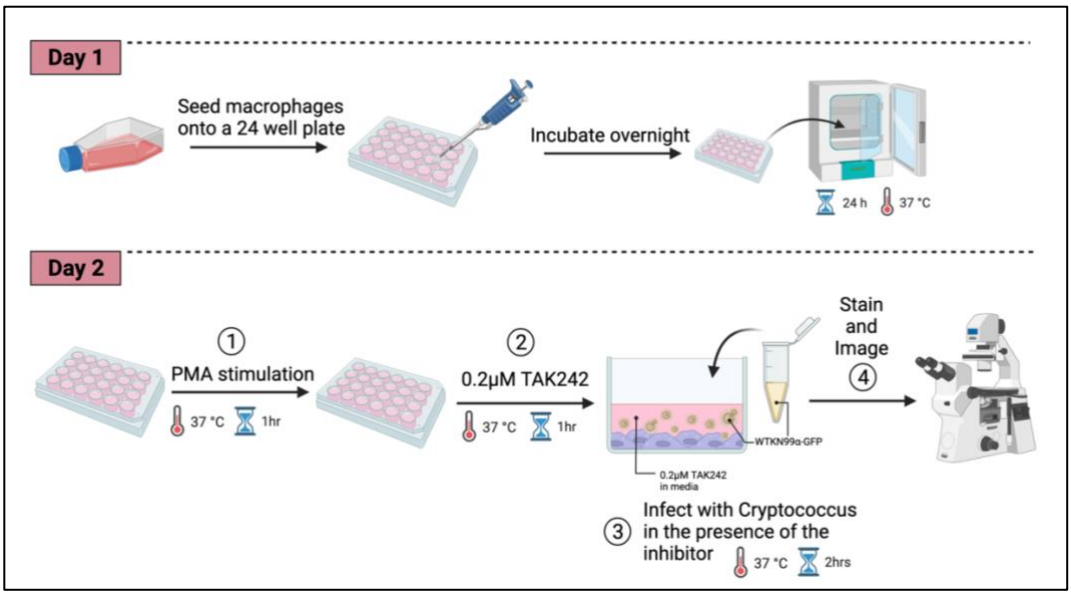

Figure 2-1: Representative phagocytosis assay in J774 macrophages treated with the TLR4 inhibitor, TAK-242. Figure created with BioRender.com.

Table 2.2: List of all inhibitors, competitive ligands, and blocking antibodies used to interfere with macrophage pattern recognition receptor (PRR) activity.

Molecule Name	Target Receptor	Concentration Used	Mode of Action	Cat# [Brand]
TAK-242	TLR4	0.2 µM	Selectively binds to Cys747 of TLR4 and disrupts its interaction with the adaptor molecules, TIRAP and TRAM.	614316 [Sigma-Aldrich]
Low Density Lipoprotein from Human Plasma, oxidised (ox-LDL)	Scavenger Receptors	10 µg/mL	A known scavenger receptor ligand	L34357 [ThermoFisher]
CU CPT 22	TLR2/1	1µM	Competes with lipoproteins for binding to TLR2/1 and inhibits the release of proinflammatory cytokines TNF-α and IL-1β.	4884 [Tocris]

ODN-2088	TLR9	1µM	An inhibitory sequence that disrupts the colocalization of CpG oligonucleotides with TLR9 in the endosome	tlrl-2088 [InvivoGen]
TLR3/dsRNA Complex Inhibitor	TLR3	1 µM – 10 µM	A specific and competitive inhibitor of dsRNA binding to TLR3	614310 [Sigma-Aldrich]
Pepinh-MYD	MyD88	20 µM	A peptide that inhibits the homodimerization of MyD88	tlrl-pimyd [InvivoGen]
Pepinh-TRIF	TRIF	20 µM	An inhibitory peptide that obstructs TLR-TRIF interaction.	tlrl-pitrif [InvivoGen]
B1605906	Inhibitor of nuclear factor kappa-B kinase subunit beta (IKKβ)	5 µM	Binds to IKKβ and prevents the activation of NF-κB.	A kind gift from Dario Alessi, University of Dundee
MRT67307	TANK-binding kinase 1 (TBK1)	10 µM	Blocks the activity of TBK1 and IKKε thereby preventing the activation of IRF3.	A kind gift from Dario Alessi, University of Dundee
Piceatannol	Spleen Tyrosine Kinase (SYK)	50 µM and 75 µM	Blocks SYK-dependent downstream signalling	P0453 [Sigma]
Wortmannin	Phosphatidyl inositol 3-kinase (PI3K)	0.1 µM and 20 µM	Irreversible covalent inhibitor of PI3K	S2758 [Selleck Chemicals)

Rat anti-mouse CD16/CD32	FcγRIII/ FcγRII	1.25 μg/mL; 2.5 μg/mL	Recognises a shared extracellular epitope on FcγRIII (CD16) and FcγRII (CD32).	553142 [BD Biosciences]
Rat IgG2b κ	Rat isotype control	1.25 μg/mL	Isotype control	15228759 [Invitrogen]
PD184352	Extracellular signal-regulated kinase 1/2 (ERK1/2)	5 μM	A selective inhibitor of MEK1/2, kinases directly upstream of ERK1/2. MEK inhibition blocks the phosphorylation of ERK1/2	A kind gift from Dario Alessi, University of Dundee
VX-745	p38	5 μM	Binds to p38α and inhibits its downstream signalling	A kind gift from Dario Alessi, University of Dundee
JNK-IN-8	c-Jun N-terminal kinase (JNK)	10 μM	Binds the catalytic site of JNK1/2, thereby preventing the phosphorylation of c-Jun transcription factor.	A kind gift from Dario Alessi, University of Dundee
Polyguanylic Acid Potassium Salt	MARCO	400 μg/mL	A MARCO ligand that acts as a competitive inhibitor	P4404 [Sigma]
Rat anti-mouse MARCO ED31 clone	MARCO	1 μg/mL; 10 μg/mL	Recognises epitope on the C-terminal cysteine rich domain of MARCO and blocks ligand binding.	MCA1849 [Bio-Rad]
Rat IgG1 κ	Rat isotype control	1 μg/mL	Isotype control	14-4301-82 [Invitrogen]

2.5 Traditional Intracellular Proliferation Rate (IPR) Assay

To measure proliferation of *C. neoformans* in macrophages, an intracellular proliferation rate assay was performed by lysing macrophages 0 h and 18 h post infection and counting the number of cryptococcus in the lysate. To perform a conventional intracellular proliferation rate (IPR) assay, a phagocytosis assay was carried out as described in Chapter 2.4. After 2 h of infection, extracellular fungi were washed off using 1X DPBS, marking 0 h post infection (T0). For the T18 wells, 400 µl of culture medium was added back into the wells after washing and returned to the incubator at 37°C and 5% CO_2 for 18 h. Meanwhile, for the T0 wells, 200 µl of sterile distilled water was added and incubated at 37°C for 20-30mins to lyse the macrophages. The 200 µl lysate was collected and added to 1.5 mL Eppendorf tubes, then an additional 200 µl of sterile distilled water was added to collect any leftover cells, resulting in a final volume of 400 µl lysate recovered from each T0 well. The number of *C. neoformans* cells in the lysate was quantified using a haemocytometer. The same procedure was carried out after 18 hours, then IPR was calculated by dividing the number of fungi in the lysate at T18 by the number of fungi in the lysate at T0 (IPR = T18/T0).

The viability of *C. neoformans* in each lysate was determined by diluting the lysate to get a concentration of 200 yeast cells per 100 µl and plating it onto YPD agar. Plates were incubated at 25°C for 48 h after which the colony forming units (CFU) were counted.

This method of measuring IPR has several drawbacks. Firstly, it is very difficult to ensure that all the extracellular fungi have been wash off, therefore, the lysate likely includes

fungal cells that were never phagocytosed. Additionally, the counting of fungi using haemocytometer is time consuming and leaves room for human error. Therefore, an alternative approach to quantifying IPR that involved live-cell imaging was also utilised. This technique will be described in Chapter 2.6.2.

2.6 Microscopy

2.6.1 Fluorescence Microscopy Imaging

Having washed off extracellular cryptococci, the number of phagocytosed fungi was quantified from images from a fluorescent microscope. To distinguish between phagocytosed and extracellular *C. neoformans,* wells were treated with 10 µg/mL calcofluor white (CFW) [Sigma-Aldrich], a fluorochrome that recognises cellulose and chitin in cell walls of fungi, parasite and plants (Hageage and Harrington, 1984), for 10 mins at 37°C. The wells were then washed twice with PBS. Fluorescent microscopy images were acquired using the Zeiss Axio Observer [Zeiss Microscopy] fitted with the ORCA-Flash4.0 C11440 camera [Hamamatsu] at 20X magnification. The phase contrast objective, EGFP channel (excitation wavelength: 489 nm; emission wavelength: 509 nm) and CFW channel (excitation wavelength: 350 nm; emission wavelength: 432 nm) were used. Image acquisition was performed using the ZEN 3.1 Blue software [Zeiss Microscopy] and the resulting images were analysed using the Fiji image processing software [ImageJ] (Figure 2-2).

When *Cryptococcus* strains were not fluorescently labelled, images were acquired using the Nikon Eclipse Ti inverted microscope [Nikon] fitted with the QICAM Fast 1394

camera [Hamamatsu]. This was because the camera provided more contrast between macrophages and internalised fungi than the Zeiss Axio Observer. Images were acquired on the Nikon NIS Elements software [Nikon] using the phase contrast objective and CFW channel. Images were analysed using the Fiji image processing software [ImageJ].

To quantify the number of phagocytosed *Cryptococcus*, the total number of ingested *C. neoformans* was counted in 200 macrophages, then the values were applied to the following equation: ((number of phagocytosed *C. neoformans*/ total number of macrophages counted) * 100). Alternatively, when infecting macrophages with non-fluorescent *Cryptococcus*, a measure termed phagocytic index (PI) was used to quantify the percentage of macrophages that phagocytosed at least one *Cryptococcus* cell. This was because it was more difficult to quantify the precise number of internalised fungi without introducing excessive human error. PI was calculated using the following equation: ((number of infected macrophages/ total number of macrophages counted) * 100%).

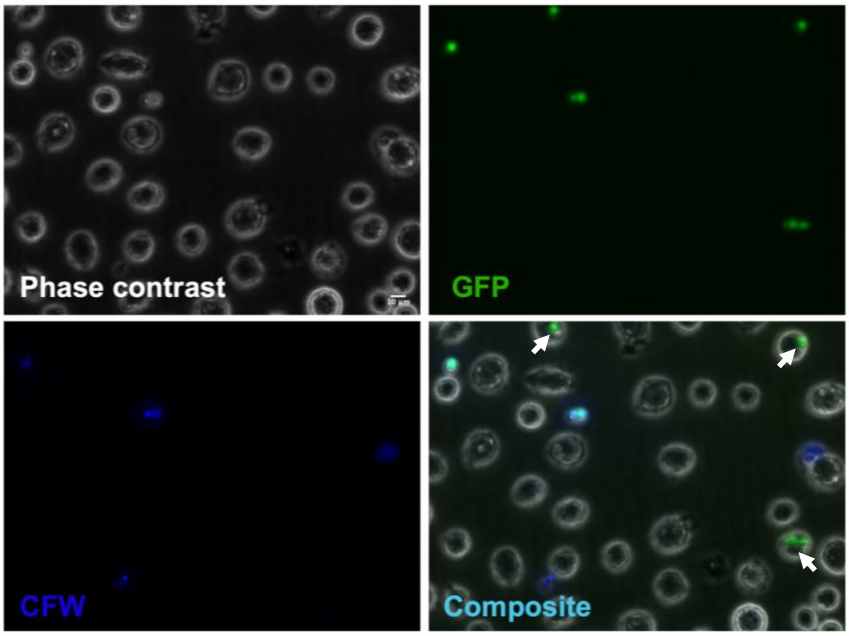

Figure 2-2: A typical fluorescent microscopy image following a phagocytosis assay. In this figure, *Marco*$^{-/-}$ macrophages were infected with non-opsonised WTKN99α-GFP. After infection, calcofluor white (CFW) was used to distinguish between intracellular and extracellular cryptococci. To quantify phagocytosis, the number of individual *Cryptococcus* cells within 200 macrophages were counted then expressed as the number of internalised fungi per 100 macrophages. White arrows show macrophages with internalised fungi.

2.6.2 Timelapse Imaging

As an alternative approach to assess the IPR of *Cryptococcus* strains within macrophages, infected macrophages were captured at a regular interval over an extended period. Live-cell imaging was performed by running the phagocytosis assay as usual, then after washing off extracellular *Cryptococcus* with PBS 4 times, the corresponding media for the macrophage cell line was added back into the well before imaging. Live-cell imaging occurred using either the Zeiss Axio Observer or the Nikon Eclipse Ti at 20X magnification. Images were acquired every 5 min for 18 h at 37 °C and 5% CO_2.

The resulting videos were analysed using Fiji [ImageJ] and IPR was determined by quantifying the total number of internalised fungi in 200 macrophages at the 'first frame' (time point 0 (T0)) and 'last frame' (T10). The resulting values were used in the following equation: ((number of phagocytosed *C. neoformans*/ total number of macrophages counted) * 100). Then, the number of phagocytosed fungi per 100 macrophages at T10 was divided by the number of phagocytosed fungi at T0 to give the IPR (IPR = T10/T0). With the timelapse approach of quantifying IPR, IPR was quantified after 10 h and not 18 h because macrophages began to lyse after 10 h, and the wells began to be dominated by extracellular fungi that were not washed off or fungi proliferating within the media.

To quantify vomocytosis/ non-lytic expulsion, at least 200 macrophages were observed, and the time-lapse videos were scored according to the following guidelines established by Gilbert et al 2017:

1. One vomocytosis event is the expulsion of internalized cryptococci from an infected macrophage, regardless of the number of cryptococci expelled if they do so simultaneously.
2. Vomocytosis events are scored as independent phenomena if they occur in different frames or from different macrophages.
3. Vomocytosis events are discounted if the host macrophage subsequently undergoes lysis or apoptosis within 30 min.

2.6.3 Staining and Confocal Microscopy

Immunofluorescence was used to investigate receptor localisation on macrophages. Firstly, 13 mm cover slips were placed onto 24-well plates prior to seeding with desired number of macrophages. After overnight incubation, macrophages were used in a standard phagocytosis assay as described in chapter 2.4. Before staining, macrophages were fixed with 4% paraformaldehyde for 10 min at room temperature and permeabilised with 0.1% Triton X-100 diluted in PBS for 10 min at room temperature. Cells were treated with 1% BSA diluted in 1X DPBS for 30 min to block non-specific interactions. To stain for MSR1 localisation after infection with GFP-expressing *C. neoformans*, 5 μg/mL rat anti-mouse CD204-PE [Fisher Scientific; Cat#: 12-204-682; Clone M204PA] diluted in 1% BSA was used as the primary antibody. Cells were incubated with the primary antibody for 1 h at room temperature. After washing twice with DPBS, macrophages were incubated with 5 μg/mL AlexaFluor 594 goat anti-rat IgG secondary antibody [ThermoFisher Scientific; Cat#: A-11007] diluted in 1% BSA for 1 h at room temperature in the dark.

Alternatively, MSR1 was stained using rabbit anti-mouse MSR1 (E4H1C) (1:100) [Cell Signalling Technology; Cat#: 91119; Clone E4H1C] as the primary antibody, and Alexa Fluor 594 conjugated anti-rabbit IgG F(ab')$_2$ fragment secondary antibody (1:500) [Cell Signalling Technology; Cat#: 8889S] for 1 h at room temperature and in the dark.

F-actin filaments were stained using 2 units of rhodamine-conjugated phalloidin stain [Invitrogen; Cat#: R415] diluted in 400 μl 1% BSA in 1X DPBS and incubated for 20 mins at room temperature.

Next, macrophages were washed with DPBS two times, then counterstained with 0.5 μg/mL DAPI for 5 mins at room temperature to visualize the nucleus. After DPBS washes and a final wash with sterile dH_20, coverslips were carefully removed from the wells, blotted to remove excess water, and mounted using Fluoromount mounting medium [Sigma; Cat#: F4680] onto glass slides. Slides were left to set prior to imaging. Images were acquired using the Zeiss LSM880 Confocal with Airyscan2, laser lines 405, 488, 561 and 640 nm, and at 63X or 100X oil magnification. Image acquisition was performed using the ZEN 3.0 Black software [Zeiss Microscopy] and the resulting images were analysed using the Fiji image processing software [ImageJ].

2.7 Flow Cytometry

Flow cytometry was used to measure the surface expression of scavenger receptors on macrophages or to measure the immunofluorescence of macrophages. Macrophages were seeded at desired density in a 24-well plate, then incubated overnight at 37°C and 5% CO_2. The following day, macrophages were exposed to desired treatments prior to staining.

To stain macrophages, wells were incubated with 200 μL 1X TrypLE Express Enzyme [ThermoFisher] for 5-10 mins at 37°C to detach the cells from the wells. After incubation,

200 μL 1X PBS was added to each well and the bottom of the wells was scratched with a pipette tip to lift any cells still adhered to the well. The suspension was then transferred to a 1.5 mL Eppendorf tube. An extra 200 μL PBS was added to each well to recover any leftover cells. Eppendorf tubes were centrifuged at 400xg for 3 mins at 10°C, supernatant was discarded, and pellet was resuspended in 400 μL PBS. Samples were centrifuged again, then pellet was resuspended in 50 μL Fc block and incubated on ice for 10 mins. To prepare Fc block mixture, 2.5 μg/mL rat anti-mouse CD16/CD32 Fc block [BD Biosciences; Cat#: 553142; Clone 2.4G2] diluted in FACS buffer (1X PBS without Mg^{2+} and Ca^{2+} supplemented with 2% heat-inactivated FBS and 2 mM EDTA). EDTA was included in the FACS buffer to limit the formation of aggregates. Fc blocking was performed to minimise the non-specific binding of the Fc region of receptor-directed antibodies to Fc receptors on the surface of macrophages. This ensures that antibodies bind to the target antigen via the Fab region. After Fc blocking, the desired concentration of fluorochrome-conjugated antibodies diluted in FACS buffer was added into each tube still in the presence of Fc block mixture. The following fluorochrome-conjugated antibodies were used: 0.5 μg/mL anti-mouse CD45-PerCP-Cyanine5.5 [ThermoFisher; Cat#: 45-0451-82; Clone 30-F11], 0.25 μg/100 μL anti-mouse CD204-PE [Fisher Scientific; Cat#: 12-204-682; Clone M204PA], 0.25 μg/100 μL CD36-BB515 [BD Biosciences; Cat#: 565933; Clone CRF D-2712], and 10 μL/100 μL anti-mouse MARCO-Fluorescein [Biotechne; Cat#: FAB2956F; Clone 579511]. Fluorescent minus one (FMO) controls, where the samples were stained with all fluorophores except one, were included to aid in setting gating boundaries. Isotype controls were used to check for non-specific binding. The following isotype control antibodies were used: 0.25 μg/100

μL PE rat IgG2a, κ isotype control [Fisher Scientific; Cat#: 15248769; Clone eBR2a], 0.25 μg/100 μL BB515 Mouse IgA, κ isotype control [BD Biosciences; Cat#: 565095; Clone M18-254], and 10 μL/100 μL Rat IgG_1 Fluorescein isotype control [Biotechne; Cat#: IC005F; Clone IC0057]. Finally, samples stained with only one fluorophore were used as compensation controls. Antibody staining was incubated on ice and in the dark for 10 min. After staining, samples were washed twice using FACS buffer. Final resuspension was in FACS buffer for single staining and unstained controls and FACS buffer plus 0.2 μg/mL DAPI [ThermoFisher], a live dead stain, for all other samples. Samples were left on ice and in the dark until they were run on the flow cytometer.

Stained samples were run on the Attune NxT flow cytometer [ThermoFisher] configured with four violet filters (440/50, 512/25, 603/48, 710/50), three blue filters (530/30, 590/40, 695/40), and four yellow filters (585/16, 620/15, 695/40, 780/60). Data was acquired using the Attune NxT software v3.1.2 [ThermoFisher]. The resulting data was analysed using the FlowJo v10.8.1 software for MacOS [BD Life Sciences]. Before determining the proportion of macrophages positive for a particular fluorochrome, a gating strategy was employed to achieve the sequential exclusion of debris and doublets. Firstly, a 'Time gate' where Time was presented on the x-axis and forward scatter (FSC)-Area was presented on the y-axis was applied to identify and exclude any gaps or disruption in the flow of cells during the sample run that may be caused by bubbles or clogs. Next, FSC-Area was plotted against side scatter (SSC)-Area to exclude debris, FSC-Height was plotted against FSC-Area to exclude doublets, anti-CD45-PerCP-Cyanine5.5 was used to identify total leukocytes, and DAPI was used to exclude dead cells. The

result of the gating strategy is a CD45-positive population of live macrophages which can then be analysed for their expression of target receptors and immunofluorescence (Figure 2-3).

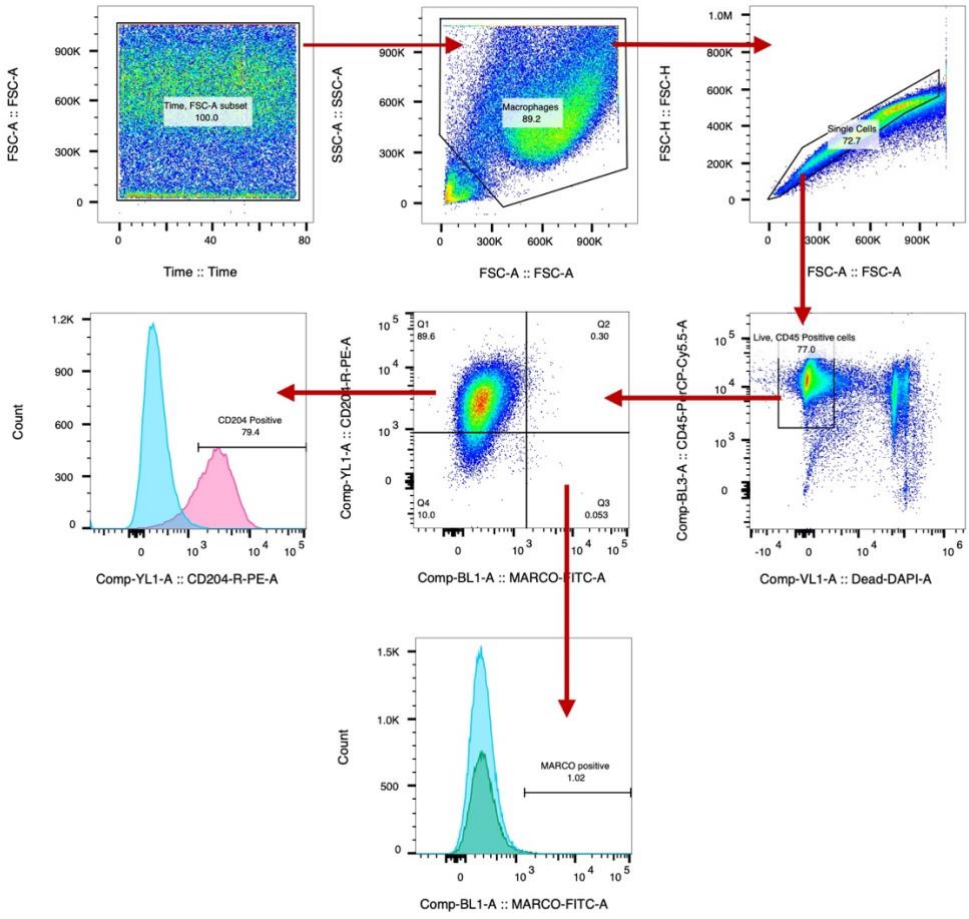

Figure 2-3: Representative gating strategy used to measure PRR expression in macrophages. The above data corresponds to PMA-unstimulated *Tlr4*$^{-/-}$ macrophages tested for MARCO and MSR1 expression using fluorochrome-conjugated antibodies. Macrophages were stained with CD45-PerCP-Cy5.5 to isolate leukocytes, DAPI to exclude dead cells, CD204 (MSR1)-PE and MARCO-Fluorescein. Isotype controls were used to check for non-specific antibody binding, while fluorescent minus one (FMO) controls were used to set gates. Gating was performed to exclude debris, doublets, and dead cells and to isolate MARCO and MSR1 positive live macrophages. Blue histogram represents Isotype Control. Pink histogram represents MSR1 (CD204) staining. Green histogram represents MARCO staining. FSC, forward scatter; SSC, side scatter

2.8 India Ink Staining

The *C. neoformans* capsule has anti-phagocytic properties, thus, to examine whether the capsule size of various *C. neoformans* strains contributed to variation in their susceptibility to phagocytosis by macrophages, India ink was used to visualize the fungal capsule. With India ink staining, the background is stained dark but the acidic stain is excluded from the capsule due to the negative charge of the polysaccharide capsule. As a result, a transparent halo, which represents the capsule, is visible around the *Cryptococcus* cell (Nichols, 2021) Figure 2-4.

To stain *Cryptococcus* with India Ink, a fungal colony was resuspended in 3mL YPD both and incubated overnight at 25°C under constant rotation (20 rpm). The following day, 1 mL overnight culture was transferred to a 1.5 mL Eppendorf tube, centrifuged at 6500 rpm for 2.5 mins and the pellet was resuspended in 1X PBS. The cells were centrifuged again and then resuspended in 100 μL PBS. To stain, 1 μL *Cryptococcus* suspension was transferred to a microscope slide followed by 3 μL India ink [ThermoFisher]. They were then mixed using a pipette tip and covered with a coverslip. Images were acquired using the Zeiss Axio Observer [Zeiss Microscopy], phase contrast objective and 40X magnification.

To measure the capsule size images were opened on the Fiji software [ImageJ] then the straight-line tool was used to measure cell body diameter (Figure 2-4; red line), which excludes the polysaccharide capsule, and total cell diameter (Figure 2-4; yellow line)

manually. The size of capsule, termed capsule radius, was determined using the following equation: ((total cell diameter – cell body diameter)/2).

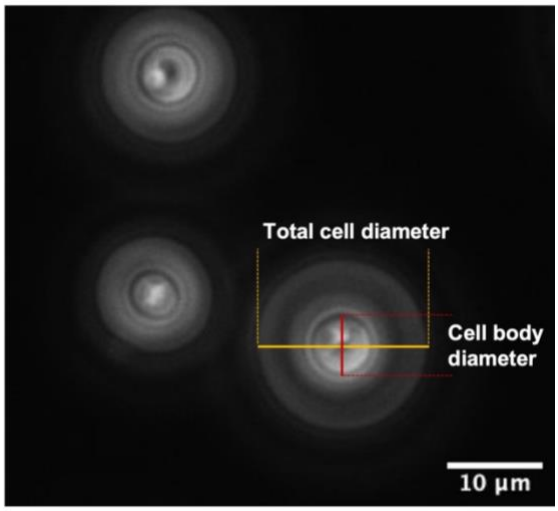

Figure 2-4: India ink staining of the Bt22 *Cryptococcus* strain. Yellow bar shows total cell diameter; Red bar shows cell body diameter. Capsule radius was determined by subtracting cell body diameter from total cell diameter and dividing by 2.

2.9 Extracellular Vesicle (EV) Isolation

To investigate the ability of wildtype EVs to rescue the phagocytosis of EV-deficient mutant *Cryptococcus* strains, three approaches were tested. The first approach utilised trans-well inserts with 400 nm pores to separate wildtype cryptococci from EV-deficient mutants during the phagocytosis assay. To do this, PMA stimulated J774A.1 macrophages were infected with WTKN99α, *gat5Δ* and *hap2Δ* at an MOI of 10 fungi to 1 macrophage, then ThinCert™ trans-well inserts with 400 nm pores [Greiner Bio-One] were inserted into each well and WTKN99α was added onto the trans-well insert. For the "blank" control, serum-free DMEM was added onto the trans-well insert. With a

pore size of 400 nm, EVs secreted by WTKN99α during the course of infection should be able to travel across the membrane.

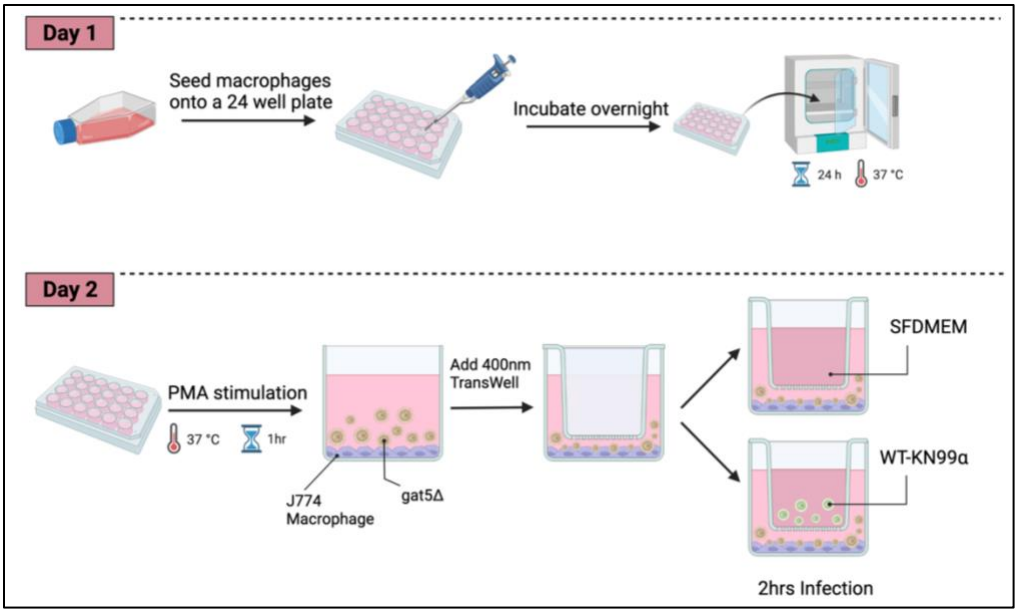

Figure 2-5: Schematic representation of a trans-well assay. Method is adapted from the standard phagocytosis assay with the inclusion of a trans-well insert with a 400 nm pore size into each well following the inoculation of cryptococci into wells with macrophages. Figure created with BioRender.com.

In the second approach, cell culture media conditioned with WTKN99α was used to investigate the effect of wildtype EVs on the phagocytosis of mutant strains (Figure 2-6). To prepare EV-conditioned media to be used in the infection of J774A.1 macrophages, WTKN99α was cultured at a density of $1x10^6$ cells/mL in 10 mL serum-free DMEM in a T25 flask [Greiner Bio-One] and incubated at 37°C and 5% CO_2 for 24 h. The next day, media was collected, centrifuged at 4000 rpm for 3 mins, and the supernatant was used for infection.

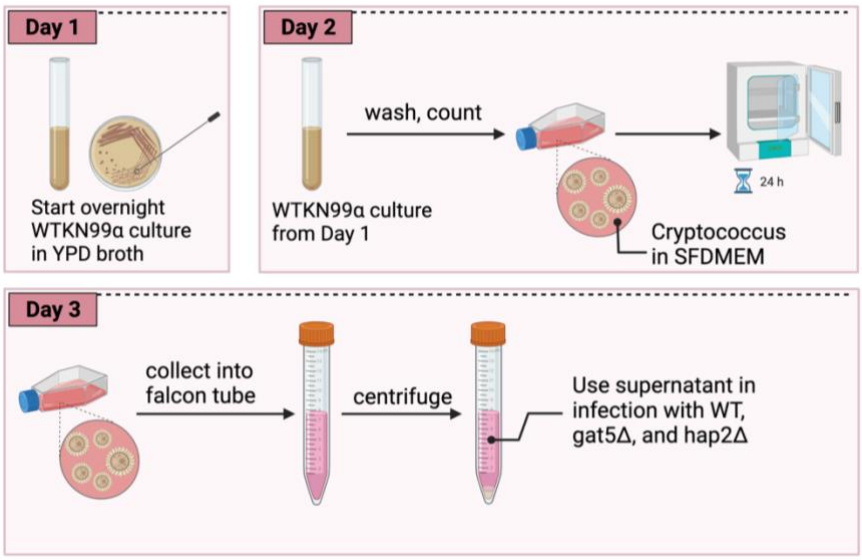

Figure 2-6: Schematic representation of the protocol used for preparing WTKN99α-conditioned serum free DMEM culture media (SFDMEM). Figure created with BioRender.com.

The final approach involved the exposure of *Cryptococcus* strains to EVs isolated from wildtype fungi. To isolate EVs from WTKN99α, a colony of WTKN99α was picked from agar plate, resuspended in 10 mL YPD broth, and incubated at 30°C, 180 rpm for 24 h (Figure 2-7). The following day, the *Cryptococcus* culture was washed twice with sterile pyrolyzed H_2O and counted with a haemocytometer. The cells were adjusted to a density of $3.5x10^7$ cells/mL in sterile H_2O and 300 µl of cell suspension was plated onto sabouraud dextrose (SD) agar, which was prepared using sabouraud 4% dextrose agar [Millipore] at a concentration of 65 g/L. The plates were incubated at 30°C for 24 h. Next, the lawn of *Cryptococcus* cells that had grown on all three SD agar plates were recovered by gently scraping the agar plates with a 10 µL inoculation loop and resuspending the cells in 10 mL YPD broth or 5 mL of 0.22 µm-filtered PBS. The cell suspension was centrifuged at 5000xg for 15 mins at 4°C and the supernatant was collected. The recovered supernatant was centrifuged again at 5000xg for 20 mins at 4°C. The resulting

supernatant was filtered through a 0.45 μm syringe filter to ensure that all WTKN99α cells have been removed while retaining the EVs which are around 20 to 500 nm in diameter. When EVs were isolated in YPD broth, 3 mL of the EV conditioned YPD broth was used to start an overnight culture of WTKN99α, *gat5Δ* and *hap2Δ*. Cells grown in standard YPD broth were used as controls. The *Cryptococcus* cultures were used in a phagocytosis assay as described in Chapter 2.4. Meanwhile, when EVs were isolated in PBS, the EV+PBS solution was used to "opsonise" 1x10^6 WTKN99α, *gat5Δ* and *hap2Δ* per well for 1 h under constant rotation (20 rpm). After 1 h, the opsonisation reaction was used to infect macrophages.

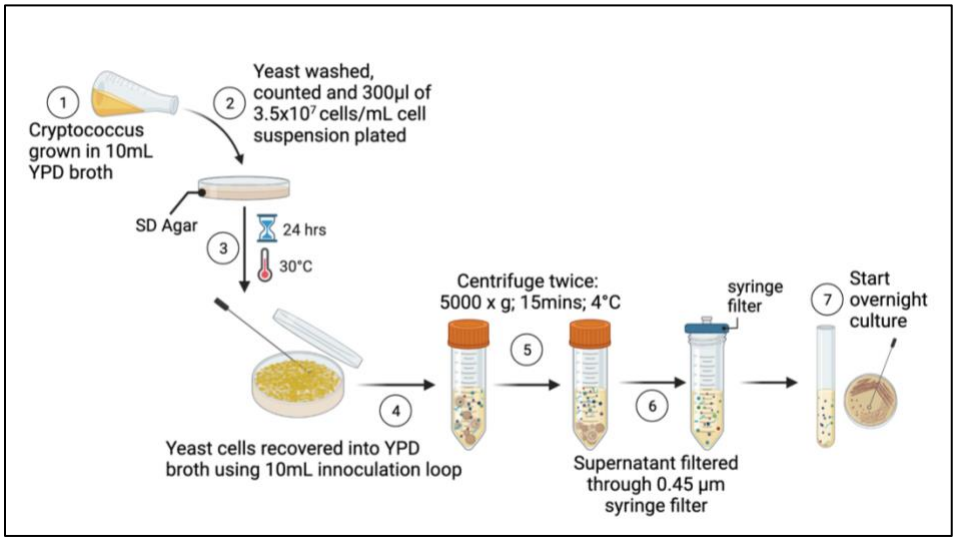

Figure 2-7: Extracellular vesicle isolation in YPD broth. This protocol is adapted from the EV isolation protocol described in (Reis et al., 2019). Figure created with BioRender.com.

2.10 *C. neoformans* Growth Curve

To explore the effect of exogenous EV exposure to the growth of wildtype and EV-deficient *C. neoformans* strains, a growth curve was generated. EV isolation was carried out in PBS or YPD broth as described above. For growth curves using EVs isolated in PBS, the solution was diluted 1:3 in YPD broth, then 400 μL was dispensed into each well of

a 24-well plate and inoculated with $1x10^6$ *C. neoformans.* For growth curves using EVs isolated in YPD broth, the resulting solution was used as is and 400 μL was dispensed into each well. Plates were incubated in the FLUOstar Omega microplate reader at 30°C and no shaking. Absorbance was measured every 1 h at 600 nm.

2.11 Statistical Analysis

GraphPad Prism Version 9.5.0 for MacOS (GraphPad Software, San Diego, CA) was used to generate graphical representations of experimental data. Violin plots were generated using R programming. Inferential statistical tests were performed using Prism. The data set was assumed to be normally distributed based on the results of a Shapiro-Wilk test for normality. Therefore, to compare the means between treatments, the following parametric tests were performed: unpaired two-sided t test, one-way ANOVA, and two-way ANOVA. ANOVA tests were followed up with Tukey's post-hoc test. When data failed the normality test, Mann-Whitney U nonparametric test was used. Variation between treatments was considered statistically significant if the p-value was less than 0.05.

Chapter 3 Reciprocal regulation of Toll-Like Receptor 4 and Macrophage Scavenger Receptor 1 regulates non-opsonic phagocytosis of the fungal pathogen *Cryptococcus neoformans*.

The following thesis chapter contains work that has been published in Nature Communications. I am the first author in this paper and was responsible for writing the entire manuscript. Though I received feedback from my supervisor and collaborators, their contribution to the text in this chapter were not substantial.

*Onyishi, C.U., Desanti, G.E., Wilkinson, A.L. et al. Toll-like receptor 4 and macrophage scavenger receptor 1 crosstalk regulates phagocytosis of a fungal pathogen. Nat Commun **14**, 4895 (2023). https://doi.org/10.1038/s41467-023-40635-w*

3.1 Introduction

Following the inhalation of *C. neoformans* into the lungs, lung-resident macrophages are amongst the first immune cells the fungi encounter (Osterholzer et al., 2009a), thus, the interaction between host macrophages and invading fungi is believed to be an important determinant of disease progression and outcome. Non-opsonised cryptococci are phagocytosed poorly (Lim et al., 2018), but since opsonising antibodies are thought to be negligible within the healthy lung (Mitchell and Perfect, 1995), this low level of uptake is likely a critical determinant of the subsequent course of an infection. However, there is no clear understanding of the mechanism by which macrophages detect and

phagocytose *C. neoformans* in the absence of opsonins (Shao et al., 2005; Osterholzer et al., 2009a).

TLR4 is a well-known and well-studied PRR in the context of bacterial infection; specifically gram-negative infection, since TLR4 is the major receptor for the recognition of LPS (Chow et al., 1999). However, as discussed in the chapter 1.2.3, its role during *C. neoformans* infection remains unclear. Before I joined the lab, a previous master's student in the lab, Alex Wilkinson, found that J774 macrophages treated with a TLR4 inhibitor showed a modest decrease in vomocytosis compared to control, but no differences were observed in phagocytosis or intracellular proliferation (unpublished data). This study made use of 18B7 antibody opsonised fungi; thus, my initial aim was to explore the role of TLR4 in the phagocytosis of non-opsonised *C. neoformans* with the hypothesis that the loss of TLR4 signalling would reduce the phagocytosis of non-opsonised *C. neoformans*.

3.2 Both the chemical and genetic loss of TLR4 function unexpectedly increased the phagocytosis of non-opsonised *C. neoformans.*

To determine the role of TLR4 in the phagocytosis of non-opsonised *C. neoformans*, I began by pre-treating J774A.1 murine macrophages with TAK-242, a TLR4-specific inhibitor. Contrary to my hypothesis, I found that the chemical inhibition of TLR4 resulted in a 1.7-fold increase in the phagocytosis of *C. neoformans* (Figure 3-1A). As an alternative approach to investigate the role of TLR4 in the phagocytosis of cryptococci, macrophages isolated from *Tlr4*$^{-/-}$ mice were utilised. Similar to the finding with J774A.1

macrophages, the genetic knockout of TLR4 resulted in a significant 8-fold increase in the phagocytosis of *C. neoformans* (Figure 3-1B and D).

To explore the human relevance of this finding, 2 h serum-starved human monocyte-derived macrophages (HMDMs) were exposed to TAK-242 and infected with non-opsonised cryptococci. I found that TLR4 inhibition also led to an unexpected increase in the number of internalised *C. neoformans* in human macrophages (Figure 3-1C), providing further validation for this unexpected result.

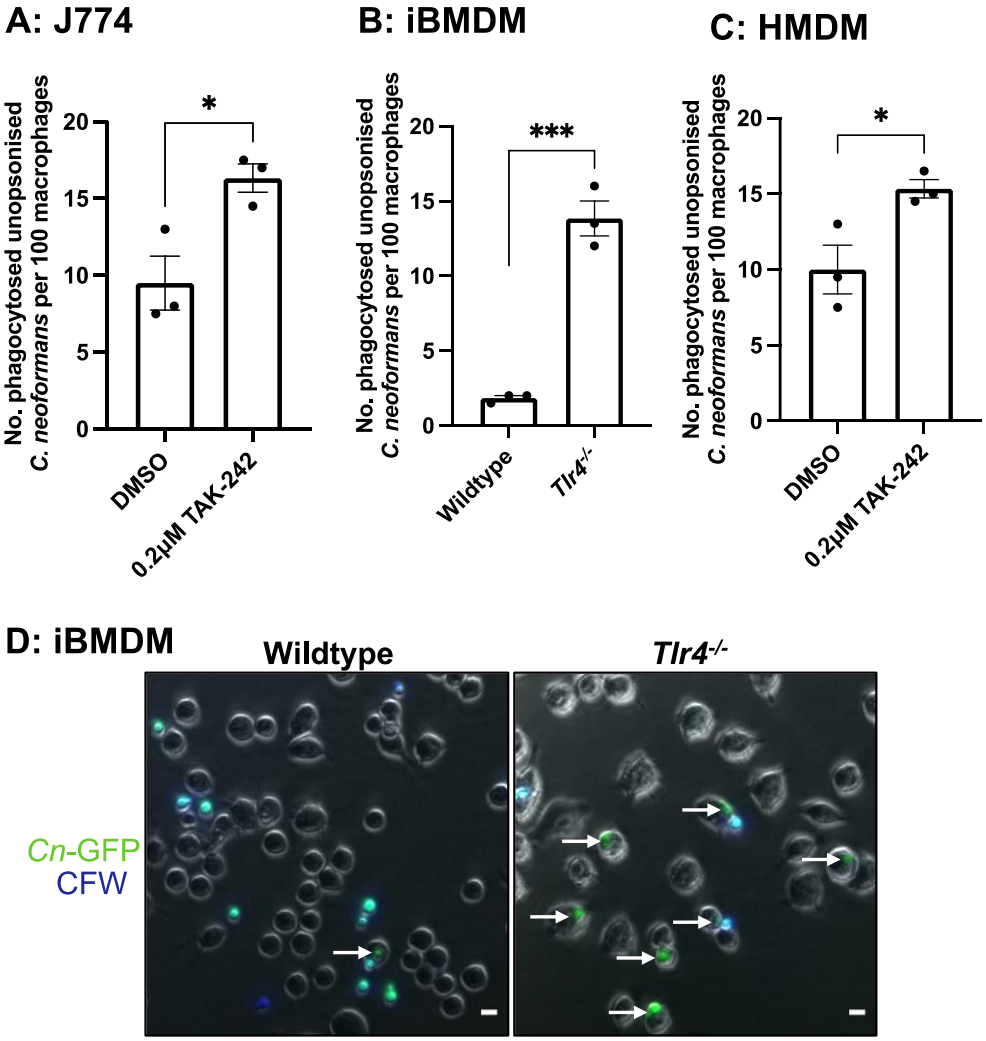

Figure 3-1: Both chemical inhibition and genetic loss of TLR4 results in an increase in the phagocytosis of *C. neoformans*. (A) J774A.1 macrophages were treated with DMSO (control) or 0.2 μM TAK-242, a TLR4-specific inhibitor, for 1 h before infection with non-opsonised *C. neoformans*. **(B)** Immortalised bone marrow-derived macrophages from wildtype and *Tlr4*$^{-/-}$ macrophages were infected with non-opsonised *C. neoformans*. **(C)** Peripheral blood mononuclear cells were isolated from leukocyte cones, then macrophages were differentiated using GM-CSF. Naïve M0 macrophages were serum-starved for 2 h, treated with DMSO (control) or 0.2 μM TAK-242 for 1 h, then infected with non-opsonised *C. neoformans* for 2 h, still in the presence of the inhibitor. Phagocytosis was quantified as the number of individual internalised cryptococci within 100 macrophages. Figures are representative of at least three independent experiments. HMDM data represents two independent experiments with separate donors. For all graphs individual data points represent technical replicates (n = 3 per condition). Data shown as mean ± SEM; statistical significance was evaluated using an unpaired two-sided t-test: *p<0.05, ***p<0.001. **(D)** Representative image showing the phagocytosis of GFP-labelled *C. neoformans* (*Cn*-GFP) by wildtype and TLR4$^{-/-}$ iBMDM. Calcofluor White (CFW) was used to stain extracellular fungi. White arrows show phagocytosed fungi. Scale bar = 10 μm.

3.3 The increased uptake observed in TLR4 deficient macrophages is not a consequence of increased intracellular proliferation.

Proinflammatory responses, such as those driven by TLR4, have been shown to restrict the intracellular proliferation of cryptococci (Voelz et al., 2009), thus the perceived increase in phagocytosis might instead reflect increased proliferation in the absence of TLR4 activity. To test this, I quantified the proliferation of *C. neoformans* within macrophages using a timelapse-microscopy-based approach. I carried out live-cell imaging of infected macrophages over 18 h and quantified the number of internalised fungi at the beginning of the video (T0) and 10 hours post-infection (T10) to determine the intracellular proliferation rate (IPR). This timelapse-based IPR assay revealed that neither TLR4 inhibition using TAK-242 (Figure 3-2A) nor *TLR4* knockout (Figure 3-2B) altered the IPR of cryptococci compared to control cells. When the traditional IPR assay was used to measure proliferation within TAK-242-treated macrophages, there was also no difference in IPR between untreated and TAK-242-treated macrophages (Figure 3-3B). This suggests that the observed intracellular burden of *C. neoformans* is representative of the initial rate of uptake and not due to differences in the subsequent proliferation of the fungi within macrophages.

Notably, the traditional IPR approach reiterates that loss of TLR4 signalling increases the number of internalised *C. neoformans* (Figure 3-3A). When phagocytosed *C. neoformans* was recovered by lysing macrophages and plating onto agar plates, there was no difference in fungal viability between TAK-242 treated and untreated macrophages at both T0 and T18 (Figure 3-3C). However, there was a reproducible trend toward

increased fungal viability in TAK-242-treated macrophages at T18, though this trend was quite marginal.

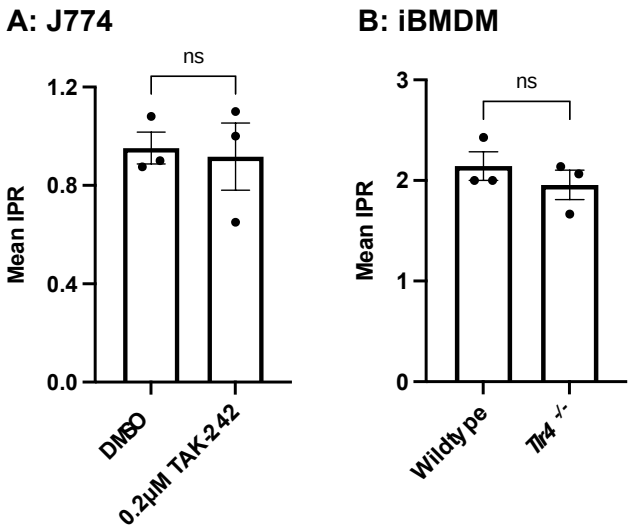

Figure 3-2: Intracellular Proliferation Rate (IPR) of *C. neoformans* within macrophages using live cell imaging approach. After 2 h infection with *C. neoformans*, J774A.1 **(A)** and iBMDMs **(B)** were imaged every 5 minutes for 18 h. To determine IPR, the number of internalised fungi per 100 macrophages at the 'first frame' (T0) and 'last frame' (T10) was quantified and IPR was calculated using the equation: IPR = T10/T0. Data is representative of two independent experiments. For both graphs individual data points represent technical replicates (n = 3 per condition). Data shown as mean ± SEM; ns, not significant in an unpaired two-sided t-test.

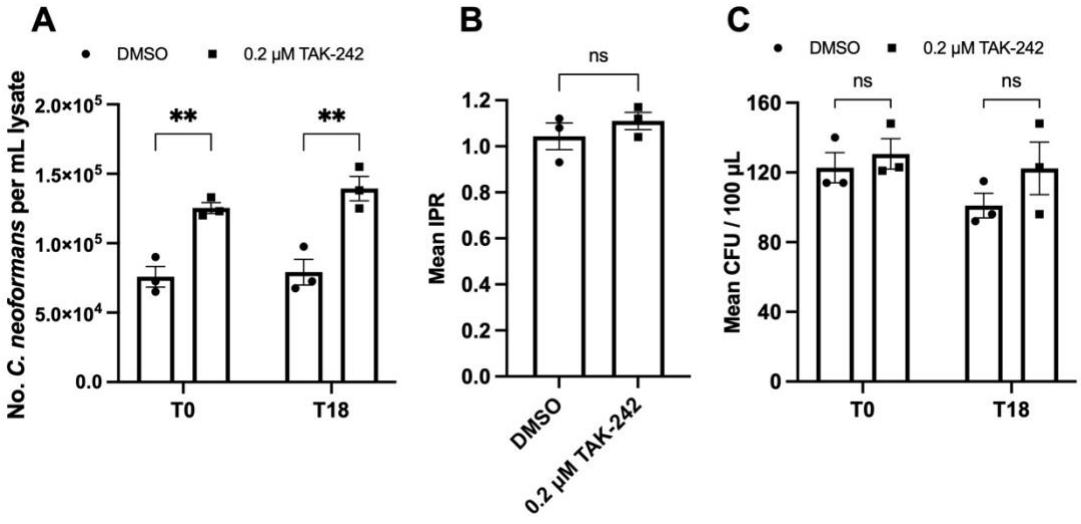

Figure 3-3: Intracellular Proliferation Rate (IPR) of *C. neoformans* within J774A.1 macrophages using the traditional IPR assay approach. J774 macrophages were treated with TAK-242 and infected with *C. neoformans* for 2 h. After 2 h of infection, extracellular fungi were washed off and macrophages were lysed immediately (T0) or 18 h later (T18). **(A)** The number of cryptococci in the lysate was counted using

a haemocytometer. **(B)** The resulting cell count was used to determine IPR using the formula T18/T0. **(C)** *Cryptococcus* from the lysate was plated onto YPD agar plates and the number of colonies was counted. Data is representative of two independent experiments. For both graphs individual data points represent technical replicates (*n* = 3 per condition). Data shown as mean ± SEM; ns, not significant; **p<0.01 in a t-test **(B)** or two-way ANOVA **(A, C)**.

3.4 Oxidised low-density lipoprotein (ox-LDL) competitively inhibits the phagocytosis of non-opsonised *C. neoformans*.

Having shown that the increased intracellular burden of infection following TLR4 inhibition or knockout is a result of elevated phagocytosis and not proliferation, we next sought to identify the plasma membrane receptor responsible for this increase in uptake. Notably, plasma membrane TLRs, including TLR4, are not bona fide phagocytic receptors, since they are not directly responsible for the engulfment of whole microorganisms (Freeman and Grinstein, 2014). Consequently, I considered whether TLR4 modulates the availability or activity of one or more bona fide non-opsonic phagocytic receptors, which are then responsible for direct binding to *C. neoformans*.

Since the role of CLRs in non-opsonic uptake of *C. neoformans* have already been investigated and found to be minimal (Lim et al., 2018), I decided to begin by exploring the role of scavenger receptors in *Cryptococcus* uptake. It has been shown that the expression of several scavenger receptors is upregulated in *Tlr4*$^{-/-}$ mice (Meng et al., 2011) and that TLR agonists increase the phagocytosis of *Escherichia coli* by inducing the expression of scavenger receptors (Doyle et al., 2004). Therefore, I posited that the loss of TLR4 signalling increases the phagocytosis of non-opsonised *C. neoformans* through the upregulation of scavenger receptors.

To explore this hypothesis, I treated macrophages with oxidised low-density lipoprotein (ox-LDL), a general scavenger receptor ligand which would also act as a competitive inhibitor, prior to infection with *C. neoformans*. I observed that ox-LDL was able to inhibit the phagocytosis of *C. neoformans* in both wildtype and *Tlr4*$^{-/-}$ macrophages (Figure 3-4A and B). This competitive inhibition of *C. neoformans* uptake was lost when macrophages were infected with 18B7 antibody-opsonised fungi (Figure 3-4C), indicating that the inhibition is specific to non-opsonic uptake. Antibody-opsonised microbes are phagocytosed through the FcγR pathway; therefore, it is not too surprising that ox-LDL pre-treatment had no impact on opsonic uptake. Next, I exposed HMDMs to ox-LDL and similar to the finding in a mice cell line, HMDMs pre-treated with ox-LDL showed reduced phagocytosis of non-opsonic *C. neoformans* (Figure 3-4D), implicating scavenger receptors as a broadly relevant family of receptors involved in the uptake of non-opsonised *C. neoformans*.

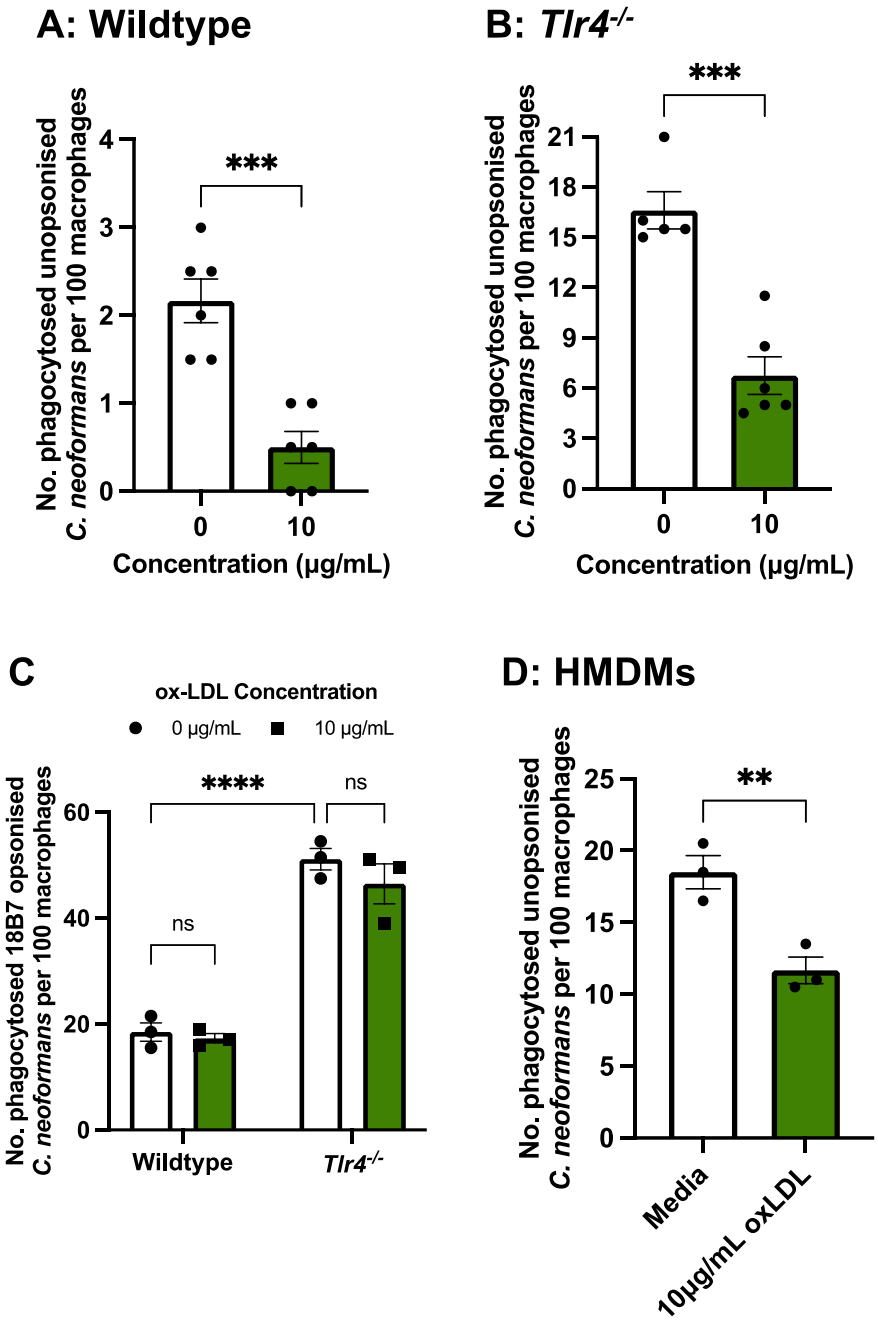

Figure 3-4: The increased phagocytosis observed in *Tlr4*$^{-/-}$ macrophages is partially driven by scavenger receptors. (A) Wildtype immortalised bone marrow-derived macrophages (BMDMs), **(B)** *Tlr4*$^{-/-}$ iBMDMs and **(D)** Human monocyte-derived macrophages (HMDMs) were treated with oxidised low-density lipoprotein (ox-LDL), a general scavenger receptor ligand, for 30 mins prior to infection with non-opsonised *C. neoformans*. iBMDM data is pooled from two independent experiments resulting in *n* = 6 per condition. HMDM data represents two independent experiments with separate donors and data points represent technical replicates (*n* = 3). **(C)** Wildtype and *Tlr4*$^{-/-}$ iBMDMs were treated with 10 µg/mL ox-LDL for 30 mins, then infected with *C. neoformans* opsonised with the anti-capsular 18B7 antibody. Experiment was performed once, and each data point represents a technical repeat (*n* = 3). The number of internalised fungi per 100 macrophages was quantified from fluorescent microscopy images. Data shown as mean ± SEM; ns, not significant, ***p<0.001, ****p<0.0001 in an unpaired two-sided t-test **(A, B, D)** or two-way ANOVA followed by Tukey's post-hoc test **(C).**

3.5 *Tlr4*$^{-/-}$ macrophages have increased expression of Macrophage Scavenger Receptor 1 (MSR1).

Treatment with ox-LDL was able to competitively inhibit the uptake of non-opsonised *C. neoformans*; however, since ox-LDL is a general scavenger receptor ligand, the precise scavenger receptor involved in the uptake of *C. neoformans* remains unknown. To try and discern which receptor may be responsible for the phagocytosis of *C. neoformans*, I analysed the surface expression of the scavenger receptors Macrophage Scavenger Receptor 1 (MSR1) (also known as CD204), CD36 and MAcrophage Receptor with COllagenous structure (MARCO) using flow cytometry. Wildtype and *Tlr4*$^{-/-}$ macrophages had similar levels of CD36 expression (Figure 3-5, A1-A3). Both cell types expressed very little MARCO (Figure 3-5, B1-B3), but this was in line with studies that show that iBMDMs do not express MARCO (Fejer et al., 2013). Notably, however, MSR1 expression was significantly higher in *Tlr4*$^{-/-}$ macrophages compared to wildtype macrophages (Figure 3-5, C1-C3), suggesting that the increased phagocytosis of *C. neoformans* observed in *Tlr4*$^{-/-}$ macrophages may be due to their increased expression of MSR1.

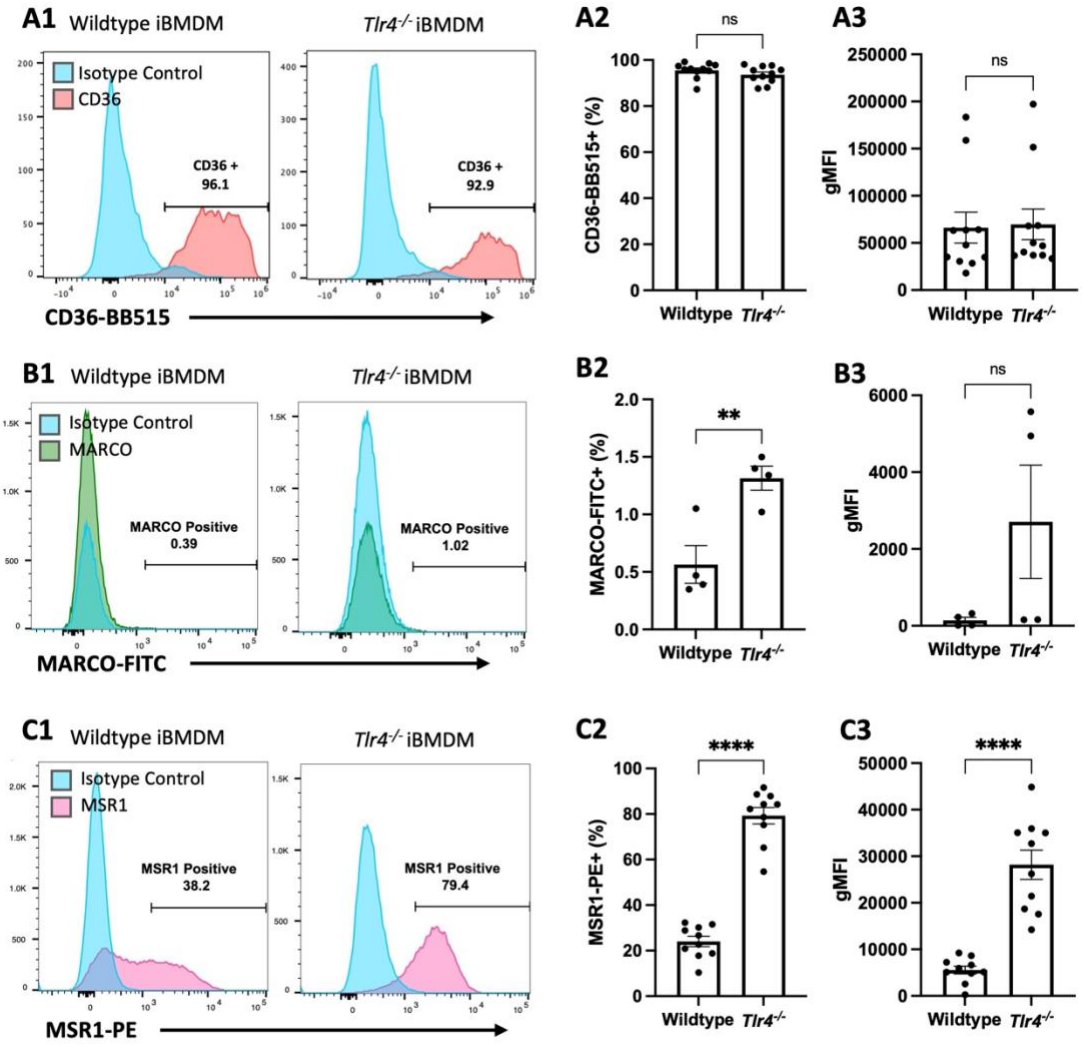

Figure 3-5: Cell surface expression of scavenger receptors in wildtype and *Tlr4*$^{-/-}$ macrophages. Baseline surface expression of **(A1-A3)** CD36 stained with anti-mouse CD36-BB515 antibody (red histogram); **(B1-B3)** MAcrophage Receptor with COllagenous structure (MARCO) stained with anti-mouse MARCO-Fluorescein antibody (green histogram); and **(C1-C3)** Macrophage Scavenger Receptor 1 (MSR1), also known as CD204, stained with anti-mouse CD204-PE antibody (pink histogram) on wildtype and *Tlr4*$^{-/-}$ macrophages. A corresponding isotype control antibody was used for each receptor (blue histogram). Receptor expression was measured using flow cytometry. **(A2, B2, C2)** Bar graphs showing percent positive population. **(A3, B3, C3,)** Bar graphs showing normalised geometric mean fluorescent intensity (gMFI). Data is pooled from at least two independent experiments each performed in duplicates. Data shown as mean ± SEM; ns, not significant, **p<0.01, ****p<0.0001 in an unpaired two-sided t-test.

3.6 MSR1 is a major PRR for the phagocytosis of non-opsonised *C. neoformans.*

Having shown that MSR1 is upregulated in *Tlr4*$^{-/-}$ macrophages, I next wanted to explore the direct role of individual scavenger receptors during *Cryptococcus* uptake. To achieve

this aim, we infected MPI cells derived from wildtype, *Msr1*$^{-/-}$, *Marco*$^{-/-}$ or double knockout (DKO) C57BL/6 mice with *C. neoformans*. *Marco*$^{-/-}$ macrophages were not affected in their capacity to infect macrophages, while macrophages derived from *Msr1*$^{-/-}$ mice showed a 75% decrease in phagocytosis of non-opsonised cryptococci (Figure 3-6) suggesting that MSR1 is a critical phagocytic receptor for *C. neoformans*. Notably, we still observe some non-opsonic uptake in MSR1 and DKO macrophages implying a role for some other PRR in the non-opsonic uptake of cryptococci.

To provide further support that MSR1 is directly involved in the phagocytosis of *C. neoformans*, I explored the localisation of MSR1 in infected macrophages using confocal microscopy. I first used the same MSR1 antibody used in the flow cytometry experiment and amplified the fluorescence signalling using an AlexaFluor 594 conjugated secondary antibody. Prior to staining, macrophages were blocked with 1% bovine serum albumin (BSA) to minimise non-specific binding of the antibodies. Using this set of primary and secondary antibodies, I observed an area of intense MSR1 staining that colocalised with some phagocytosed *C. neoformans* (Figure 3-7A, white arrows) but not others (Figure 3-7B, green arrows). I reasoned that the absence of MSR1 colocalization with some cryptococci and not others might reflect internalised versus surface-bound fungi. Alternatively, it may reflect phagosomes at different stages of maturation, such that more mature phagosomes lack MSR1 due to the receptor being recycled back to the plasma membrane. Surprisingly, when I imaged macrophages that were only incubated with a secondary antibody, I observed non-specific binding of the secondary antibody that colocalised with some cryptococci, but not others (Figure 3-7A, No 1° Ab Ctrl, white

arrows). Although the intensity of AF594 conjugated secondary antibody fluorescence was more intense when macrophages are exposed to MSR1 1° Ab, the presence of some non-specific binding in the 'No 1° Ab' control casts doubt on whether this is robust evidence of colocalization between MSR1 and phagocytosed *C. neoformans*.

To better control for non-specific binding of the secondary antibody, I repeated the experiment using an AlexaFluor 594 conjugated secondary antibody composed of the $F(ab')_2$ fragment alone, which prevents non-specific binding of the secondary antibody to Fc receptors on cells. I also purchased a new MSR1 primary antibody that has specifically been validated for use in immunofluorescence staining. Using this new set of antibodies, I observed some accumulation of MSR1 around phagosomes containing *C. neoformans* (Figure 3-7B, white arrows), and no evidence of non-specific binding (Figure 3-7B, No 1° Ab Ctrl). The enrichment of MSR1 around internalised *C. neoformans* is not as intense as expected; however, this may be because not many MSR1 molecules are needed to trigger pathogen engulfment resulting in a moderate signal. Moreover, the recycling time of MSR1 molecules is not known and rapid recycling could significantly reduce the intensity of colocalization. Macrophages transfected with fluorescent MSR1 could be used as an alternative imaging approach to combat these limitations, particularly if combined with live-cell super-resolution approaches.

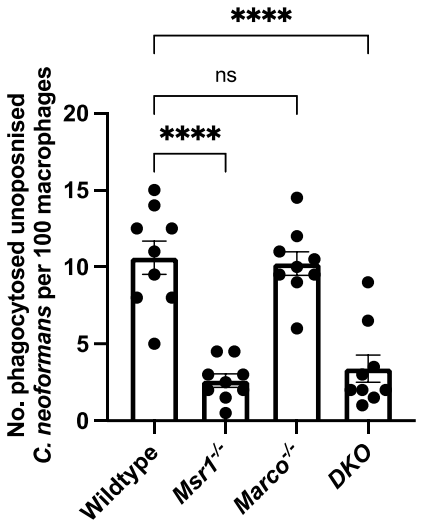

Figure 3-6: MSR1 mediates non-opsonic phagocytosis of *C. neoformans*. MPI cells, a non-transformed GM-CSF-dependent murine macrophage cell line, were isolated from wildtype, *Msr1*$^{-/-}$, *Marco*$^{-/-}$ and double knockout (DKO) mice. Macrophages were infected with non-opsonised *C. neoformans*. The data shown are pooled from three independent experimental repeats ($n = 9$). Data is presented as mean ± SEM; ns, not significant, ****p<0.0001 in a one-way ANOVA followed by Tukey's post-hoc test.

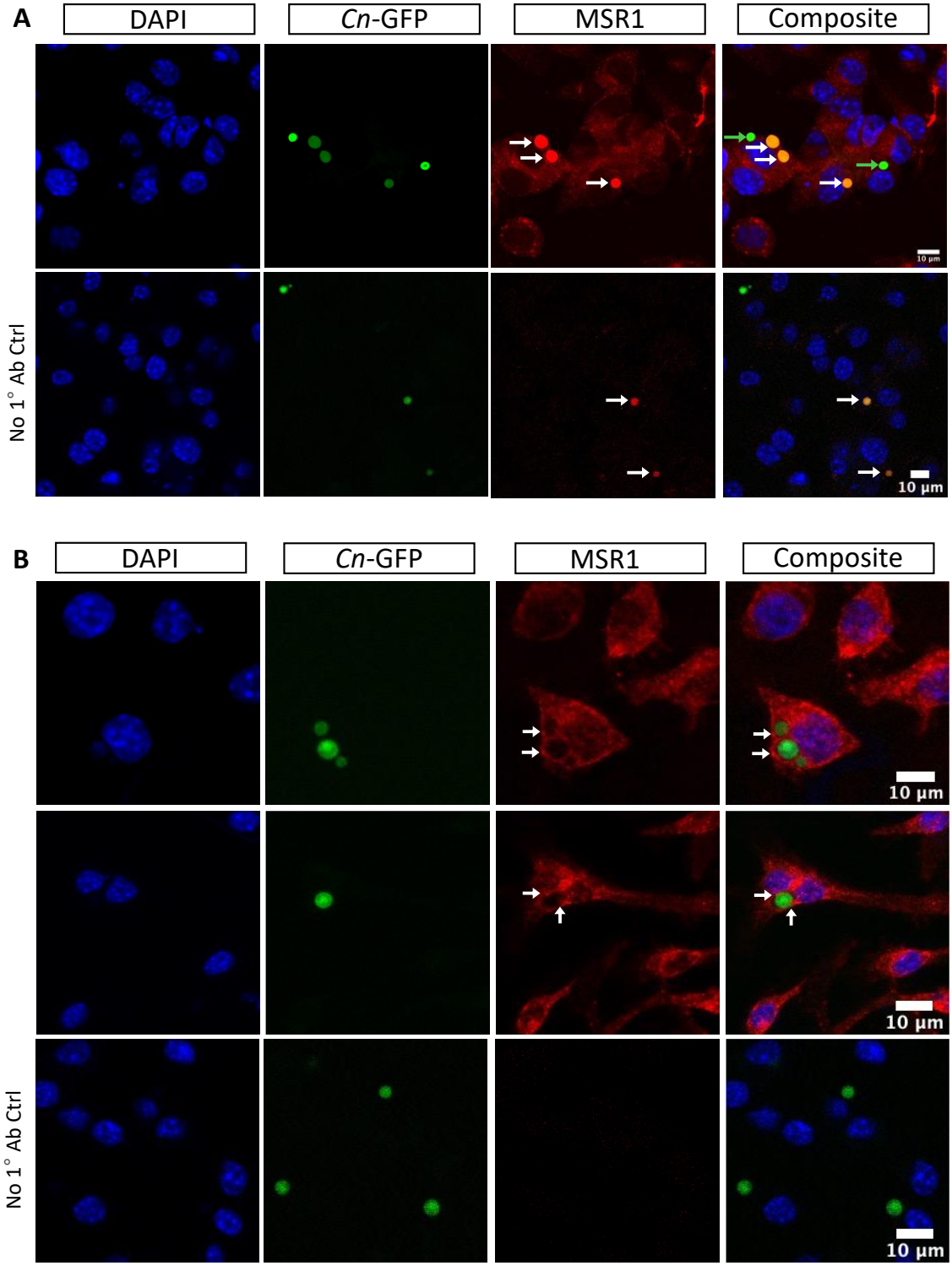

Figure 3-7: Immunofluorescence analysis of MSR1 localisation on *Tlr4*$^{-/-}$ macrophages after infection with GFP-expressing *C. neoformans* (*Cn*-GFP). Post-infection, **(A)** macrophages were fixed, permeabilised and stained with rat anti-mouse CD204-PE (MSR1) followed by AlexaFluor 594 goat anti-rat IgG secondary antibody; alternatively, **(B)** macrophages were stained with rabbit anti-mouse MSR1 followed by Alexa Fluor 594 conjugated anti-rabbit IgG F(ab')$_2$ fragment secondary antibody. To control for non-specific binding of the primary antibody, macrophages were exposed to secondary antibody alone (No 1°Ab Ctrl). Cells were counterstained with DAPI to visualize the nucleus**.** Samples were captured on the Zeiss LSM880

confocal microscope using 63X Oil magnification, except '**(A)** No 1° Ab Ctrl', which was captured using 40X magnification. White arrows show colocalization of cryptococcus and MSR1. Green arrows show phagocytosed cryptococci not localised with MSR1. Scale bar = 10 μm

3.7 The increased uptake observed in *Tlr4*$^{-/-}$ macrophages is partially driven by TLR3 signalling, without affecting cell surface expression of MSR1.

Having identified the exitance of crosstalk between TLR4 and MSR1 in the non-opsonic phagocytosis of *C. neoformans*, I then sought to explore the mechanism of MSR1-mediated phagocytosis as well as the mechanism of TLR4 mediated regulation of MSR1 activity. Scavenger receptors lack a clear intracellular signalling domain; thus, it is hypothesized that scavenger receptor-mediated internalization requires coreceptors and adaptor molecules leading to the formation of multimolecular signalling complexes (Canton et al., 2013). Since increased *C. neoformans* uptake in *Tlr4*$^{-/-}$ macrophages is likely driven by the increased expression of MSR1 in these cells, I decided to use *Tlr4*$^{-/-}$ macrophages as a tool to identify potential coreceptors involved in MSR1-mediated phagocytosis.

There is substantial evidence of TLR-TLR crosstalk modulating cytokine expression (Bagchi et al., 2007). Given that the loss of TLR4 increased phagocytosis, we concluded that TLR4 normally has phagocytosis limiting activity. Consequently, we hypothesized that TLR-TLR crosstalk may influence phagocytosis such that the loss of TLR4 signalling may lead to increased signalling through other, phagocytosis-promoting, TLRs. To explore the existence of such TLR-TLR crosstalk, I treated wildtype and *Tlr4*$^{-/-}$ iBMDMs with inhibitors of TLR2 (CU CPT22), TLR3 (TLR3/dsRNA complex inhibitor), and TLR9

(ODN 2088) prior to infection with *C. neoformans*. These inhibitors were chosen because only TLR4, TLR2, TLR9, and TLR3 have been studied previously in the context of *C. neoformans* infection (Yauch et al., 2004; Redlich et al., 2013; Zhang et al., 2010; Biondo et al., 2005).

The inhibition of TLR3, but not TLR2 or TLR9, led to a statistically significant decrease in the phagocytosis of non-opsonised *C. neoformans* by wildtype macrophages (Figure 3-8A), though it is worth noting that the overall number of internalised fungi is generally quite low in these cells. Meanwhile, in *Tlr4*$^{-/-}$ macrophages, TLR3 inhibition, but not TLR2 or TLR9 inhibition, led to a 42% decrease in the number of phagocytosed fungi (Figure 3-8B). Interestingly, when macrophages were infected with *C. neoformans* opsonised with the anti-capsular 18B7 antibody, TLR4-deficiency resulted in an increase in uptake compared to wildtype macrophages, but the effect of TLR3 inhibition was lost in both wildtype and *Tlr4*$^{-/-}$ cells (Figure 3-8C). Therefore, the role of TLR3 in modulating the phagocytosis of *C. neoformans* is specific to non-opsonic uptake.

Given the role of TLR3 in the increased uptake observed in *Tlr4*$^{-/-}$ macrophages, I hypothesized that loss of TLR4 signalling triggers increased TLR3 signalling, leading to upregulation of MSR1. This would shed light on the mechanism by which TLR4 signalling modulated MSR1 expression leading to increased uptake. To test this hypothesis, I measured MSR1 expression in wildtype and *Tlr4*$^{-/-}$ iBMDMs after 1 h TLR3 inhibition. I found no significant changes in MSR1 expression after both wildtype and *Tlr4*$^{-/-}$ macrophages were treated with the TLR3 inhibitor (Figure 3-8D, E), suggesting that the

interaction between MSR1 and TLR3 is not at the level of direct TLR3-mediated regulation of MSR1 expression. Instead, TLR3 may act on a coreceptor needed for the completion of MSR1-mediated uptake.

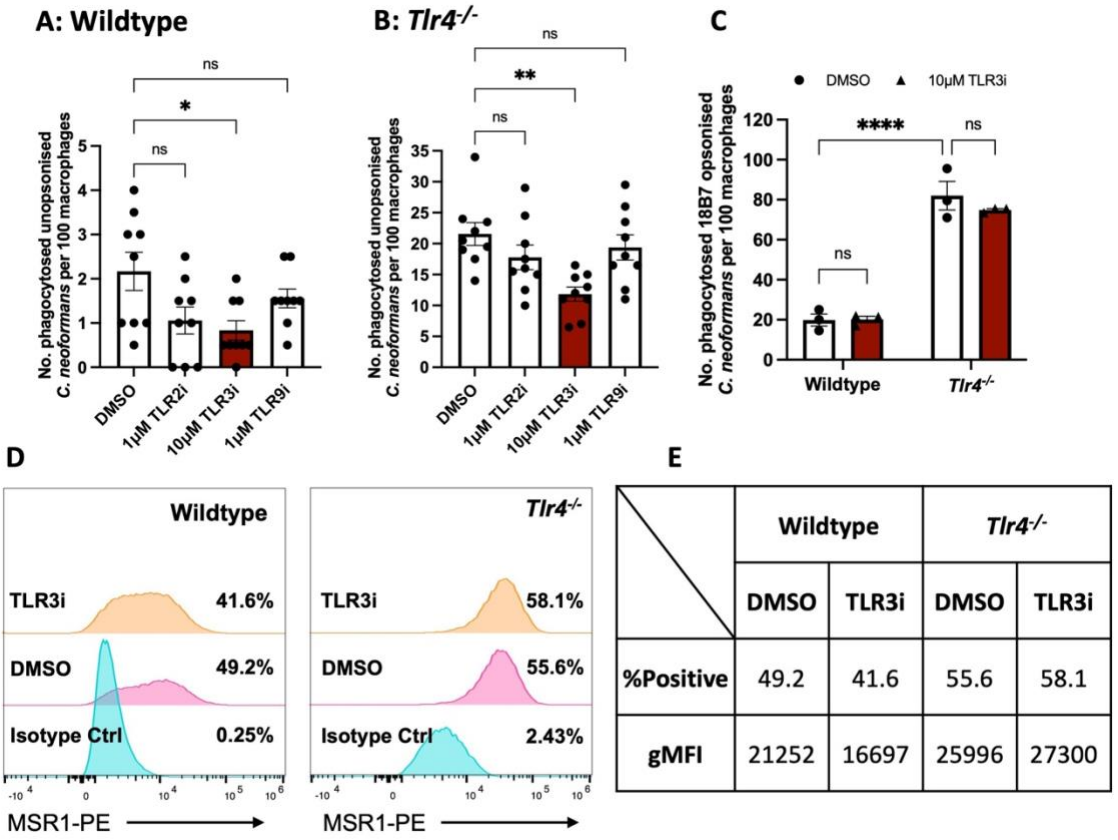

	Wildtype		Tlr4-/-	
	DMSO	TLR3i	DMSO	TLR3i
%Positive	49.2	41.6	55.6	58.1
gMFI	21252	16697	25996	27300

Figure 3-8: The increased phagocytosis observed in *Tlr4*$^{-/-}$ macrophages is dependent on TLR3 signalling. Wildtype **(A)** and *Tlr4*$^{-/-}$ **(B)** iBMDMs were treated with chemical inhibitors of TLR2, TLR3 and TLR9 for 1 h, then infected with non-opsonised *C. neoformans*. Data are pooled from three independent experiments (n = 9). **(C)** Wildtype and *Tlr4*$^{-/-}$ iBMDMs were treated with a TLR3 inhibitor then infected with *C. neoformans* opsonised with the anti-capsular 18B7 antibody. Experiment was performed once, and each data point represents a technical repeat (n = 3). Phagocytosis was quantified as the number of internalised cryptococci within 100 macrophages. Data shown as mean ± SEM; ns, not significant, *p<0.05, **p<0.01, ****p<0.0001 in a one-way analysis of variance (ANOVA) **(A, B)** or two-way ANOVA followed by Tukey's post-hoc test **(C)**. Red solid fill was used to highlight the results of TLR3 inhibition, given its statistical significance over TLR2 and TLR9 inhibition. **(D)** Wildtype and *Tlr4*$^{-/-}$ iBMDMs were treated with 0.025% DMSO (control) (pink histogram) or 10 μM TLR3 inhibitor (yellow histogram) for 1 h. MSR1 (also known as CD204) expression was measured using anti-mouse CD204-PE monoclonal antibody. PE-labelled rat IgG2a kappa was used as an isotype control (blue histogram). Percentages represent the percentage of MSR1-positive cells. **(E)** Table showing MSR1 percent positive population (%) and geometric mean fluorescent intensity (gMFI). Experiment was performed once. Each treatment was carried in duplicates. Duplicates were pooled prior to antibody staining. Samples were run through the Attune NxT flow cytometer and analysed in the FlowJo software.

3.8 TLR3 and Scavenger Receptors act along the same pathway to modulate phagocytosis.

To further explore the connection between TLR3 and scavenger receptors, *Tlr4*$^{-/-}$ iBMDMs were pre-treated with TLR3i and ox-LDL individually and in combination. When macrophages were treated with the effective concentrations of TLR3i (10 μM) and ox-LDL (10 μg/mL), the combined treatment did not dampen phagocytosis any more than the individual treatments (Figure 3-9A). The absence of an additive/synergistic effect at high concentrations may reflect saturation of each receptor individually, resulting in no further suppression when both inhibitors are used. Alternatively, it could reflect antagonism between the different inhibitors (e.g. via steric hindrance).

Next, inspired by a study which showed that *Msr1*$^{+/-}$ or *Tlr4*$^{+/-}$ single heterozygote mice showed no impairment in the phagocytosis of *E. coli*, but double heterozygotes were defective in phagocytosis (Amiel et al., 2009), I imagined that using high concentrations of TLR3 inhibitor and ox-LDL may be masking synergistic interaction between TLR3 and scavenger receptors due to saturation of the receptors. Consequently, I treated macrophages with a less optimal concentration of ox-LDL and TLR3i individually and in combination. When *Tlr4*$^{-/-}$ macrophages were treated with 1 μM TLR3i or 1 μg/mL ox-LDL, there was no difference in the phagocytosis of *C. neoformans* compared to untreated cells (Figure 3-9B). However, when treated with 1 μM TLR3i and 1 μg/mL ox-LDL simultaneously, there was a decrease in phagocytosis (Figure 3-9B). I interpret this data to mean that both receptors act in synergy along the same pathway since residual 'flux'

through the pathway when a low dose of inhibitor is used was further dampened by treatment with both inhibitors.

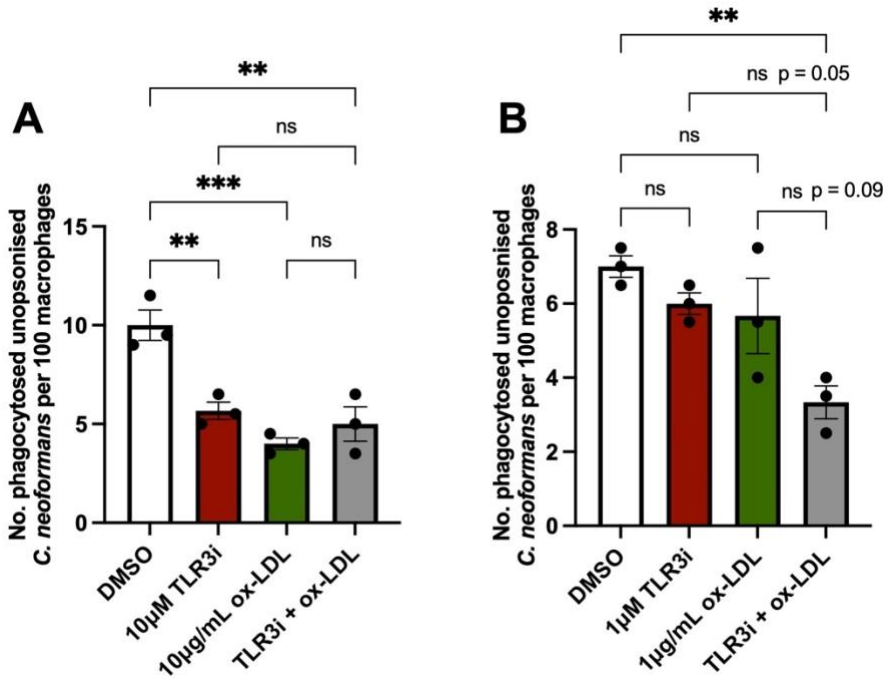

Figure 3-9: TLR4-deficient macrophages treated with TLR3 inhibitor and ox-LDL individually and in combination. *Tlr4*$^{-/-}$ macrophages were pre-treated with optimal **(A)** and suboptimal **(B)** concentrations of TLR3 inhibitor and ox-LDL individually and in combination. The number of internalised fungi per 100 macrophages was quantified. Each data point represents a technical repeat (*n* = 3). Data is representative of two independent experiments and is shown as mean ± SEM; ns, not significant, **p<0.01, ***p<0.001, in a one-way ANOVA followed by Tukey's post-hoc test.

3.9 MyD88 and TRIF are important for the phagocytosis of non-opsonised *C. neoformans*.

Since TLR4 and TLR3 signalling require the downstream adaptor molecules MyD88 (used by all TLRs except TLR3) and TRIF (used by TLR4 and TLR3 only) (Kawai and Akira, 2010), I then wanted to understand the effect of these downstream signalling molecules on the uptake of cryptococci. To achieve this aim, macrophages were exposed to inhibitors of MyD88, TRIF, IKKβ (a kinase downstream of MyD88 that is necessary for NF-κB

activation (Liu et al., 2017)), and TBK1 (a kinase downstream of TRIF that phosphorylates and activates IRF3 (Tsukamoto et al., 2018)). I found that treatment with all four inhibitors dampened phagocytosis in both wildtype and TLR4-deficient macrophages (Figure 3-10A and B).

To validate the findings from the inhibitor treatments, macrophages derived from *Myd88*$^{-/-}$ and *Trif*$^{-/-}$ mice were infected with *C. neoformans*. These macrophages showed significant defect in the phagocytosis of *C. neoformans* (Figure 3-10C). To ensure that the decrease in uptake in MyD88- and TRIF-deficient macrophages was not caused by an inherent deficiency in phagocytic capacity, I infected iBMDMs with CAF2-dTomato *Candida albicans* (Gratacap et al., 2013). The level of *C. albicans* uptake in *Myd88*$^{-/-}$ and *Trif*$^{-/-}$ macrophages was similar to that observed in wildtype macrophages (Figure 3-10D). This is expected since non-TLR PRRs such as Dectin-1, which is recognised as the key PRR involved in the phagocytosis of *C. albicans* (Gantner et al., 2005; Taylor et al., 2007), remain intact in *Myd88*$^{-/-}$ and *Trif*$^{-/-}$ macrophages. Notably, however, the loss of TLR4 also led to an increase in the phagocytosis of *C. albicans* (Figure 3-10D) suggesting the existence of some shared host response to both fungi. Overall, the phagocytosis of non-opsonised *C. neoformans*, but not *C. albicans*, is dependent on MyD88 and TRIF.

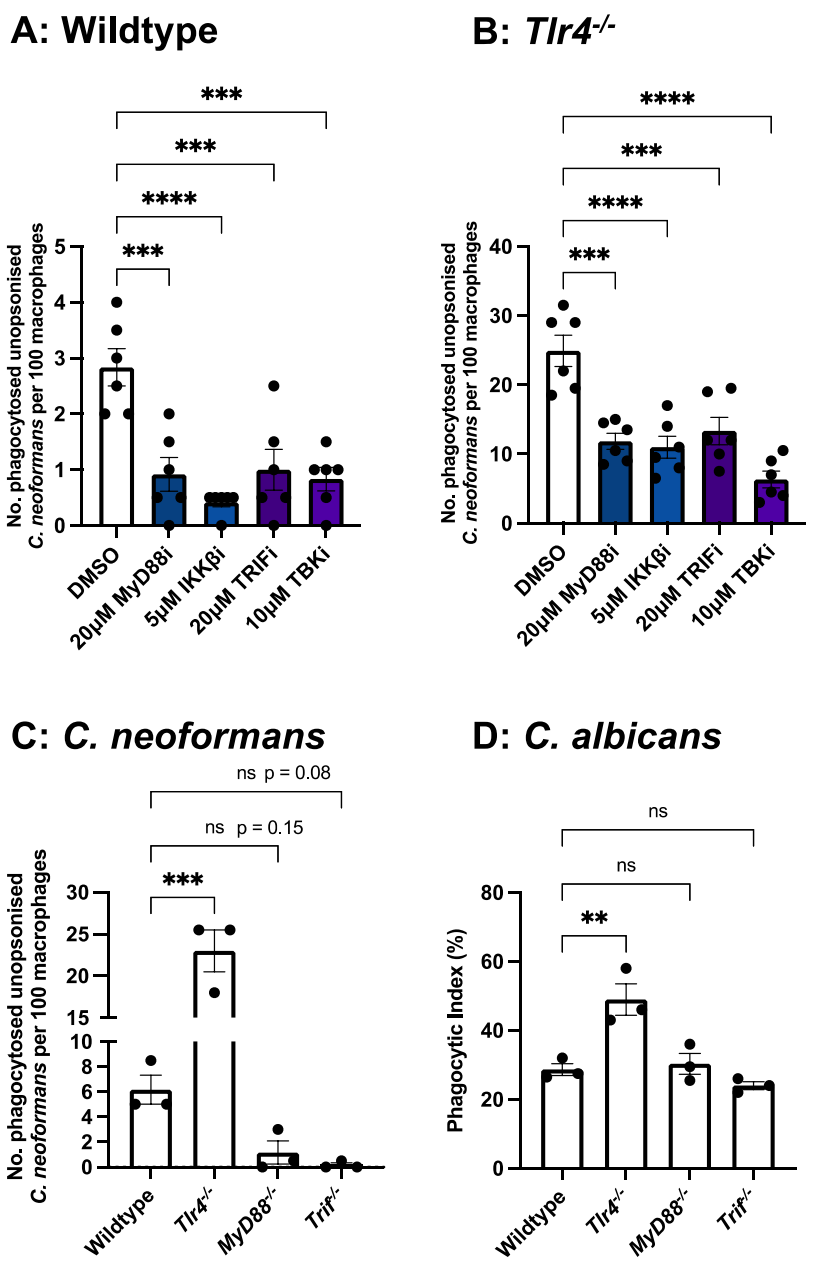

Figure 3-10: MyD88 and TRIF are required for non-opsonic uptake of *C. neoformans*. (A) Wildtype and **(B)** *Tlr4*$^{-/-}$ macrophages were treated with inhibitors of MyD88, IKKβ (a kinase downstream of MyD88 that is necessary for NF-κB activation), TRIF, and TBK1 (a kinase downstream of TRIF that phosphorylates and activates IRF3). Following pre-treatment with the various inhibitors, cells were infected with non-opsonised *C. neoformans*. Data are pooled from two independent experiments (n = 6 per condition). Immortalised BMDMs from wildtype, *Tlr4*$^{-/-}$, *MyD88*$^{-/-}$ and *Trif*$^{-/-}$ mice were infected with **(C)** non-opsonised *C. neoformans* or **(D)** *Candida albicans* at a multiplicity of infection of 5 *C. albicans* to 1 macrophage for 45 mins. Experiments for *C. neoformans* infection was performed more than three times. Infection with *C. albicans* was performed twice. Phagocytosis was quantified as the number of internalised cryptococci within 100 macrophages. Phagocytic index (%) represents the percentage of macrophages that internalised at least one fungus. Data shown as mean ± SEM; ns, not significant, **p<0.01, ***p<0.001, ****p<0.0001 in a one-way analysis of variance (ANOVA) followed by Tukey's post-hoc test.

3.10 MSR1 expression is elevated in *Myd88*$^{-/-}$ and *Trif*$^{-/-}$ macrophages.

Given that *Myd88*$^{-/-}$ and *Trif*$^{-/-}$ macrophages showed significant impairment in the uptake of *C. neoformans*, I hypothesized that these cells express very little MSR1. To test this, the surface expression of MSR1 on these macrophages was measured using flow cytometry. Surprisingly, as with *Tlr4*$^{-/-}$ macrophages, *Myd88*$^{-/-}$ and *Trif*$^{-/-}$ cells showed increased MSR1 expression compared to wildtype iBMDMs (Figure 3-11, A1-A3). This implies that increased MSR1 expression alone is not sufficient to drive increased phagocytosis. Either MyD88 and TRIF themselves or some yet-to-be-identified MyD88- and TRIF-dependent molecules may serve as adaptor proteins or coreceptors necessary to drive pathogen engulfment.

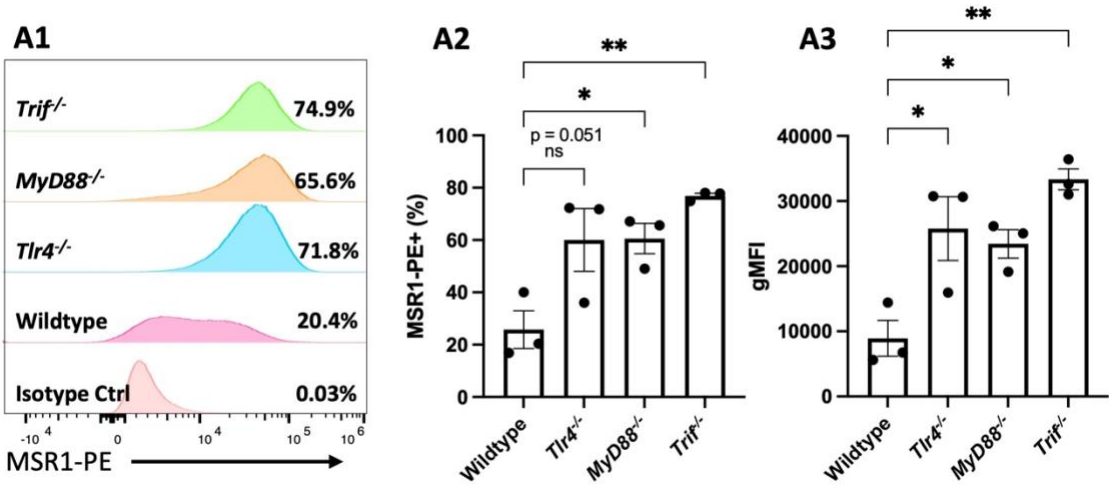

Figure 3-11: Macrophage scavenger receptor 1 (MSR1) expression in wildtype, *Tlr4*$^{-/-}$, *Myd88*$^{-/-}$ and *Trif*$^{-/-}$ macrophages. Baseline surface expression of MSR1 was measured using anti-mouse CD204-PE antibody. PE-labelled rat IgG2a kappa was used as an isotype control. Receptor expression was measured using flow cytometry and analysed using the FlowJo software. **(A1)** Histogram showing the distribution of MSR1-PE positive macrophages. Percentages represent the percentage of MSR1-positive cells. Light pink histogram represents isotype control. Dark pink histogram represents wildtype iBMDM. Blue histogram represents *Tlr4*$^{-/-}$ iBMDM. Yellow histogram represents *MyD88*$^{-/-}$ iBMDM. Green histogram represents *Trif*$^{-/-}$ iBMDM. Data is representative of three independent experiments. **(A2)** Bar graph showing the percentage of MSR1-PE positive macrophages. **(A3)** Bar graph showing normalised geometric mean fluorescence intensity (gMFI). Each data point on bar graphs represents the result from an independent experiment. Experiment was performed three times. Statistical significance was measured using One-Way ANOVA followed by Tukey's post-hoc test; ns, not significant, *p<0.05, **p<0.01.

3.11 MARCO is also involved in the phagocytosis of non-opsonised *C. neoformans*.

There is evidence to suggest that MARCO expression requires LPS stimulation (Kraal et al., 2000); however, my early experiments utilised PMA-stimulated macrophages. Therefore, to test whether a role for MARCO will be unveiled when macrophages are stimulated with LPS instead of PMA, I pre-treated MPI cells with 10 ng/mL LPS for 24 hours prior to infection with *C. neoformans*. In LPS-stimulated macrophages, the loss of both MSR1 and MARCO resulted in a decrease in *C. neoformans* uptake, though MSR1 still appears to be most relevant for *C. neoformans* phagocytosis (Figure 3-12A). This suggests that the lack of MARCO involvement observed in PMA-stimulated macrophages may be due to an absence of MARCO expression in the wildtype cells such that a difference between wildtype and *Marco*$^{-/-}$ macrophages could not be discerned. Surprisingly, DKO MPI showed no difference in uptake compared to wildtype cells (Figure 3-12A), implying the existence of some LPS-induced compensatory mechanism.

To further explore the role of MARCO in non-opsonic uptake, primary peritoneal macrophages (PMϕ) were isolated from wildtype, *Msr1*$^{-/-}$, *Marco*$^{-/-}$ and DKO mice. MARCO expression is predominantly restricted to peritoneal macrophages, alveolar macrophages, and spleen marginal zone macrophages (Kraal et al., 2000; Maler et al., 2017), hence I used primary PMϕs to explore *Cryptococcus* uptake in a "MARCO high" background. I found that MARCO, but not MSR1, was significantly involved in uptake by PMϕ (Figure 3-12B). This suggests the existence of tissue-specific differences in the

involvement of individual scavenger receptors. It has been shown that resident peritoneal macrophages express little to no MSR1, but thioglycolate-elicited PMϕs express more (Winther et al., 1999). Therefore, the lack of a role for MSR1 in uptake by PMϕs may be due to the use of resident PMϕs macrophages and not thioglycolate-elicited PMϕs in this experiment. Finally, the lack of MSR1 involvement in PMϕ could also be due to localisation of MSR1 in intracellular organelle membranes and not on the plasma membrane. However, it is worth noting that due to time constraints this experiment was only conducted once.

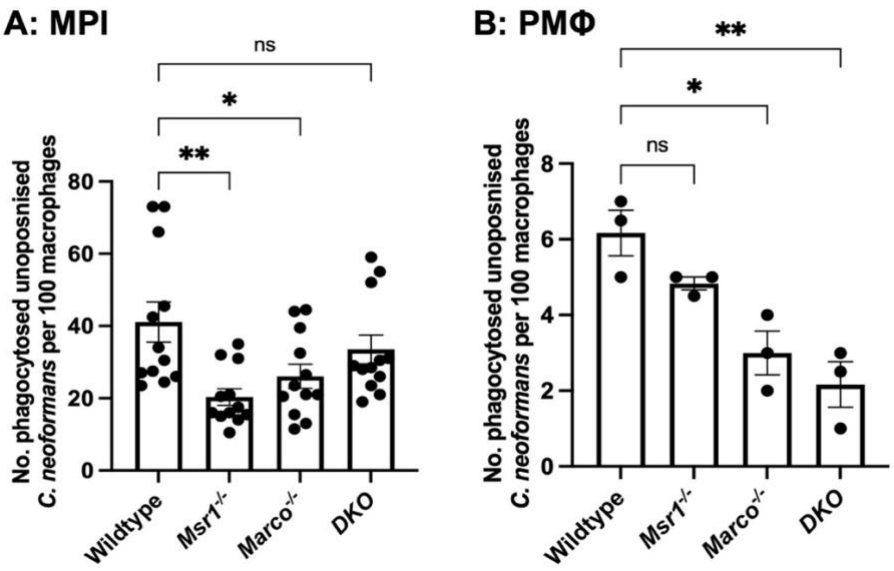

Figure 3-12: MARCO in the non-opsonised phagocytosis of *C. neoformans*. (A) Alveolar-like MPI cells from wildtype, *Msr1*$^{-/-}$, *Marco*$^{-/-}$ and double knockout (DKO) mice were stimulated with 10 ng/mL LPS for 24 h prior to infection with non-opsonised *C. neoformans*. Data shown are pooled from four independent experimental repeats performed in triplicates. **(B)** Primary peritoneal macrophages (PMϕ) from wildtype, *Msr1*$^{-/-}$, *Marco*$^{-/-}$ and double knockout (DKO) mice were stimulated with PMA and then infected with non-opsonised *C. neoformans*. Experiment was performed once, and individual data points represent technical repeats (n = 3) Data is presented as mean ± SEM; ns, not significant; *p<0.05; **p<0.01 in a one-way ANOVA followed by Tukey's post-hoc test.

3.12 Inhibitor screening to identify additional proteins involved in the increased uptake observed in *Tlr4*$^{-/-}$ macrophages.

Still using *Tlr4*$^{-/-}$ macrophages as a model for MSR1-mediated uptake, we carried an inhibitor screen to further probe the mechanism of MSR1-mediated phagocytosis. A study looking into the mechanism of CD36-mediated ligand internalization showed that CD36 forms a signalling complex involving FcRs, integrins and tetraspanins leading to SYK activation and particle internalisation (Heit et al., 2013). Though FcγRs are known to mediate the phagocytosis of antibody-opsonised *C. neoformans*, inspired by Heit et al. (2013), I tested whether they might also be involved in non-opsonic phagocytosis by blocking FcγRII and FcγRIII using the anti-CD16/CD32 monoclonal antibody. Interestingly, we found that FcγRII/III blocking decreased the phagocytosis of non-opsonic phagocytosis (Figure 3-13A).

Engagement of FcγRs is followed by the phosphorylation of their ITAM motifs (Mócsai et al., 2010). Phosphorylated ITAMs lead to the recruitment and activation of SYK, a cytoplasmic tyrosine kinase that is recruited to phosphorylated ITAM domains found on a range of receptors including CLRs and FcγR (Mócsai et al., 2010). Downstream of SYK is phosphoinositide 3-kinase (PI3K), a lipid-modifying enzyme that catalyses the conversion of PtdIns(4,5)P_2 into PtdIns(3,4,5)P_3 in the plasma membrane (Vanhaesebroeck et al., 2012). This ultimately leads to a range of biological responses including actin cytoskeleton remodelling, respiratory burst and cell proliferation and differentiation (Vanhaesebroeck et al., 2012). Next, I tested the involvement of these downstream kinases in MSR1-mediated non-opsonic phagocytosis. I found that the

inhibition of SYK, using piceatannol, and PI3K, using wortmannin, led to a dose-dependent decrease in the phagocytosis of cryptococci by macrophages (Figure 3-13B). This implies a model where *C. neoformans* binding to MSR1 triggers the formation of a signalling complex with FcγRs. The ITAM domain of FcγRs enables SYK and PI3K activation which then drives actin-remodelling and fungal internalisation. It would be interesting to carry out immunoprecipitation and immunoblotting experiments to investigate direct association between MSR1 and these proteins.

It has previously been shown that TLRs induce a phagocytic gene program through the mitogen-activated protein kinase p38 (Doyle et al., 2004), thus I hypothesized that the increased uptake seen in *Tlr4*$^{-/-}$ macrophages is also dependent on the MAPK signalling pathway. To test this hypothesis, I pre-treated macrophages with inhibitors of the three classical MAPKs, namely, extracellular signalling kinases (ERK1/2), p38 and c-Jun N-terminal kinase (JNK). ERK1/2 and p38, but not JNK, were involved in non-opsonic phagocytosis (Figure 3-13C). MAPKs are downstream of SYK signalling and have a range of effector functions including proinflammatory cytokine production and cytoskeletal remodelling (Miller et al., 2012), supporting the proposed model where SYK-recruitment to MSR1 via ITAM-containing coreceptors drives ligand internalisation. ERK1/2 and p38 activation is also triggered by MyD88 and TRIF signalling (Gay et al., 2014). Given the decreased uptake seen following MyD88 and TRIF inhibition (Figure 3-10A and B) and in *Myd88*$^{-/-}$ and *Trif*$^{-/-}$ macrophages (Figure 3-10C), MyD88 and TRIF may also function as adaptor proteins for MSR1-mediated ligand internalisation.

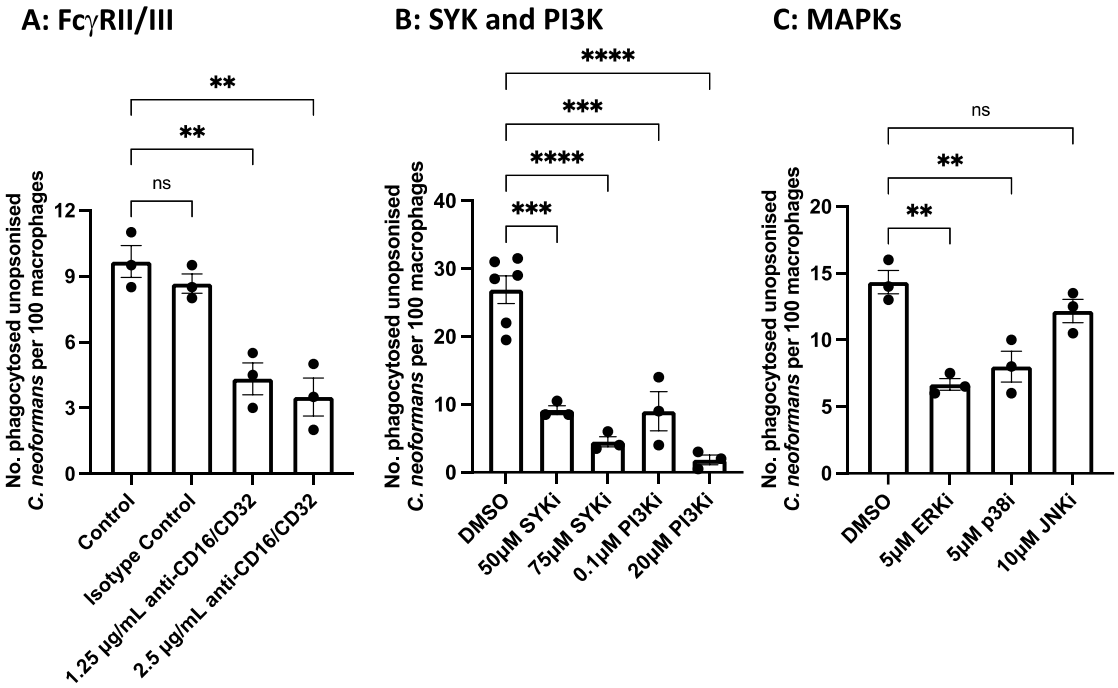

Figure 3-13: Increased uptake in *Tlr4*$^{-/-}$ macrophages is dependent on FcγRs, SYK, PI3K, ERK1/2 and p38, but not JNK. *Tlr4*$^{-/-}$ macrophages were pre-treated with inhibitors of **(A)** FcγRs, **(B)** SYK and PI3K, and **(C)** Mitogen Activate Protein Kinases (MAPKs) for 1 h, then infected with non-opsonised *C. neoformans*. The number of internalised fungi per 100 macrophages was quantified. Data is representative of at least two independent experiments. Each data point represents technical replicates. Data shown as mean ± SEM; ns, not significant, **p<0.01, ***p<0.001, ****p<0.0001 in a one-way ANOVA followed by Tukey's post-hoc test.

3.13 MAPK signalling does not regulate MSR1 expression.

Finally, given that some groups have identified a role for MAPKs in LPS-induced expression of scavenger receptors (Doyle et al., 2004; Hashimoto et al., 2017, 2020), to further explore the mechanism of TLR4-mediated regulation of MSR1 expression, I hypothesized that MAPKs may also modulate baseline MSR1 expression. To test this hypothesis, wildtype and *Tlr4*$^{-/-}$ macrophages were treated with MAPK inhibitors for 24 h, then MSR1 expression was measured using flow cytometry. I observed no difference in MSR1 expression following p38 or JNK inhibition in both wildtype and knockout

macrophages (Figure 3-14A and B). However, according to the normalised gMFI, there was increased MSR1 expression in *Tlr4*$^{-/-}$ macrophages treated with ERK1/2 inhibitor (Figure 3-14, B3) and a similar trend was observed in wildtype macrophages (Figure 3-14, A3).

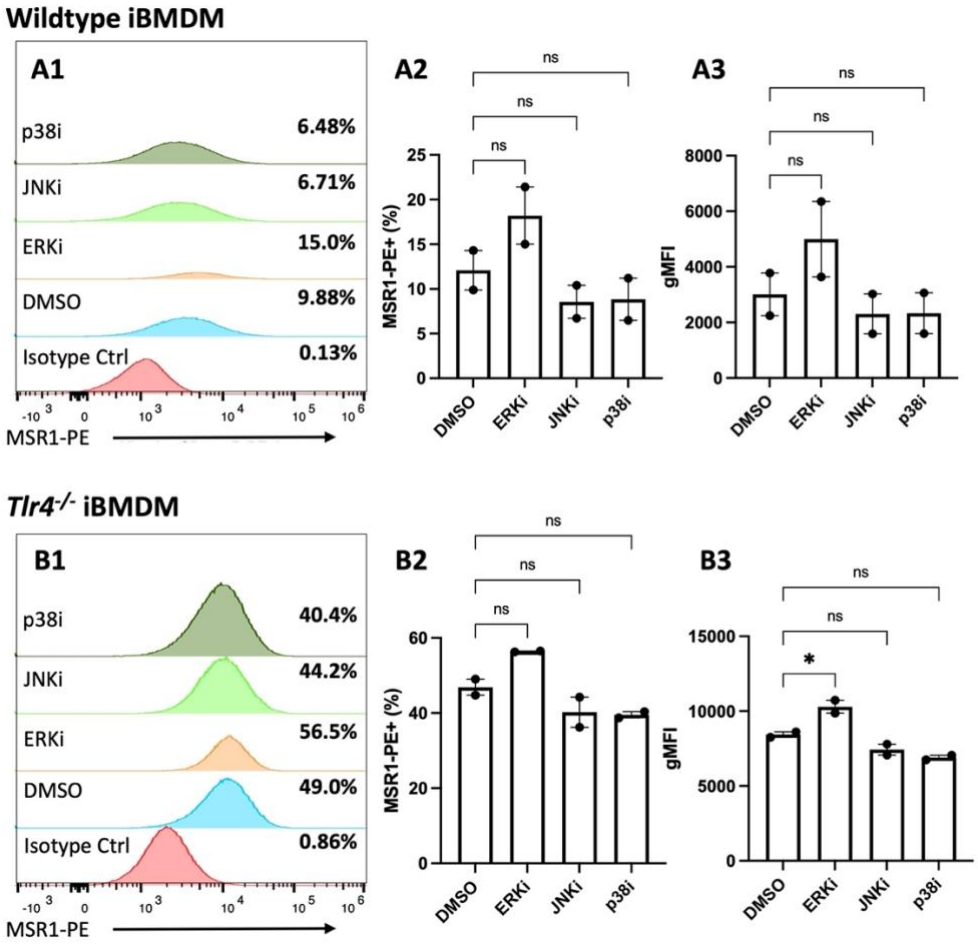

Figure 3-14: MSR1 expression after treatment with MAPK inhibitors. (A1-A3) Wildtype and **(B1-B3)** *Tlr4*$^{-/-}$ iBMDMs were exposed to MAPK inhibitors for 24 h, then cell surface expression of MSR1 was detected using anti-mouse CD204-PE antibody. PE-labelled rat IgG2a kappa was used as an isotype control. Receptor expression was measured using flow cytometry and analysed using the FlowJo software. **(A1 and B1)** Histogram showing the distribution of MSR1-PE positive macrophages. Red graphs represent isotype control. Blue graphs show DMSO treated macrophages. Yellow graphs show macrophages treated with ERK1/2 inhibitor (ERKi). Light green graphs show macrophages treated with JNK inhibitor (JNKi). Dark green graphs show macrophages treated with p38 inhibitor (p38i). Data is representative of two independent experiments. Percentages refer to the percentage of MSR1-positive cells. **(A2 and B2)** Bar graph showing the percentage of MSR1-PE positive macrophages. **(A3 and B3)** Bar graph showing normalised geometric mean fluorescence intensity (gMFI). Each data point on bar graphs represents the result from an independent experiment. Experiment was performed twice and gave similar results.

Statistical significance was measured using One-Way ANOVA followed by Tukey's post-hoc test; ns, not significant.

3.14 Discussion

In this chapter, I provide novel insight into the role of host TLR4 in the non-opsonic phagocytosis of *C. neoformans* by macrophages. I show that TLR4 signalling is important for the uptake of *C. neoformans* not because it is directly involved in the binding and phagocytosis and *C. neoformans*, but because it modulates, through a still unknown mechanism, the abundance of MSR1 on the surface of macrophages. MSR1 is then responsible for the uptake of *C. neoformans* as evidenced by the dramatic decrease in *C. neoformans* uptake in *Msr1*$^{-/-}$ macrophages and the enrichment of MSR1 around phagocytosed *C. neoformans*. This finding is significant as it identifies MSR1 as the key receptor for the non-opsonic phagocytosis of *C. neoformans*. Moreover, the work reveals a previously unknown importance for crosstalk between MSR1 and TLR4 in regulating phagocytic uptake of non-opsonised cryptococci, which is likely of particular importance during the early stages of lung infection. Within medical mycology, C-type lectin receptors, such as Dectin-1, are recognised as the dominant PRRs since they recognise β-glucan molecules found on fungal cell walls (Brown and Gordon, 2001). Moreover, Dectin-1 has long been identified as the key PRR involved in the phagocytosis of *Candida albicans* (Gantner et al., 2005; Taylor et al., 2007). However, Dectin-1 has only shown moderate involvement in the uptake of cryptococci (Nakamura et al., 2007; Lim et al., 2018). The identification of a significant role for MSR1 in uptake provides an explanation for the minimal involvement of Dectin-1 in host response to *C. neoformans* reported thus far.

Given my findings, I propose a model where TLR4 modulates the surface expression of MSR1. Alternatively, TLR4 may modulate intracellular scavenger receptor reservoirs such that suppression of TLR4 signalling drives MSR1 to the plasma membrane. MSR1 is then responsible for the direct binding and internalisation of *C. neoformans* (Figure 3-15). MSR1-mediated uptake may rely on the formation of a signalling complex with FcγRII/III. The ITAM domain of FcγRs enables SYK and PI3K activation which then activates Rac GTPases that drive WASP-Arp2/3 dependent actin cytoskeleton rearrangement leading to phagocytosis (Freeman and Grinstein, 2014). Aside from phagocytosis, the phosphorylation and activation of SYK also lead to the production of ROS, NF-κB expression and MAPK activation (Miller et al., 2012). Notably, SYK-dependent activation of ERK1/2 also drives Rac GTPases-dependent cytoskeleton rearrangement (Choi et al., 2009; Miller et al., 2012). At the same time, TLR3, MyD88 and TRIF can also serve as coreceptors or adaptor proteins leading to the activation of ERK1/2 and p38 which will also drive actin remodelling and pathogen uptake (Figure 3-15). Future research could utilise immunoprecipitation followed by immunoblotting to investigate direct interaction of MSR1 with these molecules, especially TLR3 and FcγRII/III due to their known role as PRRs.

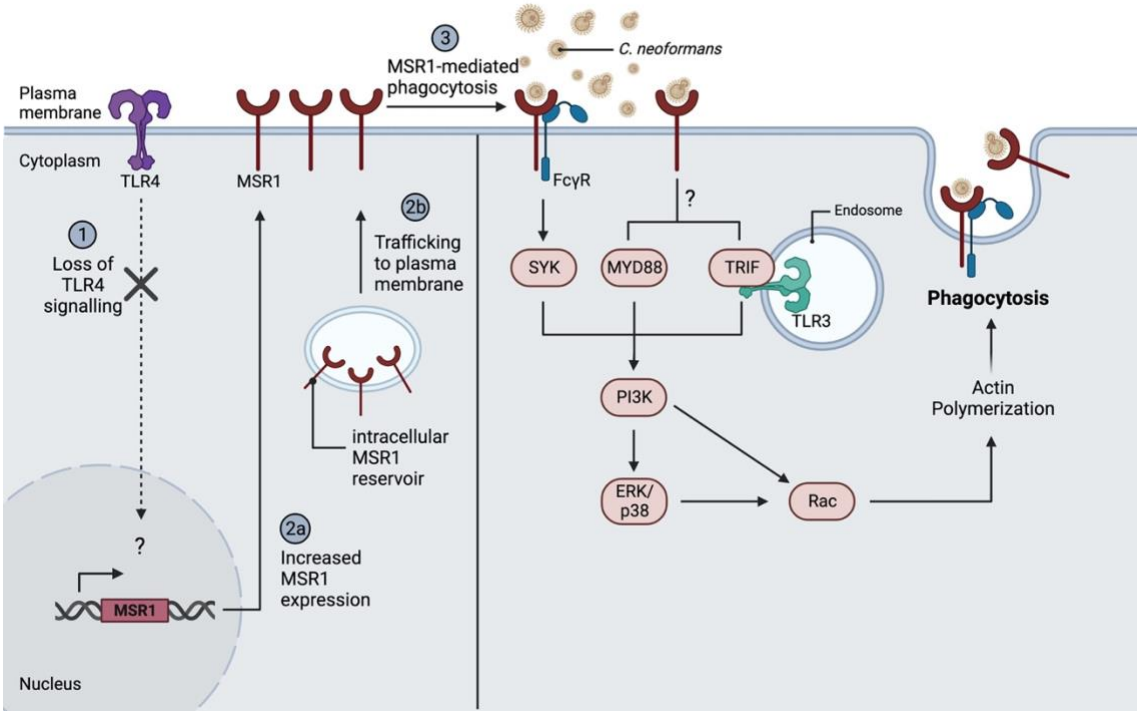

Figure 3-15: Proposed model of MSR1-mediated non-opsonic phagocytosis. TLR4 modulates the surface expression of MSR1 through a yet-to-be-identified mechanism, such that loss of TLR4 signalling drives increased surface expression of MSR1. MSR1 is then responsible for the direct binding and internalisation of *C. neoformans*. MSR1-mediated uptake may rely on the formation of a signalling complex with FcγRII/III. The ITAM domain of FcγRs enables SYK and PI3K activation which then activates Rac GTPases that drive actin polymerization and phagocytosis. At the same time, TLR3, MyD88 and TRIF may also serve as coreceptors or adaptor proteins leading to the activation of ERK1/2 and p38 which will also drive actin remodelling and pathogen uptake. Figure created with BioRender.com.

As described extensively in Chapter 1.2.3, others have investigated the role of TLR4 during host response to *Cryptococcus* infection; however, these studies have revealed contradictory results (Shoham et al., 2001; Yauch et al., 2004, 2005; Nakamura et al., 2006). An *in vitro* study found that the stimulation of microglial cells isolated from the brain of wildtype mice with the TLR4 agonist, lipopolysaccharide (LPS), resulted in increased phagocytosis and killing of *C. neoformans* in a MyD88-dependent manner (Redlich et al., 2013). Additionally, CHO cells transfected with TLR4 were able to bind *Cryptococcus* capsule polysaccharide and activate NF-κB (Shoham et al., 2001).

Interestingly, *in vivo* studies using *Tlr4*$^{-/-}$ mice have found that the receptor is dispensable during host response to infection (Biondo et al., 2005; Nakamura et al., 2006; Yauch et al., 2004). These *in vivo* findings are contradictory to my conclusion that TLR4 is important during macrophage response to infection. However, some of these studies that found no or minimal involvement of TLR4 in mice response to infection used a TLR4 mutant C3H/HeJ and control C3H/HeOuJ mice (Yauch et al., 2004; Biondo et al., 2005), which is different from the C57Bl/6 background of the mice cells used in this project. Even when a TLR4 knockout was generated in C57Bl/6 background, they found no role for TLR4 as well as TLR2 in mice response to infection (Nakamura et al., 2006), even though others have used the same TLR2 knockout in C57Bl/6 background and found a role for TLR2 in mice mortality. A role (or lack thereof) for TLRs may also depend heavily on factors such as the infectious dose and route of infection. Additionally, the data presented in this chapter suggests a role for varying levels of MSR1 expression in mice which was unaccounted for in these studies. Alternatively, the effect of TLR4 deficiency in increasing MSR1 surface expression may be relevant *in vitro*, meanwhile, compensatory mechanisms present *in vivo* may return MSR1 expression to wildtype levels.

Here we show that the knockout of *TLR4* increased MSR1 expression; however, others have shown that LPS-mediated stimulation of TLR4 was also capable of increasing the expression of scavenger receptors leading to increased uptake (Hashimoto et al., 2017; Doyle et al., 2004). Despite expecting TLR4-deficiency and pre-treatment with a TLR4 agonist to have opposing effects, our data imply that any perturbation of TLR4 signalling

increases scavenger receptor expression which could impact macrophage response to infection. Further analysis is needed to investigate the possible existence of compensatory mechanisms in *Tlr4*$^{-/-}$ (as well as *MyD88*$^{-/-}$ and *TRIF*$^{-/-}$ macrophages) that allow for increased scavenger receptor expression.

Crosstalk between MSR1 and TLRs to regulate phagocytosis has been reported in the context of bacterial pathogens. It has been reported that TLR4 synergises with MSR1 to promote the phagocytosis of Gram-negative *E. coli*, while TLR2 synergises with MSR1 in the phagocytosis of Gram-positive *Staphylococcus aureus* (Amiel et al., 2009). They also found that MSR1-mediated phagocytosis of bacteria was regulated by a TLR-MyD88 signalling pathway. Similarly, MSR1 was involved in the phagocytosis of the Gram-negative bacteria *Neisseria meningitidis*, which is also recognised by TLR4 (Mukhopadhyay et al., 2011). At the same time, MSR1-mediated uptake of *N. meningitidis*, downregulated TLR4-dependent inflammatory response to *N. meningitidis* infection by scavenging TLR4 ligands and limiting their availability to TLR4 (Mukhopadhyay et al., 2011). Despite these studies on bacterial pathogens, my data provides the first example of TLR4/MSR1 crosstalk in fungi. It is therefore likely that TLR-MSR1 crosstalk to regulate phagocytosis and cytokine expression is a general phenomenon of host-pathogen interactions.

It was beyond the scope of this study to explore the *in vivo* consequence of MSR1 during *C. neoformans* infection. However, one 2013 study found that *Msr1*$^{-/-}$ knockout mice had reduced lung fungal burden, decreased expression of the non-protective Th2 cytokines,

and increased iNOS expression, indicating activation of anti-cryptococcal immune response (Qiu et al., 2013). Thus, the authors concluded that MSR1 is normally hijacked by *C. neoformans* to promote its pathogenesis. Although the authors provide no data on mice survival over the course of infection, this implies the increased expression of MSR1 I observe in *Tlr4*$^{-/-}$ macrophages could correlate with poor disease outcome. In support of this idea is the finding that *C. neoformans* clinical isolates that are more readily phagocytosed showed increased brain fungal burden, reduced mice survival and polarization towards the nonprotective Th2 response (Hansakon et al., 2020). Similarly, clinical isolates with low phagocytic indexes were associated with poor fungal clearance (even with antifungal treatment) in the cerebrospinal fluid (Alanio et al., 2011). Meanwhile, isolates with high phagocytic indexes were associated with increased mortality (Alanio et al., 2011; Sabiiti et al., 2014b). Therefore, both very high (e.g. as seen in *Tlr4*$^{-/-}$ iBMDMs) and very low (e.g. as seen in *Msr1*$^{-/-}$ MPI cells) phagocytosis are predictors of poor disease outcome, implying the existence of a 'Goldilocks' level of uptake. Determining whether MSR1-driven uptake is advantageous to the host, by aiding in fungal clearance, or the pathogen, by aiding in dissemination, is a fascinating question that will require future investigation using murine models and, ultimately, clinical investigation.

A role for MARCO in phagocytosis was observed following LPS stimulation, but not PMA stimulation. It has been reported that MARCO expression is inducible by LPS, leading to increased phagocytosis of bacteria (Mukhopadhyay et al., 2004; Doyle et al., 2004). However, even with LPS stimulation, MSR1 appeared to have a greater role in the non-

opsonic uptake of *C. neoformans*. The involvement of MARCO during phagocytosis is likely tissue-specific since MARCO expression is limited to macrophages in the lungs, spleen, liver and peritoneum, while MSR1 is more broadly expressed (Maler et al., 2017). More generally, an *in vivo* study found that *Marco*$^{-/-}$ mice infected with *C. neoformans* had a significantly higher lung fungal burden compared to control mice, likely due to their impaired production of CCL2 and CCl7 chemokines needed for the recruitment of dendritic cells and monocytes to the site of infection (Xu et al., 2017b). Additionally, *Marco*$^{-/-}$ mice produced less IFNγ and iNOS, suggesting a role for MARCO in promoting antifungal response. Moreover, they showed that alveolar macrophages isolated from *Marco*$^{-/-}$ mice had decreased phagocytosis, which is in line with my findings using LPS-stimulated cells.

Why does TLR3, an endosomal receptor, impact *C. neoformans* uptake?

Surprisingly, I found that TLR3 inhibition decreased the non-opsonic uptake of *C. neoformans* by wildtype and *Tlr4*$^{-/-}$ macrophages (Figure 3-8A and B). The mechanism by which TLR4-TLR3 crosstalk regulates the expression and/or activity of MSR1 remains unclear. This is particularly difficult to decipher since most SRs, including MSR1, have very short cytoplasmic tails with no discernible signalling domains (Canton et al., 2013). Additionally, since TLR3 is a dsRNA receptor, there is no obvious TLR3 ligand in *C. neoformans*, hence it is uncertain how TLR3 contributes to the modulation of *C. neoformans* uptake by macrophages. It is known that various scavenger receptors, including MSR1, mediate the uptake of extracellular dsRNA (DeWitte-Orr et al., 2010; Limmon et al., 2008). They then serve as vehicles to deliver dsRNA to intracellular

dsRNA-sensing PRRs such as TLR3 (Dieudonné et al., 2012). This raised the concern that the decreased uptake seen following TLR3 inhibition was caused by non-specific binding of the TLR3/dsRNA inhibitor to scavenger receptors. To test this possibility, I treated macrophages with TLR3/dsRNA inhibitor for 1 h, incubated with DiI conjugated ox-LDL and measured ox-LDL uptake using flow cytometry. I found no impact of TR3 inhibition on ox-LDL endocytosis, suggesting the absence of cross-reactivity of the TLR3 inhibitor with scavenger receptors (Figure 3-16).

In our study, the treatment of macrophages with a TLR3 inhibitor did not significantly alter MSR1 expression (Figure 3-8D); however, this does not exclude the possibility that some other signalling protein downstream of TLR3 or an interferon-stimulated gene is involved in the regulation of MSR1 expression. Moreover, macrophages were only treated with TLR3 inhibitor for only 1 h. Thus, it is possible that inhibition for a longer period would show decreased cell surface MSR1.

Interestingly, it has recently been shown that TLR3 is constitutively active, controlling basal levels of type 1 interferons (IFNs) and IFN-stimulated genes (ISGs) (Gao et al., 2021). These small amounts of type 1 IFN and ISGs were enough to restrict viral replication. Therefore, this basal TLR3 activity may contribute to the modulation of MSR1 expression and/or activity without the need for exogenous stimulation. The endogenous ligand responsible for constitutive TLR3 activation is unknown; however, there is evidence that TLR3 can detect self-RNA released by apoptotic cells or self-non-coding RNA (Gao et al., 2021; Takeuchi and Akira, 2010; Takemura et al., 2014). Additionally, a search of the

interferome database found 18 datasets where the treatment of immune cells with type I or type II IFNs led to an over 2-fold increase in the expression of MSR1 (Rusinova et al., 2013). This supports the potential relevance of basal TLR3/type I IFN activity in MSR1-mediated uptake, with a TLR3 inhibitor blocking this activity and leading to decreased uptake.

There was a near complete loss of phagocytosis in *Myd88*$^{-/-}$ and *Trif*$^{-/-}$ macrophages (Figure 3-10C); however, compared to wildtype macrophages, *Myd88*$^{-/-}$ and *Trif*$^{-/-}$ macrophages showed increased expression of MSR1 (Figure 3-11). Therefore, the role of MyD88 and TRIF in the phagocytosis of *C. neoformans* is probably not due to an impact on MSR1 expression. Instead, they may function as coreceptors or activators of some other partner molecule necessary for successful MSR1-mediated pathogen engulfment. Alternatively, they may be involved in a hitherto unidentified MSR1-independent mechanism of *C. neoformans* uptake.

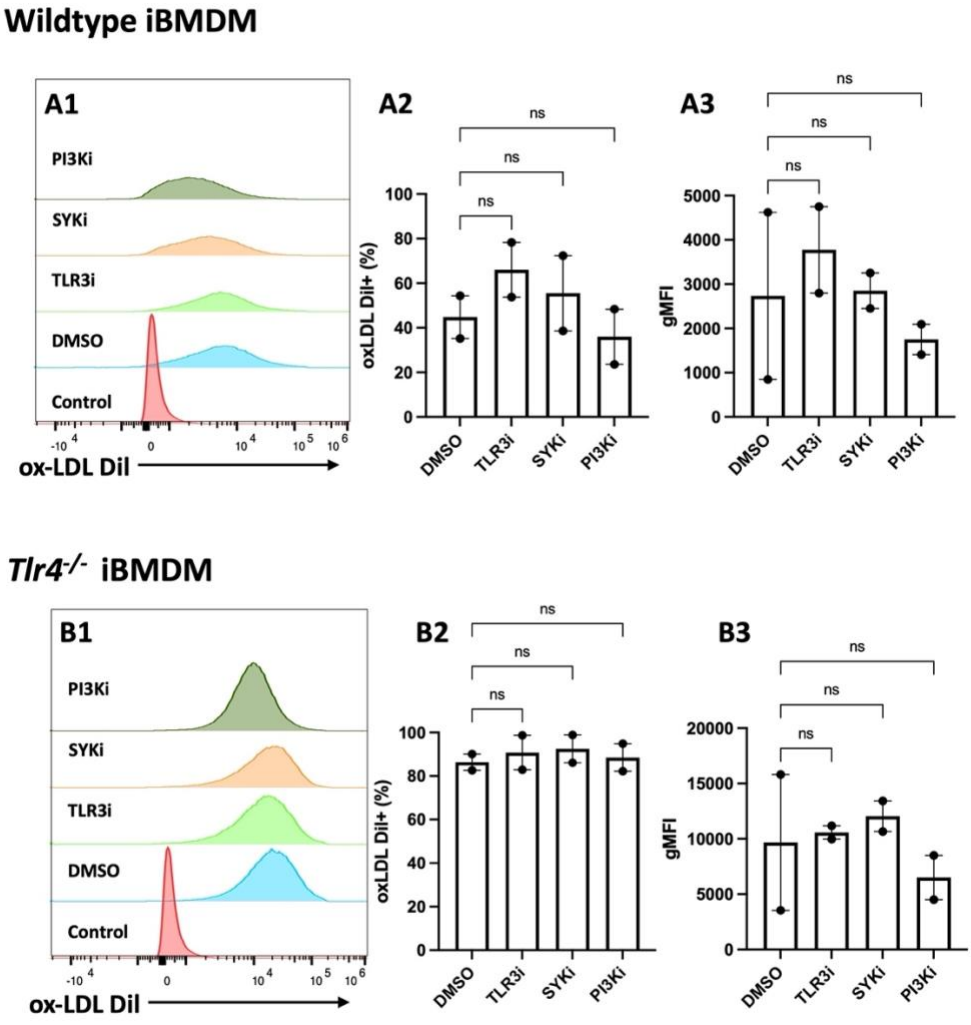

Figure 3-16: Uptake of ox-LDL by macrophages following inhibitor treatment. Wildtype **(A1-A3)** and *Tlr4*$^{-/-}$ **(B1-B3)** iBMDMs were exposed to inhibitors of TLR3 (TLR3/dsRNA complex inhibitor; 10 µg/mL), SYK (Piceatannol; 75 µM) and PI3K (Wortmannin; 20 µM). After 1 hr inhibition, macrophages were exposed to ox-LDL Dil for 30 mins, still in the presence of inhibitors. Uptake of ox-LDL was measured via Dil fluorescence using flow cytometry and analysed using the FlowJo software. **(A1 and B1)** Histogram showing the distribution of ox-LDL positive macrophages. Red graphs represent control cells that were not incubated with ox-LDL Dil. Blue graphs show DMSO treated macrophages. Light green graphs show macrophages treated with TLR3 inhibitor (TLR3i). Yellow graphs show macrophages treated with SYK inhibitor (SYKi). Dark green graphs show macrophages treated with PI3K inhibitor (PI3Ki). **(A2 and B2)** Bar graph showing ox-LDL Dil positive population. **(A3 and B3)** Bar graph showing normalised geometric mean fluorescence intensity (gMFI). Each data point on bar graphs represents the result from an independent experiment. Experiment was performed twice and gave similar results. Statistical significance was measured using One-Way ANOVA followed by Tukey's post hoc test; ns, not significant.

Limitations and Future directions

I have identified a significant role of MSR1 *in vitro*; however, this may not be relevant in an *in vivo* system where other immune response mechanisms can compensate for the loss of MSR1-mediated uptake and cytokine production. Only one study has looked at MSR1 *in vivo* in the context of *C. neoformans* infection. This was a 2013 study that is yet to be reproduced. Moreover, this project focused on phagocytosis as a singular parameter of macrophage response to infection. Nothing is known about how the observed difference in phagocytosis correlates with the cytokine profile of macrophages. It would also be relevant to explore how MSR1 deficiency affects mice survival, lung and brain fungal burden, immune cell recruitment to the site of infection and the immune polarization state.

Although I make some attempts to understand the mechanism by which TLR4 modulates MSR1 expression, the results from this study do not provide a definitive model of TLR4-mediated regulation of MSR1. Unlike other groups that implicated p38, ERK1/2 and JAK-STAT signalling in modulating LPS-induced scavenger receptor expression (Hashimoto et al., 2017, 2020; Doyle et al., 2004), I failed to find a role for MAPKs in the modulation of MSR1 expression (Figure 3-14). These studies have focused on LPS-induced expression of scavenger receptors; however, I utilised unstimulated macrophages. Therefore, future work can seek to identify modulators of baseline MSR1 expression using techniques such as electrophoretic mobility shift assay followed by mass spectrometry to identify transcription factors that bind to the MSR1 promoter. Some transcription factors already shown to modulate MSR1 expression include AP1, ATF-2, c-Jun, GATA-1 and NFE2L2 (Safran et al., 2021; Bonilla et al., 2013). In particular, in an autophagy-

related gene 7-deficient (*Atg7*$^{-/-}$) background, nuclear factor erythroid-derived 2-like 2 (NFE2L2) transcription factor was found to bind antioxidant response elements (ARE) in the MSR1 gene promoter leading to increased MSR1 mRNA and protein and ultimately increased phagocytosis of *Mycobacterium tuberculosis, E. coli and S. aureus* (Bonilla et al., 2013). This study implicates autophagy in the regulation of scavenger receptor-mediated phagocytosis.

Finally, although I implicate TLR3, MyD88, TRIF, SYK, PI3K, FcγRII/III, ERK1/2 and p38 as possible coreceptors or downstream mediators of MSR1-mediated phagocytosis, these proteins were identified using *Tlr4*$^{-/-}$ macrophages as a crude model for MSR1-mediated phagocytosis. The current data do not provide sufficient evidence for the direct involvement of these proteins in MSR1 signalling and the mechanism of action. Future research could utilise immunoprecipitation followed by immunoblotting to investigate direct interaction of MSR1 with TLR3, MyD88, TRIF and FcγRII/III. Alternatively, immunofluorescence and confocal microscopy could be used to visualise colocalization of MSR1 with various adaptor proteins and coreceptors.

Importantly, we cannot rule out the possibility of direct MSR1 signalling via its cytoplasmic tail. Human MSR1 has a 50 amino acids long cytoplasmic tail (55 amino acids long in mice). *In silico* analysis of the MSR1 protein sequence reveals the presence of a conserved serine residue in humans and mice (serine 27 in humans, and serine 32 in mice), that can be phosphorylated according to UniProt (The UniProt Consortium, 2023), suggestive of a downstream phosphorylation cascade. In fact, it has been shown that a

direct association between MSR1 and Mer receptor tyrosine kinase is needed to drive uptake of apoptotic cells by macrophages (Todt et al., 2008). Similarly, Lyn tyrosine kinase has been co-immunoprecipitated with MSR1 during uptake of acetylated LDL (Miki et al., 1996), supporting the possibility of direct MSR1-mediated signalling.

Immunoprecipitation and immunoblotting studies have also identified direct interaction between MSR1 and TRAF3, an E3 ubiquitin ligase downstream of TRIF (Xie et al., 2020), and TRAF6, an E3 ubiquitin ligase downstream of MYD88 (Yu et al., 2011) to suppress the activation of IRFs and NF-κB, respectively. It has been shown that Lysine 27 (K27) of murine MSR1 can be K63-polyubiquitinated, with the polyubiquitin chain serving as a scaffold for TAK1/MKK7/JNK signalling complex recruitment to MSR1 (Guo et al., 2019). It is possible that TRAF3 and/or TRAF6 are the E3 ubiquitin ligases responsible for the polyubiquitination identified by Guo et al. (2019).

Having shown that MSR1 is a key receptor for non-opsonic phagocytosis of *C. neoformans*, future work should aim to: (1) decipher the impact of MSR1 genetic deficiency in a mice model of *C. neoformans* infection; (2) identify the *C. neoformans* ligand recognised by MSR1; (3) provide direct evidence of members of the MSR1 signalosome; and (4) identify signalling proteins downstream of the MSR1 signalosome and how they influence innate immune response. Altogether, these findings will increase our understanding of host-*Cryptococcus* interaction and inform the development of host-directed immunotherapy.

Chapter 4 The scavenger receptor MARCO modulates the vomocytosis/ non-lytic expulsion of *Cryptococcus neoformans* from macrophages.

The following thesis chapter contains work that has been adapted for publication as a brief report. I am the first author on this manuscript and was responsible for writing the entire manuscript, though I received feedback from my supervisor and collaborators.

4.1 Introduction

In addition to survival and replication within macrophages, another outcome of the macrophage-*Cryptococcus* interaction is vomocytosis. Vomocytosis is a non-lytic expulsion mechanism where fully phagocytosed fungi are expelled from the macrophage with no evidence of host cell damage (Ma et al., 2006; Alvarez and Casadevall, 2006; Seoane and May, 2019). Vomocytosis occurs through the fusion of a *Cryptococcus*-containing phagosome with the plasma membrane in a manner that is modulated by the actin cytoskeleton (Johnston and May, 2010). Treatment of macrophages with the inhibitor of actin polymerization, cytochalasin D, enhances vomocytosis (Alvarez and Casadevall, 2006; Johnston and May, 2010), possibly due to reduced formation of "actin cages" that prevent phagosome fusion with the plasma membrane (Johnston and May, 2010). It has also been shown to require phagosome membrane permeabilization (Johnston and May, 2010) and a failure to fully acidify the phagosome (Smith et al., 2015; Fu et al., 2018). With regards to the molecular signals

that modulate vomocytosis, a screening of signalling kinase inhibitors identified the mitogen-activated protein kinase ERK5 as a regulator of vomocytosis, with ERK5 inhibition leading to increased vomocytosis (Gilbert et al., 2017). Meanwhile, deficiency of the phospholipid binding protein Annexin A2 led to decreased vomocytosis (Stukes et al., 2016). Finally, stimulation of macrophages with type 1 interferons (IFN-α and IFN-β), mimicking viral coinfection, increased cryptococcal vomocytosis (Seoane et al., 2020). Very little else is known about the host and/or fungal regulators of vomocytosis.

In this chapter, I describe the serendipitous discovery that MARCO is a critical host molecule that regulates the vomocytosis of *C. neoformans*.

4.2 *Marco*$^{-/-}$ MPI cells show elevated vomocytosis.

While using MPI cells derived from wildtype, *Msr1*$^{-/-}$, *Marco*$^{-/-}$ or double knockout (DKO) C57BL/6 mice to investigate the role of scavenger receptors in the non-opsonic uptake of *C. neoformans* (see Chapter 3), I carried out a timelapse experiment to measure the intracellular proliferation of *Cryptococcus* within these macrophages. At first glance, it appears as though there is decreased proliferation within *Marco*$^{-/-}$ macrophages (Figure 4-1). However, while analysing the timelapse videos I noticed that this decrease in perceived IPR was not due to increased killing of internalised *C. neoformans* by MARCO-deficient macrophages but rather was caused by elevated vomocytosis of *C. neoformans* from *Marco*$^{-/-}$ cells (Figure 4-2A, B and C; Appendix Supp Videos 1-4). Nearly, 100% of infected macrophages experienced at least one vomocytosis event. This dramatic increase in non-lytic expulsion was observed in both PMA-stimulated and LPS-

stimulated macrophages. Since MARCO-expression is induced by LPS, all subsequent experiments utilised LPS-stimulated macrophages.

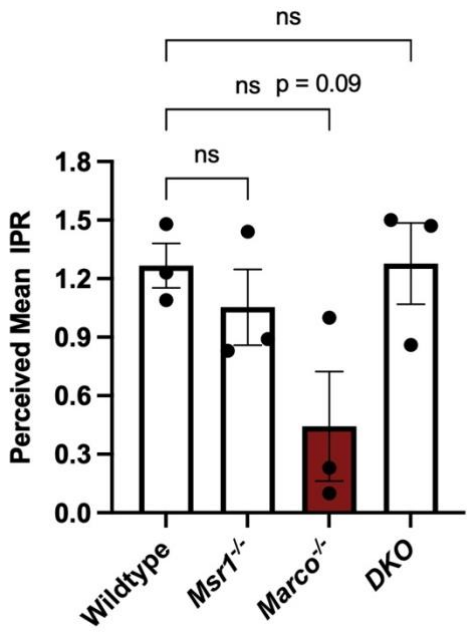

Figure 4-1: Apparent Intracellular Proliferation Rate (IPR) of *C. neoformans* in MPI cells derived from wildtype, *Msr1*$^{-/-}$, *Marco*$^{-/-}$ or double knockout (DKO) C57BL/6 mice. Macrophages were stimulated with PMA for 1 h, infected with *C. neoformans* for 2 h and imaged every 5 min for 18 h. To determine IPR, the number of internalised fungi per 100 macrophages at the 'first frame' (T0) and 'last frame' (T10) was quantified and IPR was calculated using the equation: IPR = T10/T0. Quantification of IPR was performed once. Each data point is a technical replicate. Data shown as mean ± SEM; ns, not significant in a one-way ANOVA followed by Tukey's post-hoc test. Red solid fill was used to highlight the result of *Marco*$^{-/-}$ macrophages.

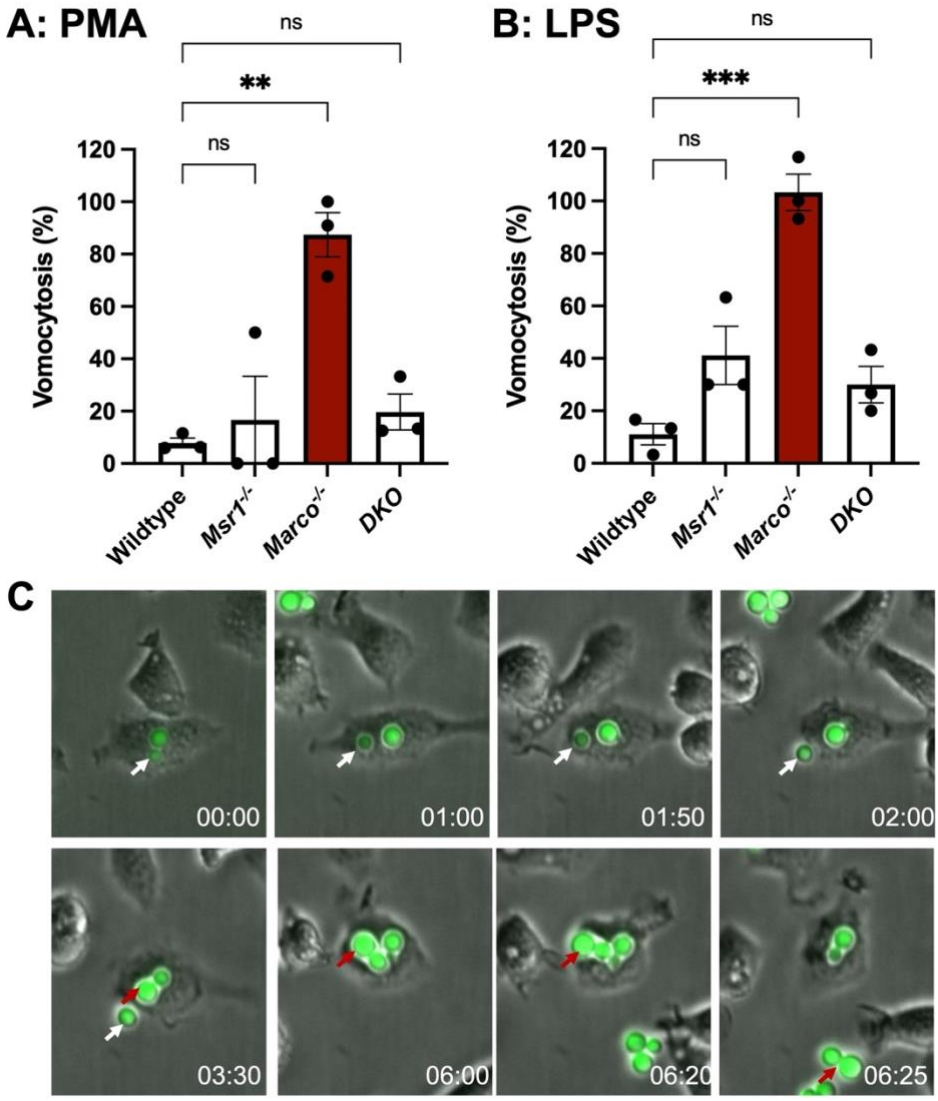

Figure 4-2: Vomocytosis in MPI cells. Wildtype, *Msr1*$^{-/-}$, *Marco*$^{-/-}$ or double knockout (DKO) MPI cells were stimulated with PMA **(A)** or LPS **(B)** prior to infection with *C. neoformans*. After 2 h infection, extracellular fungi were washed off, fresh culture media supplemented with 1% GM-CSF was added back into the wells and images were acquired every 5 mins for 18 h. Vomocytosis was quantified over a 10 h period as the percentage of infected macrophages that experienced one or more vomocytosis events. Data represents one independent experiment. Each data point is a technical replicate (n = 3). Data shown as mean ± SEM; ns, not significant; **p<0.01; ***p<0.001 in a one-way ANOVA followed by Tukey's post-hoc test. Red solid fill was used to highlight the result of *Marco*$^{-/-}$ macrophages. **(C)** Representative image of vomocytosis in PMA stimulated *Marco*$^{-/-}$ MPI cells infected with green fluorescent protein-expressing *C. neoformans*. Images were acquired on the Nikon Ti Microscope. Time is presented in hh:mm; white arrows follow the course of one vomocytosis event; red arrows follow the course of a second vomocytosis event by the same macrophage.

4.3 Vomocytosis in *Marco*$^{-/-}$ cells occurred within the first hour of timelapse imaging.

I extended the initial dataset by conducting several repeat experiments in *Marco*$^{-/-}$ macrophages in order to understand the distribution of vomocytosis events. Not only did *Marco*$^{-/-}$ macrophages show elevated vomocytosis (Figure 4-3A), but the majority of vomocytosis events occurred within the first five hours of the initiation of the timelapse video, with the median time to a vomocytosis event being 0.92 h (55 mins) (Figure 4-3B; Appendix Supp Video 5). Meanwhile, vomocytosis in wildtype macrophages occurred within a much wider range of time with the median time to vomocytosis being 10.6 h (10 h: 35 mins) (Figure 4-3B). Figure 4-3C shows examples of rapid vomocytosis in *Marco*$^{-/-}$ macrophages.

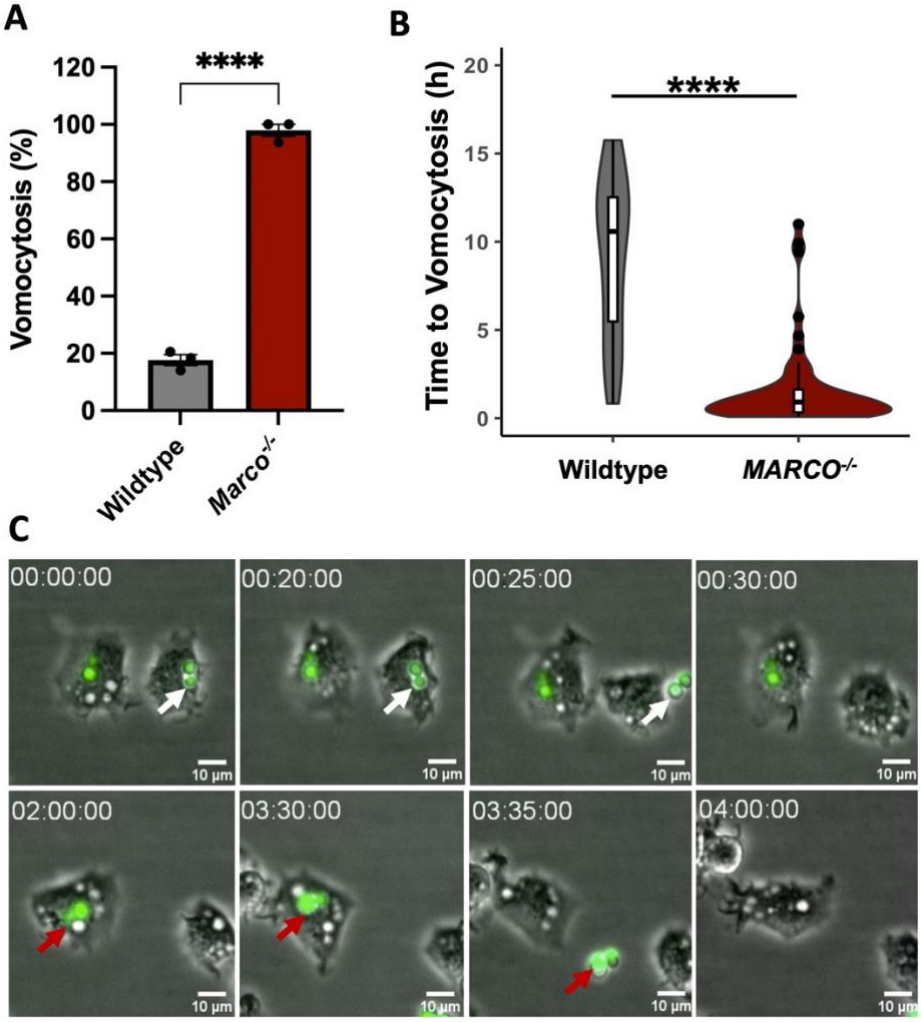

Figure 4-3: Time to Vomocytosis events. (A) LPS stimulated *Marco*$^{-/-}$ macrophages consistently show increased vomocytosis. After 2 h infection, extracellular fungi were washed off, fresh culture media supplemented with 1% GM-CSF was added back into the wells and images were acquired every 5 mins for 16 h. Vomocytosis was quantified over the entire 16 h period and expressed as the percentage (%) of infected macrophages that experienced at least one vomocytosis event. Data represents one independent experiment. Each data point is a technical replicate (n = 3). Data shown as mean ± SEM; ****p<0.0001 in a t-test. **(B)** The time at which individual vomocytosis events took place was quantified and expressed as decimals. Wildtype, n = 32, and *Marco*$^{-/-}$, n = 56, vomocytosis events were observed. A violin plot with an overlapping box plot was created using the ggplot2 package on R. ****p<0.0001 in a Mann-Whitney test. **(C)** Representative image of rapid vomocytosis in LPS stimulated *Marco*$^{-/-}$ MPI cells infected with green fluorescent protein-expressing *C. neoformans*. Images were acquired on the Nikon Ti Microscope. Time is presented in hh:mm:ss; white arrows follow the course of one vomocytosis event; red arrows follow the course of a second vomocytosis event. Scale bar = 10 µm.

4.4 Vomocytosis was observed in human serum-opsonised and 18B7 antibody-opsonised *C. neoformans*, but not in heat-killed *C. neoformans* or latex beads.

To investigate whether this increased vomocytosis in *Marco*$^{-/-}$ macrophages was specific to live non-opsonised *C. neoformans*, I infected macrophages with heat-killed *C. neoformans*, 7 μm diameter latex beads, human serum-opsonised *C. neoformans* and 18B7 anti-GXM antibody-opsonised *C. neoformans*. In line with previous data showing that inert particles do not undergo vomocytosis (Ma et al., 2006; Alvarez and Casadevall, 2006), I observed no vomocytosis of heat-killed *C. neoformans* by either wildtype or *Marco*$^{-/-}$ macrophages out of 55 infected macrophages observed (Table 3), and only a single event (amongst 239 cells) when macrophages were "infected" with latex beads (Table 4; Appendix Supp Video 6). However, *Marco*$^{-/-}$ macrophages showed decreased phagocytosis of heat-killed cryptococci (Figure 4-4A) and latex beads (Figure 4-4B; Appendix Supp Video 7) compared to wildtype cells. Moreover, I observed binding of latex beads to the surface of *Marco*$^{-/-}$ cell without successful internalisation (Appendix Supp Video 7).

Next, I infected macrophages with *C. neoformans* opsonised with 10% human serum to drive uptake via the complement pathway. Similar to the phenotype observed with non-opsonic infection, *Marco*$^{-/-}$ cells showed a significant increase in the vomocytosis of human serum-opsonised *C. neoformans* (Figure 4-5A). There was also a decrease in the uptake of serum opsonised cryptococci by *Marco*$^{-/-}$ macrophages compared to wildtype macrophages (Figure 4-5B), although this most likely reflects low levels of opsonisation

in this experiment, since the number of internalised fungi after serum opsonisation was very similar to that those seen with non-opsonised infection (Figure 3-12A).

Given the uncertainty surrounding the efficiency of human serum-mediated opsonisation, I then utilised 18B7 antibody-opsonised fungi to drive uptake via FcγRs. Significantly more *Marco*$^{-/-}$ macrophages vomocytosed antibody-opsonised fungi compared to wildtype cells (Figure 4-5C). Despite this difference in vomocytosis, there was no difference in FcγR-mediated phagocytosis between wildtype and *Marco*$^{-/-}$ macrophages (Figure 4-5D). The data suggest that the role of MARCO in vomocytosis is independent of its role in uptake.

Table 3: Quantification of the vomocytosis of heat-killed *C. neoformans* in wildtype and *Marco*$^{-/-}$ macrophages.

	# infected macrophages counted	# vomocytosis events observed
Wildtype	39	0
***Marco*$^{-/-}$**	16	0

Table 4: Quantification of the vomocytosis of latex beads in wildtype and *Marco*$^{-/-}$ macrophages.

	# infected macrophages counted	# vomocytosis events observed
Wildtype	203	1
***Marco*$^{-/-}$**	36	0

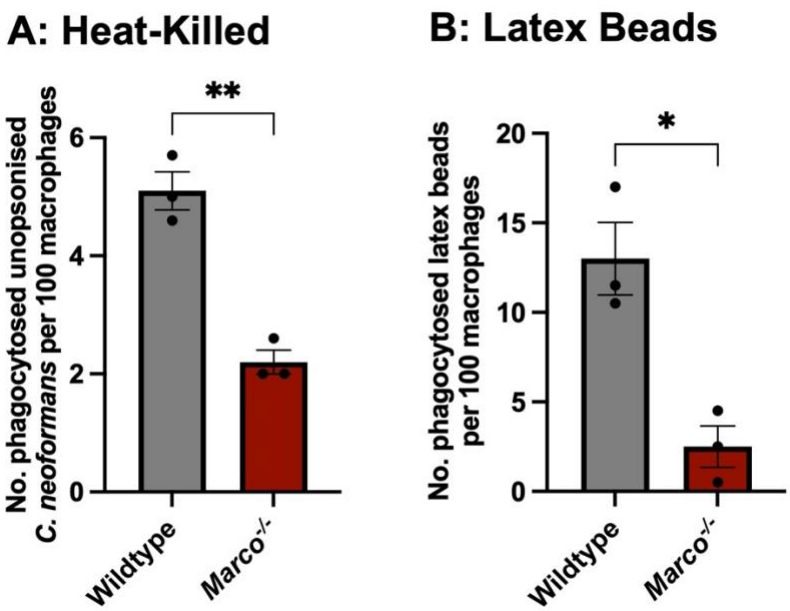

Figure 4-4: Phagocytosis of heat-killed *C. neoformans* and latex beads is decreased in *Marco*$^{-/-}$ macrophages. Wildtype and *Marco*$^{-/-}$ macrophages were infected with **(A)** *C. neoformans* killed by heating at 56°C for 30 mins or **(B)** 7 μm latex beads. After 2 h infection, images were acquired every 5 mins for 16 h. The number of internalised cryptococci or latex beads per 100 macrophages was quantified. Data represents two independent experiments. Each data point is a technical replicate (n = 3). Data shown as mean ± SEM; *p<0.05; **p<0.01 in a t-test.

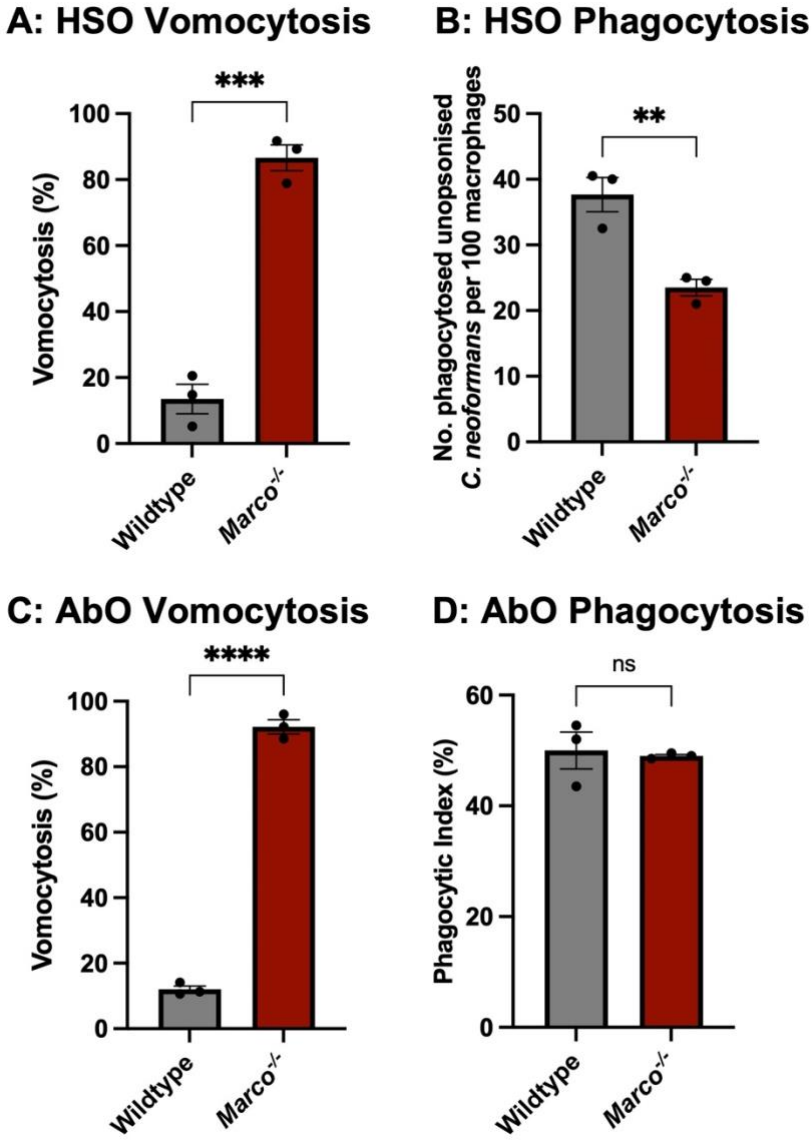

Figure 4-5: Elevated vomocytosis in *Marco*$^{-/-}$ macrophages is observed in serum and antibody-opsonised *C. neoformans*. Wildtype and *Marco*$^{-/-}$ macrophages were infected with **(A, B)** human serum-opsonised *C. neoformans* (HSO) and **(C, D)** 18B7 antibody-opsonised *C. neoformans* (AbO). After 2 h infection, images were acquired every 5 mins for 16 h. Vomocytosis was quantified over the entire 16 h period and expressed as the percentage (%) of infected macrophages that experienced at least one vomocytosis event **(A, C)**. The number of internalised *C. neoformans* **(B)** per 100 macrophages was quantified. (**D)** Phagocytic index (%) represents the percentage of macrophages that phagocytosed one or more cryptococci. Data shown as mean ± SEM; ns, not significant; **p<0.01; ***p<0.001; ****p<0.0001 in a t-test. Infection with human serum-opsonised *C. neoformans* was performed once. Infection with antibody-opsonised *C. neoformans* was performed twice.

4.5 Vomocytosis of a yeast-locked *Candida albicans* strain in wildtype and *Marco*$^{-/-}$ MPI cells

Aside from *Cryptococcus neoformans*, non-lytic expulsion has been described in other pathogens including *Cryptococcus gattii* (Gilbert et al., 2017), *Candida albicans* (Bain et al., 2012), *Mycobacterium marinum* and *M. tuberculosis* (Hagedorn et al., 2009). To investigate whether MARCO-mediated modulation of vomocytosis is unique to cryptococci or a broader phenomenon affecting other host-pathogen interactions, I infected MPI cells with a yeast-locked TetOn-NRG1 *C. albicans* strain that constitutively expresses Nrg1 transcription factor, thereby preventing yeast to hypha formation (Ost et al., 2021). Filamentation is inducible in this strain in the presence of tetracycline antibiotics (Ost et al., 2021). Infected macrophages were observed over a 6 h period and vomocytosis was quantified. I observed increased vomocytosis of yeast-locked *Candida* from MARCO-deficient macrophages compared to wildtype macrophages (Figure 4-6A and C; Appendix Supp Video 8). The percentage of *Marco*$^{-/-}$ macrophages that experienced at least one vomocytosis event was not as dramatic as that observed with *Cryptococcus*; however, vomocytosis of wildtype *C. albicans* is rare, happening at a rate of <1% in a 6-hour period (Bain et al., 2012). Therefore, a rate of 30% in a 6-hour period in *Marco*$^{-/-}$ cells, though with a yeast-locked *Candida* strain, is dramatic for this fungal pathogen. As expected, since phagocytosis of *Candida* is mainly driven by Dectin-1 (Gantner et al., 2005), there was no difference in phagocytic index between wildtype and *Marco*$^{-/-}$ macrophages (Figure 4-6B).

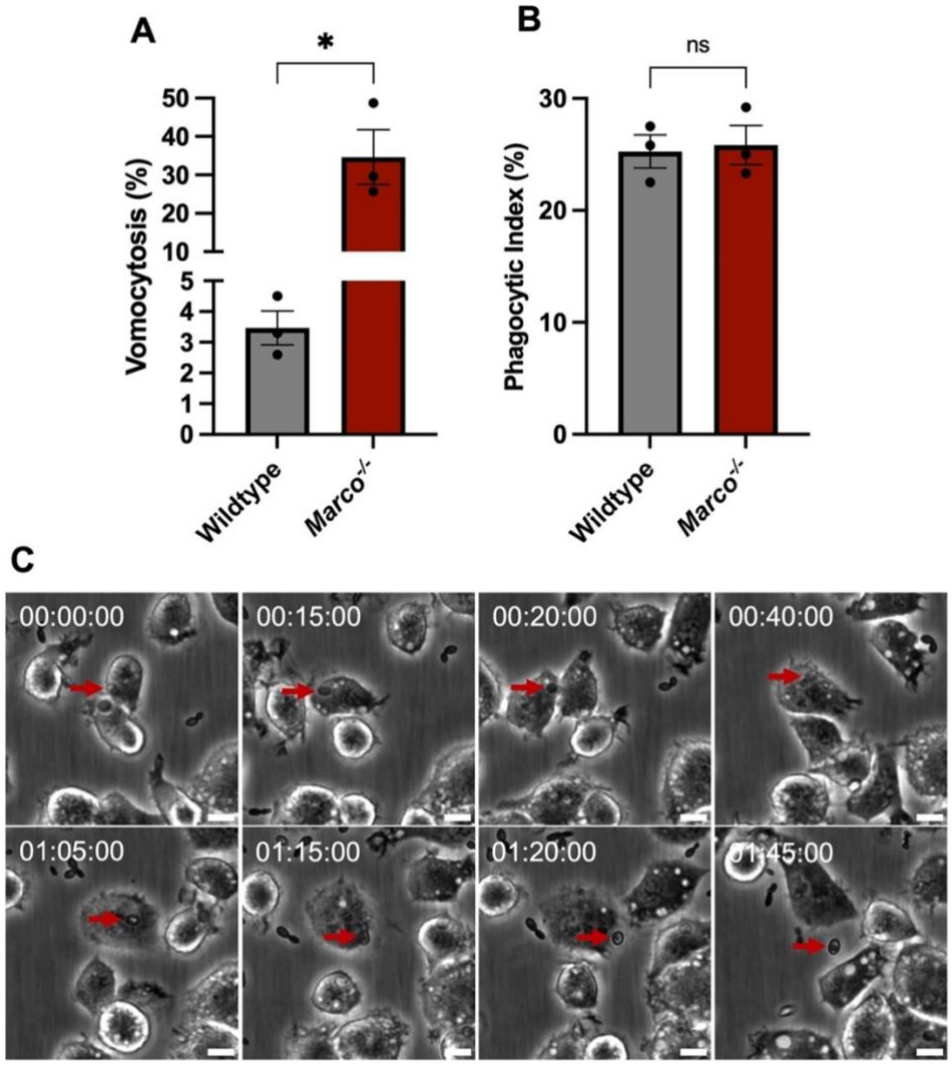

Figure 4-6: MARCO deficiency results in elevated vomocytosis of a yeast-locked *Candida albicans* strain without affecting phagocytosis. (A) MPI cells were stimulated with 10 ng/mL LPS overnight, then infected with a yeast-locked TetO-NRG1 *C. albicans* strain that constitutively expresses Nrg1 transcription factor, thereby preventing yeast to hyphae formation (Ost et al., 2021). Vomocytosis was quantified over 6 h and expressed as the percentage (%) of infected macrophages that experienced at least one vomocytosis event. **(B)** Phagocytic index (%) represents the percentage of macrophages that phagocytosed one or more candida cells 30 mins post-infection. Data shown as mean ± SEM; ns, not significant; *p<0.05 in a t-test. Data represents a single experiment. Each data point is a technical replicate. **(C)** Representative image showing vomocytosis of *C. albicans* from *Marco*$^{-/-}$ MPI cells. Images were acquired on the Nikon Ti Microscope. Time is presented in hh:mm:ss; red arrows follow the course of a vomocytosis event; scale bar = 10 μm.

4.6 Treatment of wildtype MPI cells with inhibitors of MARCO does not phenocopy increased vomocytosis seen in *Marco*$^{-/-}$ cells.

The data presented above, indicating that the impact of MARCO on vomocytosis is independent of the route of uptake, suggests that MARCO may be acting independently of ligand binding in this process. To explore this hypothesis, I tried to replicate the increased vomocytosis observed in *Marco*$^{-/-}$ cells by exposing wildtype macrophages to different MARCO inhibitors that bind to the extracellular domain. I began by exposing LPS-stimulated wildtype MPI cells to polyguanylic acid potassium salt (polyG), a MARCO ligand (Kanno et al., 2020, 2007; Elomaa et al., 1998), and quantifying the percentage of infected macrophages that experienced at least one vomocytosis event and the number of internalised cryptococci. Unlike genetic knockout, the inhibition of MARCO using polyG did not result in an increase in vomocytosis (Figure 4-7A). However, polyG was able to inhibit the phagocytosis of non-opsonic *C. neoformans* (Figure 4-7B), reminiscent of decreased uptake seen in LPS-stimulated *Marco*$^{-/-}$ macrophages. Since polyG functions as a competitive inhibitor and does not block MARCO-mediated downstream signalling, this suggests that the impact of MARCO on vomocytosis can be mechanistically separated from its ligand-binding activity.

Next, MARCO receptors on wildtype macrophages were blocked using increasing concentrations of an anti-MARCO monoclonal antibody (mAb). As with polyG pre-treatment, anti-MARCO mAb had no impact on the rate of vomocytosis in wildtype macrophages (Figure 4-7C), although it reduced MARCO-mediated phagocytosis in a dose-dependent manner (Figure 4-7D). The anti-MARCO antibody used recognises the

ligand binding domain of MARCO receptors, thus, its inhibitory activity is also due to competing for receptor binding with *C. neoformans* and may explain the observation that mAb treatment led to decreased uptake without affecting vomocytosis rate. Taken together, the role of MARCO in vomocytosis is most likely independent of its role in uptake, hence the inability of inhibitors that act on the ligand binding site to phenocopy the genetic knockout of MARCO receptor.

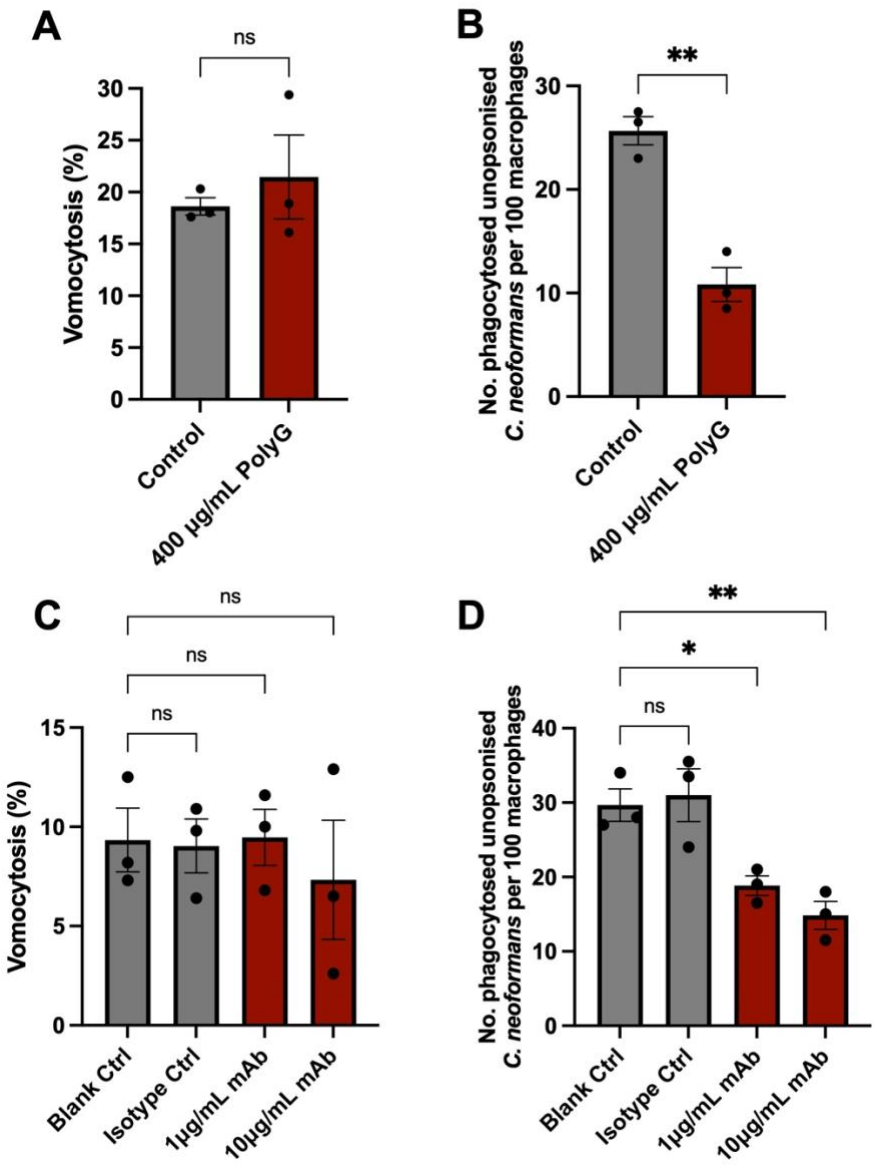

Figure 4-7: Wildtype MPI cells exposed to inhibitors of MARCO. Macrophages were stimulated overnight with 10 ng/mL LPS. The following day, cells were pre-treated with polyguanylic acid (polyG) **(A, B)** or anti-MARCO monoclonal antibody (mAb) **(C, D)** for 30 mins then infected with *C. neoformans* still in the presence of polyG or anti-MARCO mAb. After infection, extracellular fungi were washed off and fresh media containing polyG or mAb was added back into the wells. Images were acquired every 5 mins for 16 h. **(A, C)** Vomocytosis was quantified over the entire 16 h period and expressed as the percentage (%) of infected macrophages that experienced at least one vomocytosis event. **(B, D)** The number of internalised fungi at the beginning of the timelapse video was quantified. Data shown as mean ± SEM; ns, not significant; **p<0.01 in a t-test (**A, B**); ns, not significant, *, p<0.5; **p<0.01 in a one-way ANOVA followed by Tukey's post-hoc test **(C, D)**. All data represents two independent experiments. Each data point is a technical replicate (*n* = 3).

4.7 There is a noticeable difference in actin morphology between wildtype and *Marco*$^{-/-}$ macrophages.

Granucci et al. (2003) identified a role for MARCO in cytoskeletal remodelling of microglial and dendritic cells. Moreover, actin polymerization and depolymerisation have been shown to modulate vomocytosis rate (Johnston and May, 2010). Hence, I hypothesized that MARCO-deficiency similarly alters macrophage actin organisation which in turn modulates vomocytosis. To investigate the effect of MARCO deficiency on macrophage cytoskeletal arrangement, macrophages were either unstimulated or stimulated with LPS overnight, then infected with *C. neoformans* and stained with rhodamine-conjugated phalloidin to visualise F-actin filaments. Confocal microscopy images revealed that F-actin was localised near the plasma membrane in both cell types; however, *Marco*$^{-/-}$ cells appeared to have a more disorganised F-actin distribution (Figure 4-8A). The difference in actin morphology is made more visible when a maximum intensity projection is applied on z-stack images from LPS-stimulated macrophages (Figure 4-8B). Wildtype macrophages appeared more circular and compact with well-formed filopodial protrusions (Figure 4-8B; white arrows). Meanwhile, though *Marco*$^{-/-}$ cells also had instances of filopodial protrusions from the cell periphery (white arrows), these macrophages had extensive ruffle-like structures with less clear actin networks (Figure 4-8B, yellow arrows).

Variation in actin organisation between wildtype and *Marco*$^{-/-}$ macrophages is also present in LPS-stimulated or unstimulated uninfected macrophages. Wildtype unstimulated macrophages appeared more rounded and compact than MARCO-

deficient macrophages, which were much larger and less organised (Figure 4-9A). LPS stimulation led to increased filopodial protrusions in wildtype macrophages (Figure 4-9B). Meanwhile, LPS-stimulated *Marco*$^{-/-}$ macrophages display an even greater difference in shape compared to wildtype macrophages (Figure 4-9B). These knockout cells had a more disorganised morphology with expansive ruffle-like structures (Figure 4-9; yellow arrows). Taken together, there is a clear difference in actin organisation between wildtype and *Marco*$^{-/-}$ cells supporting the possibility that MARCO's role in actin remodelling and organisation is a mechanism for the elevated vomocytosis seen in *Marco*$^{-/-}$ macrophages.

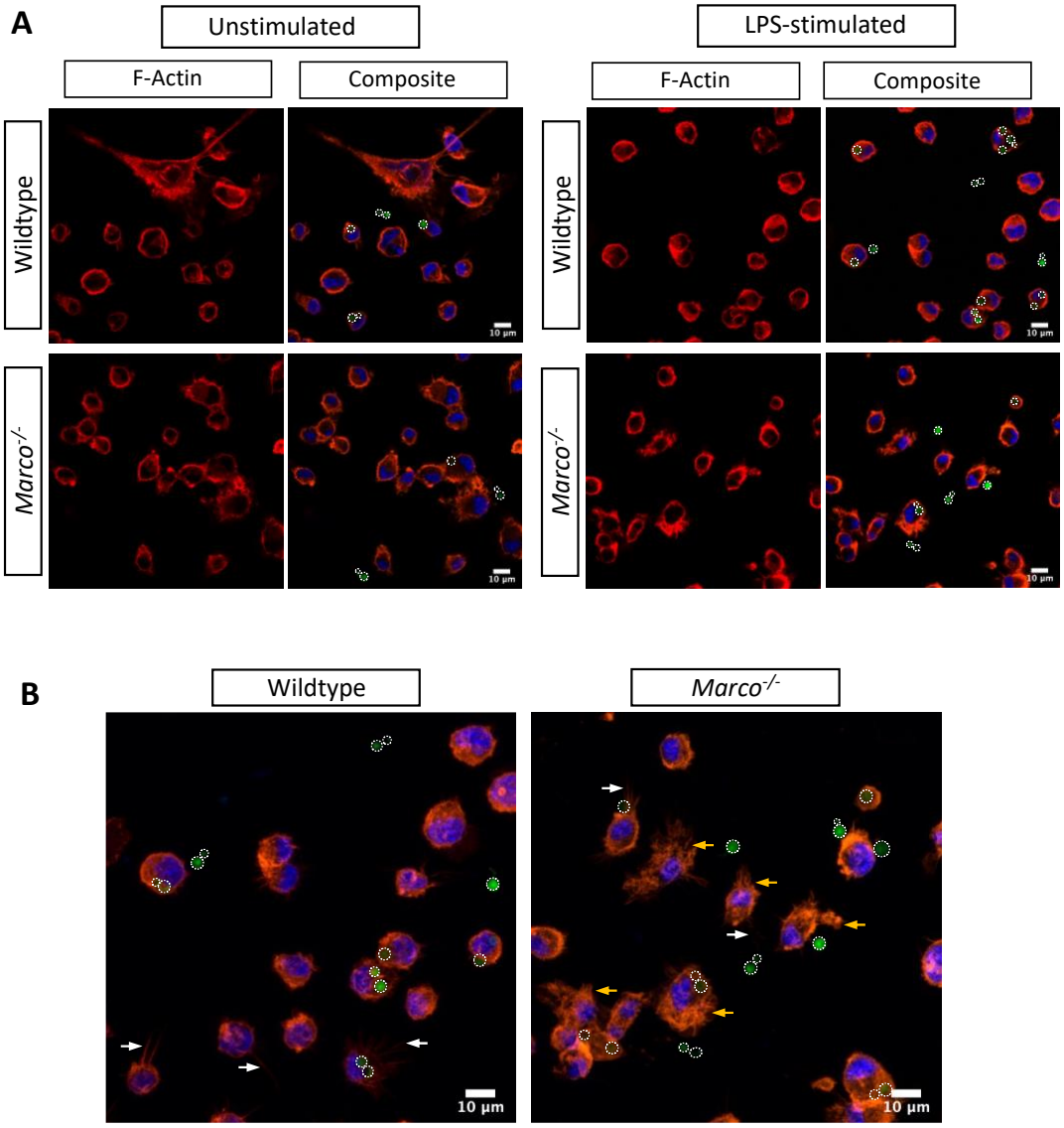

Figure 4-8: F-actin organisation in *C. neoformans* infected wildtype and *Marco*$^{-/-}$ macrophages. Macrophages were either stimulated with 10 ng/mL LPS overnight or unstimulated and then infected with GFP-expressing *C. neoformans*. Post-infection, macrophages were fixed, permeabilised and stained with rhodamine-conjugated phalloidin in 1% bovine serum albumin. Cells were counter-stained with DAPI to visualize the nucleus, then mounted onto glass slides using Fluoromount mounting medium. Samples were imaged on the Zeiss LSM880 using 63X Oil magnification. **(A)** Representative image showing actin distribution in wildtype and *Marco*$^{-/-}$ macrophages. **(B)** Z-stack maximum intensity projection was applied onto LPS stimulated wildtype and *Marco*$^{-/-}$ macrophages. Red = F-actin (Phalloidin); Blue = Nucleus; Green with white dashed circle = *C. neoformans*. White arrows show examples of filopodial protrusions. Yellow arrows show examples of macrophages with ruffle-like structures. Scale bar = 10 µm

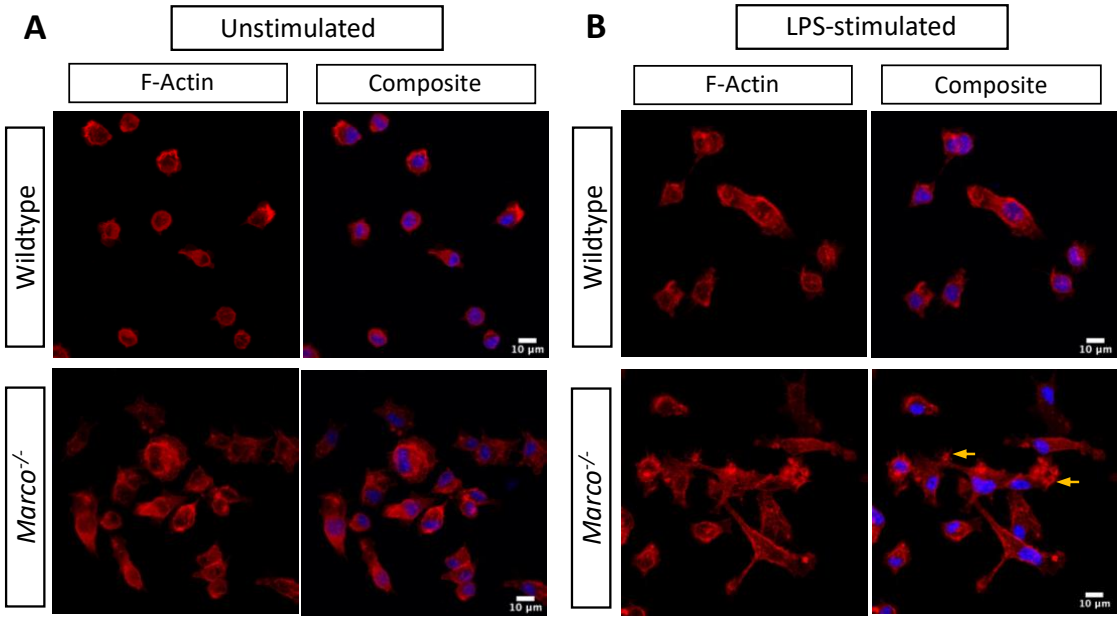

Figure 4-9: F-actin organisation in uninfected wildtype and *Marco*$^{-/-}$ macrophages. Macrophages were either **(A)** unstimulated or **(B)** stimulated with 10 ng/mL LPS overnight. After overnight incubation, macrophages were fixed, permeabilised and stained with rhodamine-conjugated phalloidin in 1% bovine serum albumin. Cells were counter-stained with DAPI to visualize the nucleus, then mounted onto glass slides using Fluoromount mounting medium. Z-stack images were acquired on the Zeiss LSM880 using 63X Oil magnification. Z-stack maximum intensity projection was applied to all images. Red = F-actin (Phalloidin); Blue = Nucleus; Yellow arrows show examples of macrophages with ruffle-like structures. Scale bar = 10 µm

4.8 Discussion

In this chapter, I identified the scavenger receptor MARCO as a modulator of vomocytosis. The increase in vomocytosis observed in *Marco*$^{-/-}$ macrophages is the most dramatic change in vomocytosis rate observed to date. MARCO inhibition does not replicate the increased rate of vomocytosis observed in *Marco*$^{-/-}$ cells but replicates the decrease in phagocytosis seen in these macrophages. The inability of MARCO inhibition using polyG or anti-MARCO mAb to phenocopy vomocytosis in *Marco*$^{-/-}$ cells does not necessarily imply a gross defect in *Marco*$^{-/-}$ macrophages or invalidate a role for MARCO as a modulator of vomocytosis. This is because, on one hand, the role of MARCO in vomocytosis may be independent of its role in phagocytosis since elevated vomocytosis

in *Marco*$^{-/-}$ cells was observed when phagocytosis was mediated by opsonic receptors and in *Candida albicans* where uptake is mediated by Dectin-1. On the other hand, inert latex beads and heat-killed *C. neoformans* were not vomocytosis by *Marco*$^{-/-}$ macrophages, suggesting that MARCO-deficiency does not lead to unregulated expulsion of all phagosome cargo. This is consistent with many other studies that have failed to observe vomocytosis of latex beads and heat-killed cryptococcus (Gilbert et al., 2017; Alvarez and Casadevall, 2006; Ma et al., 2006).

I am not the first to propose a role for MARCO outside of ligand internalisation. MARCO has been implicated in cytoskeletal organization of splenic dendritic cells and microglia (Granucci et al., 2003) and in various cell lines (Pikkarainen et al., 1999). Host actin cytoskeleton has been implicated in the modulation of vomocytosis. Actin polymerization and depolarization are crucial for *Cryptococcus* engulfment (Guerra et al., 2014), hence a role for actin in vomocytosis is not far-fetched. Pre-treatment of macrophages with cytochalasin D, a drug that inhibits actin polymerization led to elevated non-lytic expulsion (Alvarez and Casadevall, 2006). Johnston and May (2010) observed that actin repeatedly assembles and dissembles around phagosomes containing cryptococci, a process they termed actin 'flashes'. These actin flashes were mediated by the WASP-Arp2/3 pathway and led to the formation of actin cages around the phagosome that tried to prevent vomocytosis (Johnston and May, 2010). Similar to Granucci et al. (2003) and Pikkarainen et al. (1999), I also observe variation in actin cytoskeleton organisation in MARCO-expressing versus MARCO-deficient cells; though it remains unclear how this difference in cytoskeleton results in increased vomocytosis

in *Marco*$^{-/-}$ cells. Therefore, given that loss of MARCO leads to elevated vomocytosis, one role for MARCO may be to sense phagosomal content and prevent premature expulsion, potentially by regulating the formation of actin 'cages' (Johnston and May, 2010). Confocal microscopy of fixed macrophages shows actin organisation at a precise timepoint. Due to the dynamic nature of the actin cytoskeleton future work could seek to use MARCO-deficient cells stably expressing fluorescent actin to visualize, in real-time, actin remodelling in *Cryptococcus*-infected macrophages as they undergo vomocytosis. This could test the hypothesis that MARCO knockout destabilises the actin cytoskeleton leading to decreased 'actin cages' and thus increased vomocytosis. It would also be interesting to investigate whether MARCO influences WASP-Arp2/3 signalling. This would provide a molecular mechanism of MARCO's influence on actin organisation.

The noncanonical MAPK, extracellular-signal-regulated kinase 5 (ERK5), has been associated with vomocytosis with both pharmacological and genetic inhibition of ERK5 leading to increased vomocytosis. (Gilbert et al., 2017). It is also possible that MARCO activity is linked to the MAPK ERK5, since ERK5 activity has been implicated in disruptions in actin cytoskeleton during oncogenic transformation (Barros and Marshall, 2005; Schramp et al., 2008). In addition to ERK5, the phospholipid binding protein Annexin A2 has been identified as a regulator of vomocytosis, with Annexin A2 deficiency leading to decreased vomocytosis (Stukes et al., 2016). Annexin A2 is Ca^{2+}-dependent and is involved in a range of cellular processes including endocytosis, exocytosis and binding to actin to modulate cytoskeleton arrangement (Hayes et al.,

2006; Gabel and Chasserot-Golaz, 2016). Its role in actin and plasma membrane remodelling makes its involvement in non-lytic expulsion highly plausible.

Altogether, I propose a model where, in addition to its role in mediating *C. neoformans* uptake, MARCO also functions by sensing the contents of the phagosome, determining the efficiency of phagosome maturation and initiating a signal transduction process, possibly involving Annexin A2, ERK5 and Arp2/3, that determines the fate of the phagosome content— persist or expel. Such a model presents MARCO as the master regulator of *C. neoformans* non-lytic expulsion from macrophages. This hitherto undocumented impact of MARCO loss on pathogen expulsion will be important for investigators to consider when using *Marco*$^{-/-}$ cells or animals for a range of other infection assays.

Is vomocytosis a macrophage- or *Cryptococcus*-directed event?

One question that has puzzled researchers for many years is whether vomocytosis is triggered by the pathogen or by the infected host cell. In support of vomocytosis being a pathogen-mediated event, it has consistently been observed that latex beads and heat-killed cryptococci are rarely vomocytosed (Ma et al., 2006; Alvarez and Casadevall, 2006; Gilbert et al., 2017), implying that the content of the phagosome needs to be alive to trigger vomocytosis. Acapsular cryptococci are not vomocytosed; however, the incubation of acapsular strain with capsule polysaccharide led to a slight increase in vomocytosis events (from 0% to 9%) (Alvarez and Casadevall, 2006). *Cryptococcus* capsule is a known virulence factor that has antiphagocytic properties and suppresses

proinflammatory cytokine production (Monari et al., 2005; Vecchiarelli et al., 2013). It is possible the immunomodulatory activity of the *Cryptococcus* capsule also regulates vomocytosis. Other *Cryptococcus* virulence factors including urease and phospholipase B1 have been linked to vomocytosis such that macrophages infected with *ure1Δ* and *plb1Δ* mutant strains had decreased vomocytosis (Chayakulkeeree et al., 2011; Fu et al., 2018). It is thought that *Cryptococcus*-driven vomocytosis serves as a mechanism to escape the antimicrobial environment of the phagosome either during pulmonary infection or after dissemination to the brain.

There is also growing evidence of host factors that modulate vomocytosis. It is thought that host-directed vomocytosis allows macrophages that are unable to control internalised fungi to give other immune cells a chance at killing fungi. In addition to the role of the actin cytoskeleton, ERK5, and Annexin A2 already described, another host factor that influences vomocytosis rate is phagosome pH and maturation state. Pre-treatment of macrophages with concanamycin A or bafilomycin A1, drugs that inhibit V-ATPase-mediated phagosome acidification, resulted in decreased vomocytosis (Ma et al., 2006; Nicola et al., 2011). Interestingly, addition of 10 μM chloroquine, a weak base that keeps phagosome pH at or near neutral, resulted in enhanced vomocytosis (Ma et al., 2006; Nicola et al., 2011). It is uncertain why these drugs have opposing effects even though they all act to prevent phagosome acidification. It is possible the differences in vomocytosis are independent of phagosomal pH and may arise from other consequences of drug exposure such as the ability of concanamycin A or bafilomycin A1 to affect V-ATPase activity in other cellular compartments including the Golgi apparatus

and plasma membrane (Eaton et al., 2021); a direct effect of these drug on *C. neoformans* viability, though at higher concentrations than those used in the vomocytosis studies (Harrison et al., 2000); the ability of these drugs to improve host defence against infection (Mazzolla et al., 1997); and/or the ability of chloroquine to dampen LPS-induced TNFα production independent of its phagosome neutralization effects (Weber and Levitz, 2000). However, in line with the increase in vomocytosis observed after treatment with chloroquine, addition of urea (a substrate that is converted to ammonia, a base, by urease activity) resulted in increased vomocytosis of cryptococci (Fu et al., 2018). This provides a mechanism for the decreased vomocytosis seen in *ure1*Δ fungi and links increased phagosome pH to vomocytosis (Fu et al., 2018). Moreover, given the finding that phagosomes containing live *C. neoformans* are rarely acidified, as measured by lysotracker red colocalization, while those that contain heat-killed or UV-killed cryptococci do (Smith et al., 2015), and the observation that killed *C. neoformans* are rarely vomocytosed support the idea that increased or neutral phagosome pH contributes to vomocytosis rate.

Lastly, host cytokine expression influences the rate of vomocytosis. Pre-treatment of both murine and human macrophages with the nonprotective Th2 cytokines IL-4 or IL-13 resulted in a decrease in non-lytic expulsion (Voelz et al., 2009). Meanwhile, pre-treatment with Th1 or Th17 cytokines had no impact on vomocytosis rate. Since *Cryptococcus* is an opportunistic pathogen, typically in HIV/AIDS patients, Seoane et al. (2020) investigated the consequence of viral infection on non-lytic expulsion. They found that viral infection increased the vomocytosis of *C. neoformans* from human

monocyte-derived macrophages without affecting phagocytosis and IPR. The increase in vomocytosis was mediated by viral-induced type 1 IFN signalling (Seoane et al., 2020).

What is the biological and clinical consequence of vomocytosis?

Since the initial observation of *Cryptococcus* vomocytosis from macrophages in 2006, it has been proposed as a mechanism of fungal dissemination, particularly its dissemination to the CNS via the "Trojan horse" model (Figure 4-10) (Ma et al., 2006; Alvarez and Casadevall, 2006). According to the "Trojan Horse" model, cryptococci hijack macrophages for transport via the blood to the CNS. They then cross the BBB within macrophages and can escape from within macrophages via vomocytosis, though vomocytosis is yet to be directly observed *in vivo* or in the brain (Sorrell et al., 2016; May et al., 2016; Kaufman-Francis et al., 2018). Direct crossing of *Cryptococcus*-containing phagocytes across the BBB was observed using *an in vitro* model of blood-brain barrier where human cerebral microvascular endothelial cells were seeded on top of a permeable trans-well insert (Santiago-Tirado et al., 2017). The study also observed non-lytic expulsion of cryptococci from macrophages prior to crossing the model blood-brain barrier. Although Santiago-Tirado et al. (2017) provides evidence in support of the Trojan horse model to cross endothelial cells *in vitro*, crossing of the brain endothelium does not equate to entry into brain tissue since brain endothelium is separated from brain parenchyma by a perivascular space and glia limitans, a protective layer separating the perivascular space from the brain parenchyma (Kaufman-Francis et al., 2018) (Figure 4-10). To provide more clarity on the role of the "Trojan horse" model in dissemination, recent data found that phagocytes containing cryptococci were only present in the

perivascular space, whilst free cryptococci were able to cross the perivascular space into the brain parenchyma (Kaufman-Francis et al., 2018). This finding aligns with the mechanism presented in Figure 4-10; 3b. Therefore, the role of vomocytosis in dissemination may be to deliver cryptococci from within phagocytes into the perivascular space. Free cryptococci in the perivascular space can then enter the brain parenchyma, possibly by transcytosis, where they can replicate and cause meningitis (Figure 4-10). Crossing of free *C. neoformans* from brain microvasculature to the brain parenchyma has been observed in live mice using intravital microscopy (Shi et al., 2010); though the mechanism remains unclear.

With the identification of MARCO as a potent modulator of vomocytosis, *Marco*$^{-/-}$ mice could provide a unique tool to investigate the impact of vomocytosis on *Cryptococcus* dissemination. Elevated vomocytosis could promote dissemination due to increased escape of intra-phagocyte cryptococci after dissemination to the perivascular space. Alternatively, given the finding that vomocytosis in *Marco*$^{-/-}$ macrophages occurred within the first 1 to 5 hours of imaging, elevated vomocytosis may also decrease dissemination due to rapid vomocytosis occurring before macrophages are able to reach the CNS. This would be in line with the finding that ERK5 inhibition led to an increase in vomocytosis, but decreased dissemination in a zebrafish model of infection (Gilbert et al., 2017). Future work should explore the consequence of MARCO deficiency using an *in vivo* model of infection. Such a study should investigate mice survival, brain and lung fungal burden over time, and follow *Cryptococcus* dissemination from the lungs to the brain in real-time using techniques such as intravital microscopy and bioluminescence

imaging (BLI). BLI is a non-invasive technique that has been used successfully to follow the spatial and temporal distribution of *C. neoformans* expressing the luciferase gene in live mice (Vanherp et al., 2019). In addition to BLI, micro-computed tomography (µCT) of the lung and magnetic resonance imaging (MRI) of the brain provided clinical information on disease progression (Vanherp et al., 2019).

The host and pathogen factors that regulate vomocytosis have remained elusive for over a decade. However, the dramatic increase in vomocytosis seen in *Marco*$^{-/-}$ macrophages implicate MARCO as a master regulator of host-directed vomocytosis. Research that builds upon this finding could result in a greater understanding of the mechanism and consequence of vomocytosis.

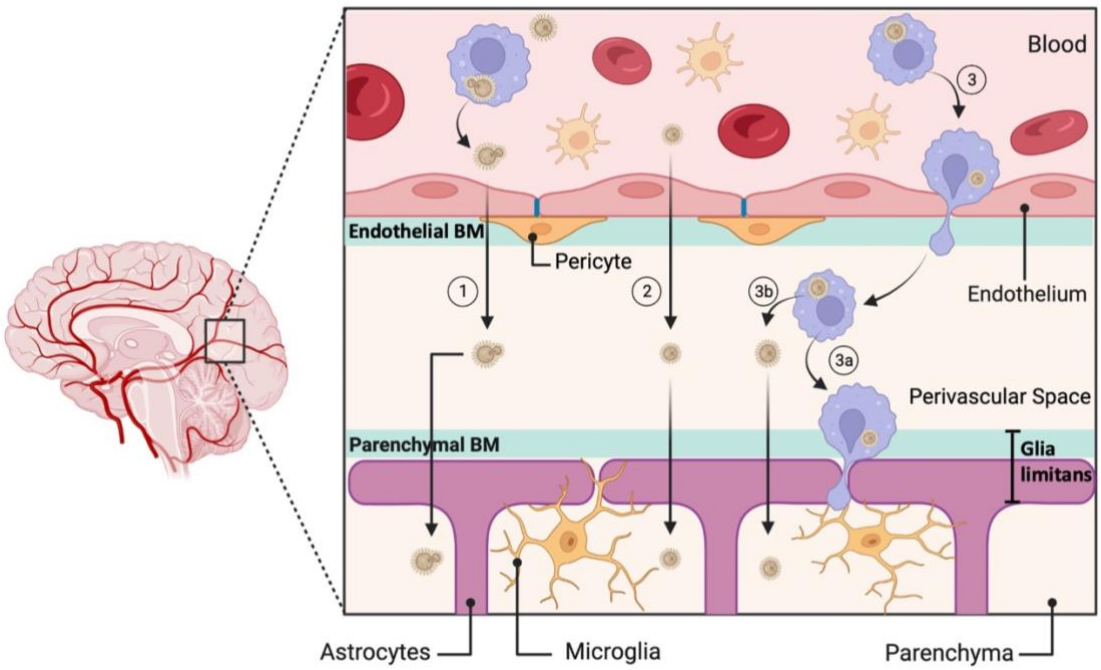

Figure 4-10: Proposed roles of vomocytosis during *C. neoformans* traversal through the blood-brain barrier. *C. neoformans* can travel through the blood within phagocytes or as free fungi. **(1)** *C. neoformans* that reach the CNS through travel within phagocytes can get vomocytosed in the vicinity of the brain endothelium. **(1, 2)** Free *C. neoformans* can cross the endothelium via transcytosis or paracytosis, gain

access to the perivascular space, then cross the glia limitans, a protective layer separating the perivascular space from the brain parenchyma, as a free fungus. **(3)** According to the "Trojan horse" model, macrophages are hijacked and used for *C. neoformans* transport through the blood. Infected macrophages then traverse endothelial cells into the perivascular space. **(3a)** *C. neoformans* could either remain within macrophages to cross the glia limitans into the brain parenchyma. **(3b)** Alternatively, *C. neoformans* may be released from within macrophages through non-lytic expulsion. Then gain access to the brain parenchyma as a free fungus. BM, basement membrane.

Chapter 5 Extracellular Vesicle production modulates the phagocytosis of non-opsonised *C. neoformans* through its role in yeast-to-yeast communication.

5.1 Introduction

This chapter presents data from a collaborative project I undertook with Dr Juliana Rizzo and Dr Guilhem Janbon (Pasteur Institute, Paris, France). Based on a prior genetic screen, Drs Rizzo and Janbon had identified two genes whose loss significantly impacted the ability of cryptococci to produce EVs: *GAT5* and *HAP2*. I received five *C. neoformans* strains from their group: WTKN99α, *gat5Δ*, *gat5Δ::GAT5* (complemented strain), *hap2Δ* and *hap2Δ::HAP2* (complemented strain). GAT5 and HAP2 are transcription factors and CryoEM experiments performed by Juliana Rizzo showed that *C. neoformans* strains lacking these transcription factors produce few or no EVs. My role in this collaboration was to explore the consequence of EV-deficiency on *Cryptococcus*-macrophage interaction, with a specific interest in its effect on phagocytosis.

5.2 EV-deficient *C. neoformans* strains are defective in non-opsonic phagocytosis by J774A.1 murine macrophages.

To investigate the effect of EV-deficiency on the non-opsonised uptake of *C. neoformans*, all five strains were used to infect J774A.1 macrophages and immortalised bone marrow-derived macrophages (iBMDMs). The phagocytosis assay revealed that compared to WTKN99α, both *gat5Δ* and *hap2Δ* showed decreased phagocytosis by J774

macrophages (Figure 5-1A) and iBMDMs (Figure 5-1B), whereas the complemented strains were phagocytosed to a similar extent as wildtype cryptococci (Figure 5-1A and B). Thus, EV-deficiency decreases the uptake of cryptococci. When intracellular proliferation rate was quantified, I observed no difference between wildtype *C. neoformans* and *gat5Δ* and *hap2Δ* mutants (Figure 5-2), though there was a modest increase in *hap2Δ* IPR compared to *gat5Δ* strain.

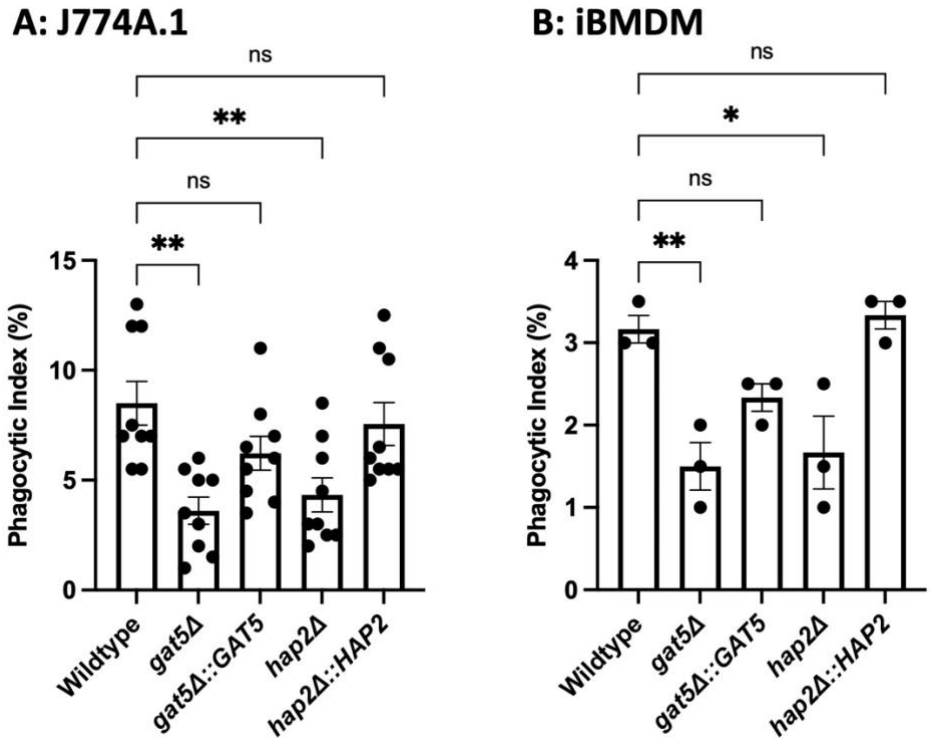

Figure 5-1: Non-opsonised phagocytosis of EV-deficient *C. neoformans* strains by (A) J774A.1 macrophages and (B) immortalised BMDMs. Macrophages were infected with wildtype (WTKN99α), EV-deficient mutants (*gat5Δ* and *hap2Δ*) and complemented (*gat5Δ::GAT5* and *hap2Δ::HAP2*) *C. neoformans* strains at an MOI of 10 fungi to 1 macrophage. After 2 h infection, phagocytosis was quantified using images from a fluorescent microscope. The phagocytic index represents the percentage of macrophages that ingested at least one yeast cell. The bars represent the mean ± SEM. Data for J774A.1 macrophages were pooled from three independent experiments (*n* = 9). Phagocytosis assay using iBMDM was performed once and each data point is a technical repeat. Statistical significance was determined by performing a One-Way ANOVA (ns, not significant; *, p<0.05; **, p<0.01.

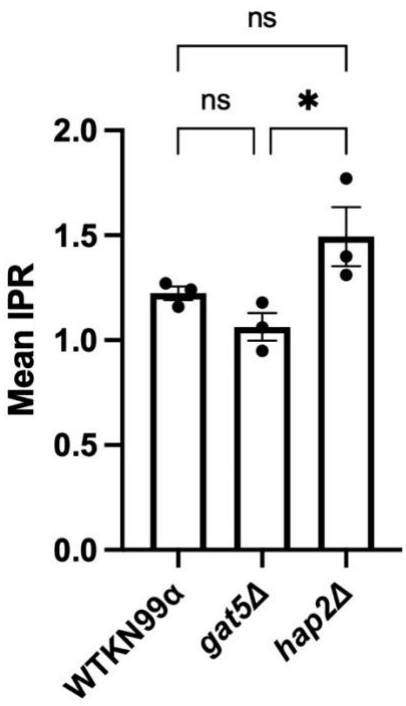

Figure 5-2: Intracellular Proliferation Rate (IPR) of EV-deficient mutants. J774A.1 murine macrophages were infected with WTKN99α, *gat5Δ* and *hap2Δ C. neoformans* strains. IPR of *C. neoformans* within macrophages was quantified using the live-cell imaging approach. After 2 h infection with *C. neoformans*, extracellular fungi were washed off and macrophages were imaged every 5 minutes for 18 hours. To determine IPR, the number of internalised fungi per 100 macrophages at the 'first frame' (T0) and 'last frame' (T10) was quantified and IPR was calculated using the equation: IPR = T10/T0. Data is representative of three independent experiments. Data shown as mean ± SEM; ns, not significant; *p<0.05 in a One-Way ANOVA.

5.3 EV-deficient mutants are not defective in 18B7 antibody-opsonised phagocytosis.

Next, I wanted to examine the effect of EV-deficiency on antibody-opsonised fungi. WTKN99α, *gat5Δ*, *gat5Δ::GAT5*, *hap2Δ* and *hap2Δ::HAP2* were opsonised with the anti-capsular 18B7 antibody prior to infection. I observed no difference in phagocytosis between the mutants and wildtype cryptococci (Figure 5-3), suggesting that antibody opsonisation can offset the phagocytosis defect induced by EV-deficiency. The rest of this project focused on non-opsonised phagocytosis since it appears that only this condition is affected by EV-mediated defects in phagocytosis.

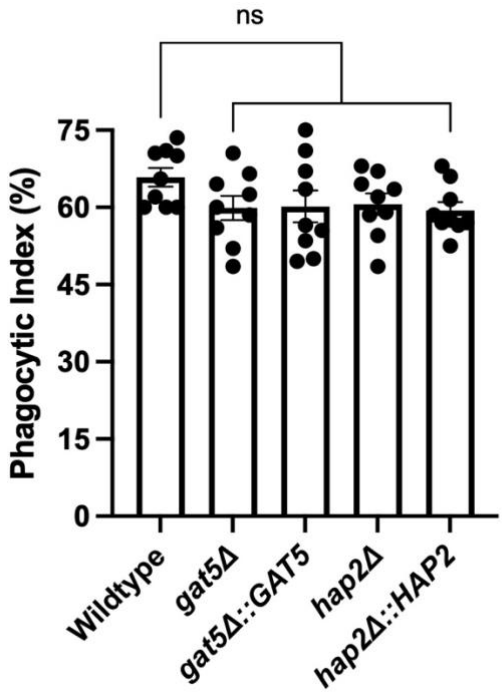

Figure 5-3: Anti-capsular 18B7 antibody-opsonised phagocytosis of EV-deficient *C. neoformans* strain by J774A.1 macrophages. Prior to infection, *C. neoformans* was opsonised with the anti-glucuronoxylomannan 18B7 antibody for 1 h. Macrophages were infected with wildtype (WTKN99α), EV-deficient mutants (*gat5Δ* and *hap2Δ*) and complemented (*gat5Δ::GAT5* and *hap2Δ::HAP2*) *C. neoformans* strains at an MOI of 10:1 for 2 h. Phagocytosis was quantified using images from a fluorescent microscope. The phagocytic index represents the percentage of macrophages that ingested at least one yeast cell. The bars represent the mean ± SEM. Statistical significance was determined by performing a One-Way ANOVA; ns, not significant. Data is pooled from three independent experiments (*n* = 9).

5.4 The presence of WTKN99α in a trans-well insert does not rescue the phagocytosis of *gat5Δ* and *hap2Δ* mutants.

Having shown that both *gat5Δ* and *hap2Δ* have decreased non-opsonic uptake compared to wildtype cryptococci, I next wanted to confirm that this defect is a direct consequence of EV deficiency and not due to some other confounding variable. To explore this question, I hypothesized that the presence of EVs from wildtype *C. neoformans* during macrophage infection with EV-deficient mutant strains would increase phagocytosis to or near wildtype levels. In other words, the presence of

wildtype EVs would rescue the ability of macrophages to phagocytose *gat5Δ* and *hap2Δ* mutants.

To test this hypothesis, I first employed a trans-well assay using a 400 nm ThinCert to separate WTKN99α from macrophages infected with *gat5Δ* or *hap2Δ* mutants. A schematic representation of the experimental design is shown in Figure 2-5. Theoretically, the 400 nm pore size would allow EVs from wildtype *C. neoformans* to pass through, while retaining the *Cryptococcus* cells within the trans-well insert. Unexpectedly, I found that the presence of WTKN99α had no impact on the phagocytosis of all three cryptococcus strains compared to blank control (Figure 5-4). It is possible that the lack of a difference between the presence and absence of WTKN99α in the trans-well insert is a result of insufficient time for EVs to pass through the pores and have an effect on macrophages and/or cryptococci. In my experimental design, macrophage infection with *C. neoformans* is allowed to take place for 2 h, which may be insufficient for the production and transport of EVs across the pores. Moreover, any EVs produced during the overnight culture of *C. neoformans* is removed during the washes with PBS prior to infection. Thus, new EVs need to be produced by the cells in the trans-well insert.

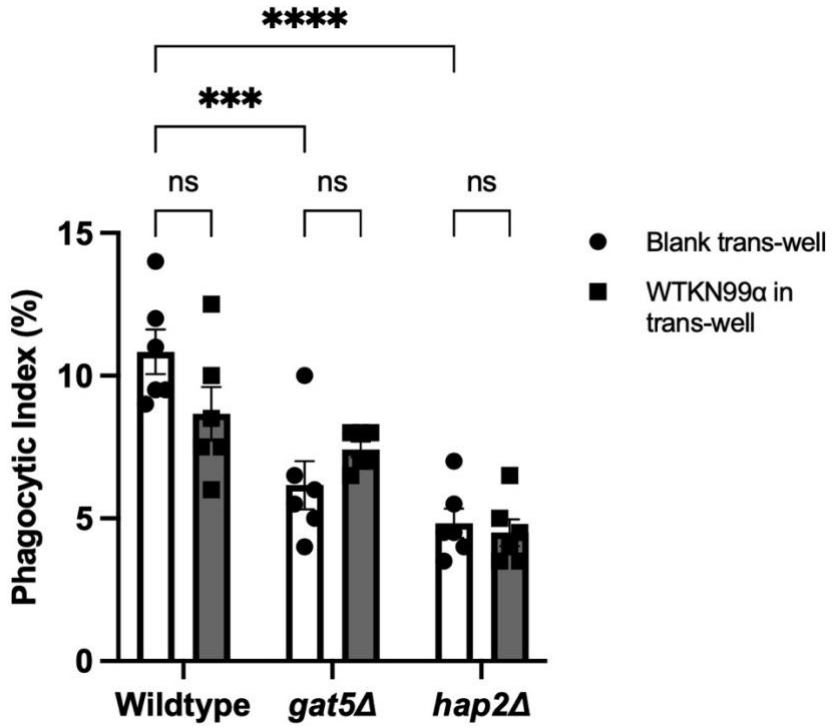

Figure 5-4: The effect of WTKN99α in a 400 nm trans-well insert on phagocytosis. J774A.1 murine macrophages were infected with WTKN99α, *gat5Δ* and *hap2Δ*, then trans-well insert with 400 nm pores were inserted into each well and WTKN99α or culture media (Blank trans-well) was added into the trans-well insert. After 2 h infection, macrophages were washed, and phagocytosis was quantified using images from a fluorescent microscope. The phagocytic index represents the percentage of macrophages that ingested at least one yeast cell. The bars represent the mean ± SEM. Data is pooled from two independent experiments, and each was performed in triplicates (n = 6). Statistical significance was determined by performing a two-way analysis of variance; ns, not significant; ***p<0.001; ****p<0.0001.

5.5 Culture media conditioned with WTKN99α did not rescue the phagocytosis of *gat5Δ* and *hap2Δ* mutants.

Given the limitations of the trans-well approach, I decided to culture WTKN99α cryptococci in serum-free DMEM (the media used in the phagocytosis assay), such that any EVs produced by *C. neoformans* will be present during the phagocytosis assay (Figure 2-6). When the supernatant was recovered and used in phagocytosis assays, I found that WTKN99α-conditioned media decreased the phagocytosis of wildtype

cryptococci while having no statistically significant effect on both EV-deficient mutants (Figure 5-5). However, there appeared to be a trend towards decreased phagocytosis in the *hap2Δ* mutant when infection occurred using conditioned media. The decrease in phagocytosis seen using conditioned media may reflect the presence of *C. neoformans* secreted molecules that negatively impact the health of macrophages and their ability to carry out phagocytosis. Whether or not this effect is specifically due to EVs is not clear.

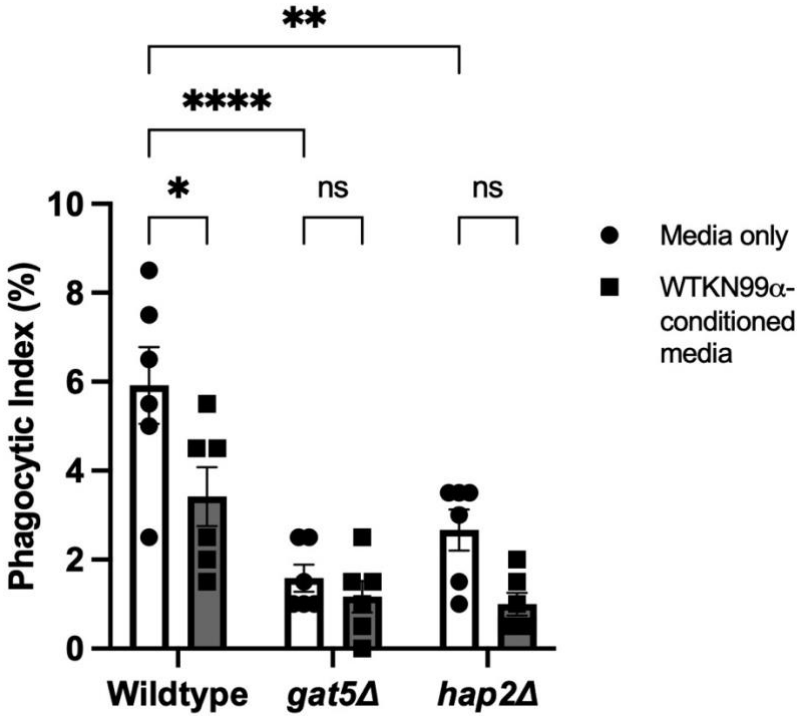

Figure 5-5: Phagocytosis assay using WTKN99α conditioned media had no effect on the phagocytosis of EV-deficient mutants. Cell culture media was conditioned with WTKN99α for 24 h, then supernatant was collected and used in a phagocytosis assay. After 2 h infection, macrophages were washed, and phagocytosis was quantified using images from a fluorescent microscope. The phagocytic index represents the percentage of macrophages that ingested at least one yeast cell. The bars represent the mean ± SEM. Data is pooled from two independent experiments, and each was performed in triplicates (n = 6). Statistical significance was determined by performing a two-way analysis of variance; ns, not significant; *p<0.05; **p<0.01; ****p<0.0001.

5.6 EV isolated from WTKN99α rescued the phagocytosis of *hap2Δ*, but not *gat5Δ*.

The approaches used thus far have failed to identify a role for exogenous EVs acting on macrophages (i.e. the host) to rescue the phagocytosis of EV-deficient mutants. Given that EVs are thought to be involved in yeast-to-yeast communication (Rodrigues and Casadevall, 2018; Bielska et al., 2018), I then wanted to investigate whether exogenous EVs acting on *Cryptococcus* cells directly would rescue the phagocytosis of EV-deficient mutants.

To test this, EV-deficient mutant strains were cultured in YPD broth containing EVs isolated from wildtype cryptococci (Figure 2-7). I found that WTKN99α and *hap2Δ* strains cultured overnight in YPD broth containing EVs were phagocytosed more readily than those cultured in control YPD broth (Figure 5-6A). Therefore, EV exposure not only rescues the uptake of *hap2Δ*, but further increases the uptake of WTKN99α. Interestingly, the phagocytosis of *gat5Δ* was not affected by the presence of EVs, implying that the phagocytosis defect seen in *gat5Δ* is at least partially EV-independent.

To gain some insight into the speed to which EV exposure rescues the phagocytosis of *hap2Δ*, I isolated EVs in PBS and used the PBS-containing solution to "opsonise" cryptococci for 1 h before macrophage infection. With just 1 h of EV exposure, termed EV "opsonisation", the uptake of *hap2Δ* was elevated in comparison to those that were not exposed to EVs, termed "unopsonised" (Figure 5-6B). Unlike with overnight

EV exposure, WTKN99α cryptococci did not show a further increase in uptake. This could be because WTKN99α cells are already exposed to some self-made EVs during overnight culture such that 1 h EV "opsonisation" does not offer sufficient stimuli to elicit a further increase in uptake. Meanwhile, *hap2Δ* cells that have not been exposed to any EVs will be affected by even a short exposure to EVs. It is important to note that the magnitude to which EV exposure rescued the uptake of *hap2Δ* is greater when cells were cultured overnight in YPD broth containing EVs (205% increase) (Figure 5-6A) than when "opsonised" with EVs for 1 h (125% increase) (Figure 5-6B), suggesting a time and/or dose-dependent effect.

The trans-well approach and EV-conditioned media approach were founded on the hypothesis that EVs would act on the macrophage to elicit its effect on phagocytosis. However, the EV isolation approach suggests that exogenous EVs may be taken up by fungal cells resulting in changes in their cell wall and/or capsule physiology that impact their recognition and phagocytosis by macrophages. This provides further evidence of the role of EVs in cell-to-cell communication.

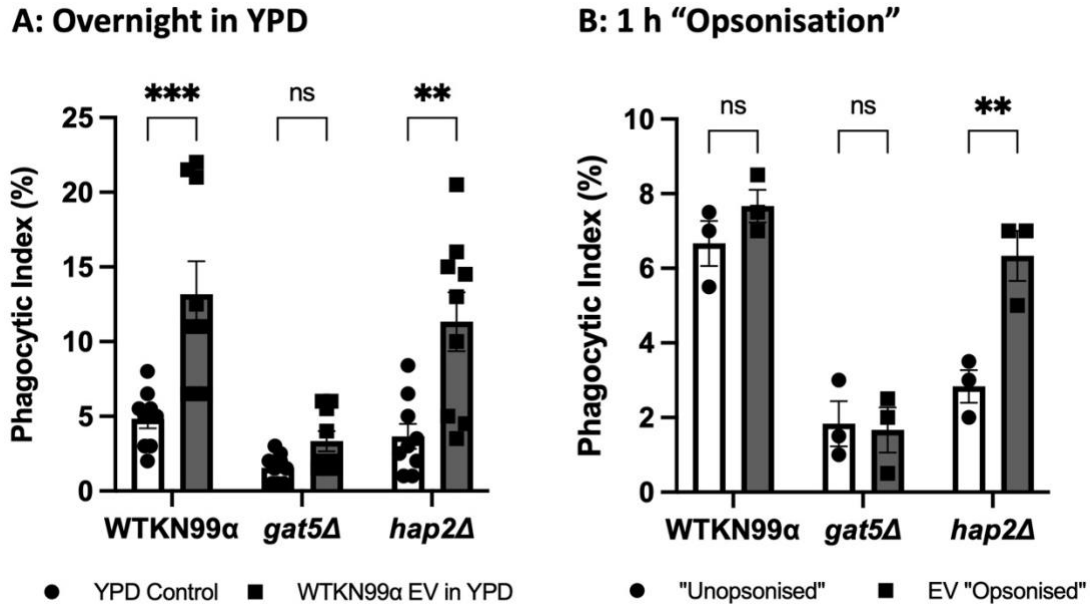

Figure 5-6: The consequence of direct EV exposure on the phagocytosis of WTKN99α, *gat5Δ* and *hap2Δ* by J774 macrophages. (A) EVs were isolated from wildtype *C. neoformans* (WTKN99α) into YPD broth. Overnight cultures were started in YPD broth containing wildtype EVs or control YPD broth with no EVs. The following day a phagocytosis assay was performed. Data is pooled from three independent experiments, and each was performed in triplicates (*n* = 9). **(B)** EVs were isolated from wildtype *C. neoformans* into PBS. Cultured WTKN99α, *gat5Δ* and *hap2Δ* were "opsonised" with PBS containing EV or PBS alone. After 1 h "opsonisation" a phagocytosis assay was performed. Experiment was performed once, and each data point is a technical repeat. Phagocytic index was measured as the percentage of macrophages that ingested at least one yeast cell. Data shown as mean ± SEM. Statistical significance was determined by performing a two-way analysis of variance; ns, not significant; **p<0.01; ***p<0.001. Data is representative of at least three independent experiments.

5.7 Increased phagocytosis observed following EV exposure was independent of growth phase.

Next, I hypothesized that increased uptake seen following exogenous EV exposure may be due to variations in cell wall and/or capsule components caused by EV-induced differences in growth phase. In other words, cells at early vs. late stationary phase or at stationary vs. exponential phase may differ in cell wall and capsule components which could impact their interaction with macrophages and alter the level of uptake. To

investigate this hypothesis, a growth curve was generated by measuring optical density at 30°C in media with or without isolated EVs.

There was a moderate difference in growth rate between WTKN99α grown in the presence of exogenous EVs compared to those inoculated in control YPD broth (Figure 5-7). This increase was only observed in the first 16 h of growth, after which WTKN99α in added EVs reached stationary phase, while those in control YPD broth remained in the exponential phase even after 36 h of growth. There was no difference in the growth rate of *hap2Δ* cells grown in the presence or absence of EVs up until the 20 h time point. After this point, *hap2Δ* cells exposed to EVs entered the stationary phase, while those in control YPD broth remained in the exponential phase even after 36 h of growth (Figure 5-7). It is striking that both WTKN99α and *hap2Δ* cells grown in the presence of EVs reached stationary phase earlier than those grown in control YPD broth. Meanwhile, in the absence of added EVs, they continued to grow beyond stationary phase, indicating that EVs alter the growth kinetics of *C. neoformans* and drive fungi to enter stationary phase earlier than control conditions. The *gat5Δ* growth curve revealed the existence of a growth defect when cells are grown in control YPD (Figure 5-7; Figure 5-8). This growth defect was rescued by exposure to wildtype EVs. Though the optical density was consistently higher for *gat5Δ* cells grown in the presence of wildtype EVs, the general pattern of the growth curve was similar in the presence and absence of EVs.

Since cryptococci were used in the phagocytosis assays after a 20 h to 24 h overnight culture, the observed differences in growth phase between WTKN99α and *hap2Δ* cells

may signify differences in the physiological state of the fungi between 20 h to 24 h, which could influence its interaction with macrophages and its ability to be phagocytosed. To investigate whether EV-mediated variation in growth phase could explain part of the increase in phagocytosis, macrophages were infected with fungi cultured for only 12 h, a time point where EV-exposed and unexposed cells were in the same growth phase. There was a generally low level of uptake of these cells, but I still observed EV-mediated rescue of *hap2Δ* uptake (Figure 5-9). Meanwhile, there was no difference in uptake, between WTKN99α and *gat5Δ* mutant cultured in the presence or absence of isolate EVs (Figure 5-9).

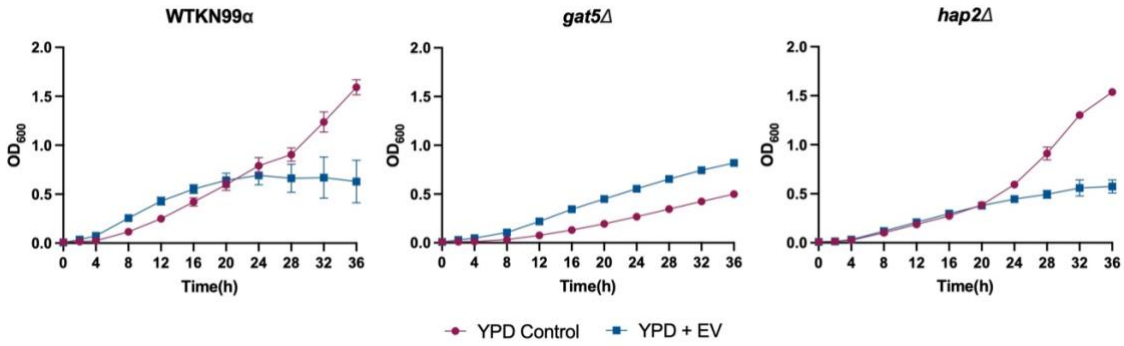

Figure 5-7: Growth curves of WTKN99α, *gat5Δ* and *hap2Δ* cryptococci in the presence or absence of extracellular vesicles. 1x10^6 cryptococci were inoculated in YPD broth (YPD Control) or YPD broth used in EV isolation (YPD + EV) in a 24-well plate. Growth was measured as a function of optical density at a wavelength of 600 nm. Measurements were acquired at 30°C every 1 h for 36h. The above graph is representative of three independent experiments.

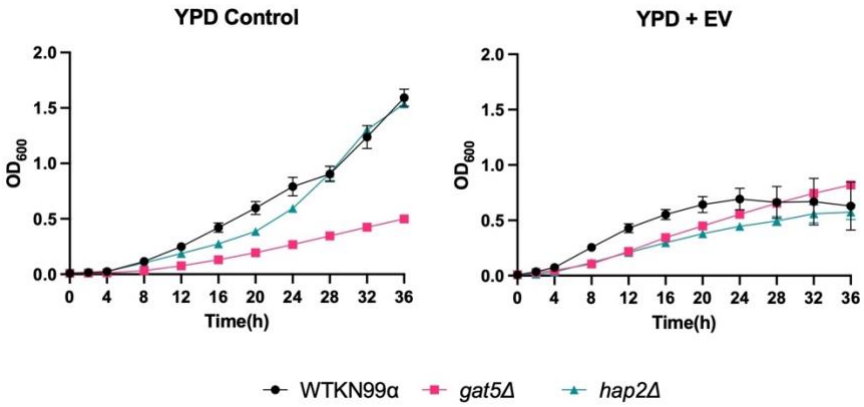

Figure 5-8: Comparison of WTKN99α, *gat5Δ* and *hap2Δ* growth curves in relation to each other. This figure provides an alternative representation of the data presented in Figure **5-7**. Here the three *Cryptococcus* strains are compared to each other in YPD broth or YPD + EV. $1x10^6$ cryptococci were inoculated into each culture media and optical density at a wavelength of 600 nm was measured every 1 h for 36 h at 30°C. The above graph is representative of three independent experiments.

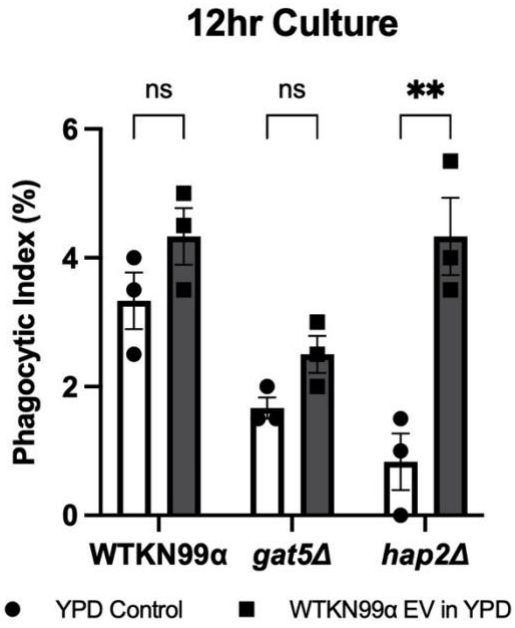

Figure 5-9: The consequence of EV exposure on the phagocytosis of WTKN99α, *gat5Δ* and *hap2Δ* by J774 macrophages. EVs were isolated from wildtype *C. neoformans* (WTKN99α) into YPD broth. WTKN99α, *gat5Δ* and *hap2Δ* strains were cultured in YPD broth with or without wildtype EVs for 12 h only. A phagocytosis assay was performed, and phagocytic index was measured as the percentage of macrophages that ingested at least one yeast cell. Data shown as mean ± SEM. Experiment was performed once. Each data point is a technical replicate (n = 3). Statistical significance was determined by performing a two-way analysis of variance; ns, not significant; **p<0.01; ***p<0.001.

5.8 There is no correlation between cell body and capsule measurements and phagocytosis phenotype.

To begin to investigate the mechanism by which EV-deficiency decreases the phagocytosis of *C. neoformans* by macrophages, I hypothesized that since the *C. neoformans* capsule has anti-phagocytic properties (Kozel and Gotschlich, 1982) decreased uptake of EV-deficient fungi may reflect an increase in cell size and/or capsule size. To investigate this hypothesis, I stained *Cryptococcus* cells from an overnight YPD culture with India ink and measured total cell diameter and cell body diameter. Only the *hap2Δ* mutant exhibited a statistically-significant difference in cell measurements, with this strain showing increased cell body diameter (Figure 5-10A), capsule radius (Figure 5-10B) and total cell diameter (Figure 5-10C) compared to WTKN99α and *gat5Δ* strains. However, although statistically significant, an average total cell diameter of 6.9 μm for *hap2Δ* and 6.4 μm for WTKN99α may not be biologically relevant since macrophages are highly dynamic and are capable of phagocytosing particles from 0.1 to 19.3 μm (Chikaura et al., 2016), though particles with a diameter between 2-3 μm were the most readily phagocytosed by macrophages (Paul et al., 2013; Champion et al., 2008). Moreover, since there was no difference between WTKN99α and *gat5Δ* strains, it is unlikely that cell body size and capsule radius are the determinants of the phagocytosis phenotypes observed for the EV-deficient mutants.

I also measured cell body diameter, capsule radius and total cell diameter after all three *Cryptococcus* strains were cultured overnight in EVs from WTKN99α. EV exposure increased the cell body diameter and total cell diameter of *gat5Δ* without affecting the

capsule radius (Figure 5-11A-C), increased the capsule radius of *hap2Δ*, without affecting the cell body diameter and total cell diameter (Figure 5-11A-C) and had no impact of wildtype capsule radius, cell body diameter or total cell diameter (Figure 5-11A-C). Though statistically significant in some cases, the magnitude of the difference in cell body diameter and/or capsule radius does not appear large enough to explain the observed difference in macrophage phagocytosis of EV-deficient mutants. Therefore, some yet-to-be-identified mechanisms, potentially acting on cell wall and/or capsule composition, and not size, may be responsible.

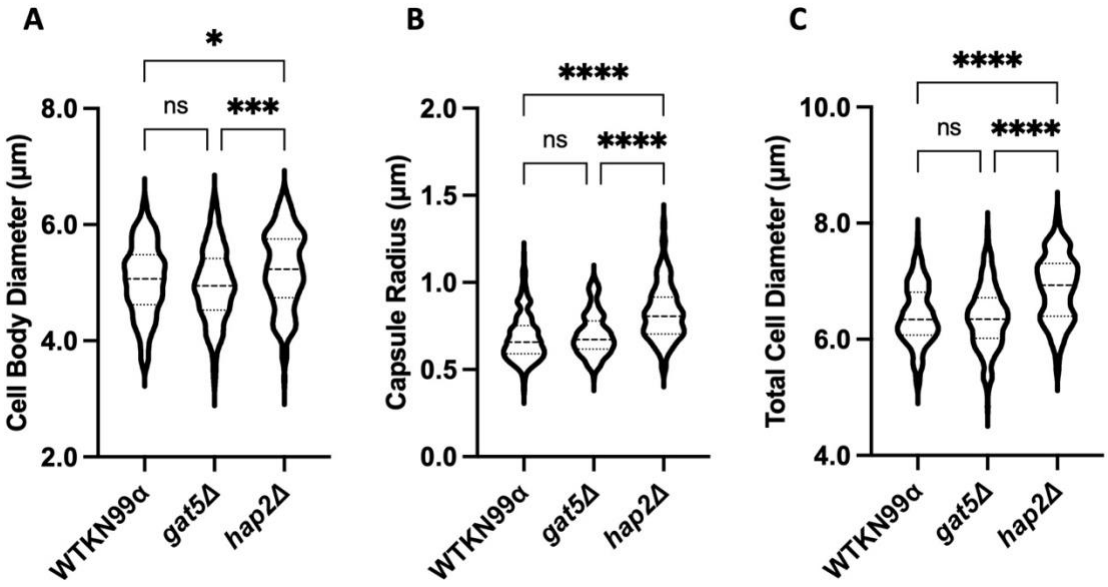

Figure 5-10: Cell body measurements of EV-deficient mutants. WTKN99α, *gat5Δ* and *hap2Δ* were cultured overnight in YPD broth. The following day, cells were stained with India Ink and imaged using the Nikon Ti Eclipse fluorescence microscope under 60X magnification. *n* = 200 *C. neoformans* cells were measured per strain. Data is presented as a violin plot. Statistical significance was determined using one-way ANOVA; ns, not significant; *P<0.05; ***p<0.001; ****p<0.0001.

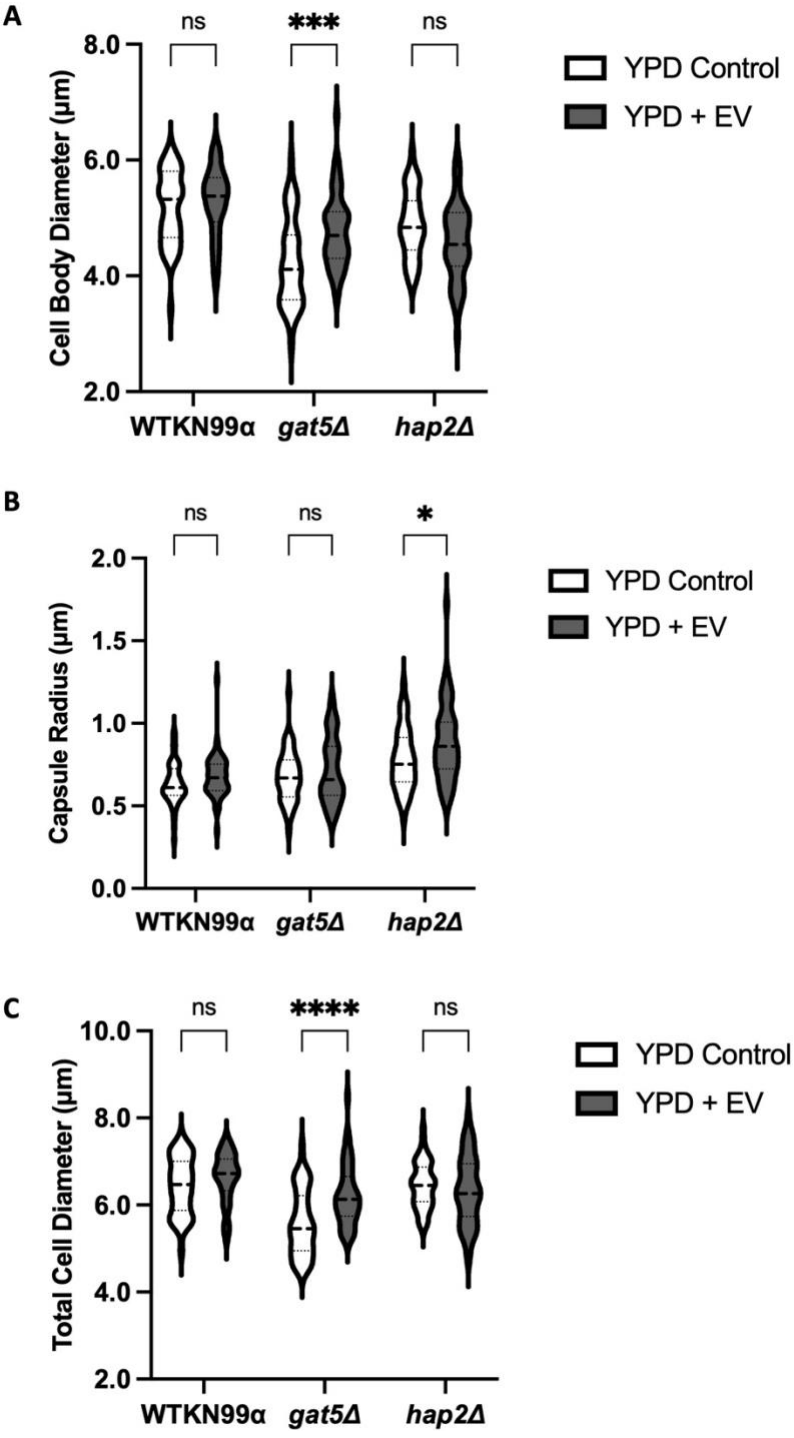

Figure 5-11: Cell body measurements of EV-deficient mutants after exposure to exogenous EVs. WTKN99α, *gat5Δ* and *hap2Δ* were cultured overnight in YPD broth alone (YPD Control) or YPD broth containing EVs isolated from WTKN99α *C. neoformans* (YPD + EV). The following day, cells were stained with India Ink and imaged using the Nikon Ti Eclipse fluorescence microscope under 60X magnification. *n* = 50 *C. neoformans* cells were measured per strain and per condition. Data is presented as a violin plot. Statistical significance was determined using two-way ANOVA; ns, not significant; *P<0.05; ***p<0.001; ****p<0.0001.

5.9 Discussion

The data presented above investigated the phagocytosis of two EV-deficient *C. neoformans* strains by murine macrophages. Although both the *gat5Δ* and *hap2Δ* mutants were less readily phagocytosed by macrophages, only the uptake of *hap2Δ* was rescued by exposure to exogenous EVs from wildtype *C. neoformans* after 1 h, 12 h and 24 h of exposure. There are many possible interpretations of this data. One is that the phagocytosis defect in *gat5Δ* is independent of EVs, instead, it is caused by another consequence of *gat5Δ* knockout. This is highly likely since GAT5 and HAP2 are transcription factors with pleiotropic effects (Jung et al., 2015). The growth curve generated when all three *C. neoformans* strains were grown in YPD broth revealed a defect in *gat5Δ* growth rate. This defect in growth rate could be a confounding variable to the phagocytosis phenotype observed for this strain. Alternatively, *gat5Δ* mutants may also be defective in their ability to detect and internalise EVs, resulting in the inability of exogenous EVs from WTKN99α to rescue the phagocytosis of *gat5Δ*.

It was interesting that the phagocytosis of *hap2Δ* was rescued when the fungal cells were cultured in the presence of wildtype EVs, but not when macrophages themselves were exposed to EVs. This implies the relevance of yeast-to-yeast communication via the transfer of EVs in modulating the rate of phagocytosis. My finding suggests that the mechanism through which EVs impact phagocytosis is unlikely to be at the level of capsule size or cell body diameter, since capsule and cell body measurements were not considerably changed when *C. neoformans* strains were cultured in media containing exogenous EVs. Future work seeking to investigate the effect EVs have on *C. neoformans*

cells that makes them more readily phagocytosed than cells unexposed to EVs could test the hypothesis that EV-deficient mutants have altered cell wall and/or capsule structure that hinders their recognition by murine macrophages. EVs have been found to modulate cell wall remodelling in *S. cerevisiae* (Zhao et al., 2019); therefore, immunofluorescent staining and mass spectrometry could be used to investigate variations in the distribution and composition of capsular polysaccharides, cell wall glucans and chitins between wildtype and EV-deficient strains. Investigating the polysaccharide composition is particularly relevant since GXM is a known virulence factor (Vecchiarelli et al., 2003), highly prevalent within EVs (Rodrigues et al., 2007) and is the main component of the fibrillar decoration seen around EVs (Rizzo et al., 2021). In my experimental design, cells cultured in the presence of wildtype EVs are washed prior to macrophage infection; therefore, the effect on phagocytosis must represent a physical change in cell wall/ capsule structure during overnight culture and not a signalling process triggered during macrophage infection.

There is evidence that EVs are internalised by fungal cells (Cai et al., 2018; Walker et al., 2018; Zhao et al., 2019), though little is known about the mechanism. It is thought that the *C. neoformans* cell wall is viscoelastic, such that cell wall remodelling can allow particles larger than the porosity of the cell wall (~5.8 nm) to pass through, such as 60 to 80 nm liposomes containing the antifungal drug amphotericin B (Walker et al., 2018). Notable, EVs are 30 – 500 nm in diameter, thus it remains to be discovered whether the viscoelasticity of the *C. neoformans* cell wall permits traversal of vesicles larger than 60

to 80 nm. However, this study implies that the fungal cell wall is less rigid than originally thought.

Although I found no evidence of EVs acting on macrophages to modulate phagocytosis, it is worth noting that EVs from fungi are also internalised by mammalian phagocytes (Bielska et al., 2018; Oliveira et al., 2010a). EV internalisation by mammalian cells has been found to be mediated by a range of endocytic pathways including clathrin-mediated endocytosis (Feng et al., 2010; Escrevente et al., 2011), PI3K-dependent phagocytosis (Feng et al., 2010), macropinocytosis (Fitzner et al., 2011; Costa Verdera et al., 2017) and lipid-raft mediated endocytosis (Bielska et al., 2018; Huang et al., 2012).

Others have explored the consequence of EV exposure on the phagocytosis of various fungal pathogens. Pre-treatment of BMDMs with isolated EVs led to increased phagocytosis and killing of the dermatophyte *Trichophyton interdigitale* (Bitencourt et al., 2018). It also induced expression of M1-associated markers such as iNOS and proinflammatory cytokines such as TNF-α, IL-6 and IL-1β. Similarly, macrophage stimulation with EVs from *C. neoformans* showed increased fungal uptake, increased fungal killing and increased pro-inflammatory TNF-α and anti-inflammatory IL-10 and TGF-β production (Oliveira et al., 2010a). However, there are also studies that have found no impact of EV exposure on phagocytosis rate (Bielska et al., 2018) or found that EV pre-treatment led to decreased phagocytosis and decreased killing of *Histoplasma capsulatum* (Baltazar et al., 2018), suggesting that the results might vary depending on the fungal pathogen, host cell type, or the makeup of EV cargo or cell membrane.

In all these studies, macrophages themselves were pre-exposed to isolated EVs prior to infection with fungi. This is contrary to my data which saw phagocytosis recover when fungi themselves were pre-treated with EVs. This may be because the trans-well approach did not provide enough time for EVs to pass through the pores and elicit an effect on macrophages, since infection was only allowed to take place for 2 h. The second approach in which the phagocytosis assay was carried out in serum-free culture media conditioned with WTKN99α, surprisingly had a negative effect on macrophage phagocytosis capacity, particularly the phagocytosis of wildtype fungi and to some extent the *hap2Δ* mutant. This may reflect the presence of *Cryptococcus* secreted molecules other than EVs, such as CPL1, which is known to promote the non-protective type 2 response (Dang et al., 2022). There may also be secreted GXM that competes for binding with PRRs needed for *Cryptococcus* uptake. There is evidence that *C. albicans* secrete EVs when cultured in mammalian cell culture medium such as DMEM and RPMI (Wei et al., 2023); however, it would be worth validating the presence of *C. neoformans* EVs in supernatant using nanoparticle tracking analysis.

The role of GAT5 and HAP2 (studied in this chapter), along with LIV4 and BZP2, in EV production were first identified using a *C. neoformans* transcription factor deletion library containing 155 mutants (Rizzo et al., 2023). The amount of EVs produced by these cells were less than 10% of that produced by wildtype fungi. Given their roles as transcription factors, these genes likely modulate EV production through the regulation of gene expression. BZP2 and GAT5 belong to the GATA family of transcription factors

and were found to be important for *Cryptococcus* resistance to radiation (Cui et al., 2019). LIV4 is highly conserved across various model yeasts and fungi and plays an important role in *C. neoformans* virulence, such that mice infected with *liv4Δ* strain showed increased survival and reduced lung, spleen and brain fungal burden (Jung et al., 2015; Yi et al., 2020). Finally, HAP2 is one of four components of the CCAAT-binding heme activator protein complex (Hap2/3/5/X), and was found to modulate iron utilisation and mating (Kim and Bahn, 2022). Interestingly, the *hap3Δ* and *hap5Δ* mutant strains, but not *hapXΔ*, were also defective in EV production without affecting growth rate (Rizzo et al., 2023).

Given that the *hap2Δ* mutant had no growth defect, showed normal EV morphology (Rizzo et al., 2023), and had a phagocytosis phenotype that was fully rescued by culture in YPD broth conditioned with wildtype EVs, I propose that *hap2Δ* is a true EV mutant. The growth defect seen in the *gat5Δ* strain and the inability of WT EVs to rescue their phagocytosis suggest there are other EV-independent processes at play in this strain, in addition to EV-mediated processes. Additionally, deletion of LIV4 and BZP2 also results in a growth defect (Jung et al., 2015; Rizzo et al., 2023), suggesting that reduced EV production in these strains may also result in decreased phagocytosis but not be rescued by treatment with WT EVs.

Rizzo et al (2023) performed RNA-seq analysis of *gat5Δ*, *hap2Δ*, and wildtype cryptococci, to investigate the mechanism by which these transcription factors influence EV production. Firstly, they found that genes involved in ribosome biogenesis were the

most upregulated genes in *gat5Δ* and *hap2Δ* mutants, suggesting that the suppression of translation is needed for EV production. Next, they showed that genes involved in protein glycosylation, cell wall organization and biogenesis and vesicle-mediated transport were downregulated in *gat5Δ* and *hap2Δ* mutants compared to wildtype. Interestingly, they found that GAT5 is downregulated in the *hap2Δ* mutant suggesting that the HAP2 transcription factor is upstream of GAT5. Earlier work by (Rizzo et al., 2021) identified 39 proteins that were most commonly associated with secreted EVs. Twenty-one of these 39 proteins were downregulated in *gat5Δ* and *hap2Δ* mutants. The most abundant EV proteins in *C. neoformans*, Mp88 and Vep1 (Rizzo et al., 2021), were downregulated in *gat5Δ* and *hap2Δ* mutants (Rizzo et al., 2023). All these findings point to a key role for GAT5 and HAP2 in modulating EV production.

Although I tried various approaches to validate that the decreased phagocytosis seen when macrophages were infected with *gat5Δ* and *hap2Δ C. neoformans* was a consequence of EVs, it is a widely recognised challenge within the field to attribute specific physiological outcomes to the activity of EVs themselves (van Niel et al., 2022). How can we ensure the phenotypes observed are truly a consequence of EV trafficking to, and EV uptake by, a recipient cell? This challenge is largely due to technological limitations. The isolation of EVs currently relies on various centrifugation approaches; however, in addition to EVs, this process can pellet down other extracellular molecules such as non-EV associated nucleic acid, protein complex and lipoproteins which could lead to false attribution of a phenotype to EV activity (van Niel et al., 2022; Meldolesi, 2018).

Another limitation of my experiment is the inability to control for variability in the quantity of EVs *C. neoformans* cultures are exposed to between independent experiments. Some EV preparations used in my experiments may have had a greater yield than others; however, this is difficult to account for since I was unable to quantify the concentration of EVs in each preparation. To try and mitigate this, I plated the same number of cells ($3.5x10^7$cells/mL per plate) onto three SD agar plates for all experiments. However, confirmation of EV concentration will require at the very least measuring total sterol concentration in supernatant.

There is also inherent heterogeneity in EV populations, such that when centrifugation-based approaches are used, the result is a heterogenous population of EVs that vary in size, membrane composition and cargo content (van Niel et al., 2022). Some EVs, called exosomes, originate from endosomal membranes and have a diameter of 50 – 150 nm (Meldolesi, 2018). Meanwhile, the second class of EVs, called ectosomes, are derived from outward budding of the plasma membrane and have a diameter of 100 – 500 nm (Meldolesi, 2018). There is also variation within each class of EVs which could have unpredictable effects on target cells. Notably, there is evidence for the existence of all of these various types of EVs in fungi (Wolf et al., 2014; Reis et al., 2021). Therefore, when a heterogenous EV population is used, it is difficult to understand the contribution of distinct EV subpopulations to physiological outcomes and could lead to misleading interpretations of experimental results. These challenges will require novel tools and methodology to overcome. There is much to be done in understanding the biogenesis,

secretion and function of fungal EVs; however, this work provides further evidence that EVs are biologically active, contribute to yeast-to-yeast communication and impact fungal phagocytosis by murine macrophages. Whether this is beneficial to the host or fungi remains unknown.

Chapter 6 *Cryptococcus neoformans* resistance to Amoebae does not correlate with resistance to phagocytosis by mammalian macrophages.

The following thesis chapter contains work carried out in collaboration with Dr Thomas Sauters and Dr Paul Magwene (Duke University, North Carolina, USA). The bulk of the work was carried out by Thomas Sauters as part of his PhD thesis and has been accepted for publication in PLOS Pathogens. I was responsible for the experiments involving Cryptococcus uptake by, and proliferation within, macrophages. Sauters wrote the majority of the manuscript. A preprint version of this paper is available on bioRxiv.

6.1 Background

As a fungal pathogen that is prevalent in the environment, *C. neoformans* do not depend on their host for survival and replication (Casadevall and Pirofski, 2007). Moreover, they do not share an evolutionary history with humans and are incapable of natural person-to-person transmission. Therefore, the mechanism by which *C. neoformans* acquired virulence in human hosts remains a puzzle. One widely propagated model to explain *C. neoformans* virulence in humans is the accidental pathogenesis hypothesis. First presented in 2001, this is the idea that *C. neoformans* virulence in human hosts evolved as an accidental by-product of its evolutionary history with its natural predators, such as amoebae (Steenbergen et al., 2001). More recently, this phenomena has been termed the amoeboid predator-animal virulence hypothesis (Casadevall et al., 2019).

The hypothesis is supported by the well-known fact that amoebae and macrophages share a range of similarities including: the ability to phagocytose particles, initiate an oxidative burst, migrate towards a target organism or chemical signal, and undergo non-lytic expulsion (Bajgar and Krejčová, 2023; Chrisman et al., 2010). It is also supported by early findings that the amoeba, *Acanthamoeba castellanii*, was able to phagocytose *C. neoformans* and that the fungus was able to replicate within amoebae (Steenbergen et al., 2001). Additionally, *Cryptococcus* virulence factors such as melanisation, polysaccharide capsule, and phospholipase B were important for fungal survival and replication in amoebae, which is reminiscent of their importance during *Cryptococcus*-macrophage interaction (Steenbergen et al., 2001; Chrisman et al., 2010, 2011). It has also been found that when *C. neoformans* are co-incubated with the amoeba *Dictyostelium discoideum* for 72 h and then used to infect A/Jcr female mice, fungi passaged in amoebae were more virulent as measured by mice survival (Steenbergen et al., 2003). Similarly, *C. neoformans* recovered from 24 h co-incubation with *A. castellanii* led to increased killing of *Galleria mellonella* (Rizzo et al., 2017). *C. neoformans* exposed to *A. castellanii* produced more urease, were more resistant to reactive oxygen species (H_2O_2) and reactive nitrogen species ($NaNO_2$), and had increased deposition of chitin on the cell wall (Rizzo et al., 2017). These studies provide more direct evidence that adaptation in amoebae influence interaction with mammalian. However, given that *C. neoformans* was only incubated with amoebae for 72 h (Steenbergen et al., 2003) or 24 h (Rizzo et al., 2017), this is unlikely to provide sufficient selection pressure for the mechanism of increased virulence to be explained by spontaneous mutagenesis and positive selection. Rather, acquired virulence in these experiments would most likely

represent epigenetic changes and may be reversible, although hypermutator *Cryptococcus* isolates have been identified and may potentially also play a role (Magditch et al., 2012; Billmyre et al., 2017).

There is theoretical and experimental basis for the amoeboid predator-animal virulence hypothesis; however, these studies only tested virulence factors that are already known to play a role in mammalian infection and relied on knockout *Cryptococcus* strains. They have also failed to utilise a long-term experiential evolution approach to explore this hypothesised evolutionary dynamic. It was with this backdrop that Dr Thomas Sauters set out to further evaluate the accidental pathogenesis model by first identifying genes and alleles that influence *Cryptococcus* virulence in amoebae using quantitative trait loci (QTL) mapping, then testing the virulence of these evolved strains in a mammalian host.

The remainder of this chapter will discuss some of the findings from Sauter's PhD research, present the data I acquired to support this work, and provide a critical discussion on the amoeboid predator-animal virulence hypothesis.

6.2 Results & Discussion

Firstly, taking advantage of the natural genetic diversity in *C. neoformans*, Thomas surveyed the ability of 15 *C. neoformans* strains spanning the VNBI, VNBII and VNI lineages to resist *A. castellanii* predation in a plate-based assay (Figure 6-1) (Sauters et al., 2022). In this assay, a lawn of *C. neoformans* is grown, *A. castellanii* is dropped onto the centre of the *Cryptococcus* lawn, plates are incubated for 12 – 18 days at 25°C, then

the area of the lawn cleared by amoebae is measured. The greater the area cleared by amoebae, the less resistant the fungal strain is to amoeboid predation (Table 5). Conversely, the smaller the clearance area, the more resistant the strain is to *A. castellanii*. Interestingly, there was no correlation between clinical vs environmental vs laboratory or strain lineage and amoebae resistance. In other words, these parameters were not predictors of amoebae resistance (Table 5).

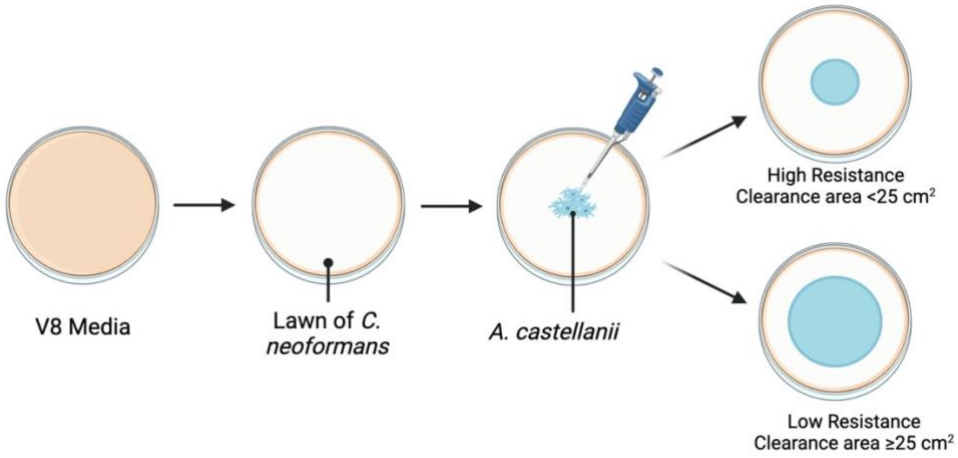

Figure 6-1: Plate-based assay of *C. neoformans* resistance to the amoeba, *Acanthamoeba castellanii*. *Cryptococcus neoformans* are cultured overnight in YPD broth, diluted, then spread onto V8 agar to create a lawn. Plates were grown at 30°C for 60 h. At the same time *A. castellanii* were cultured, then 50 µl of a $1x10^6$ cells/mL dilution was pipetted onto the middle of the lawn of *C. neoformans*. Plates were incubated at 25°C for 18 days then the area of clearance was measured on days 1 and days 18. Final measurement was determined by subtracting the day 1 measurement from day 18 measurement. Clearance area less than 25 cm^2 identifies a high amoeba resistant strain; Clearance area greater than or equal to 25 cm^2 represents a low amoeba resistant strain. Figure adapted from (Sauters et al., 2022). Figure created with Biorender.com.

To perform QTL mapping to identify alleles associated with amoebae resistance, two strains were selected on the basis that they are of opposite mating types, showed differential resistance to amoebae, and had good sporulation and germination efficiency. The two strains selected for crossing were the medium resistance Bt22 clinical isolate (median clearance area: 40 cm^2) and the high resistance Ftc555-1 environmental isolate

(median clearance area: 9 cm^2) (Table 5; **). The F_1 progeny from Bt22 x Ftc555-1 cross were sequenced and their resistance to amoebae were analysed using the plate-based assay. The amoeba predation assay on the F_1 progeny (>300 progeny) revealed a wide range of response to amoebae with the average clearance area being 23.46 cm^2 (SD = 14.99 cm^2).

Table 5: Selection of *C. neoformans* strains surveyed and their associated resistance to amoebae*

Strain	Lineage	Site of Isolation	Amoeba Resistance (Median clearance area cm^2) ***
H99	VNI	Clinical	Low (51 cm^2)
Bt22**	VNBI	Clinical	Low (40 cm^2)
Bt75	VNBII	Clinical	Low (28 cm^2)
Ftc192-1	VNBI	Environmental	High (20 cm^2)
Bt130	VNBII	Clinical	High (18 cm^2)
Bt45	VNBI	Clinical	High (16 cm^2)
Ftc267-1	VNBI	Environmental	High (12 cm^2)
Bt206	VNBII	Clinical	High (11 cm^2)
Ftc555-1**	VNBI	Environmental	High (9 cm^2)
Bt102	VNBI	Clinical	High (9 cm^2)
Bt65	VNBII	Clinical	High (4 cm^2)

* Table includes data from experiments carried out by Thomas Sauters, PhD, Duke University, North Carolina. Adapted from Figure 1C and Table 2 (Sauters et al., 2022).
** Strains selected for crossing and QTL analysis
*** Area ranged from 0 – 50 cm^2, therefore, I used 25 cm^2 as the cut-off between high and low amoeba resistance. Clearance area less than 25 cm^2 represent high amoeba resistance; Clearance area greater than or equal to 25 cm^2 represent low amoeba resistance.

Before testing whether observed *C. neoformans* resistance to amoebae correlated with resistance to mammalian cells as measured by phagocytosis index and intracellular proliferation, segregants from the Bt22 x Ftc555-1 cross were used in QTL analysis to

identify alleles associated with amoeba resistance. A single QTL peak at chromosome 8 was identified and progeny with the Bt22 haplotypes at this site were more sensitive to amoeba predation than those with the Ftc555-1 haplotype. Within this haplotype, an intergenic 1789 bp deletion upstream of the BZP4 gene was identified in the Bt22 background that shortened the 5'UTR of BZP4 by 100 bp. This deletion resulted in decreased expression of BZP4. When BZP4 was deleted in the high resistance Ftc555-1 parental strain, this strain become more sensitive to amoeba predation. BZP4 is a transcription factor identified for its role in melanin synthesis, with loss of BZP4 expression resulting in decreased melanin production (Yu et al., 2019; Desjardins et al., 2017; Lee et al., 2019). Sauters identified a positive correlation between melanin production and amoeba resistance, suggesting that BZP4's role in melanin production is a mechanism driving *C. neoformans* resistance to *A. castellanii*.

Having identified BZP4 as a key gene responsible for modulating amoeba resistance, the next question was to explore whether resistance to *A. castellanii* predicts resistance to mammalian challenge. To test this, I received the Bt22 and Ftc555-1 parental strains along with 5 segregants that were found to have differential resistance to amoeba predation. J774A.1 murine macrophages were infected with parental strains along with low and high resistance strains and the number of phagocytosed *C. neoformans* and the intracellular proliferation of *C. neoformans* were quantified. I found no correlation between a strain's resistance to amoebae and its resistance to phagocytosis by murine macrophages (Figure 6-2A). There was no difference in the phagocytosis of the parental strains despite their varying susceptibility to amoeba predation. Segregant 2 (S2) and S4

both had increased numbers of internalised fungi, even though S2 has low resistance to amoebae and carries the BZP4 allele corresponding to the Bt22 parent, while S4 has high resistance to amoebae and has the BZP4 allele corresponding to the Ftc555-1 parent. Next, I observed no difference in IPR between parental strains and segregants (Figure 6-2B). In fact, there was no difference in IPR between any of the pair wise comparisons, further implying no parallel between amoeba resistance and interaction with macrophages.

To further investigate this, Thomas infected A/J mice with Bt22 and Ftc555-1 parental strains or segregants. Similar to the *in vitro* findings, there was no obvious link between amoeba resistance and virulence in mice. Instead, there was extensive variation in virulence to mice with low and high amoeba resistance strains being both avirulent and highly virulent as measured by mice mortality over 180 days. For example, the classic laboratory strain H99 had very low amoeba resistance but had a time to 50% lethality (LT50) of ~21 days making it highly virulent to mice. The high amoeba resistant Ftc555-1 parent was avirulent in mice while the low amoeba resistant Bt22 parent was more virulent with an LT50 of ~92 days. At the same time, some strain with high amoeba resistance were highly virulent in mice. Therefore, amoeba resistance could not be used to predict virulence in mice, challenging the accidental pathogenesis model of *C. neoformans* evolution.

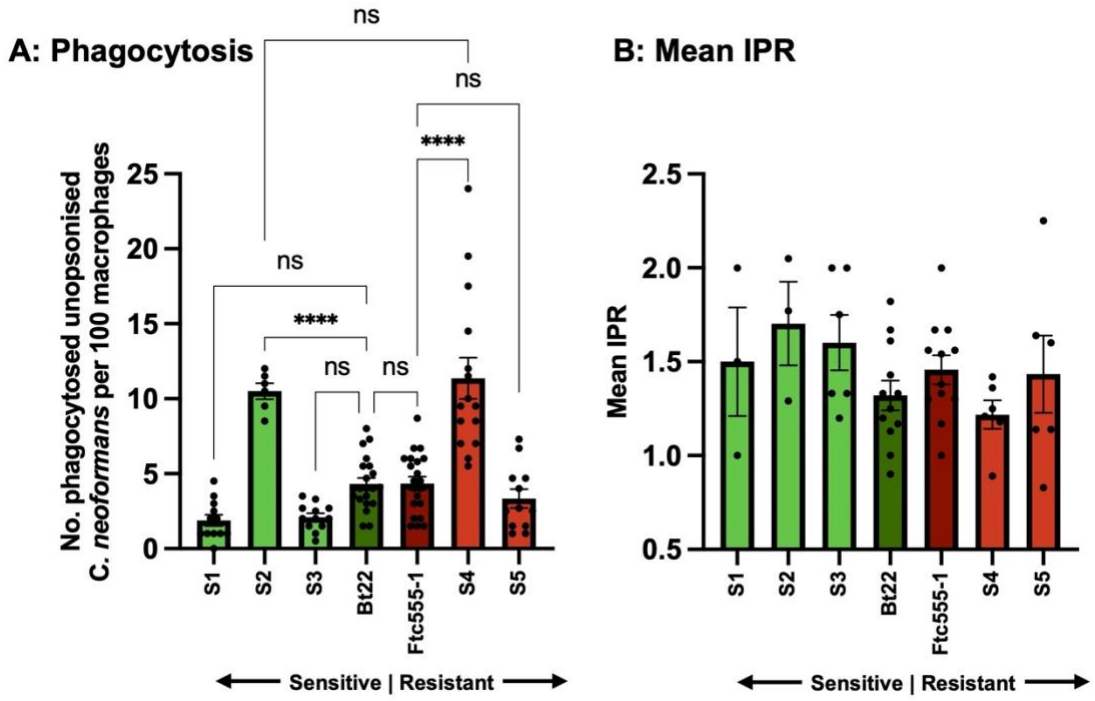

Figure 6-2: *C. neoformans* resistance to *Acanthamoeba castellanii* does not predict interaction with macrophages. Macrophages were infected with low resistance Bt22 parental strain (dark green), high resistance Ftc555-1 parental strain (dark red) and five segregants (S1 to S5; coloured according to BZP4 allele). **(A)** Phagocytosis was quantified as the number of internalised *C. neoformans* per 100 macrophages. Each *Cryptococcus* strain was used in a phagocytosis assay at least twice. Then data was pooled to form a single graph. Each data point represents a technical repeat. **(B)** Intracellular proliferation of *C. neoformans* was quantified using the time-lapse approach. The number of internalised fungi per 100 macrophages at the 'first frame' (T0) and 'last frame' (T10) was quantified and IPR was calculated using the equation: IPR = T10/T0. Data is pooled from independent experiments to form a single graph. Strains are organised left to right from most sensitive to amoeba predation to most resistant to amoeba predation. Data shown as mean ± SEM. Statistical significance was determined by performing a one-way analysis of variance; ns, not significant; ****p<0.0001. All comparisons in **(B)** were not significant.

There are some limitations to our experimental design that may explain the lack of association between *C. neoformans* resistance to *A. castellanii* and response to macrophage/mice. Firstly, mouse infection utilised a large inoculum size ($4x10^6$ CFU/mL); however, it has been found that *C. neoformans* capacity for virulence is dependent on inoculum with infection with low inoculum surprisingly resulting in higher pathogenic potential (Smith and Casadevall, 2022). Therefore, using lower inoculum could help tease out further variation between strains and provide a more accurate representation

of the pathogenic potential of individual fungal cells of each strain. However, it is hard to think that a low inoculum would alter the overall conclusion that there is no correlation between resistance to amoebae and mammalian cells. Secondly, this study found and focused on the role of BZP4 in *Cryptococcus* virulence to amoebae; however, it is very likely that not all interactions with *A. castellanii* necessarily results in evolution of virulence in mammalian cells. Just because the BZP4 allele is important for resistance to amoebae doesn't mean it will be important for virulence in mammalian hosts. There is not necessarily a one to one relationship between virulence in amoebae and virulence in mammalian hosts (Casadevall et al., 2019). It is interesting that although BZP4 is implicated in regulating melanin production (Desjardins et al., 2017), which is a known virulence factor in mammalian cells (Liu et al., 1999; Wang et al., 1995; McClelland et al., 2006), there was still no correlation between amoebae resistance driven by BZP4 polymorphism and virulence in mammalian cells. However, this may not be so surprising since environmental isolates of *C. neoformans* express more melanin than clinical isolates (Yu et al., 2019; Desjardins et al., 2017). Therefore, melanin may not be a significant virulence factor during mammalian infection when other virulence factors such as the polysaccharide capsule are intact. In fact, in the 2001 paper by Steenbergen et al. that first presented the idea of accidental pathogenesis to explain *C. neoformans* virulence, they observed that amoebae were equally able to kill encapsulated melanized versus non-melanised *C. neoformans*. However, when using the acapsular cap67 strain, melanised *C. neoformans* was more resistant to amoebae predation than non-melanised acapsular *C. neoformans* strain (Steenbergen et al., 2001), suggesting that melanisation

might be a secondary/ redundant virulence factor important only when a primary virulence factor such as capsule polysaccharide is absent.

A recent study performed experimental evolution to identify phenotypic and genetic adaptations in three *C. neoformans* strains (H99, Ftc555-1, and A1-35-8) following one-month long coincubation with *A. castellanii* (Fu et al., 2021). They identified pseudo-hyphal formation, increased capsule thickness, increased urease production, decreased melanin production, nonsynonymous mutations in the OPT1 oligopeptide transporter involved in transporting quorum-sensing peptides into the recipient cell, and duplication of chromosome 8 as adaptations promoting increased resistance to amoebae. It is interesting that, unlike Sauters et al (2022), Fu et al. (2021) identified reduced melanin production as a mechanism of increased resistance to amoebae. However, the identification of a chromosome 8 duplication, the same chromosome carrying the BZP4 gene identified by Sauters, highlights a need to explore the consequence of BZP4 duplication on amoeba resistance. Similar to the findings presented here, Fu et al (2021) failed to identify a relationship between amoebae resistance and virulence in macrophages, as measured by IPR, and virulence in mice and *Galleria mellonella*, as measured by survival. Though the identified mechanism of adaptation to amoebae varied between the two studies, both studies conclude that resistance to *A. castellanii* does not necessarily predict resistance to mammalian cells. Many of the earlier studies utilised *Cryptococcus* strains deficient in known mammalian virulence factors and identified concordance between the function of these genes in mammalian cells and amoebae. However, this concordance may represent a general reduction in fitness and

does not directly prove the virulence factors evolved from coevolution with amoeboid predators.

Although the accidental pathogenesis hypothesis has been widely propagated over the past two decades, more recent experiments suggest that this model may be too simplistic to explain the evolution of *C. neoformans* in the complex soil environment. Many of the studies investigating the accidental pathogenesis model utilise a single amoeba strain, *A. castellanii*, when the soil environment contains a myriad other fungal predators and selection pressures acting on the fungi. Thus, in spite of the similarities between amoebae and mammalian phagocytes, it is important to explore these other hosts as distinct niches where cryptococci can develop varying survival solutions. What is clear, however, is that *C. neoformans* can undergo phenotypic (Fu et al., 2021) and genetic (Fu et al., 2021; Sauters et al., 2022) changes after co-incubation with amoebae. It is unlikely that *C. neoformans*-amoebae interaction always results in adaptations that favour increased fungal virulence to mammalian hosts. Instead, the generation of genetic diversity through mutations and aneuploidy may represent shared drivers of microevolution during *Cryptococcus* interaction with mammalian cells and environmental predators.

Chapter 7 Conclusion

The aim of this thesis was to shed light on host and pathogen factors that modulate the non-opsonic phagocytosis of *C. neoformans*. Looking from the perspective of the mammalian host, I first asked the question of whether the classic pattern recognition receptor, TLR4, is necessary for the phagocytosis of *C. neoformans*. To my surprise, loss of TLR4 signalling led to a counterintuitive increase in the phagocytosis of cryptococci. This increased uptake corresponded to increased MSR1 expression in *Tlr4*$^{-/-}$ iBMDMs and accumulation of MSR1 around phagosomes containing cryptococci. Furthermore, macrophages derived from MSR1 knock out mice were dramatically impaired in the uptake of cryptococci. Therefore, although TLR4 does not directly mediate *C. neoformans* uptake, it modulates the surface expression of MSR1 which is then critical for the non-opsonic phagocytosis of *C. neoformans*, presenting a novel TLR4/MSR1 crosstalk in the modulation of *C. neoformans* uptake. This finding provides an explanation for the minimal involvement of Dectin-1, the classic PRR for fungal β-glucan (Brown and Gordon, 2001; Gantner et al., 2005), in host response to *C. neoformans*.

Previous work that found no contribution of TLR4 in mice response to *C. neoformans* (Biondo et al., 2005; Yauch et al., 2004) may reflect a difference in MSR1 expression between mice of differing genetic backgrounds which has, thus far, been unaccounted for. Future work should explore how TLR4, MSR1 and TLR4/MSR1 double knockout influence mice response to intranasal or intravenous infection. There is also a need to understand the mechanism by which TLR4 activity modulates MSR1 cell surface expression. Alternatively, TLR4 may modulate intracellular scavenger receptor

reservoirs such that suppression of TLR4 signalling drives MSR1 to the plasma membrane.

While investigating the role of scavenger receptors in *C. neoformans* uptake, I made the observation that MARCO is dispensable for uptake in PMA stimulated, but not LPS stimulated macrophages. However, in both conditions, as well as for *C. albicans* and antibody-opsonised *C. neoformans*, MARCO deficiency led to a glaring increase in non-lytic expulsion of *C. neoformans*. The magnitude of increase was greater than anything reported in the literature to date with the rate of non-lytic expulsion reaching 80% to 100% in MARCO knockout macrophages compared to 10% to 20% in wildtype macrophages. Pointing to MARCO as a potential master regulator of host-directed non-lytic expulsion. Moreover, I concluded that the role of MARCO in non-lytic expulsion was independent of the mechanism of uptake. Instead, it may reflect dysfunctional actin cytoskeleton in *Marco*$^{-/-}$ macrophages. More work is needed to understand the mechanism of MARCO-mediated modulation of cytoskeletal remodelling. Additional work can also investigate the effect of MARCO on ERK5 (Gilbert et al., 2017), Arp2/3 (Johnston and May, 2010), Annexin A2 (Stukes et al., 2016), and type 1 interferon (Seoane et al., 2020) expression and/or activity, as these were the only host molecules that had been identified as modulators of non-lytic expulsion. A role for MARCO in modulating these proteins will support the claim that MARCO is a master regulator of non-lytic expulsion. Moreover, since non-lytic expulsion is theorised to be a key step in the Trojan horse model of *C. neoformans* dissemination (Gilbert et al., 2017), *Marco*$^{-/-}$ mice could be used as a tool to investigate non-lytic expulsion *in vivo* and explore the

involvement of non-lytic expulsion in dissemination to the brain possibly using intravital microscopy or bioluminescent imaging.

Moving onto pathogen factors that influence *C. neoformans* uptake, I found that the secretion of EVs and subsequent *Cryptococcus* cell response to EVs in the culture environment influences the extent to which *C. neoformans* is phagocytosed by murine macrophages. Our understanding of fungal EVs is still in its infancy; however, this finding highlights the significance of considering pathogen physiological processes during *Cryptococcus*-macrophage interaction. EV secretion can alter the cell wall and capsule composition which then impacts the ability of PRRs to detect *Cryptococcus* PAMPs. Finally, using genetically diverse *Cryptococcus* strains that differed in their resistance to amoebae predation and the resulting F1 progeny from their crosses, I found no association between *Cryptococcus* resistance to amoebae and virulence to macrophages. This does not necessarily negate the accidental pathogenesis hypothesis of *C. neoformans* evolution. However, it highlights a need for greater nuance in this hypothesis and a view of amoebae and mammalian cells as distinct niches where *C. neoformans* can undergo adaptation.

Overall, this thesis has contributed to minimising the gap in our understanding of host PRRs involved in the non-opsonic uptake of C*. neoformans*, by identifying MSR1 as a key receptor for uptake and MARCO as a conditional receptor involved in non-opsonic phagocytosis but critical to the inhibition of phagosome expulsion. It has also identified *C. neoformans* EV production, release, and potential uptake by recipient fungal cells in

modulating uptake and highlighted amoeboid predators and macrophages as distinct niches that impose shared, but also unique selection pressures on *C. neoformans* calling for increased nuance to the accidental pathogenesis model of *C. neoformans* evolution of virulence towards mammalian hosts.

List of References

Abdul Zani, I., Stephen, S.L., Mughal, N.A., et al. (2015) Scavenger Receptor Structure and Function in Health and Disease. *Cells*, 4 (2): 178–201. doi:10.3390/cells4020178.

Abe, K., Kadota, J., Ishimatsu, Y., et al. (2000) Th1-Th2 cytokine kinetics in the bronchoalveolar lavage fluid of mice infected with Cryptococcus neoformans of different virulences. *Microbiology and Immunology*, 44 (10): 849–855. doi:10.1111/j.1348-0421.2000.tb02573.x.

Ackerman, S.K., Friend, P.S., Hoidal, J.R., et al. (1978) Production of C2 by human alveolar macrophages. *Immunology*, 35 (2): 369–372.

Alanio, A., Desnos-Ollivier, M. and Dromer, F. (2011) Dynamics of Cryptococcus neoformans-macrophage interactions reveal that fungal background influences outcome during cryptococcal meningoencephalitis in humans. *mBio*, 2 (4): e00158-11. doi:10.1128/mBio.00158-11.

Almeida, F., Wolf, J.M. and Casadevall, A. (2015) Virulence-Associated Enzymes of Cryptococcus neoformans. *Eukaryotic Cell*, 14 (12): 1173–1185. doi:10.1128/EC.00103-15.

Alvarez, M. and Casadevall, A. (2006) Phagosome Extrusion and Host-Cell Survival after Cryptococcus neoformans Phagocytosis by Macrophages. *Current Biology*, 16 (21): 2161–2165. doi:10.1016/j.cub.2006.09.061.

Amiel, E., Alonso, A., Uematsu, S., et al. (2009) Pivotal Advance: Toll-like receptor regulation of scavenger receptor-A-mediated phagocytosis. *Journal of Leukocyte Biology*, 85 (4): 595–605. doi:10.1189/jlb.1008631.

Applen Clancey, S., Ruchti, F., LeibundGut-Landmann, S., et al. (2020) A Novel Mycovirus Evokes Transcriptional Rewiring in the Fungus Malassezia and Stimulates Beta Interferon Production in Macrophages. *mBio*, 11 (5): e01534-20. doi:10.1128/mBio.01534-20.

Arango-Franco, C.A., Migaud, M., Ramírez-Sánchez, I.C., et al. (2023) Anti-GM-CSF Neutralizing Autoantibodies in Colombian Patients with Disseminated Cryptococcosis. *Journal of Clinical Immunology*, pp. 1–12. doi:10.1007/s10875-023-01451-5.

van Asbeck, E.C., Hoepelman, A.I., Scharringa, J., et al. (2008) Mannose binding lectin plays a crucial role in innate immunity against yeast by enhanced complement activation and enhanced uptake of polymorphonuclear cells. *BMC Microbiology*, 8: 229. doi:10.1186/1471-2180-8-229.

Bagchi, A., Herrup, E.A., Warren, H.S., et al. (2007) MyD88-Dependent and MyD88-Independent Pathways in Synergy, Priming, and Tolerance between TLR Agonists. *The Journal of Immunology*, 178 (2): 1164–1171. doi:10.4049/jimmunol.178.2.1164.

Bain, J.M., Lewis, L.E., Okai, B., et al. (2012) Non-lytic expulsion/exocytosis of Candida albicans from macrophages. *Fungal Genetics and Biology*, 49 (9): 677–678. doi:10.1016/j.fgb.2012.01.008.

Bajgar, A. and Krejčová, G. (2023) On the origin of the functional versatility of macrophages. *Frontiers in Physiology*, 14. doi:https://doi.org/10.3389/fphys.2023.1128984.

Baltazar, L.M., Zamith-Miranda, D., Burnet, M.C., et al. (2018) Concentration-dependent protein loading of extracellular vesicles released by Histoplasma capsulatum after antibody treatment and its modulatory action upon macrophages. *Scientific Reports*, 8 (1): 8065. doi:10.1038/s41598-018-25665-5.

Balzar, S., Strand, M., Rhodes, D., et al. (2007) Immunoglobulin (Ig)E Expression Pattern in Lung: Relation to Systemic IgE and Asthma Phenotypes. *The Journal of allergy and clinical immunology*, 119 (4): 855–862. doi:10.1016/j.jaci.2006.12.642.

Barrio, M.B., Rainard, P., Gilbert, F.B., et al. (2003) Assessment of the Opsonic Activity of Purified Bovine sIgA Following Intramammary Immunization of Cows with Staphylococcus aureus. *Journal of Dairy Science*, 86 (9): 2884–2894. doi:10.3168/jds.S0022-0302(03)73885-5.

Barros, J.C. and Marshall, C.J. (2005) Activation of either ERK1/2 or ERK5 MAP kinase pathways can lead to disruption of the actin cytoskeleton. *Journal of Cell Science*, 118 (8): 1663–1671. doi:10.1242/jcs.02308.

Beenhouwer, D.O., Yoo, E.M., Lai, C.-W., et al. (2007) Human Immunoglobulin G2 (IgG2) and IgG4, but Not IgG1 or IgG3, Protect Mice against Cryptococcus neoformans Infection. *Infection and Immunity*, 75 (3): 1424–1435. doi:10.1128/IAI.01161-06.

Beisswenger, C., Hess, C. and Bals, R. (2012) Aspergillus fumigatus conidia induce interferon-β signalling in respiratory epithelial cells. *European Respiratory Journal*, 39 (2): 411–418. doi:10.1183/09031936.00096110.

Ben-Ali, M., Barbouche, M.-R., Bousnina, S., et al. (2004) Toll-like receptor 2 Arg677Trp polymorphism is associated with susceptibility to tuberculosis in Tunisian patients. *Clinical and Diagnostic Laboratory Immunology*, 11 (3): 625–626. doi:10.1128/CDLI.11.3.625-626.2004.

Bergman, F. and Linell, F. (1961) Cryptococcosis as a Cause of Pulmonary Alveolar Proteinosis. *Acta Pathologica Microbiologica Scandinavica*, 53 (2): 217–224. doi:10.1111/j.1699-0463.1961.tb00403.x.

Bhatti, M.F., Bignell, E.M. and Coutts, R.H.A. (2011) Complete nucleotide sequences of two dsRNAs associated with a new partitivirus infecting Aspergillus fumigatus. *Archives of Virology*, 156 (9): 1677–1680. doi:10.1007/s00705-011-1045-5.

Bielska, E., Sisquella, M.A., Aldeieg, M., et al. (2018) Pathogen-derived extracellular vesicles mediate virulence in the fatal human pathogen Cryptococcus gattii. *Nature Communications*, 9 (1): 1556. doi:10.1038/s41467-018-03991-6.

Billmyre, R.B., Clancey, S.A. and Heitman, J. (2017) Natural mismatch repair mutations mediate phenotypic diversity and drug resistance in Cryptococcus deuterogattii Rokas, A. (ed.). *eLife*, 6: e28802. doi:10.7554/eLife.28802.

Bin, L.-H., Nielson, L.D., Liu, X., et al. (2003) Identification of Uteroglobin-Related Protein 1 and Macrophage Scavenger Receptor with Collagenous Structure as a Lung-Specific Ligand-Receptor Pair. *The Journal of Immunology*, 171 (2): 924–930. doi:10.4049/jimmunol.171.2.924.

Biondo, C., Midiri, A., Messina, L., et al. (2005) MyD88 and TLR2, but not TLR4, are required for host defense against Cryptococcus neoformans. *European Journal of Immunology*, 35 (3): 870–878. doi:10.1002/eji.200425799.

Bitencourt, T.A., Rezende, C.P., Quaresemin, N.R., et al. (2018) Extracellular Vesicles From the Dermatophyte Trichophyton interdigitale Modulate Macrophage and Keratinocyte Functions. *Frontiers in Immunology*, 9. doi:doi.org/10.3389/fimmu.2018.02343.

Bloom, A.L.M., Jin, R.M., Leipheimer, J., et al. (2019) Thermotolerance in the pathogen Cryptococcus neoformans is linked to antigen masking via mRNA decay-dependent reprogramming. *Nature Communications*, 10: 4950. doi:10.1038/s41467-019-12907-x.

Bolger, M.S., Ross, D.S., Jiang, H., et al. (2007) Complement levels and activity in the normal and LPS-injured lung. *American Journal of Physiology-Lung Cellular and Molecular Physiology*, 292 (3): L748–L759. doi:10.1152/ajplung.00127.2006.

Bongomin, F., Gago, S., Oladele, R.O., et al. (2017) Global and Multi-National Prevalence of Fungal Diseases—Estimate Precision. *Journal of Fungi*, 3 (4). doi:10.3390/jof3040057.

Bonilla, D.L., Bhattacharya, A., Sha, Y., et al. (2013) Autophagy Regulates Phagocytosis by Modulating the Expression of Scavenger Receptors. *Immunity*, 39 (3): 537–547. doi:10.1016/j.immuni.2013.08.026.

Bournazos, S., Wang, T.T. and Ravetch, J.V. (2016) The Role and Function of Fcγ Receptors on Myeloid Cells. *Microbiology spectrum*, 4 (6). doi:10.1128/microbiolspec.MCHD-0045-2016.

Brandsma, A.M., ten Broeke, T., van Dueren den Hollander, E., et al. (2017) Single Nucleotide Polymorphisms of the High Affinity IgG Receptor FcγRI Reduce Immune Complex Binding and Downstream Effector Functions. *The Journal of Immunology*, 199 (7): 2432–2439. doi:10.4049/jimmunol.1601929.

Brizendine, K.D., Baddley, J.W. and Pappas, P.G. (2013) Predictors of Mortality and Differences in Clinical Features among Patients with Cryptococcosis According to Immune Status. *PLOS ONE*, 8 (3): e60431. doi:10.1371/journal.pone.0060431.

Brown, G.D. (2006) Dectin-1: a signalling non-TLR pattern-recognition receptor. *Nature Reviews Immunology*, 6 (1): 33–43. doi:10.1038/nri1745.

Brown, G.D. and Gordon, S. (2001) A new receptor for β-glucans. *Nature*, 413 (6851): 36–37. doi:10.1038/35092620.

Browne, S.K., Burbelo, P.D., Chetchotisakd, P., et al. (2012) Adult-onset immunodeficiency in Thailand and Taiwan. *The New England journal of medicine*, 367 (8): 725–734. doi:10.1056/NEJMoa1111160.

Burnett, D. (1986) Immunoglobulins in the lung. *Thorax*, 41 (5): 337–344. doi:10.1136/thx.41.5.337.

Cai, J.-P., Liu, L.-L., To, K.K.W., et al. (2015) Characterization of the antigenicity of Cpl1, a surface protein of Cryptococcus neoformans var. neoformans. *Mycologia*, 107 (1): 39–45. doi:10.3852/14-074.

Cai, Q., Qiao, L., Wang, M., et al. (2018) Plants send small RNAs in extracellular vesicles to fungal pathogen to silence virulence genes. *Science*, 360 (6393): 1126–1129. doi:10.1126/science.aar4142.

Campuzano, A., Castro-Lopez, N., Wozniak, K.L., et al. (2017) Dectin-3 Is Not Required for Protection against Cryptococcus neoformans Infection. *PLoS ONE*, 12 (1). doi:10.1371/journal.pone.0169347.

Campuzano, A. and Wormley, F. (2018) Innate Immunity against Cryptococcus, from Recognition to Elimination. *Journal of Fungi*, 4 (1): 33. doi:10.3390/jof4010033.

Canton, J., Neculai, D. and Grinstein, S. (2013) Scavenger receptors in homeostasis and immunity. *Nature Reviews Immunology*, 13 (9): 621–634. doi:10.1038/nri3515.

Casadevall, A. (2008) Evolution of Intracellular Pathogens. *Annual Review of Microbiology*, 62 (1): 19–33. doi:10.1146/annurev.micro.61.080706.093305.

Casadevall, A., Fu, M.S., Guimaraes, A.J., et al. (2019) The 'Amoeboid Predator-Fungal Animal Virulence' Hypothesis. *Journal of Fungi*, 5 (1): 10. doi:10.3390/jof5010010.

Casadevall, A. and Pirofski, L. (2007) Accidental Virulence, Cryptic Pathogenesis, Martians, Lost Hosts, and the Pathogenicity of Environmental Microbes. *Eukaryotic Cell*, 6 (12): 2169–2174. doi:10.1128/ec.00308-07.

Casadevall, A., Rosas, A.L. and Nosanchuk, J.D. (2000) Melanin and virulence in Cryptococcus neoformans. *Current Opinion in Microbiology*, 3 (4): 354–358. doi:10.1016/S1369-5274(00)00103-X.

Chaka, W., Verheul, A.F., Vaishnav, V.V., et al. (1997) Induction of TNF-alpha in human peripheral blood mononuclear cells by the mannoprotein of Cryptococcus neoformans involves human mannose binding protein. *The Journal of Immunology*, 159 (6): 2979–2985.

Champion, J.A., Walker, A. and Mitragotri, S. (2008) Role of Particle Size in Phagocytosis of Polymeric Microspheres. *Pharmaceutical Research*, 25 (8): 1815–1821. doi:10.1007/s11095-008-9562-y.

Chang, Y.C., Stins, M.F., McCaffery, M.J., et al. (2004) Cryptococcal Yeast Cells Invade the Central Nervous System via Transcellular Penetration of the Blood-Brain Barrier. *Infection and Immunity*, 72 (9): 4985–4995. doi:10.1128/IAI.72.9.4985-4995.2004.

Chanput, W., Mes, J.J. and Wichers, H.J. (2014) THP-1 cell line: An in vitro cell model for immune modulation approach. *International Immunopharmacology*, 23 (1): 37–45. doi:10.1016/j.intimp.2014.08.002.

Charlier, C., Nielsen, K., Daou, S., et al. (2009) Evidence of a Role for Monocytes in Dissemination and Brain Invasion by Cryptococcus neoformans. *Infection and Immunity*, 77 (1): 120–127. doi:10.1128/IAI.01065-08.

Chayakulkeeree, M., Johnston, S.A., Oei, J.B., et al. (2011) SEC14 is a specific requirement for secretion of phospholipase B1 and pathogenicity of Cryptococcus neoformans. *Molecular Microbiology*, 80 (4): 1088–1101. doi:10.1111/j.1365-2958.2011.07632.x.

Chen, J., Ryu, S., Gharib, S.A., et al. (2008) Exploration of the normal human bronchoalveolar lavage fluid proteome. *Proteomics. Clinical applications*, 2 (4): 585–595. doi:10.1002/prca.200780006.

Chen, S.C., Wright, L.C., Santangelo, R.T., et al. (1997a) Identification of extracellular phospholipase B, lysophospholipase, and acyltransferase produced by Cryptococcus neoformans. *Infection and Immunity*, 65 (2): 405–411. doi:10.1128/iai.65.2.405-411.1997.

Chen, S.C.A., Muller, M., Zhou, J.Z., et al. (1997b) Phospholipase Activity in Cryptococcus neoformans: A New Virulence Factor? *The Journal of Infectious Diseases*, 175 (2): 414–420. doi:10.1093/infdis/175.2.414.

Chigaleĭchik, A.G., Belova, L.A., Grishchenko, V.M., et al. (1977) [Several properties of the extracellular vesicles of Candida tropicalis yeasts grown on n-alkanes]. *Mikrobiologiia*, 46 (3): 467–471.

Chikaura, H., Nakashima, Y., Fujiwara, Y., et al. (2016) Effect of particle size on biological response by human monocyte-derived macrophages. *Biosurface and Biotribology*, 2 (1): 18–25. doi:10.1016/j.bsbt.2016.02.003.

Choi, S.-H., Harkewicz, R., Lee, J.H., et al. (2009) Lipoprotein accumulation in macrophages via TLR4-dependent fluid phase uptake. *Circulation research*, 104 (12): 1355–1363. doi:10.1161/CIRCRESAHA.108.192880.

Chow, J.C., Young, D.W., Golenbock, D.T., et al. (1999) Toll-like Receptor-4 Mediates Lipopolysaccharide-induced Signal Transduction. *Journal of Biological Chemistry*, 274 (16): 10689–10692. doi:10.1074/jbc.274.16.10689.

Chrisman, C.J., Albuquerque, P., Guimaraes, A.J., et al. (2011) Phospholipids Trigger Cryptococcus neoformans Capsular Enlargement during Interactions with Amoebae and Macrophages. *PLOS Pathogens*, 7 (5): e1002047. doi:10.1371/journal.ppat.1002047.

Chrisman, C.J., Alvarez, M. and Casadevall, A. (2010) Phagocytosis of Cryptococcus neoformans by, and Nonlytic Exocytosis from, Acanthamoeba castellanii. *Applied and Environmental Microbiology*, 76 (18): 6056–6062. doi:10.1128/AEM.00812-10.

Coelho, C., Bocca, A.L. and Casadevall, A. (2014) The Intracellular Life of Cryptococcus neoformans. *Annual Review of Pathology: Mechanisms of Disease*, 9 (1): 219–238. doi:10.1146/annurev-pathol-012513-104653.

Cole, F.S., Matthews, W.J., Rossing, T.H., et al. (1983) Complement biosynthesis by human bronchoalveolar macrophages. *Clinical Immunology and Immunopathology*, 27 (2): 153–159. doi:10.1016/0090-1229(83)90065-x.

Collins, H.L. and Bancroft, G.J. (1992) Cytokine enhancement of complement-dependent phagocytosis by macrophages: synergy of tumor necrosis factor-α and granulocyte-macrophage colony-stimulating factor for phagocytosis ofCryptococcus neoformans. *European Journal of Immunology*, 22 (6): 1447–1454. doi:10.1002/eji.1830220617.

Coonrod, J.D. (1981) Pulmonary opsonins in Klebsiella pneumoniae pneumonia in rats. *Infection and Immunity*, 33 (2): 533–539.

Costa Verdera, H., Gitz-Francois, J.J., Schiffelers, R.M., et al. (2017) Cellular uptake of extracellular vesicles is mediated by clathrin-independent endocytosis and macropinocytosis. *Journal of Controlled Release*, 266: 100–108. doi:10.1016/j.jconrel.2017.09.019.

Cox, G.M., McDade, H.C., Chen, S.C.A., et al. (2001) Extracellular phospholipase activity is a virulence factor for Cryptococcus neoformans. *Molecular Microbiology*, 39 (1): 166–175. doi:10.1046/j.1365-2958.2001.02236.x.

Cox, G.M., Mukherjee, J., Cole, G.T., et al. (2000) Urease as a Virulence Factor in Experimental Cryptococcosis. *Infection and Immunity*, 68 (2): 443–448. doi:10.1128/IAI.68.2.443-448.2000.

Crabtree, J.N., Okagaki, L.H., Wiesner, D.L., et al. (2012) Titan Cell Production Enhances the Virulence of Cryptococcus neoformans. *Infection and Immunity*, 80 (11): 3776–3785. doi:10.1128/IAI.00507-12.

Cross, C.E. and Bancroft, G.J. (1995) Ingestion of acapsular Cryptococcus neoformans occurs via mannose and beta-glucan receptors, resulting in cytokine production and increased phagocytosis of the encapsulated form. *Infection and Immunity*, 63 (7): 2604–2611.

Cross, C.E., Collins, H.L. and Bancroft, G.J. (1997) CR3-dependent phagocytosis by murine macrophages: different cytokines regulate ingestion of a defined CR3 ligand and complement-opsonized *Cryptococcus neoformans*. *Immunology*, 91 (2): 289–296. doi:10.1046/j.1365-2567.1997.00238.x.

Cui, W., Li, X., Hull, L., et al. (2019) GATA-type transcription factors play a vital role in radiation sensitivity of Cryptococcus neoformans by regulating the gene expression of specific amino acid permeases. *Scientific Reports*, 9: 6385. doi:10.1038/s41598-019-42778-7.

Cunha, C. and Carvalho, A. (2018) Host Genetics Takes a Toll on Immunity to Cryptococcus. *EBioMedicine*, 37: 9–10. doi:10.1016/j.ebiom.2018.10.064.

Cuomo, C.A., Rhodes, J. and Desjardins, C.A. (2018) Advances in Cryptococcus genomics: insights into the evolution of pathogenesis. *Memórias do Instituto Oswaldo Cruz*, 113 (7): e170473. doi:10.1590/0074-02760170473.

Dan, J.M., Kelly, R.M., Lee, C.K., et al. (2008) Role of the Mannose Receptor in a Murine Model of Cryptococcus neoformans Infection. *Infection and Immunity*, 76 (6): 2362–2367. doi:10.1128/IAI.00095-08.

Dang, E.V., Lei, S., Radkov, A., et al. (2022) Secreted fungal virulence effector triggers allergic inflammation via TLR4. *Nature*, 608 (7921): 161–167. doi:10.1038/s41586-022-05005-4.

Davies, J., Turner, M. and Klein, N. (2001) The role of the collectin system in pulmonary defence. *Paediatric Respiratory Reviews*, 2 (1): 70–75. doi:10.1053/prrv.2000.0104.

Davis, M.J., Eastman, A.J., Qiu, Y., et al. (2015) Cryptococcus neoformans-induced macrophage lysosome damage crucially contributes to fungal virulence. *Journal of immunology (Baltimore, Md. : 1950)*, 194 (5): 2219–2231. doi:10.4049/jimmunol.1402376.

Dennehy, K.M., Ferwerda, G., Faro-Trindade, I., et al. (2008) Syk kinase is required for collaborative cytokine production induced through Dectin-1 and Toll-like receptors. *European Journal of Immunology*, 38 (2): 500–506. doi:10.1002/eji.200737741.

Derengowski, L. da S., Paes, H.C., Albuquerque, P., et al. (2013) The Transcriptional Response of Cryptococcus neoformans to Ingestion by Acanthamoeba castellanii and Macrophages Provides Insights into the Evolutionary Adaptation to the Mammalian Host. *Eukaryotic Cell*, 12 (5): 761–774. doi:10.1128/EC.00073-13.

Deshaw, M. and Pirofski, L.A. (1995) Antibodies to the Cryptococcus neoformans capsular glucuronoxylomannan are ubiquitous in serum from HIV+ and HIV- individuals. *Clinical and Experimental Immunology*, 99 (3): 425–432. doi:10.1111/j.1365-2249.1995.tb05568.x.

Desjardins, C.A., Giamberardino, C., Sykes, S.M., et al. (2017) Population genomics and the evolution of virulence in the fungal pathogen Cryptococcus neoformans. *Genome Research*, 27 (7): 1207–1219. doi:10.1101/gr.218727.116.

DeWitte-Orr, S.J., Collins, S.E., Bauer, C.M.T., et al. (2010) An Accessory to the 'Trinity': SR-As Are Essential Pathogen Sensors of Extracellular dsRNA, Mediating Entry and Leading to Subsequent Type I IFN Responses. *PLoS Pathogens*, 6 (3): e1000829. doi:10.1371/journal.ppat.1000829.

Diamond, R.D., May, J.E., Kane, M., et al. (1973) The role of late complement components and the alternate complement pathway in experimental cryptococcosis. *Proceedings of the Society for Experimental Biology and Medicine*, 144 (1): 312–315. doi:10.3181/00379727-144-37580.

Diamond, R.D., May, J.E., Kane, M.A., et al. (1974) The Role of the Classical and Alternate Complement Pathways in Host Defenses Against Cryptococcus Neoformans Infection. *The Journal of Immunology*, 112 (6): 2260–2270.

Diamond, R.D., Root, R.K. and Bennett, J.E. (1972) Factors Influencing Killing of Cryptococcus neoformans by Human Leukocytes In Vitro. *The Journal of Infectious Diseases*, 125 (4): 367–376. doi:10.1093/infdis/125.4.367.

Dieudonné, A., Torres, D., Blanchard, S., et al. (2012) Scavenger Receptors in Human Airway Epithelial Cells: Role in Response to Double-Stranded RNA. *PLOS ONE*, 7 (8): e41952. doi:10.1371/journal.pone.0041952.

Doering, T.L., Nosanchuk, J.D., Roberts, W.K., et al. (1999) Melanin as a potential cryptococcal defence against microbicidal proteins. *Medical Mycology*, 37 (3): 175–181.

Doyle, S.E., O'Connell, R.M., Miranda, G.A., et al. (2004) Toll-like Receptors Induce a Phagocytic Gene Program through p38. *The Journal of Experimental Medicine*, 199 (1): 81–90. doi:10.1084/jem.20031237.

Driemeyer, C., Falci, D.R., Oladele, R.O., et al. (2022) The current state of clinical mycology in Africa: a European Confederation of Medical Mycology and International Society for Human and Animal Mycology survey. *The Lancet Microbe*, 0 (0). doi:10.1016/S2666-5247(21)00190-7.

Dromer, F., Charreire, J., Contrepois, A., et al. (1987) Protection of mice against experimental cryptococcosis by anti-Cryptococcus neoformans monoclonal antibody. *Infection and Immunity*, 55 (3): 749–752.

Duin, D. van, Casadevall, A. and Nosanchuk, J.D. (2002) Melanization of Cryptococcus neoformans and Histoplasma capsulatum Reduces Their Susceptibilities to Amphotericin B and Caspofungin. *Antimicrobial Agents and Chemotherapy*, 46 (11): 3394–3400. doi:10.1128/AAC.46.11.3394-3400.2002.

den Dunnen, J., Vogelpoel, L.T.C., Wypych, T., et al. (2012) IgG opsonization of bacteria promotes Th17 responses via synergy between TLRs and FcγRIIa in human dendritic cells. *Blood*, 120 (1): 112–121. doi:10.1182/blood-2011-12-399931.

Eaton, A.F., Merkulova, M. and Brown, D. (2021) The H+-ATPase (V-ATPase): from proton pump to signaling complex in health and disease. *American Journal of Physiology - Cell Physiology*, 320 (3): C392–C414. doi:10.1152/ajpcell.00442.2020.

Edwards, L., Williams, A.E., Krieg, A.M., et al. (2005) Stimulation via Toll-like receptor 9 reduces Cryptococcus neoformans-induced pulmonary inflammation in an IL-12-dependent manner. *European Journal of Immunology*, 35 (1): 273–281. doi:10.1002/eji.200425640.

Elomaa, O., Sankala, M., Pikkarainen, T., et al. (1998) Structure of the Human Macrophage MARCO Receptor and Characterization of Its Bacteria-binding Region*. *Journal of Biological Chemistry*, 273 (8): 4530–4538. doi:10.1074/jbc.273.8.4530.

Escrevente, C., Keller, S., Altevogt, P., et al. (2011) Interaction and uptake of exosomes by ovarian cancer cells. *BMC Cancer*, 11 (1): 108. doi:10.1186/1471-2407-11-108.

Esher, S.K., Zaragoza, O. and Alspaugh, J.A. (2018) Cryptococcal pathogenic mechanisms: a dangerous trip from the environment to the brain. *Memórias do Instituto Oswaldo Cruz*, 113 (7): e180057. doi:10.1590/0074-02760180057.

Evans, R.J., Li, Z., Hughes, W.S., et al. (2015) Cryptococcal phospholipase B1 is required for intracellular proliferation and control of titan cell morphology during macrophage infection. *Infection and Immunity*, 83 (4): 1296–1304. doi:10.1128/IAI.03104-14.

Ezekowitz, R.A.B., Williams, D.J., Koziel, H., et al. (1991) Uptake of Pneumocystis carinii mediated by the macrophage mannose receptor. *Nature*, 351 (6322): 155–158. doi:10.1038/351155a0.

Farhi, F., Bulmer, G.S. and Tacker, J.R. (1970) Cryptococcus neoformans IV. The Not-So-Encapsulated Yeast. *Infection and Immunity*, 1 (6): 526–531. doi:10.1128/iai.1.6.526-531.1970.

Fejer, G., Wegner, M.D., Györy, I., et al. (2013) Nontransformed, GM-CSF–dependent macrophage lines are a unique model to study tissue macrophage functions.

Proceedings of the National Academy of Sciences of the United States of America, 110 (24): E2191–E2198. doi:10.1073/pnas.1302877110.

Feng, D., Zhao, W.-L., Ye, Y.-Y., et al. (2010) Cellular internalization of exosomes occurs through phagocytosis. *Traffic*, 11 (5): 675–687. doi:10.1111/j.1600-0854.2010.01041.x.

Ferwerda, G., Meyer-Wentrup, F., Kullberg, B.-J., et al. (2008) Dectin-1 synergizes with TLR2 and TLR4 for cytokine production in human primary monocytes and macrophages. *Cellular Microbiology*, 10 (10): 2058–2066. doi:10.1111/j.1462-5822.2008.01188.x.

Fidler, K.J., Hilliard, T.N., Bush, A., et al. (2009) Mannose-binding lectin is present in the infected airway: a possible pulmonary defence mechanism. *Thorax*, 64 (2): 150–155. doi:10.1136/thx.2008.100073.

Fitzner, D., Schnaars, M., van Rossum, D., et al. (2011) Selective transfer of exosomes from oligodendrocytes to microglia by macropinocytosis. *Journal of Cell Science*, 124 (3): 447–458. doi:10.1242/jcs.074088.

Fleuridor, R., Zhong, Z. and Pirofski, L. (1998) A human IgM monoclonal antibody prolongs survival of mice with lethal cryptococcosis. *The Journal of Infectious Diseases*, 178 (4): 1213–1216. doi:10.1086/515688.

Floto, R.A., Clatworthy, M.R., Heilbronn, K.R., et al. (2005) Loss of function of a lupus-associated FcγRIIb polymorphism through exclusion from lipid rafts. *Nature Medicine*, 11 (10): 1056–1058. doi:10.1038/nm1288.

Fonseca, F.L., Nohara, L.L., Cordero, R.J.B., et al. (2010) Immunomodulatory Effects of Serotype B Glucuronoxylomannan from Cryptococcus gattii Correlate with Polysaccharide Diameter. *Infection and Immunity*, 78 (9): 3861–3870. doi:10.1128/IAI.00111-10.

Freeman, S.A. and Grinstein, S. (2014) Phagocytosis: receptors, signal integration, and the cytoskeleton. *Immunological Reviews*, 262 (1): 193–215. doi:10.1111/imr.12212.

Fu, M.S., Coelho, C., De Leon-Rodriguez, C.M., et al. (2018) Cryptococcus neoformans urease affects the outcome of intracellular pathogenesis by modulating phagolysosomal pH May, R.C. (ed.). *PLOS Pathogens*, 14 (6): e1007144. doi:10.1371/journal.ppat.1007144.

Fu, M.S., Liporagi-Lopes, L.C., dos Santos, S.R., et al. (2021) Amoeba Predation of Cryptococcus neoformans Results in Pleiotropic Changes to Traits Associated with Virulence. *mBio*, 12 (2): e00567-21. doi:10.1128/mBio.00567-21.

Fu, Y.L. and Harrison, R.E. (2021) Microbial Phagocytic Receptors and Their Potential Involvement in Cytokine Induction in Macrophages. *Frontiers in Immunology*, 12. doi:10.3389/fimmu.2021.662063.

Fumagalli, M., Sironi, M., Pozzoli, U., et al. (2011) Signatures of environmental genetic adaptation pinpoint pathogens as the main selective pressure through human evolution. *PLoS genetics*, 7 (11): e1002355. doi:10.1371/journal.pgen.1002355.

Gabel, M. and Chasserot-Golaz, S. (2016) Annexin A2, an essential partner of the exocytotic process in chromaffin cells. *Journal of Neurochemistry*, 137 (6): 890–896. doi:10.1111/jnc.13628.

Galán, J.E. (2009) Common themes in the design and function of bacterial effectors. *Cell host & microbe*, 5 (6): 571–579. doi:10.1016/j.chom.2009.04.008.

Gantner, B.N., Simmons, R.M. and Underhill, D.M. (2005) Dectin-1 mediates macrophage recognition of Candida albicans yeast but not filaments. *The EMBO Journal*, 24 (6): 1277–1286. doi:10.1038/sj.emboj.7600594.

Gao, D., Ciancanelli, M.J., Zhang, P., et al. (2021) TLR3 controls constitutive IFN-β antiviral immunity in human fibroblasts and cortical neurons. *The Journal of Clinical Investigation*, 131 (1). doi:10.1172/JCI134529.

García-Barbazán, I., Trevijano-Contador, N., Rueda, C., et al. (2016) The formation of titan cells in Cryptococcus neoformans depends on the mouse strain and correlates with induction of Th2-type responses. *Cellular Microbiology*, 18 (1): 111–124. doi:10.1111/cmi.12488.

Garelnabi, M. and May, R.C. (2018) Variability in innate host immune responses to cryptococcosis. *Memórias do Instituto Oswaldo Cruz*, 113 (7). doi:10.1590/0074-02760180060.

Garelnabi, M., Taylor-Smith, L.M., Bielska, E., et al. (2018) Quantifying donor-to-donor variation in macrophage responses to the human fungal pathogen Cryptococcus neoformans Nielsen, K. (ed.). *PLOS ONE*, 13 (3): e0194615. doi:10.1371/journal.pone.0194615.

Gay, N.J., Symmons, M.F., Gangloff, M., et al. (2014) Assembly and localization of Toll-like receptor signalling complexes. *Nature Reviews Immunology*, 14 (8): 546–558. doi:10.1038/nri3713.

Gaynor, C.D., McCormack, F.X., Voelker, D.R., et al. (1995) Pulmonary surfactant protein A mediates enhanced phagocytosis of Mycobacterium tuberculosis by a direct interaction with human macrophages. *Journal of Immunology*, 155 (11): 5343–5351.

George, I.A., Spec, A., Powderly, W.G., et al. (2018) Comparative Epidemiology and Outcomes of Human Immunodeficiency virus (HIV), Non-HIV Non-transplant, and Solid Organ Transplant Associated Cryptococcosis: A Population-Based Study. *Clinical Infectious Diseases*, 66 (4): 608–611. doi:10.1093/cid/cix867.

Gerstein, A.C., Jackson, K.M., McDonald, T.R., et al. (2019) Identification of Pathogen Genomic Differences That Impact Human Immune Response and Disease during Cryptococcus neoformans Infection. *mBio*, 10 (4): e01440-19. doi:10.1128/mBio.01440-19.

Getahun, A. and Cambier, J.C. (2015) Of ITIMs, ITAMs and ITAMis, revisiting Immunoglobulin Fc Receptor signaling. *Immunological reviews*, 268 (1): 66–73. doi:10.1111/imr.12336.

Geunes-Boyer, S., Beers, M.F., Perfect, J.R., et al. (2012) Surfactant Protein D Facilitates Cryptococcus neoformans Infection. *Infection and Immunity*, 80 (7): 2444–2453. doi:10.1128/IAI.05613-11.

Geunes-Boyer, S., Oliver, T.N., Janbon, G., et al. (2009) Surfactant Protein D Increases Phagocytosis of Hypocapsular Cryptococcus neoformans by Murine Macrophages and Enhances Fungal Survival. *Infection and Immunity*, 77 (7): 2783–2794. doi:10.1128/IAI.00088-09.

Giannoni, E., Sawa, T., Allen, L., et al. (2006) Surfactant Proteins A and D Enhance Pulmonary Clearance of Pseudomonas aeruginosa. *American Journal of Respiratory Cell and Molecular Biology*, 34 (6): 704–710. doi:10.1165/rcmb.2005-0461OC.

Gibson, R.K. and Peberdy, J.F. (1972) Fine Structure of Protoplasts of Aspergillus nidulans. *Microbiology*, 72 (3): 529–538. doi:10.1099/00221287-72-3-529.

Gilbert, A.S., Seoane, P.I., Sephton-Clark, P., et al. (2017) Vomocytosis of live pathogens from macrophages is regulated by the atypical MAP kinase ERK5. *Science Advances*, 3 (8): e1700898. doi:10.1126/sciadv.1700898.

Giles, S.S., Zaas, A.K., Reidy, M.F., et al. (2007) Cryptococcus neoformans Is Resistant to Surfactant Protein A Mediated Host Defense Mechanisms. *PLOS ONE*, 2 (12): e1370. doi:10.1371/journal.pone.0001370.

Goldman, D.L., Khine, H., Abadi, J., et al. (2001) Serologic Evidence for Cryptococcus neoformansInfection in Early Childhood. *Pediatrics*, 107 (5): e66. doi:10.1542/peds.107.5.e66.

Goupil de Bouillé, J., Epelboin, L., Henaff, F., et al. (2022) Case Report: Invasive Cryptococcosis in French Guiana: Immune and Genetic Investigation in Six Non-HIV Patients. *Frontiers in Immunology*, 13: 881352. doi:10.3389/fimmu.2022.881352.

Granucci, F., Petralia, F., Urbano, M., et al. (2003) The scavenger receptor MARCO mediates cytoskeleton rearrangements in dendritic cells and microglia. *Blood*, 102 (8): 2940–2947. doi:10.1182/blood-2002-12-3651.

Gratacap, R.L., Rawls, J.F. and Wheeler, R.T. (2013) Mucosal candidiasis elicits NF-κB activation, proinflammatory gene expression and localized neutrophilia in zebrafish. *Disease Models & Mechanisms*, 6 (5): 1260–1270. doi:10.1242/dmm.012039.

Guerra, C.R., Seabra, S.H., Souza, W. de, et al. (2014) Cryptococcus neoformans Is Internalized by Receptor-Mediated or 'Triggered' Phagocytosis, Dependent on Actin Recruitment. *PLOS ONE*, 9 (2): e89250. doi:10.1371/journal.pone.0089250.

Guo, M., Härtlova, A., Gierliński, M., et al. (2019) Triggering MSR1 promotes JNK-mediated inflammation in IL-4-activated macrophages. *The EMBO Journal*, 38 (11): e100299. doi:10.15252/embj.2018100299.

Haagsman, H.P., Hawgood, S., Sargeant, T., et al. (1987) The major lung surfactant protein, SP 28-36, is a calcium-dependent, carbohydrate-binding protein. *Journal of Biological Chemistry*, 262 (29): 13877–13880. doi:10.1016/S0021-9258(18)47873-8.

Häcker, H., Redecke, V., Blagoev, B., et al. (2006) Specificity in Toll-like receptor signalling through distinct effector functions of TRAF3 and TRAF6. *Nature*, 439 (7073): 204–207. doi:10.1038/nature04369.

Hageage, G. and Harrington, B. (1984) *Use of Calcofluor White in Clinical Mycology*. doi:10.1093/LABMED/15.2.109.

Hagedorn, M., Rohde, K.H., Russell, D.G., et al. (2009) Infection by Tubercular Mycobacteria Is Spread by Nonlytic Ejection from Their Amoeba Hosts. *Science*, 323 (5922): 1729–1733. doi:10.1126/science.1169381.

Hai, T.P., Tuan, T.L., Anh, D.V., et al. (2020) The virulence of the Cryptococcus neoformans VNIa-5 lineage is highly plastic and associated with isolate background. *bioRxiv*. doi:10.1101/2020.02.24.962134.

Hamed, M.F., Araújo, G.R. de S., Munzen, M.E., et al. (2023) Phospholipase B Is Critical for Cryptococcus neoformans Survival in the Central Nervous System. *mBio*, pp. e02640-22. doi:10.1128/mbio.02640-22.

Hansakon, A., Jeerawattanawart, S., Pattanapanyasat, K., et al. (2020) IL-25 Receptor Signaling Modulates Host Defense against Cryptococcus neoformans Infection. *The Journal of Immunology*, 205 (3): 674–685. doi:10.4049/jimmunol.2000073.

Hansakon, A., Mutthakalin, P., Ngamskulrungroj, P., et al. (2018) Cryptococcus neoformans and Cryptococcus gattii clinical isolates from Thailand display diverse phenotypic interactions with macrophages. *Virulence*, 10 (1): 26–36. doi:10.1080/21505594.2018.1556150.

Hargreaves, C.E., Rose-Zerilli, M.J.J., Machado, L.R., et al. (2015) Fcγ receptors: genetic variation, function, and disease. *Immunological Reviews*, 268 (1): 6–24. doi:10.1111/imr.12341.

Harris, J., Hartman, M., Roche, C., et al. (2011) Autophagy Controls IL-1β Secretion by Targeting Pro-IL-1β for Degradation. *The Journal of Biological Chemistry*, 286 (11): 9587–9597. doi:10.1074/jbc.M110.202911.

Harrison, T.S., Griffin, G.E. and Levitz, S.M. (2000) Conditional Lethality of the Diprotic Weak Bases Chloroquine and Quinacrine against Cryptococcus neoformans. *The Journal of Infectious Diseases*, 182 (1): 283–289. doi:10.1086/315649.

Hashimoto, R., Kakigi, R., Miyamoto, Y., et al. (2020) JAK-STAT-dependent regulation of scavenger receptors in LPS-activated murine macrophages. *European Journal of Pharmacology*, 871: 172940. doi:10.1016/j.ejphar.2020.172940.

Hashimoto, R., Kakigi, R., Nakamura, K., et al. (2017) LPS enhances expression of CD204 through the MAPK/ERK pathway in murine bone marrow macrophages. *Atherosclerosis*, 266: 167–175. doi:10.1016/j.atherosclerosis.2017.10.005.

Hayes, M.J., Shao, D., Bailly, M., et al. (2006) Regulation of actin dynamics by annexin 2. *The EMBO Journal*, 25 (9): 1816–1826. doi:10.1038/sj.emboj.7601078.

Heit, B., Kim, H., Cosío, G., et al. (2013) Multimolecular Signaling Complexes Enable Syk-Mediated Signaling of CD36 Internalization. *Developmental Cell*, 24 (4): 372–383. doi:10.1016/j.devcel.2013.01.007.

Heung, L.J. (2017) Innate Immune Responses to Cryptococcus. *Journal of Fungi*, 3 (3). doi:10.3390/jof3030035.

Hidore, M.R., Nabavi, N., Sonleitner, F., et al. (1991) Murine natural killer cells are fungicidal to Cryptococcus neoformans. *Infection and Immunity*, 59 (5): 1747–1754. doi:10.1128/iai.59.5.1747-1754.1991.

Hoepel, W., Newling, M., Vogelpoel, L.T.C., et al. (2019) FcγR-TLR Cross-Talk Enhances TNF Production by Human Monocyte-Derived DCs via IRF5-Dependent Gene Transcription and Glycolytic Reprogramming. *Frontiers in Immunology*, 10: 739. doi:10.3389/fimmu.2019.00739.

Holcomb, Z.E., Steinbrink, J.M., Zaas, A.K., et al. (2022) Transcriptional Profiles Elucidate Differential Host Responses to Infection with Cryptococcus neoformans and Cryptococcus gattii. *Journal of Fungi*, 8 (5): 430. doi:10.3390/jof8050430.

Hole, C.R., Bui, H., Wormley, F.L., et al. (2012) Mechanisms of Dendritic Cell Lysosomal Killing of Cryptococcus. *Scientific Reports*, 2 (1): 739. doi:10.1038/srep00739.

Hu, W., Zhang, Y., Sun, X., et al. (2019) FcγRIIB-I232T polymorphic change allosterically suppresses ligand binding Taniguchi, T., Kurosaki, T., Takai, T., et al. (eds.). *eLife*, 8: e46689. doi:10.7554/eLife.46689.

Hu, X.-P., Wu, J.-Q., Zhu, L.-P., et al. (2012) Association of Fcγ Receptor IIB Polymorphism with Cryptococcal Meningitis in HIV-Uninfected Chinese Patients. *PLOS ONE*, 7 (8): e42439. doi:10.1371/journal.pone.0042439.

Huang, H.-R., Li, F., Han, H., et al. (2018) Dectin-3 Recognizes Glucuronoxylomannan of Cryptococcus neoformans Serotype AD and Cryptococcus gattii Serotype B to Initiate Host Defense Against Cryptococcosis. *Frontiers in Immunology*, 9. doi:10.3389/fimmu.2018.01781.

Huang, S.-H., Wu, C.-H., Chang, Y.C., et al. (2012) Cryptococcus neoformans-Derived Microvesicles Enhance the Pathogenesis of Fungal Brain Infection. *PLOS ONE*, 7 (11): e48570. doi:10.1371/journal.pone.0048570.

Huffnagle, G.B., Boyd, M.B., Street, N.E., et al. (1998) IL-5 Is Required for Eosinophil Recruitment, Crystal Deposition, and Mononuclear Cell Recruitment During a Pulmonary Cryptococcus neoformans Infection in Genetically Susceptible Mice (C57BL/6). *The Journal of Immunology*, 160 (5): 2393–2400.

Hünniger, K. and Kurzai, O. (2019) Phagocytes as central players in the defence against invasive fungal infection. *Seminars in Cell & Developmental Biology*, 89: 3–15. doi:10.1016/j.semcdb.2018.03.021.

Ikeda, R., Sugita, T., Jacobson, E.S., et al. (2003) Effects of Melanin upon Susceptibility of Cryptococcus to Antifungals. *Microbiology and Immunology*, 47 (4): 271–277. doi:10.1111/j.1348-0421.2003.tb03395.x.

van Iwaarden, J.F., van Strijp, J.A., Ebskamp, M.J., et al. (1991) Surfactant protein A is opsonin in phagocytosis of herpes simplex virus type 1 by rat alveolar macrophages. *American Journal of Physiology-Lung Cellular and Molecular Physiology*, 261 (2): L204–L209. doi:10.1152/ajplung.1991.261.2.L204.

Jain, A.V., Zhang, Y., Fields, W.B., et al. (2009) Th2 but not Th1 immune bias results in altered lung functions in a murine model of pulmonary Cryptococcus neoformans infection. *Infection and Immunity*, 77 (12): 5389–5399. doi:10.1128/IAI.00809-09.

Jambo, K.C., French, N., Zijlstra, E., et al. (2007) AIDS patients have increased surfactant protein D but normal mannose binding lectin levels in lung fluid. *Respiratory Research*, 8 (1): 42. doi:10.1186/1465-9921-8-42.

Janda, A., Eryilmaz, E., Nakouzi, A., et al. (2015) Variable Region Identical IgA and IgE to Cryptococcus neoformans Capsular Polysaccharide Manifest Specificity Differences. *The Journal of Biological Chemistry*, 290 (19): 12090–12100. doi:10.1074/jbc.M114.618975.

Jarvis, J.N., Bicanic, T., Loyse, A., et al. (2014) Determinants of Mortality in a Combined Cohort of 501 Patients With HIV-Associated Cryptococcal Meningitis: Implications for Improving Outcomes. *Clinical Infectious Diseases*, 58 (5): 736–745. doi:10.1093/cid/cit794.

Jiang, Y.-K., Wu, J.-Q., Zhao, H.-Z., et al. (2018) Genetic influence of Toll-like receptors on non-HIV cryptococcal meningitis: An observational cohort study. *EBioMedicine*, 37: 401–409. doi:10.1016/j.ebiom.2018.10.045.

Jing, J., Yang, I.V., Hui, L., et al. (2013) Role of MARCO in Innate Immune Tolerance. *Journal of immunology (Baltimore, Md. : 1950)*, 190 (12): 6360–6367. doi:10.4049/jimmunol.1202942.

Johnston, S.A. and May, R.C. (2010) The Human Fungal Pathogen Cryptococcus neoformans Escapes Macrophages by a Phagosome Emptying Mechanism That Is Inhibited by Arp2/3 Complex-Mediated Actin Polymerisation. *PLOS Pathogens*, 6 (8): e1001041. doi:10.1371/journal.ppat.1001041.

Johnston, S.A. and May, R.C. (2013) Cryptococcus interactions with macrophages: evasion and manipulation of the phagosome by a fungal pathogen. *Cellular Microbiology*, 15 (3): 403–411. doi:10.1111/cmi.12067.

Jong, A., Wu, C.-H., Shackleford, G.M., et al. (2008) Involvement of human CD44 during Cryptococcus neoformans infection of brain microvascular endothelial cells. *Cellular Microbiology*, 10 (6): 1313–1326. doi:10.1111/j.1462-5822.2008.01128.x.

Jung, K.-W., Yang, D.-H., Maeng, S., et al. (2015) Systematic functional profiling of transcription factor networks in Cryptococcus neoformans. *Nature Communications*, 6 (1): 6757. doi:10.1038/ncomms7757.

Kagan, J.C., Su, T., Horng, T., et al. (2008) TRAM couples endocytosis of Toll-like receptor 4 to the induction of interferon-β. *Nature immunology*, 9 (4): 361–368. doi:10.1038/ni1569.

Kampmann, B., Hemingway, C., Stephens, A., et al. (2005) Acquired predisposition to mycobacterial disease due to autoantibodies to IFN-γ. *Journal of Clinical Investigation*, 115 (9): 2480–2488. doi:10.1172/JCI19316.

Kannambath, S., Jarvis, J.N., Wake, R.M., et al. (2020) Genome-Wide Association Study Identifies Novel Colony Stimulating Factor 1 Locus Conferring Susceptibility to Cryptococcosis in Human Immunodeficiency Virus-Infected South Africans. *Open Forum Infectious Diseases*, 7 (11): ofaa489. doi:10.1093/ofid/ofaa489.

Kanno, S., Furuyama, A. and Hirano, S. (2007) A Murine Scavenger Receptor MARCO Recognizes Polystyrene Nanoparticles. *Toxicological Sciences*, 97 (2): 398–406. doi:10.1093/toxsci/kfm050.

Kanno, S., Hirano, S., Sakamoto, T., et al. (2020) Scavenger receptor MARCO contributes to cellular internalization of exosomes by dynamin-dependent endocytosis and macropinocytosis. *Scientific Reports*, 10 (1): 21795. doi:10.1038/s41598-020-78464-2.

Karikó, K., Ni, H., Capodici, J., et al. (2004) mRNA Is an Endogenous Ligand for Toll-like Receptor 3 *. *Journal of Biological Chemistry*, 279 (13): 12542–12550. doi:10.1074/jbc.M310175200.

Kaufman-Francis, K., Djordjevic, J.T., Juillard, P.-G., et al. (2018) The Early Innate Immune Response to, and Phagocyte-Dependent Entry of, Cryptococcus neoformans Map to the Perivascular Space of Cortical Post-Capillary Venules in Neurocryptococcosis. *The American Journal of Pathology*, 188 (7): 1653–1665. doi:10.1016/j.ajpath.2018.03.015.

Kawai, T. and Akira, S. (2010) The role of pattern-recognition receptors in innate immunity: update on Toll-like receptors. *Nature Immunology*, 11 (5): 373–384. doi:10.1038/ni.1863.

Kawakami, K., Kohno, S., Kadota, J., et al. (1995) T Cell-Dependent Activation of Macrophages and Enhancement of Their Phagocytic Activity in the Lungs of Mice Inoculated with Heat-Killed Cryptococcus neoformans: Involvement of IFN-γ and Its Protective Effect against Cryptococcal Infection. *Microbiology and Immunology*, 39 (2): 135–143. doi:10.1111/j.1348-0421.1995.tb02180.x.

Kawasaki, T. and Kawai, T. (2014) Toll-Like Receptor Signaling Pathways. *Frontiers in Immunology*, 5. doi:10.3389/fimmu.2014.00461.

Kechichian, T.B., Shea, J. and Del Poeta, M. (2007) Depletion of Alveolar Macrophages Decreases the Dissemination of a Glucosylceramide-Deficient Mutant of Cryptococcus neoformans in Immunodeficient Mice. *Infection and Immunity*, 75 (10): 4792–4798. doi:10.1128/IAI.00587-07.

Khajo, A., Bryan, R.A., Friedman, M., et al. (2011) Protection of Melanized Cryptococcus neoformans from Lethal Dose Gamma Irradiation Involves Changes in Melanin's Chemical Structure and Paramagnetism. *PLOS ONE*, 6 (9): e25092. doi:10.1371/journal.pone.0025092.

Kim, J.-Y. and Bahn, Y.-S. (2022) Role of the Heme Activator Protein Complex in the Sexual Development of Cryptococcus neoformans. *mSphere*, 7 (3): e00170-22. doi:10.1128/msphere.00170-22.

Kinsella, C.M., Deijs, M., Gittelbauer, H.M., et al. (2022) Human Clinical Isolates of Pathogenic Fungi Are Host to Diverse Mycoviruses. *Microbiology Spectrum*, 10 (5): e01610-22. doi:10.1128/spectrum.01610-22.

Kissick, H.T., Dunn, L.K., Ghosh, S., et al. (2014) The Scavenger Receptor MARCO Modulates TLR-Induced Responses in Dendritic Cells. *PLoS ONE*, 9 (8): e104148. doi:10.1371/journal.pone.0104148.

Kitai, Y., Sato, K., Tanno, D., et al. (2021) Role of Dectin-2 in the phagocytosis of Cryptococcus neoformans by dendritic cells. *Infection and Immunity*. doi:10.1128/IAI.00330-21.

Kitamura, T., Tanaka, N., Watanabe, J., et al. (1999) Idiopathic Pulmonary Alveolar Proteinosis as an Autoimmune Disease with Neutralizing Antibody against Granulocyte/Macrophage Colony-Stimulating Factor. *The Journal of Experimental Medicine*, 190 (6): 875–880.

Kozel, T.R. and Gotschlich, E.C. (1982) The capsule of cryptococcus neoformans passively inhibits phagocytosis of the yeast by macrophages. *Journal of Immunology*, 129 (4): 1675–1680.

Kozel, T.R., Wilson, M.A. and Murphy, J.W. (1991) Early events in initiation of alternative complement pathway activation by the capsule of Cryptococcus neoformans. *Infection and Immunity*, 59 (9): 3101–3110.

Kraal, G., van der Laan, L.J.W., Elomaa, O., et al. (2000) The macrophage receptor MARCO. *Microbes and Infection*, 2 (3): 313–316. doi:10.1016/S1286-4579(00)00296-3.

Kwon-Chung, K.J., Boekhout, T., Wickes, B.L., et al. (2010) "Systematics of the Genus Cryptococcus and Its Type Species C. neoformans." In *Cryptococcus*. John Wiley & Sons, Ltd. pp. 1–15. doi:10.1128/9781555816858.ch1.

Kwon-Chung, K.J., Polacheck, I. and Popkin, T.J. (1982) Melanin-lacking mutants of Cryptococcus neoformans and their virulence for mice. *Journal of Bacteriology*, 150 (3): 1414–1421.

Kyogoku, C., Dijstelbloem, H.M., Tsuchiya, N., et al. (2002) Fcgamma receptor gene polymorphisms in Japanese patients with systemic lupus erythematosus: contribution of FCGR2B to genetic susceptibility. *Arthritis and Rheumatism*, 46 (5): 1242–1254. doi:10.1002/art.10257.

Latty, S.L., Sakai, J., Hopkins, L., et al. (2018) Activation of Toll-like receptors nucleates assembly of the MyDDosome signaling hub. *eLife*, 7: e31377. doi:10.7554/eLife.31377.

Lee, D., Jang, E.-H., Lee, M., et al. (2019) Unraveling Melanin Biosynthesis and Signaling Networks in Cryptococcus neoformans. *mBio*, 10 (5): e02267-19. doi:10.1128/mBio.02267-19.

Lennartz, M. and Drake, J. (2018) Molecular mechanisms of macrophage Toll-like receptor–Fc receptor synergy. *F1000Research*, 7 (21). doi:10.12688/f1000research.12679.1.

Leopold Wager, C.M., Hole, C.R., Wozniak, K.L., et al. (2015) STAT1 signaling within macrophages is required for antifungal activity against Cryptococcus neoformans. *Infection and Immunity*, 83 (12): 4513–4527. doi:10.1128/IAI.00935-15.

Leopold Wager, C.M., Hole, C.R., Wozniak, K.L., et al. (2016) Cryptococcus and Phagocytes: Complex Interactions that Influence Disease Outcome. *Frontiers in Microbiology*, 7: 105. doi:10.3389/fmicb.2016.00105.

LeVine, A.M., Elliott, J., Whitsett, J.A., et al. (2004) Surfactant Protein-D Enhances Phagocytosis and Pulmonary Clearance of Respiratory Syncytial Virus. *American Journal of Respiratory Cell and Molecular Biology*, 31 (2): 193–199. doi:10.1165/rcmb.2003-0107OC.

Levitz, S.M. and Tabuni, A. (1991) Binding of Cryptococcus neoformans by human cultured macrophages. Requirements for multiple complement receptors and actin. *Journal of Clinical Investigation*, 87 (2): 528–535.

Li, K. and Underhill, D.M. (2020) *C-Type Lectin Receptors in Phagocytosis*. In . Current Topics in Microbiology and Immunology. Berlin, Heidelberg: Springer. pp. 1–18. doi:10.1007/82_2020_198.

Li, S.S., Kyei, S.K., Timm-McCann, M., et al. (2013) The NK Receptor NKp30 Mediates Direct Fungal Recognition and Killing and Is Diminished in NK Cells from HIV-Infected Patients. *Cell Host & Microbe*, 14 (4): 387–397. doi:10.1016/j.chom.2013.09.007.

Li, W., Yan, J. and Yu, Y. (2019) Geometrical reorganization of Dectin-1 and TLR2 on single phagosomes alters their synergistic immune signaling. *Proceedings of the National Academy of Sciences*, 116 (50): 25106–25114. doi:10.1073/pnas.1909870116.

Li, X., Ptacek, T.S., Brown, E.E., et al. (2009) Fcγ Receptors: Structure, Function and Role as Genetic Risk Factors in SLE. *Genes and immunity*, 10 (5): 380–389. doi:10.1038/gene.2009.35.

Lim, J., Coates, C.J., Seoane, P.I., et al. (2018) Characterizing the Mechanisms of Nonopsonic Uptake of Cryptococci by Macrophages. *The Journal of Immunology Author Choice*, 200 (10): 3539–3546. doi:10.4049/jimmunol.1700790.

Limmon, G.V., Arredouani, M., McCann, K.L., et al. (2008) Scavenger receptor class-A is a novel cell surface receptor for double-stranded RNA. *FASEB journal: official publication of the Federation of American Societies for Experimental Biology*, 22 (1): 159–167. doi:10.1096/fj.07-8348com.

Litvack, M.L. and Palaniyar, N. (2010) Review: Soluble innate immune pattern-recognition proteins for clearing dying cells and cellular components: implications on exacerbating or resolving inflammation. *Innate Immunity*, 16 (3): 191–200. doi:10.1177/1753425910369271.

Litvintseva, A.P. and Mitchell, T.G. (2009) Most environmental isolates of Cryptococcus neoformans var. grubii (serotype A) are not lethal for mice. *Infection and Immunity*, 77 (8): 3188–3195. doi:10.1128/IAI.00296-09.

Liu, L., Tewari, R.P. and Williamson, P.R. (1999) Laccase Protects Cryptococcus neoformans from Antifungal Activity of Alveolar Macrophages. *Infection and Immunity*, 67 (11): 6034–6039.

Liu, O.W., Chun, C.D., Chow, E.D., et al. (2008) Systematic Genetic Analysis of Virulence in the Human Fungal Pathogen Cryptococcus neoformans. *Cell*, 135 (1): 174–188. doi:10.1016/j.cell.2008.07.046.

Liu, T., Zhang, L., Joo, D., et al. (2017) NF-κB signaling in inflammation. *Signal Transduction and Targeted Therapy*, 2 (1): 1–9. doi:10.1038/sigtrans.2017.23.

Love, G.L., Boyd, G.D. and Greer, D.L. (1985) Large Cryptococcus neoformans isolated from brain abscess. *Journal of Clinical Microbiology*, 22 (6): 1068–1070.

Loyse, A., Thangaraj, H., Easterbrook, P., et al. (2013) Cryptococcal meningitis: improving access to essential antifungal medicines in resource-poor countries. *The Lancet Infectious Diseases*, 13 (7): 629–637. doi:10.1016/S1473-3099(13)70078-1.

Ma, H., Croudace, J.E., Lammas, D.A., et al. (2006) Expulsion of Live Pathogenic Yeast by Macrophages. *Current Biology*, 16 (21): 2156–2160. doi:10.1016/j.cub.2006.09.032.

Ma, L.L., Wang, C.L.C., Neely, G.G., et al. (2004) NK Cells Use Perforin Rather than Granulysin for Anticryptococcal Activity. *The Journal of Immunology*, 173 (5): 3357–3365. doi:10.4049/jimmunol.173.5.3357.

Mada, P., Nowack, B., Cady, B., et al. (2017) Disseminated cryptococcosis in an immunocompetent patient. *Case Reports*, 2017. doi:10.1136/bcr-2016-218461.

Madan, T., Eggleton, P., Kishore, U., et al. (1997) Binding of pulmonary surfactant proteins A and D to Aspergillus fumigatus conidia enhances phagocytosis and killing by human neutrophils and alveolar macrophages. *Infection and Immunity*, 65 (8): 3171–3179. doi:10.1128/iai.65.8.3171-3179.1997.

Magditch, D.A., Liu, T.-B., Xue, C., et al. (2012) DNA Mutations Mediate Microevolution between Host-Adapted Forms of the Pathogenic Fungus Cryptococcus neoformans. *PLOS Pathogens*, 8 (10): e1002936. doi:10.1371/journal.ppat.1002936.

Maler, M.D., Nielsen, P.J., Stichling, N., et al. (2017) Key Role of the Scavenger Receptor MARCO in Mediating Adenovirus Infection and Subsequent Innate Responses of Macrophages. *mBio*, 8 (4): e00670-17. doi:10.1128/mBio.00670-17.

Malhotra, R., Haurum, J., Thiel, S., et al. (1993) Pollen grains bind to lung alveolar type II cells (A549) via lung surfactant protein A (SP-A). *Bioscience Reports*, 13 (2): 79–90. doi:10.1007/BF01145960.

Mantis, N.J., Rol, N. and Corthésy, B. (2011) Secretory IgA's complex roles in immunity and mucosal homeostasis in the gut. *Mucosal Immunology*, 4 (6): 603–611. doi:10.1038/mi.2011.41.

Martinez, F.O. and Gordon, S. (2014) The M1 and M2 paradigm of macrophage activation: time for reassessment. *F1000Prime Reports*, 6: 13. doi:10.12703/P6-13.

Maruvada, R., Zhu, L., Pearce, D., et al. (2012) Cryptococcus neoformans phospholipase B1 activates host cell Rac1 for traversal across the blood–brain barrier. *Cellular Microbiology*, 14 (10): 1544–1553. doi:10.1111/j.1462-5822.2012.01819.x.

May, R.C., Stone, N.R.H., Wiesner, D.L., et al. (2016) Cryptococcus: from environmental saprophyte to global pathogen. *Nature Reviews Microbiology*, 14 (2): 106–117. doi:10.1038/nrmicro.2015.6.

Maziarz, E.K. and Perfect, J.R. (2016) Cryptococcosis. *Infectious disease clinics of North America*, 30 (1): 179–206. doi:10.1016/j.idc.2015.10.006.

Mazzolla, R., Barluzzi, R., Brozzetti, A., et al. (1997) Enhanced resistance to Cryptococcus neoformans infection induced by chloroquine in a murine model of meningoencephalitis. *Antimicrobial Agents and Chemotherapy*, 41 (4): 802–807. doi:10.1128/AAC.41.4.802.

McClelland, E.E., Bernhardt, P. and Casadevall, A. (2006) Estimating the Relative Contributions of Virulence Factors for Pathogenic Microbes. *Infection and Immunity*, 74 (3): 1500–1504. doi:10.1128/IAI.74.3.1500-1504.2006.

Means, T.K., Mylonakis, E., Tampakakis, E., et al. (2009) Evolutionarily conserved recognition and innate immunity to fungal pathogens by the scavenger receptors SCARF1 and CD36. *The Journal of Experimental Medicine*, 206 (3): 637–653. doi:10.1084/jem.20082109.

Mei, K. and Guo, W. (2018) The exocyst complex. *Current Biology*, 28 (17): R922–R925. doi:10.1016/j.cub.2018.06.042.

Meldolesi, J. (2018) Exosomes and Ectosomes in Intercellular Communication. *Current Biology*, 28 (8): R435–R444. doi:10.1016/j.cub.2018.01.059.

Meletiadis, J., Walsh, T.J., Hwa Choi, E., et al. (2007) Study of common functional genetic polymorphisms of FCGR2A, 3A and 3B genes and the risk for cryptococcosis in HIV-uninfected patients. *Medical Mycology*, 45 (6): 513–518. doi:10.1080/13693780701390140.

Meng, J., Gong, M., Björkbacka, H., et al. (2011) Genome wide expression profiling and mutagenesis studies reveal that LPS responsiveness appears to be absolutely dependent on TLR4 and MD-2 expression and is dependent upon intermolecular ionic interactions. *Journal of immunology (Baltimore, Md. : 1950)*, 187 (7): 3683–3693. doi:10.4049/jimmunol.1101397.

Miki, S., Tsukada, S., Nakamura, Y., et al. (1996) Functional and possible physical association of scavenger receptor with cytoplasmic tyrosine kinase Lyn in monocytic THP-1-derived macrophages. *FEBS letters*, 399 (3): 241–244. doi:10.1016/s0014-5793(96)01332-4.

Miller, G.P. and Kohl, S. (1983) Antibody-dependent leukocyte killing of Cryptococcus neoformans. *The Journal of Immunology*, 131 (3): 1455–1459.

Miller, Y.I., Choi, S.-H., Wiesner, P., et al. (2012) The SYK side of TLR4: signalling mechanisms in response to LPS and minimally oxidized LDL. *British Journal of Pharmacology*, 167 (5): 990–999. doi:10.1111/j.1476-5381.2012.02097.x.

Mitchell, T.G. and Perfect, J.R. (1995) Cryptococcosis in the era of AIDS--100 years after the discovery of Cryptococcus neoformans. *Clinical Microbiology Reviews*, 8 (4): 515–548.

Mockenhaupt, F.P., Cramer, J.P., Hamann, L., et al. (2006) Toll-like receptor (TLR) polymorphisms in African children: Common TLR-4 variants predispose to severe malaria. *Proceedings of the National Academy of Sciences of the United States of America*, 103 (1): 177–182. doi:10.1073/pnas.0506803102.

Mócsai, A., Ruland, J. and Tybulewicz, V.L.J. (2010) The SYK tyrosine kinase: a crucial player in diverse biological functions. *Nature Reviews Immunology*, 10 (6): 387–402. doi:10.1038/nri2765.

Monari, C., Bistoni, F., Casadevall, A., et al. (2005) Glucuronoxylomannan, a Microbial Compound, Regulates Expression of Costimulatory Molecules and Production of Cytokines in Macrophages. *The Journal of Infectious Diseases*, 191 (1): 127–137. doi:10.1086/426511.

Monari, C., Retini, C., Casadevall, A., et al. (2003) Differences in outcome of the interaction between Cryptococcus neoformans glucuronoxylomannan and human monocytes and neutrophils. *European Journal of Immunology*, 33 (4): 1041–1051. doi:10.1002/eji.200323388.

Montoya, M.C., Magwene, P.M. and Perfect, J.R. (2021) Associations between Cryptococcus Genotypes, Phenotypes, and Clinical Parameters of Human Disease: A Review. *Journal of Fungi*, 7 (260). doi:https://doi.org/ 10.3390/jof7040260.

Mosser, D.M. and Zhang, X. (2011) Measuring Opsonic Phagocytosis via Fcγ Receptors and Complement Receptors on Macrophages. *Current protocols in immunology*, 95: 1427. doi:10.1002/0471142735.im1427s95.

Mukherjee, J., Nussbaum, G., Scharf, M.D., et al. (1995) Protective and nonprotective monoclonal antibodies to Cryptococcus neoformans originating from one B cell. *The Journal of Experimental Medicine*, 181 (1): 405–409.

Mukherjee, J., Scharff, M.D. and Casadevall, A. (1992) Protective murine monoclonal antibodies to Cryptococcus neoformans. *Infection and Immunity*, 60 (11): 4534–4541.

Mukhopadhyay, S., Peiser, L. and Gordon, S. (2004) Activation of murine macrophages by Neisseria meningitidis and IFN-γ in vitro: distinct roles of class A scavenger and Toll-

like pattern recognition receptors in selective modulation of surface phenotype. *Journal of Leukocyte Biology*, 76 (3): 577–584. doi:10.1189/jlb.0104014.

Mukhopadhyay, S., Varin, A., Chen, Y., et al. (2011) SR-A/MARCO–mediated ligand delivery enhances intracellular TLR and NLR function, but ligand scavenging from cell surface limits TLR4 response to pathogens. *Blood*, 117 (4): 1319–1328. doi:10.1182/blood-2010-03-276733.

Müller, U., Stenzel, W., Köhler, G., et al. (2007) IL-13 Induces Disease-Promoting Type 2 Cytokines, Alternatively Activated Macrophages and Allergic Inflammation during Pulmonary Infection of Mice with Cryptococcus neoformans. *The Journal of Immunology*, 179 (8): 5367–5377. doi:10.4049/jimmunol.179.8.5367.

Murshid, A., Borges, T.J., Lang, B.J., et al. (2016) The Scavenger Receptor SREC-I Cooperates with Toll-Like Receptors to Trigger Inflammatory Innate Immune Responses. *Frontiers in Immunology*, 7: 226. doi:10.3389/fimmu.2016.00226.

Nakamura, K., Kinjo, T., Saijo, S., et al. (2007) Dectin-1 is not required for the host defense to Cryptococcus neoformans. *Microbiology and Immunology*, 51 (11): 1115–1119. doi:10.1111/j.1348-0421.2007.tb04007.x.

Nakamura, K., Miyagi, K., Koguchi, Y., et al. (2006) Limited contribution of Toll-like receptor 2 and 4 to the host response to a fungal infectious pathogen, Cryptococcus neoformans. *FEMS Immunology & Medical Microbiology*, 47 (1): 148–154. doi:10.1111/j.1574-695X.2006.00078.x.

Nakamura, K., Miyazato, A., Xiao, G., et al. (2008) Deoxynucleic Acids from Cryptococcus neoformans Activate Myeloid Dendritic Cells via a TLR9-Dependent Pathway. *The Journal of Immunology*, 180 (6): 4067–4074. doi:10.4049/jimmunol.180.6.4067.

Nassar, F., Brummer, E. and Stevens, D.A. (1994) Effect of in vivo macrophage colony-stimulating factor on fungistasis of bronchoalveolar and peritoneal macrophages against Cryptococcus neoformans. *Antimicrobial Agents and Chemotherapy*, 38 (9): 2162–2164.

Nichols, C.B. (2021) Visualization and documentation of capsule and melanin production in Cryptococcus neoformans. *Current protocols*, 1 (1): e27. doi:10.1002/cpz1.27.

Nicola, A.M., Robertson, E.J., Albuquerque, P., et al. (2011) Nonlytic Exocytosis of Cryptococcus neoformans from Macrophages Occurs In Vivo and Is Influenced by Phagosomal pH. *mBio*, 2 (4): e00167-11. doi:10.1128/mBio.00167-11.

van Niel, G., Carter, D.R.F., Clayton, A., et al. (2022) Challenges and directions in studying cell–cell communication by extracellular vesicles. *Nature Reviews Molecular Cell Biology*, 23 (5): 369–382. doi:10.1038/s41580-022-00460-3.

Nimmerjahn, F. and Ravetch, J.V. (2008) Fcγ receptors as regulators of immune responses. *Nature Reviews Immunology*, 8 (1): 34–47. doi:10.1038/nri2206.

Okagaki, L.H. and Nielsen, K. (2012) Titan Cells Confer Protection from Phagocytosis in Cryptococcus neoformans Infections. *Eukaryotic Cell*, 11 (6): 820–826. doi:10.1128/EC.00121-12.

Okagaki, L.H., Strain, A.K., Nielsen, J.N., et al. (2010) Cryptococcal Cell Morphology Affects Host Cell Interactions and Pathogenicity. *PLOS Pathogens*, 6 (6): e1000953. doi:10.1371/journal.ppat.1000953.

Oliveira, D.L., Freire-de-Lima, C.G., Nosanchuk, J.D., et al. (2010a) Extracellular Vesicles from Cryptococcus neoformans Modulate Macrophage Functions. *Infection and Immunity*, 78 (4): 1601–1609. doi:10.1128/IAI.01171-09.

Oliveira, D.L., Nakayasu, E.S., Joffe, L.S., et al. (2010b) Characterization of Yeast Extracellular Vesicles: Evidence for the Participation of Different Pathways of Cellular Traffic in Vesicle Biogenesis. *PLOS ONE*, 5 (6): e11113. doi:10.1371/journal.pone.0011113.

de Oliveira, H.C., Castelli, R.F., Reis, F.C.G., et al. (2020) Pathogenic Delivery: The Biological Roles of Cryptococcal Extracellular Vesicles. *Pathogens*, 9 (9): 754. doi:10.3390/pathogens9090754.

Olszewski, M.A., Noverr, M.C., Chen, G.-H., et al. (2004) Urease Expression by Cryptococcus neoformans Promotes Microvascular Sequestration, Thereby Enhancing Central Nervous System Invasion. *The American Journal of Pathology*, 164 (5): 1761–1771. doi:10.1016/S0002-9440(10)63734-0.

Ost, K.S., O'Meara, T.R., Stephens, W.Z., et al. (2021) Adaptive immunity induces mutualism between commensal eukaryotes. *Nature*, 596 (7870): 114–118. doi:10.1038/s41586-021-03722-w.

Osterholzer, J.J., Milam, J.E., Chen, G.-H., et al. (2009a) Role of Dendritic Cells and Alveolar Macrophages in Regulating Early Host Defense against Pulmonary Infection with Cryptococcus neoformans. *Infection and Immunity*, 77 (9): 3749–3758. doi:10.1128/IAI.00454-09.

Osterholzer, J.J., Surana, R., Milam, J.E., et al. (2009b) Cryptococcal Urease Promotes the Accumulation of Immature Dendritic Cells and a Non-Protective T2 Immune Response within the Lung. *The American Journal of Pathology*, 174 (3): 932–943. doi:10.2353/ajpath.2009.080673.

Ou, X.-T., Wu, J.-Q., Zhu, L.-P., et al. (2011) Genotypes Coding for Mannose-Binding Lectin Deficiency Correlated With Cryptococcal Meningitis in HIV-Uninfected Chinese Patients. *The Journal of Infectious Diseases*, 203 (11): 1686–1691. doi:10.1093/infdis/jir152.

Pandya, P.H. and Wilkes, D.S. (2014) Complement System in Lung Disease. *American Journal of Respiratory Cell and Molecular Biology*, 51 (4): 467–473. doi:10.1165/rcmb.2013-0485TR.

Panepinto, J., Komperda, K., Frases, S., et al. (2009) Sec6-dependent sorting of fungal extracellular exosomes and laccase of Cryptococcus neoformans. *Molecular Microbiology*, 71 (5): 1165–1176. doi:10.1111/j.1365-2958.2008.06588.x.

Pappas, P.G. (2013) Cryptococcal Infections in Non-Hiv-Infected Patients. *Transactions of the American Clinical and Climatological Association*, 124: 61–79.

Pappas, P.G., Alexander, B.D., Andes, D.R., et al. (2010) Invasive Fungal Infections among Organ Transplant Recipients: Results of the Transplant-Associated Infection Surveillance Network (TRANSNET). *Clinical Infectious Diseases*, 50 (8): 1101–1111. doi:10.1086/651262.

Park, B.S., Song, D.H., Kim, H.M., et al. (2009) The structural basis of lipopolysaccharide recognition by the TLR4-MD-2 complex. *Nature*, 458 (7242): 1191–1195. doi:10.1038/nature07830.

Park, Y.-D., Chen, S.H., Camacho, E., et al. (2020) Role of the ESCRT Pathway in Laccase Trafficking and Virulence of Cryptococcus neoformans. *Infection and Immunity*, 88 (7): 10.1128/iai.00954-19. doi:10.1128/iai.00954-19.

Pastva, A.M., Wright, J.R. and Williams, K.L. (2007) Immunomodulatory Roles of Surfactant Proteins A and D. *Proceedings of the American Thoracic Society*, 4 (3): 252–257. doi:10.1513/pats.200701-018AW.

Paul, D., Achouri, S., Yoon, Y.-Z., et al. (2013) Phagocytosis Dynamics Depends on Target Shape. *Biophysical Journal*, 105 (5): 1143–1150. doi:10.1016/j.bpj.2013.07.036.

Pauwels, A.-M., Trost, M., Beyaert, R., et al. (2017) Patterns, Receptors, and Signals: Regulation of Phagosome Maturation. *Trends in Immunology*, 38 (6): 407–422. doi:10.1016/j.it.2017.03.006.

Peebles, R.S., Liu, M.C., Lichtenstein, L.M., et al. (1995) IgA, IgG and IgM quantification in bronchoalveolar lavage fluids from allergic rhinitics, allergic asthmatics, and normal subjects by monoclonal antibody-based immunoenzymetric assays. *Journal of Immunological Methods*, 179 (1): 77–86. doi:10.1016/0022-1759(94)00275-2.

Peiser, L., de Winther, M.P.J., Makepeace, K., et al. (2002) The Class A Macrophage Scavenger Receptor Is a Major Pattern Recognition Receptor for Neisseria meningitidis Which Is Independent of Lipopolysaccharide and Not Required for Secretory Responses. *Infection and Immunity*, 70 (10): 5346–5354. doi:10.1128/IAI.70.10.5346-5354.2002.

Phelps, D.S. and Floros, J. (1991) Localization of Pulmonary Surfactant Proteins Using Immunohistochemistry and Tissue in Situ Hybridization. *Experimental Lung Research*, 17 (6): 985–995. doi:10.3109/01902149109064330.

Piccioni, M., Monari, C., Kenno, S., et al. (2013) A purified capsular polysaccharide markedly inhibits inflammatory response during endotoxic shock. *Infection and Immunity*, 81 (1): 90–98. doi:10.1128/IAI.00553-12.

Pikaar, J.C., Voorhout, W.F., van Golde, L.M.G., et al. (1995) Opsonic Activities of Surfactant Proteins A and D in Phagocytosis of Gram-Negative Bacteria by Alveolar Macrophages. *The Journal of Infectious Diseases*, 172 (2): 481–489. doi:10.1093/infdis/172.2.481.

Pikkarainen, T., Brännström, A. and Tryggvason, K. (1999) Expression of Macrophage MARCO Receptor Induces Formation of Dendritic Plasma Membrane Processes *. *Journal of Biological Chemistry*, 274 (16): 10975–10982. doi:10.1074/jbc.274.16.10975.

Poley, M., Koubek, R., Walsh, L., et al. (2019) Cryptococcal Meningitis in an Apparent Immunocompetent Patient. *Journal of Investigative Medicine High Impact Case Reports*, 7: 1–5. doi:10.1177/2324709619834578.

Porcaro, I., Vidal, M., Jouvert, S., et al. (2003) Mannose receptor contribution to Candida albicans phagocytosis by murine E-clone J774 macrophages. *Journal of Leukocyte Biology*, 74 (2): 206–215. doi:10.1189/jlb.1202608.

PrabhuDas, M., Bowdish, D., Drickamer, K., et al. (2014) Standardizing Scavenger Receptor Nomenclature. *Journal of immunology*, 192 (5): 1997–2006. doi:10.4049/jimmunol.1490003.

Pyrgos, V., Seitz, A.E., Steiner, C.A., et al. (2013) Epidemiology of Cryptococcal Meningitis in the US: 1997–2009. *PLoS ONE*, 8 (2): e56269. doi:10.1371/journal.pone.0056269.

Qiu, Y., Dayrit, J.K., Davis, M.J., et al. (2013) Scavenger Receptor A Modulates the Immune Response to Pulmonary Cryptococcus neoformans Infection. *The Journal of Immunology*. doi:10.4049/jimmunol.1203435.

Qiu, Y., Zeltzer, S., Zhang, Y., et al. (2012) Early induction of CCL7 downstream of TLR9 signaling promotes the development of robust immunity to cryptococcal infection. *Journal of Immunology*, 188 (8): 3940–3948. doi:10.4049/jimmunol.1103053.

Rajasingham, R., Smith, R.M., Park, B.J., et al. (2017) Global burden of disease of HIV-associated cryptococcal meningitis: an updated analysis. *The Lancet Infectious Diseases*, 17 (8): 873–881. doi:10.1016/S1473-3099(17)30243-8.

Ralph, P., Prichard, J. and Cohn, M. (1975) Reticulum cell sarcoma: an effector cell in antibody-dependent cell-mediated immunity. *Journal of Immunology*, 114 (2 pt 2): 898–905.

Rath, M., Müller, I., Kropf, P., et al. (2014) Metabolism via Arginase or Nitric Oxide Synthase: Two Competing Arginine Pathways in Macrophages. *Frontiers in Immunology*, 5: 532. doi:10.3389/fimmu.2014.00532.

Redlich, S., Ribes, S., Schütze, S., et al. (2013) Toll-like receptor stimulation increases phagocytosis of Cryptococcus neoformans by microglial cells. *Journal of Neuroinflammation*, 10 (1): 841. doi:10.1186/1742-2094-10-71.

Reis, F.C.G., Borges, B.S., Jozefowicz, L.J., et al. (2019) A Novel Protocol for the Isolation of Fungal Extracellular Vesicles Reveals the Participation of a Putative Scramblase in Polysaccharide Export and Capsule Construction in Cryptococcus gattii. *mSphere*, 4 (2): e00080-19. doi:10.1128/mSphere.00080-19.

Reis, F.C.G., Gimenez, B., Jozefowicz, L.J., et al. (2021) Analysis of Cryptococcal Extracellular Vesicles: Experimental Approaches for Studying Their Diversity Among Multiple Isolates, Kinetics of Production, Methods of Separation, and Detection in Cultures of Titan Cells. *Microbiology Spectrum*, 9 (1): e00125-21. doi:10.1128/Spectrum.00125-21.

Reynolds, H.Y., Kazmierowski, J.A. and Newball, H.H. (1975) Specificity of opsonic antibodies to enhance phagocytosis of Pseudomonas aeruginosa by human alveolar macrophages. *Journal of Clinical Investigation*, 56 (2): 376–385.

Rizzo, J., Albuquerque, P.C., Wolf, J.M., et al. (2017) Analysis of multiple components involved in the interaction between Cryptococcus neoformans and Acanthamoeba castellanii. *Fungal Biology*, 121 (6): 602–614. doi:10.1016/j.funbio.2017.04.002.

Rizzo, J., Trottier, A., Moyrand, F., et al. (2023) Coregulation of extracellular vesicle production and fluconazole susceptibility in Cryptococcus neoformans. *mBio*, pp. e00870-23. doi:10.1128/mbio.00870-23.

Rizzo, J., Wong, S.S.W., Gazi, A.D., et al. (2021) Cryptococcus extracellular vesicles properties and their use as vaccine platforms. *Journal of Extracellular Vesicles*, 10 (10): e12129. doi:10.1002/jev2.12129.

Robertson, J., Caldwell, J.R., Castle, J.R., et al. (1976) Evidence for the presence of components of the alternative (properdin) pathway of complement activation in respiratory secretions. *Journal of Immunology*, 117 (3): 900–903.

Rodman, J.S., Schlesinger, P. and Stahl, P. (1978) Rat plasma clearance of horseradish peroxidase and yeast invertase is mediated by specific recognition. *FEBS Letters*, 85 (2): 345–348. doi:10.1016/0014-5793(78)80488-8.

Rodrigues, M.L. and Casadevall, A. (2018) A two-way road: novel roles for fungal extracellular vesicles. *Molecular Microbiology*, 110 (1): 11–15. doi:10.1111/mmi.14095.

Rodrigues, M.L., Nimrichter, L., Oliveira, D.L., et al. (2007) Vesicular polysaccharide export in Cryptococcus neoformans is a eukaryotic solution to the problem of fungal trans-cell wall transport. *Eukaryotic Cell*, 6 (1): 48–59. doi:10.1128/EC.00318-06.

Rodrigues, M.L. and Nosanchuk, J.D. (2020) Fungal diseases as neglected pathogens: A wake-up call to public health officials. *PLoS Neglected Tropical Diseases*, 14 (2). doi:10.1371/journal.pntd.0007964.

Rohatgi, S., Gohil, S., Kuniholm, M.H., et al. (2013) Fc Gamma Receptor 3A Polymorphism and Risk for HIV-Associated Cryptococcal Disease. *mBio*, 4 (5): e00573-13. doi:10.1128/mBio.00573-13.

Rosen, L.B., Freeman, A.F., Yang, L.M., et al. (2013) Anti-granulocyte-macrophage colony stimulating factor autoantibodies in patients with cryptococcal meningitis. *Journal of immunology (Baltimore, Md. : 1950)*, 190 (8): 3959–3966. doi:10.4049/jimmunol.1202526.

Rosen, S.H., Castleman, B., Liebow, A.A., et al. (1958) Pulmonary Alveolar Proteinosis. *New England Journal of Medicine*, 258 (23): 1123–1142. doi:10.1056/NEJM195806052582301.

Rujirachun, P., Sangwongwanich, J. and Chayakulkeeree, M. (2020) Triple infection with Cryptococcus, varicella-zoster virus, and Mycobacterium abscessus in a patient with anti-interferon-gamma autoantibodies: a case report. *BMC Infectious Diseases*, 20: 232. doi:10.1186/s12879-020-4949-4.

Rusinova, I., Forster, S., Yu, S., et al. (2013) INTERFEROME v2.0: an updated database of annotated interferon-regulated genes. *Nucleic Acids Research*, 41 (D1): D1040–D1046. doi:10.1093/nar/gks1215.

Sabiiti, W., Robertson, E., Beale, M.A., et al. (2014a) Efficient phagocytosis and laccase activity affect the outcome of HIV-associated cryptococcosis. *The Journal of Clinical Investigation*, 124 (5): 2000–2008. doi:10.1172/JCI72950.

Sabiiti, W., Robertson, E., Beale, M.A., et al. (2014b) Efficient phagocytosis and laccase activity affect the outcome of HIV-associated cryptococcosis. *The Journal of Clinical Investigation*, 124 (5): 2000–2008. doi:10.1172/JCI72950.

Safran, M., Rosen, N., Twik, M., et al. (2021) "The GeneCards Suite." In Abugessaisa, I. and Kasukawa, T. (eds.) *Practical Guide to Life Science Databases*. Singapore: Springer Nature. pp. 27–56. doi:10.1007/978-981-16-5812-9_2.

Saijo, S., Ikeda, S., Yamabe, K., et al. (2010) Dectin-2 Recognition of α-Mannans and Induction of Th17 Cell Differentiation Is Essential for Host Defense against Candida albicans. *Immunity*, 32 (5): 681–691. doi:10.1016/j.immuni.2010.05.001.

Saijo, T., Chen, J., Chen, S.C.-A., et al. (2014) Anti-granulocyte-macrophage colony-stimulating factor autoantibodies are a risk factor for central nervous system infection by Cryptococcus gattii in otherwise immunocompetent patients. *mBio*, 5 (2): e00912-00914. doi:10.1128/mBio.00912-14.

Sakai, J., Cammarota, E., Wright, J.A., et al. (2017) Lipopolysaccharide-induced NF-κB nuclear translocation is primarily dependent on MyD88, but TNFα expression requires TRIF and MyD88. *Scientific Reports*, 7: 1428. doi:10.1038/s41598-017-01600-y.

Salas, S.D., Bennett, J.E., Kwon-Chung, K.J., et al. (1996) Effect of the laccase gene CNLAC1, on virulence of Cryptococcus neoformans. *The Journal of Experimental Medicine*, 184 (2): 377–386. doi:10.1084/jem.184.2.377.

Salvator, H., Cheng, A., Rosen, L.B., et al. (2022) Neutralizing GM-CSF autoantibodies in pulmonary alveolar proteinosis, cryptococcal meningitis and severe nocardiosis. *Respiratory Research*, 23 (1): 280. doi:10.1186/s12931-022-02103-9.

Sanford, J.E., Lupan, D.M., Schlageter, A.M., et al. (1990) Passive immunization against Cryptococcus neoformans with an isotype-switch family of monoclonal antibodies reactive with cryptococcal polysaccharide. *Infection and Immunity*, 58 (6): 1919–1923.

Santangelo, R., Zoellner, H., Sorrell, T., et al. (2004) Role of Extracellular Phospholipases and Mononuclear Phagocytes in Dissemination of Cryptococcosis in a Murine Model. *Infection and Immunity*, 72 (4): 2229–2239. doi:10.1128/IAI.72.4.2229-2239.2004.

Santiago-Tirado, F.H., Onken, M.D., Cooper, J.A., et al. (2017) Trojan Horse Transit Contributes to Blood-Brain Barrier Crossing of a Eukaryotic Pathogen. *mBio*, 8 (1): e02183-16. doi:10.1128/mBio.02183-16.

Sato, K., Yamamoto, H., Nomura, T., et al. (2015) Cryptococcus neoformans Infection in Mice Lacking Type I Interferon Signaling Leads to Increased Fungal Clearance and IL-4-Dependent Mucin Production in the Lungs. *PLoS ONE*, 10 (9): e0138291. doi:10.1371/journal.pone.0138291.

Sauters, T.J.C., Roth, C., Murray, D., et al. (2022) *Amoeba Predation of Cryptococcus: A Quantitative and Population Genomic Evaluation of the Accidental Pathogen Hypothesis*. p. 2022.12.08.519367. doi:10.1101/2022.12.08.519367.

Saylor, C.A., Dadachova, E. and Casadevall, A. (2010) Murine IgG1 and IgG3 Isotype Switch Variants Promote Phagocytosis of Cryptococcus neoformans through Different Receptors. *The Journal of Immunology*, 184 (1): 336–343. doi:10.4049/jimmunol.0902752.

Schramp, M., Ying, O., Kim, T.Y., et al. (2008) ERK5 promotes Src-induced podosome formation by limiting Rho activation. *Journal of Cell Biology*, 181 (7): 1195–1210. doi:10.1083/jcb.200801078.

Seoane, P.I. and May, R.C. (2019) Vomocytosis: What we know so far. *Cellular Microbiology*, 22 (2): e13145. doi:10.1111/cmi.13145.

Seoane, P.I., Taylor-Smith, L.M., Stirling, D., et al. (2020) Viral infection triggers interferon-induced expulsion of live Cryptococcus neoformans by macrophages. *PLOS Pathogens*, 16 (2): e1008240. doi:10.1371/journal.ppat.1008240.

Shao, X., Mednick, A., Alvarez, M., et al. (2005) An Innate Immune System Cell Is a Major Determinant of Species-Related Susceptibility Differences to Fungal Pneumonia. *The Journal of Immunology*, 175 (5): 3244–3251. doi:10.4049/jimmunol.175.5.3244.

Shi, M., Li, S.S., Zheng, C., et al. (2010) Real-time imaging of trapping and urease-dependent transmigration of Cryptococcus neoformans in mouse brain. *The Journal of Clinical Investigation*, 120 (5): 1683–1693. doi:10.1172/JCI41963.

Shoham, S., Huang, C., Chen, J.-M., et al. (2001) Toll-Like Receptor 4 Mediates Intracellular Signaling Without TNF-α Release in Response to Cryptococcus neoformans Polysaccharide Capsule. *The Journal of Immunology*, 166 (7): 4620–4626. doi:10.4049/jimmunol.166.7.4620.

Shoham, S. and Marr, K.A. (2012) Invasive fungal infections in solid organ transplant recipients. *Future microbiology*, 7 (5): 639–655. doi:10.2217/fmb.12.28.

Sionov, E., Mayer-Barber, K.D., Chang, Y.C., et al. (2015) Type I IFN Induction via Poly-ICLC Protects Mice against Cryptococcosis. *PLOS Pathogens*, 11 (8): e1005040. doi:10.1371/journal.ppat.1005040.

Sjoelund, V., Smelkinson, M. and Nita-Lazar, A. (2014) Phosphoproteome Profiling of the Macrophage Response to Different Toll-Like Receptor Ligands Identifies Differences in Global Phosphorylation Dynamics. *Journal of Proteome Research*, 13 (11): 5185–5197. doi:10.1021/pr5002466.

Skevaki, C., Pararas, M., Kostelidou, K., et al. (2015) Single nucleotide polymorphisms of Toll-like receptors and susceptibility to infectious diseases. *Clinical and Experimental Immunology*, 180 (2): 165–177. doi:10.1111/cei.12578.

Smith, D.F.Q. and Casadevall, A. (2022) On the relationship between Pathogenic Potential and Infective Inoculum. *PLoS Pathogens*, 18 (6): e1010484. doi:10.1371/journal.ppat.1010484.

Smith, L.M., Dixon, E.F. and May, R.C. (2015) The fungal pathogen Cryptococcus neoformans manipulates macrophage phagosome maturation. *Cellular Microbiology*, 17 (5): 702–713. doi:10.1111/cmi.12394.

Smith, M.E., van der Maesen, K., Somera, F.P., et al. (1998) Effects of Phorbol Myristate Acetate (PMA) on Functions of Macrophages and Microglia In Vitro. *Neurochemical Research*, 23 (3): 427–434. doi:10.1023/A:1022478005243.

Smole, U., Kratzer, B. and Pickl, W.F. (2020) Soluble pattern recognition molecules: Guardians and regulators of homeostasis at airway mucosal surfaces. *European Journal of Immunology*, 50 (5): 624–642. doi:10.1002/eji.201847811.

Sørensen, T.I., Nielsen, G.G., Andersen, P.K., et al. (1988) Genetic and environmental influences on premature death in adult adoptees. *The New England Journal of Medicine*, 318 (12): 727–732. doi:10.1056/NEJM198803243181202.

Sorrell, T.C., Juillard, P.-G., Djordjevic, J.T., et al. (2016) Cryptococcal transmigration across a model brain blood-barrier: evidence of the Trojan horse mechanism and differences between Cryptococcus neoformans var. grubii strain H99 and Cryptococcus gattii strain R265. *Microbes and Infection*, 18 (1): 57–67. doi:10.1016/j.micinf.2015.08.017.

Srikanta, D., Santiago-Tirado, F.H. and Doering, T.L. (2014) Cryptococcus neoformans: historical curiosity to modern pathogen: Cryptococcus neoformans. *Yeast*, 31 (2): 47–60. doi:10.1002/yea.2997.

Steenbergen, J.N., Nosanchuk, J.D., Malliaris, S.D., et al. (2003) Cryptococcus neoformans Virulence Is Enhanced after Growth in the Genetically Malleable Host Dictyostelium discoideum. *Infection and Immunity*, 71 (9): 4862–4872. doi:10.1128/iai.71.9.4862-4872.2003.

Steenbergen, J.N., Shuman, H.A. and Casadevall, A. (2001) Cryptococcus neoformans interactions with amoebae suggest an explanation for its virulence and intracellular pathogenic strategy in macrophages. *Proceedings of the National Academy of Sciences*, 98 (26): 15245–15250. doi:10.1073/pnas.261418798.

Stoop, J.W., Zegers, B.J.M., Sander, P.C., et al. (1969) Serum immunoglobulin levels in healthy children and adults. *Clinical and Experimental Immunology*, 4 (1): 101–112.

Strunk, R.C., Eidlen, D.M. and Mason, R.J. (1988) Pulmonary alveolar type II epithelial cells synthesize and secrete proteins of the classical and alternative complement pathways. *The Journal of Clinical Investigation*, 81 (5): 1419–1426. doi:10.1172/JCI113472.

Stukes, S., Coelho, C., Rivera, J., et al. (2016) The Membrane Phospholipid Binding Protein Annexin A2 Promotes Phagocytosis and Non-lytic Exocytosis of Cryptococcus neoformans and Impacts Survival in Fungal Infection. *Journal of immunology (Baltimore, Md. : 1950)*, 197 (4): 1252–1261. doi:10.4049/jimmunol.1501855.

Subramaniam, K., French, N. and Pirofski, L. (2005) Cryptococcus neoformans-Reactive and Total Immunoglobulin Profiles of Human Immunodeficiency Virus-Infected and Uninfected Ugandans. *Clinical and Diagnostic Laboratory Immunology*, 12 (10): 1168–1176. doi:10.1128/CDLI.12.10.1168-1176.2005.

Sulahian, T.H., Imrich, A., DeLoid, G., et al. (2008) Signaling pathways required for macrophage scavenger receptor-mediated phagocytosis: analysis by scanning cytometry. *Respiratory Research*, 9 (1): 59. doi:10.1186/1465-9921-9-59.

Sunderland, W.A., Campbell, R.A. and Edwards, M.J. (1972) Pulmonary alveolar proteinosis and pulmonary cryptococcosis in an adolescent boy. *The Journal of Pediatrics*, 80 (3): 450–456. doi:10.1016/S0022-3476(72)80503-1.

Tada, H., Nemoto, E., Shimauchi, H., et al. (2002) Saccharomyces cerevisiae- and Candida albicans-Derived Mannan Induced Production of Tumor Necrosis Factor Alpha by Human Monocytes in a CD14- and Toll-Like Receptor 4-Dependent Manner. *Microbiology and Immunology*, 46 (7): 503–512. doi:10.1111/j.1348-0421.2002.tb02727.x.

Takahashi-Nakaguchi, A., Shishido, E., Yahara, M., et al. (2020) Analysis of an Intrinsic Mycovirus Associated With Reduced Virulence of the Human Pathogenic Fungus Aspergillus fumigatus. *Frontiers in Microbiology*, 10: 3045. doi:10.3389/fmicb.2019.03045.

Takemura, N., Kawasaki, T., Kunisawa, J., et al. (2014) Blockade of TLR3 protects mice from lethal radiation-induced gastrointestinal syndrome. *Nature Communications*, 5 (1): 3492. doi:10.1038/ncomms4492.

Takeo, K., Uesaka, I., Uehira, K., et al. (1973) Fine Structure of Cryptococcus neoformans Grown In Vitro as Observed by Freeze-Etching. *Journal of Bacteriology*, 113 (3): 1442–1448. doi:10.1128/jb.113.3.1442-1448.1973.

Takeuchi, O. and Akira, S. (2010) Pattern Recognition Receptors and Inflammation. *Cell*, 140 (6): 805–820. doi:10.1016/j.cell.2010.01.022.

Tan, R.S.T., Ho, B., Leung, B.P., et al. (2014) TLR Cross-talk Confers Specificity to Innate Immunity. *International Reviews of Immunology*, 33 (6): 443–453. doi:10.3109/08830185.2014.921164.

Tanaka, N., Watanabe, J., Kitamura, T., et al. (1999) Lungs of patients with idiopathic pulmonary alveolar proteinosis express a factor which neutralizes granulocyte-macrophage colony stimulating factor. *FEBS letters*, 442 (2–3): 246–250. doi:10.1016/s0014-5793(98)01668-8.

Taylor, P.R., Brown, G.D., Reid, D.M., et al. (2002) The β-Glucan Receptor, Dectin-1, Is Predominantly Expressed on the Surface of Cells of the Monocyte/Macrophage and Neutrophil Lineages. *The Journal of Immunology*, 169 (7): 3876–3882. doi:10.4049/jimmunol.169.7.3876.

Taylor, P.R., Tsoni, S.V., Willment, J.A., et al. (2007) Dectin-1 is required for β-glucan recognition and control of fungal infection. *Nature Immunology*, 8 (1): 31–38. doi:10.1038/ni1408.

The UniProt Consortium (2023) UniProt: the Universal Protein Knowledgebase in 2023. *Nucleic Acids Research*, 51 (D1): D523–D531. doi:10.1093/nar/gkac1052.

Todt, J.C., Hu, B. and Curtis, J.L. (2008) The scavenger receptor SR-A I/II (CD204) signals via the receptor tyrosine kinase Mertk during apoptotic cell uptake by murine macrophages. *Journal of Leukocyte Biology*, 84 (2): 510–518. doi:10.1189/jlb.0307135.

Trapnell, B.C., Whitsett, J.A. and Nakata, K. (2003) Pulmonary Alveolar Proteinosis. *New England Journal of Medicine*, 349 (26): 2527–2539. doi:10.1056/NEJMra023226.

Tsukamoto, H., Takeuchi, S., Kubota, K., et al. (2018) Lipopolysaccharide (LPS)-binding protein stimulates CD14-dependent Toll-like receptor 4 internalization and LPS-induced TBK1-IKKϵ-IRF3 axis activation. *Journal of Biological Chemistry*, 293 (26): 10186–10201. doi:10.1074/jbc.M117.796631.

Underhill, D.M. (2007) Collaboration between the innate immune receptors dectin-1, TLRs, and Nods. *Immunological Reviews*, 219 (1): 75–87. doi:10.1111/j.1600-065X.2007.00548.x.

Underhill, D.M., Ozinsky, A., Hajjar, A.M., et al. (1999) The Toll-like receptor 2 is recruited to macrophage phagosomes and discriminates between pathogens. *Nature*, 401 (6755): 811–815. doi:10.1038/44605.

Uribe-Querol, E. and Rosales, C. (2020) Phagocytosis: Our Current Understanding of a Universal Biological Process. *Frontiers in Immunology*, 11. Available at: https://www.frontiersin.org/article/10.3389/fimmu.2020.01066 (Accessed: 18 April 2022).

Ushach, I. and Zlotnik, A. (2016) Biological role of granulocyte macrophage colony-stimulating factor (GM-CSF) and macrophage colony-stimulating factor (M-CSF) on cells of the myeloid lineage. *Journal of Leukocyte Biology*, 100 (3): 481–489. doi:10.1189/jlb.3RU0316-144R.

Vanhaesebroeck, B., Stephens, L. and Hawkins, P. (2012) PI3K signalling: the path to discovery and understanding. *Nature Reviews Molecular Cell Biology*, 13 (3): 195–203. doi:10.1038/nrm3290.

Vanherp, L., Ristani, A., Poelmans, J., et al. (2019) Sensitive bioluminescence imaging of fungal dissemination to the brain in mouse models of cryptococcosis. *Disease Models & Mechanisms*, 12 (6): dmm039123. doi:10.1242/dmm.039123.

Vanhove, M., Beale, M.A., Rhodes, J., et al. (2017) Genomic epidemiology of Cryptococcus yeasts identifies adaptation to environmental niches underpinning infection across an African HIV/AIDS cohort. *Molecular Ecology*, 26 (7): 1991–2005. doi:10.1111/mec.13891.

Vecchiarelli, A., Pericolini, E., Gabrielli, E., et al. (2013) Elucidating the immunological function of the Cryptococcus neoformans capsule. *Future Microbiology*, 8 (9): 1107–1116. doi:10.2217/fmb.13.84.

Vecchiarelli, A., Pietrella, D., Lupo, P., et al. (2003) The polysaccharide capsule of Cryptococcus neoformans interferes with human dendritic cell maturation and activation. *Journal of Leukocyte Biology*, 74 (3): 370–378. doi:10.1189/jlb.1002476.

van de Veerdonk, F.L., Kullberg, B.J., van der Meer, J.W., et al. (2008) Host–microbe interactions: innate pattern recognition of fungal pathogens. *Current Opinion in Microbiology*, 11 (4): 305–312. doi:10.1016/j.mib.2008.06.002.

Vidya, M.K., Kumar, V.G., Sejian, V., et al. (2018) Toll-like receptors: Significance, ligands, signaling pathways, and functions in mammals. *International Reviews of Immunology*, 37 (1): 20–36. doi:10.1080/08830185.2017.1380200.

Vilchez, R.A., Irish, W., Lacomis, J., et al. (2001) The Clinical Epidemiology of Pulmonary Cryptococcosis in Non-AIDS Patients at a Tertiary Care Medical Center. *Medicine*, 80 (5): 308.

Viola, G.M., Malek, A.E., Rosen, L.B., et al. (2021) Disseminated cryptococcosis and anti-granulocyte-macrophage colony-stimulating factor autoantibodies: An underappreciated association. *Mycoses*, 64 (6): 576–582. doi:10.1111/myc.13247.

Voelz, K., Johnston, S.A., Rutherford, J.C., et al. (2010) Automated Analysis of Cryptococcal Macrophage Parasitism Using GFP-Tagged Cryptococci. *PLOS ONE*, 5 (12): e15968. doi:10.1371/journal.pone.0015968.

Voelz, K., Lammas, D.A. and May, R.C. (2009) Cytokine signaling regulates the outcome of intracellular macrophage parasitism by Cryptococcus neoformans. *Infection and Immunity*, 77 (8): 3450–3457. doi:10.1128/IAI.00297-09.

Voelz, K. and May, R.C. (2010) Cryptococcal Interactions with the Host Immune System. *Eukaryotic Cell*, 9 (6): 835–846. doi:10.1128/EC.00039-10.

Vogelpoel, L.T.C., Hansen, I.S., Visser, M.W., et al. (2015) FcγRIIa cross-talk with TLRs, IL-1R, and IFNγR selectively modulates cytokine production in human myeloid cells. *Immunobiology*, 220 (2): 193–199. doi:10.1016/j.imbio.2014.07.016.

Vogt, S., Trendelenburg, M., Tamm, M., et al. (2020) Local and Systemic Concentrations of Pattern Recognition Receptors of the Lectin Pathway of Complement in a Cohort of Patients With Interstitial Lung Diseases. *Frontiers in Immunology*, 11: 562564. doi:10.3389/fimmu.2020.562564.

Voorhout, W.F., Veenendaal, T., Kuroki, Y., et al. (1992) Immunocytochemical localization of surfactant protein D (SP-D) in type II cells, Clara cells, and alveolar

macrophages of rat lung. *Journal of Histochemistry & Cytochemistry*, 40 (10): 1589–1597. doi:10.1177/40.10.1527377.

Vu, K., Tham, R., Uhrig, J.P., et al. (2014) Invasion of the Central Nervous System by Cryptococcus neoformans Requires a Secreted Fungal Metalloprotease. *mBio*, 5 (3): e01101. doi:10.1128/mBio.01101-14.

Wagemakers, A., Ang, C.W., Hagen, F., et al. (2019) Case report: chronic relapsing cryptococcal meningitis in a patient with low mannose-binding lectin and a low naïve CD4 cell count. *BMC Infectious Diseases*, 19. doi:10.1186/s12879-019-4515-0.

Wagener, J., Malireddi, R.K.S., Lenardon, M.D., et al. (2014) Fungal Chitin Dampens Inflammation through IL-10 Induction Mediated by NOD2 and TLR9 Activation. *PLoS Pathogens*, 10 (4). doi:10.1371/journal.ppat.1004050.

Wager, C.M.L. and Wormley, F.L. (2014) Classical versus alternative macrophage activation: the Ying and the Yang in host defense against pulmonary fungal infections. *Mucosal Immunology*, 7 (5): 1023–1035. doi:10.1038/mi.2014.65.

Walenkamp, Verheul, Scharringa, et al. (1999) Pulmonary surfactant protein A binds to Cryptococcus neoformans without promoting phagocytosis. *European Journal of Clinical Investigation*, 29 (1): 83–92. doi:10.1046/j.1365-2362.1999.00429.x.

Walker, L., Sood, P., Lenardon, M.D., et al. (2018) The Viscoelastic Properties of the Fungal Cell Wall Allow Traffic of AmBisome as Intact Liposome Vesicles. *mBio*, 9 (1): e02383-17. doi:10.1128/mBio.02383-17.

Walsh, N.M., Wuthrich, M., Wang, H., et al. (2017) Characterization of C-type lectins reveals an unexpectedly limited interaction between Cryptococcus neoformans spores and Dectin-1. *PLoS ONE*, 12 (3). doi:10.1371/journal.pone.0173866.

Wang, J.P., Lee, C.K., Akalin, A., et al. (2011) Contributions of the MyD88-dependent receptors IL-18R, IL-1R, and TLR9 to host defenses following pulmonary challenge with Cryptococcus neoformans. *PloS One*, 6 (10): e26232. doi:10.1371/journal.pone.0026232.

Wang, J.Y., Kishore, U., Lim, B.L., et al. (1996) Interaction of human lung surfactant proteins A and D with mite (Dermatophagoides pteronyssinus) allergens. *Clinical & Experimental Immunology*, 106 (2): 367–373. doi:10.1046/j.1365-2249.1996.d01-838.x.

Wang, Y., Aisen, P. and Casadevall, A. (1995) Cryptococcus neoformans melanin and virulence: mechanism of action. *Infection and Immunity*, 63 (8): 3131–3136. doi:10.1128/iai.63.8.3131-3136.1995.

Wang, Y. and Casadevall, A. (1994a) Growth of Cryptococcus neoformans in presence of L-dopa decreases its susceptibility to amphotericin B. *Antimicrobial Agents and Chemotherapy*, 38 (11): 2648–2650. doi:10.1128/AAC.38.11.2648.

Wang, Y. and Casadevall, A. (1994b) Susceptibility of melanized and nonmelanized Cryptococcus neoformans to nitrogen- and oxygen-derived oxidants. *Infection and Immunity*, 62 (7): 3004–3007.

Warkentien, T. and Crum-Cianflone, N.F. (2010) An Update on Cryptococcosis Among HIV-Infected Persons. *International journal of STD & AIDS*, 21 (10): 679–684. doi:10.1258/ijsa.2010.010182.

Warmerdam, P.A., van de Winkel, J.G., Vlug, A., et al. (1991) A single amino acid in the second Ig-like domain of the human Fc gamma receptor II is critical for human IgG2 binding. *Journal of Immunology (Baltimore, Md.: 1950)*, 147 (4): 1338–1343.

Watford, W.T., Ghio, A.J. and Wright, J.R. (2000) Complement-mediated host defense in the lung. *American Journal of Physiology-Lung Cellular and Molecular Physiology*, 279 (5): L790–L798. doi:10.1152/ajplung.2000.279.5.L790.

Weber, S.M. and Levitz, S.M. (2000) Chloroquine Interferes with Lipopolysaccharide-Induced TNF-α Gene Expression by a Nonlysosomotropic Mechanism1. *The Journal of Immunology*, 165 (3): 1534–1540. doi:10.4049/jimmunol.165.3.1534.

Wei, Y., Wang, Z., Liu, Y., et al. (2023) Extracellular vesicles of Candida albicans regulate its own growth through the l-arginine/nitric oxide pathway. *Applied Microbiology and Biotechnology*, 107 (1): 355–367. doi:10.1007/s00253-022-12300-7.

Willcocks, L.C., Smith, K.G.C. and Clatworthy, M.R. (2009) Low-affinity Fcγ receptors, autoimmunity and infection. *Expert Reviews in Molecular Medicine*, 11: e24. doi:10.1017/S1462399409001161.

Winther, M.P.J. de, Dijk, K.W. van, Vlijmen, B.J.M. van, et al. (1999) Macrophage specific overexpression of the human macrophage scavenger receptor in transgenic mice, using a 180-kb yeast artificial chromosome, leads to enhanced foam cell formation of isolated peritoneal macrophages. *Atherosclerosis*, 147 (2): 339–347. doi:10.1016/S0021-9150(99)00204-X.

Wiseman, J.C.D., Ma, L.L., Marr, K.J., et al. (2007) Perforin-Dependent Cryptococcal Microbicidal Activity in NK Cells Requires PI3K-Dependent ERK1/2 Signaling. *The Journal of Immunology*, 178 (10): 6456–6464. doi:10.4049/jimmunol.178.10.6456.

Wolf, J.M., Espadas-Moreno, J., Luque-Garcia, J.L., et al. (2014) Interaction of Cryptococcus neoformans Extracellular Vesicles with the Cell Wall. *Eukaryotic Cell*, 13 (12): 1484–1493. doi:10.1128/EC.00111-14.

Wong, S.S.W., Daniel, I., Gangneux, J.-P., et al. (2020) Differential Interactions of Serum and Bronchoalveolar Lavage Fluid Complement Proteins with Conidia of Airborne Fungal Pathogen Aspergillus fumigatus. *Infection and Immunity*, 88 (9): e00212-20. doi:10.1128/IAI.00212-20.

Wozniak, K.L., Vyas, J.M. and Levitz, S.M. (2006) In Vivo Role of Dendritic Cells in a Murine Model of Pulmonary Cryptococcosis. *Infection and Immunity*, 74 (7): 3817–3824. doi:10.1128/IAI.00317-06.

Wright, S.D., Ramos, R.A., Tobias, P.S., et al. (1990) CD14, a receptor for complexes of lipopolysaccharide (LPS) and LPS binding protein. *Science*, 249 (4975): 1431–1433. doi:10.1126/science.1698311.

Wurfel, M.M., Gordon, A.C., Holden, T.D., et al. (2008) Toll-like Receptor 1 Polymorphisms Affect Innate Immune Responses and Outcomes in Sepsis. *American Journal of Respiratory and Critical Care Medicine*, 178 (7): 710–720. doi:10.1164/rccm.200803-462OC.

Xie, M., Yin, Y., Chen, L., et al. (2020) Scavenger receptor A impairs interferon response to HBV infection by limiting TRAF3 ubiquitination through recruiting OTUB1. *The FEBS Journal*, 287 (2): 310–324. doi:10.1111/febs.15035.

Xu, J., Flaczyk, A., Neal, L.M., et al. (2017a) Exploitation of Scavenger Receptor, Macrophage Receptor with Collagenous Structure, by Cryptococcus neoformans Promotes Alternative Activation of Pulmonary Lymph Node CD11b+ Conventional Dendritic Cells and Non-Protective Th2 Bias. *Frontiers in Immunology*, 8. doi:10.3389/fimmu.2017.01231.

Xu, J., Flaczyk, A., Neal, L.M., et al. (2017b) Scavenger Receptor MARCO Orchestrates Early Defenses and Contributes to Fungal Containment during Cryptococcal Infection. *The Journal of Immunology*, 198 (9): 3548–3557. doi:10.4049/jimmunol.1700057.

Xu, M., Ji, J., Jin, D., et al. (2022) The biogenesis and secretion of exosomes and multivesicular bodies (MVBs): Intercellular shuttles and implications in human diseases. *Genes & Diseases*. doi:10.1016/j.gendis.2022.03.021.

Yamamoto, H., Nakamura, Y., Sato, K., et al. (2014) Defect of CARD9 leads to impaired accumulation of gamma interferon-producing memory phenotype T cells in lungs and increased susceptibility to pulmonary infection with Cryptococcus neoformans. *Infection and Immunity*, 82 (4): 1606–1615. doi:10.1128/IAI.01089-13.

Yauch, L.E., Mansour, M.K. and Levitz, S.M. (2005) Receptor-Mediated Clearance of Cryptococcus neoformans Capsular Polysaccharide In Vivo. *Infection and Immunity*, 73 (12): 8429–8432. doi:10.1128/IAI.73.12.8429-8432.2005.

Yauch, L.E., Mansour, M.K., Shoham, S., et al. (2004) Involvement of CD14, Toll-Like Receptors 2 and 4, and MyD88 in the Host Response to the Fungal Pathogen Cryptococcus neoformans In Vivo. *Infection and Immunity*, 72 (9): 5373–5382. doi:10.1128/IAI.72.9.5373-5382.2004.

Yi, J., Sang, J., Zhao, J., et al. (2020) Transcription factor Liv4 is required for growth and pathogenesis of Cryptococcus neoformans. *FEMS Yeast Research*, 20 (3): foaa015. doi:10.1093/femsyr/foaa015.

Yoneda, A. and Doering, T.L. (2006) A Eukaryotic Capsular Polysaccharide Is Synthesized Intracellularly and Secreted via Exocytosis. *Molecular Biology of the Cell*, 17 (12): 5131–5140. doi:10.1091/mbc.e06-08-0701.

Yu, C.-H., Chen, Y., Desjardins, C.A., et al. (2019) Landscape of gene expression variation of natural isolates of Cryptococcus neoformans in response to biologically relevant stresses. *Microbial Genomics*, 6 (1): e000319. doi:10.1099/mgen.0.000319.

Yu, H., Ha, T., Liu, L., et al. (2012) Scavenger receptor A (SR-A) is required for LPS-induced TLR4 mediated NF-κB activation in macrophages. *Biochimica Et Biophysica Acta*, 1823 (7): 1192–1198. doi:10.1016/j.bbamcr.2012.05.004.

Yu, X., Yi, H., Guo, C., et al. (2011) Pattern Recognition Scavenger Receptor CD204 Attenuates Toll-like Receptor 4-induced NF-κB Activation by Directly Inhibiting Ubiquitination of Tumor Necrosis Factor (TNF) Receptor-associated Factor 6. *Journal of Biological Chemistry*, 286 (21): 18795–18806. doi:10.1074/jbc.M111.224345.

Zal, T., Volkmann, A. and Stockinger, B. (1994) Mechanisms of tolerance induction in major histocompatibility complex class II-restricted T cells specific for a blood-borne self-antigen. *Journal of Experimental Medicine*, 180 (6): 2089–2099. doi:10.1084/jem.180.6.2089.

Zaragoza, O., Alvarez, M., Telzak, A., et al. (2007) The Relative Susceptibility of Mouse Strains to Pulmonary Cryptococcus neoformans Infection Is Associated with Pleiotropic Differences in the Immune Response. *Infection and Immunity*, 75 (6): 2729–2739. doi:10.1128/IAI.00094-07.

Zaragoza, O. and Casadevall, A. (2004) Antibodies Produced in Response to Cryptococcus neoformans Pulmonary Infection in Mice Have Characteristics of Nonprotective Antibodies. *Infection and Immunity*, 72 (7): 4271–4274. doi:10.1128/IAI.72.7.4271-4274.2004.

Zaragoza, O., Chrisman, C.J., Castelli, M.V., et al. (2008) Capsule enlargement in Cryptococcus neoformans confers resistance to oxidative stress suggesting a mechanism for intracellular survival. *Cellular microbiology*, 10 (10): 2043–2057. doi:10.1111/j.1462-5822.2008.01186.x.

Zaragoza, O., García-Rodas, R., Nosanchuk, J.D., et al. (2010) Fungal Cell Gigantism during Mammalian Infection. *PLoS Pathogens*, 6 (6): e1000945. doi:10.1371/journal.ppat.1000945.

Zarnowski, R., Sanchez, H., Covelli, A.S., et al. (2018) Candida albicans biofilm–induced vesicles confer drug resistance through matrix biogenesis. *PLOS Biology*, 16 (10): e2006872. doi:10.1371/journal.pbio.2006872.

Zhang, S.-Y., Jouanguy, E., Ugolini, S., et al. (2007) TLR3 deficiency in patients with herpes simplex encephalitis. *Science*, 317 (5844): 1522–1527. doi:10.1126/science.1139522.

Zhang, Y., Wang, F., Bhan, U., et al. (2010) TLR9 Signaling Is Required for Generation of the Adaptive Immune Protection in Cryptococcus neoformans-Infected Lungs. *The American Journal of Pathology*, 177 (2): 754–765. doi:10.2353/ajpath.2010.091104.

Zhang, Y., Wang, F., Tompkins, K.C., et al. (2009) Robust Th1 and Th17 Immunity Supports Pulmonary Clearance but Cannot Prevent Systemic Dissemination of Highly Virulent Cryptococcus neoformans H99. *The American Journal of Pathology*, 175 (6): 2489–2500. doi:10.2353/ajpath.2009.090530.

Zhao, K., Bleackley, M., Chisanga, D., et al. (2019) Extracellular vesicles secreted by Saccharomyces cerevisiae are involved in cell wall remodelling. *Communications Biology*, 2 (1): 1–13. doi:10.1038/s42003-019-0538-8.

Zhou, H., Coveney, A.P., Wu, M., et al. (2019) Activation of Both TLR and NOD Signaling Confers Host Innate Immunity-Mediated Protection Against Microbial Infection. *Frontiers in Immunology*, 9: 3082. doi:10.3389/fimmu.2018.03082.

Zipfel, P.F. and Skerka, C. (2009) Complement regulators and inhibitory proteins. *Nature Reviews Immunology*, 9 (10): 729–740. doi:10.1038/nri2620.

Appendix

Supplementary Video 1: WT MPI cells infected with non-opsonised *C. neoformans.* https://youtube.com/shorts/KPfuMBMPzXk?feature=share

Supplementary Video 2: MSR1 knockout MPI cells infected with non-opsonised *C. neoformans.* https://youtube.com/shorts/g23YCDhora8?feature=share

Supplementary Video 3: MARCO knockout MPI cells infected with non-opsonised *C. neoformans.* https://youtube.com/shorts/Ask6Xj97XOM?feature=share

Supplementary Video 4: Double Knockout MPI cells infected with non-opsonised *C. neoformans.* https://youtube.com/shorts/BRSZurPd8as?feature=share

Supplementary Video 5: Rapid Vomocytosis in MARCO-deficient macrophages https://youtube.com/shorts/qlDevXuURzM?feature=share

Supplementary Video 6: Wildtype MPI cells 'infected' with latex beads. https://youtu.be/341dd5CkXco

Supplementary Video 7: *Marco*$^{-/-}$ macrophages 'infected' with latex beads. https://youtu.be/cEuAm9Dqfuc

Supplementary Video 8: Vomocytosis of yeast-locked *C. albicans* from *Marco*$^{-/-}$ macrophages. https://youtube.com/shorts/CrNF1SYIHOc?feature=share